Fisheries New Zealand
Tini a Tangaroa

Characterisation and a length-based assessment model for scampi (*Metanephrops challengeri*) at the Auckland Islands (SCI 6A), for 1989–90 to 2018–19

New Zealand Fisheries Assessment Report 2021/01

I.D. Tuck

ISSN 1179-5352 (online)
ISBN 978-1-99-004346-8 (online)

January 2021

New Zealand Government

Requests for further copies should be directed to:

Publications Logistics Officer
Ministry for Primary Industries
PO Box 2526
WELLINGTON 6140

Email: brand@mpi.govt.nz
Telephone: 0800 00 83 33
Facsimile: 04-894 0300

This publication is also available on the Ministry for Primary Industries websites at:
http://www.mpi.govt.nz/news-and-resources/publications
http://fs.fish.govt.nz go to Document library/Research reports

TABLE OF CONTENTS

EXECUTIVE SUMMARY

Tuck, I.D. (2021). Characterisation and a length-based assessment model for scampi (*Metanephrops challengeri*) at the Auckland Islands (SCI 6A), for 1989–90 to 2018–19.

***New Zealand Fisheries Assessment Report 2021/01.* 148 p.**

An assessment of the Auckland Islands (SCI 6A) scampi stock was undertaken in 2020 through Fisheries New Zealand project SCI201902 using data to the end of the 2018–19 fishing year. This work further modified and developed an existing Bayesian assessment model for this stock, which was based on previous assessment models for other scampi stocks. Considerable progress was made with the model, re-examining the commercial fishery data, exploring apparent discrepancies between photographic and trawl survey abundance indices, and updating the catchability priors, with developments also relevant to other scampi assessments. The assessment was accepted after review by the Fisheries New Zealand Deepwater Working Group. This updates the previously accepted assessment for SCI 6A conducted in 2017.

A fishery characterisation was undertaken, and a standardised Catch-Per-Unit-Effort (CPUE) index was estimated for the stock, incorporating spatial and temporal components of the fishery. Previous assessment models for this stock assumed considerable spatial structure, but following preliminary investigations in 2020, the Working Group agreed to the development of a single area model, including the fitting of an annual CPUE index as a biomass index, and photographic and trawl survey abundance indices, with informed priors for survey catchability. Length composition data were also available from fishery and survey catches. Although the base assessment model was considered most plausible, the sensitivity of the model parameter estimates to assumed constant natural mortality, catchability priors, and the exclusion of the CPUE or survey series was investigated. Parameter estimation from MCMCs were documented for four models encompassing the base model and the three sensitivities.

Although unfished spawning stock biomass (SSB_0) and stock biomass trajectories varied between the sensitivities, all models estimated recent spawning stock biomass (SSB_{2019}) to be above 40% SSB_0 (median estimates from MCMC were that SSB_{2019} was 47%–66% SSB_0). All models estimated that an above average sized year class recruited in 2017. Projections of future stock sizes using the base model through to 2025 suggested that *SSB* would remain well above 40% SSB_0 with future catches up to the TACC.

1. INTRODUCTION

This report undertakes a fishery characterisation for the Auckland Islands (SCI 6A) scampi (*Metanephrops challengeri*) stock, and applies a previously developed Bayesian, length-based, two-sex population model to this stock. The first attempt at developing a length-based population model for any scampi stock was conducted for SCI 1 (Cryer et al. 2005), which was implemented using the general-purpose stock assessment program CASAL v2.06 (September 2004). This model for SCI 1 was developed further and the same model structure was also applied to SCI 2 in a later project (Tuck & Dunn 2006). This model was first applied to the SCI 6A stock in 2011 (Tuck & Dunn 2012), and then subsequently in 2014 and 2017 (Tuck 2015, Tuck 2017) although only the latter of these assessments was accepted. The current study used CASAL v 2.22 (Bull et al. 2008) which included a slightly modified selectivity option. Developments in the model implementation and structure have been largely based on suggestions raised at the Ministry of Fisheries funded Scampi Assessment Workshop (Tuck & Dunn 2009), and subsequently at Ministry for Primary Industries/Fisheries New Zealand Shellfish Fisheries Assessment Working Group and Deepwater Working Group meetings. Assessments for SCI 1, SCI 2, and SCI 3 using this model were accepted in 2011, 2013, 2015, 2016, 2017, and 2018 (Tuck & Dunn 2012, Tuck 2014, Tuck 2016a, Tuck 2016b, Tuck 2019, Tuck 2020).

The available data and how they were used, the parameterisation of the model, and model fits and sensitivities are described. This report fulfils Fisheries New Zealand project SCI201902 "*Stock assessment of scampi*", undertaking an assessment of SCI 6A. The objective of this project was to carry out a stock assessment of scampi in SCI 6A including estimating biomass and sustainable yields.

1.1 The Auckland Islands (SCI 6A) scampi fishery

Scampi is fished all around New Zealand, in nine fishery management areas (Figure 1). The SCI 6A fishery is one of New Zealand's four main scampi fisheries (the others being SCI 1, SCI 2, and SCI 3), and over the last 5 years (2014–15 to 2018–19) has contributed an average of 243 tonnes annually, having increased from the previous 5 years (2009–10 to 2013–14 average 152 tonnes), and 283 tonnes in the five years before that. The landed catch in 2018–19 (257 tonnes) was close to the annual average since the start of the fishery (Figure 2). The Total Allowable Commercial Catch (TACC) for SCI 6A is 306 tonnes, and the total TACC for all management areas is 1224 tonnes.

The spatial distribution of targeted scampi fishing within SCI 6A is focused to the east of the Auckland Islands in water depths from 350 to 550 m (Figure 3). This fishery extends slightly deeper than other scampi fisheries around New Zealand. Scampi surveys conducted in the area have focused on the main area of the fishery, and survey strata coverage is illustrated in Figure 3.

The history of scampi management in New Zealand has been complex and subject to legal scrutiny (Carter 2003). The first reported domestic catches of scampi were in the 1987–88 fishing year, when special section 63 and section 64 permits were issued for investigative fishing and the use of small mesh trawl nets. Interpretation of the requirements for fishing under the Fisheries Act 1983 varied between regional offices of the predecessors of Fisheries New Zealand, but the fishery expanded rapidly, and by the start of the 1990–91 fishing year, 14 commercial fishing permits had been granted and 39 applications for special permits had been received.

The Ministry recognised that it needed to control the rapid expansion of the fishery, to prevent overfishing, and adopted a national approach, with a species specific prohibition on the taking of scampi imposed on 1st October 1990 under section 65 of the Fisheries Act 1983, with rules and criteria established for granting exemptions to the prohibition. These criteria included recognition of previous access to the fishery, or a demonstration of a commitment to the fishery.

Prior to the 1991–92 fishing year, there were no limits on scampi catches for any area. In the 1991–92 fishing year, Individual Quotas (IQs) were introduced for SCI 1 and SCI 2 (allocated on the basis of the

permit holder's catch in 1990–91), with competitive catch limits introduced for all other areas. The IQs were maintained for SCI 1 & 2 in 1992–93 and introduced for SCI 4 & 6A (allocated on the basis of the permit holder's catch in 1991–92), with competitive catch limits maintained for other areas. This management system (with IQs for SCI 1, 2, 4, & 6A, and competitive limits for other stocks) was maintained with the introduction of Individual Catch Entitlement (ICE) regulations in 1999, and continued until the Court of Appeal ruled in October 2001 that the scampi ICE regulations were unlawful, after which all scampi stocks were managed under competitive catch limits. Scampi was introduced into the Quota Management System (QMS) on 1st October 2004 with a Total Allowable Commercial Catch of 306 tonnes for SCI 6A, and this limit has been unchanged to date.

Coincident with the introduction of scampi to the QMS, management area boundaries were revised for SCI 3 and SCI 4, and for SCI 6A and SCI 6B (Figure 4), based on an examination of patterns in catch distribution and composition (Cryer 2000). This changed the SCI 6A area from a "bubble" encompassing the area within 50 nautical miles of the Auckland Islands to a larger box which included all the scampi fishing activity in the area.

Previous fishery characterisations have been undertaken for this area by Cryer & Coburn (2000), Tuck & Dunn (2012), and Tuck (2015, 2017).

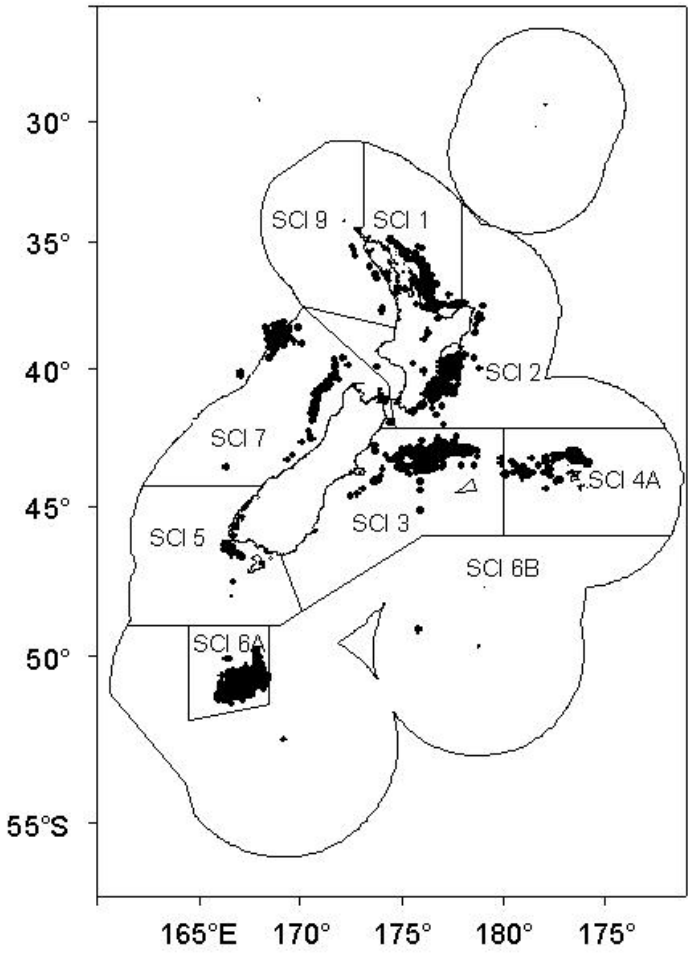

Figure 1: Spatial distribution of the scampi fishery since 1988–89. Each dot shows the midpoint of one or more tows recorded on Trawl Catch, Effort, and Processing Return (TCEPR) forms or the Electronic Reporting System (ERS) with scampi as the target species.

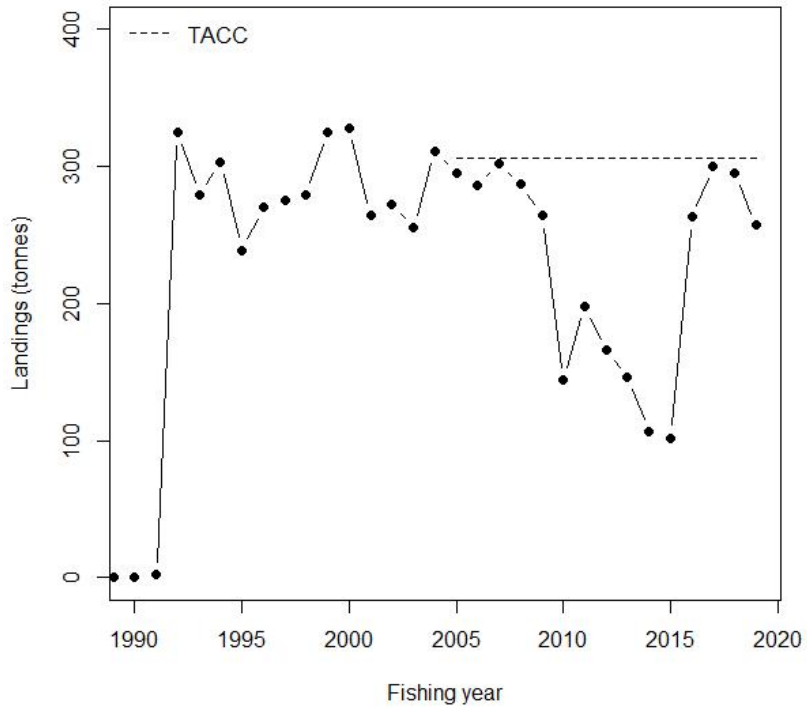

Figure 2: Time series of scampi landings from SCI 6A by fishing year (Market Harvest Return, MHR, data).

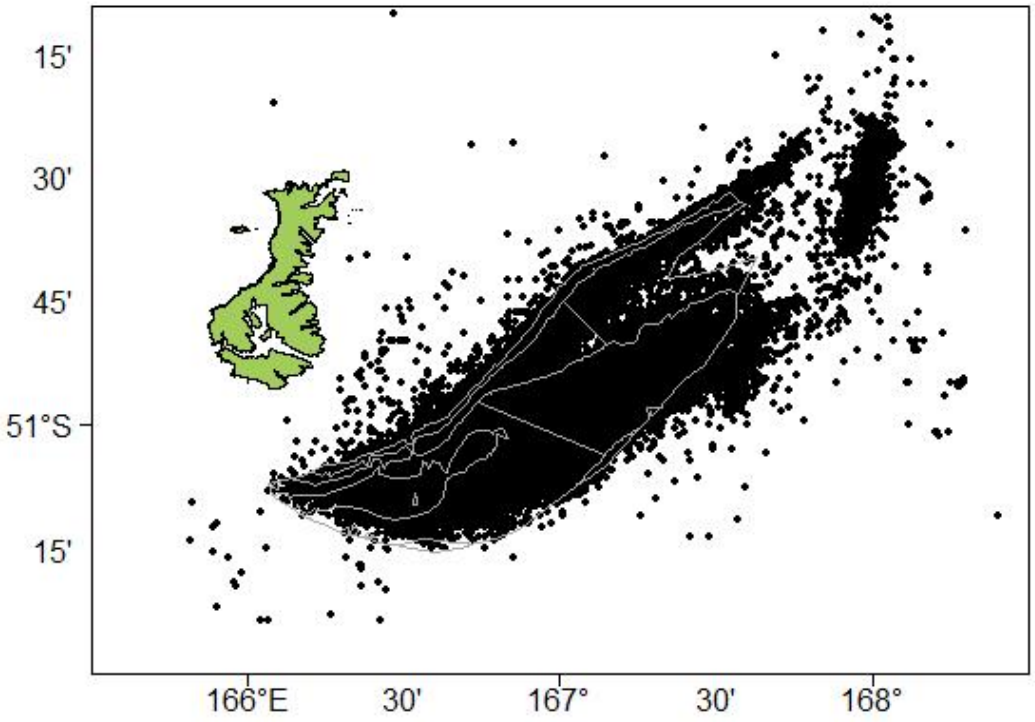

Figure 3: Spatial distribution of the scampi fishery within management area SCI 6A since 1988–89. Each dot shows the midpoint of one or more tows recorded on TCEPRs or ERS with scampi as the target species. The boundaries of the scampi survey strata are shown in grey.

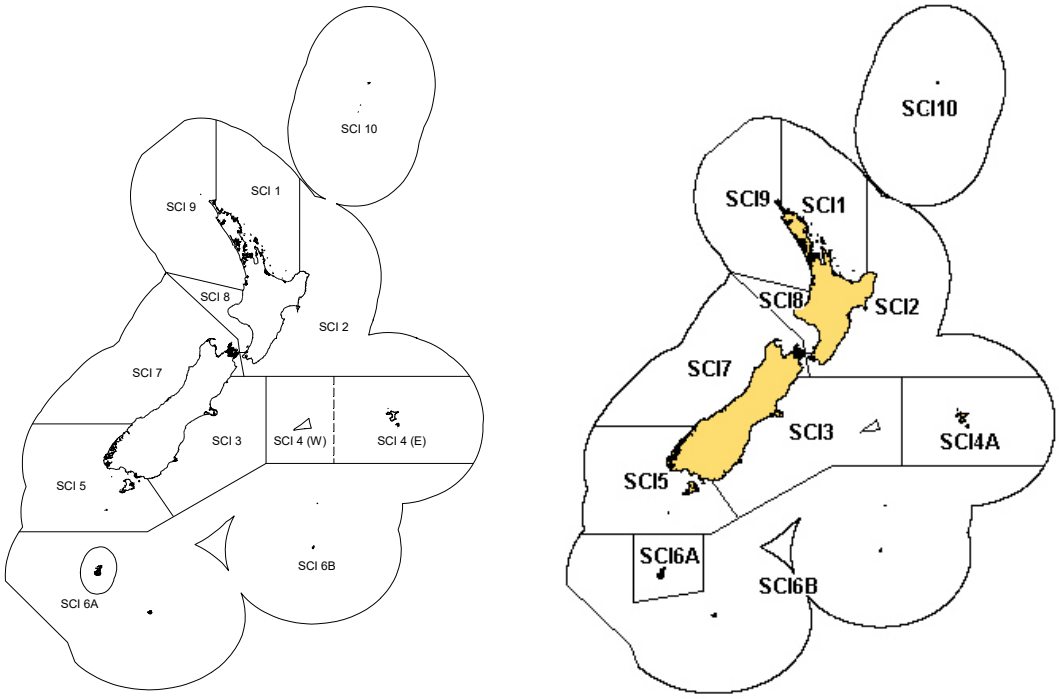

Figure 4: Left - Scampi fishery management areas, prior to 2004–05 fishing year. Right - Scampi fishery management areas, as revised at the start of the 2004–05 fishing year, when the boundaries between SCI 3 and SCI 4A, and SCI 6A and SCI 6B, were changed.

2. FISHERY CHARACTERISATION AND DATA

2.1 Commercial catch and effort data

Most scampi fishers have consistently reported catches on the Trawl Catch, Effort, and Processing Return (TCEPR) form since its introduction in 1989–90, providing a very valuable record of catch and effort on a tow-by-tow basis. This is currently being replaced by electronic reporting on the Electronic Reporting System (ERS) – Trawl data collection, and the 2017–18 and 2018–19 fishing years include an increasing proportion of data reported through this system. The ERS data collect the same tow-based variables as TCEPR.

Data were extracted from the Fisheries New Zealand *warehou* database (extract 12671), requesting all fishing events (from all areas and form types between 1 October 1989 and 31 December 2019) where scampi (SCI) was the nominated target species, or was reported in the catch from a trip. This resulted in an extract of 379 191 fishing events, with scampi target fishing events accounting for 99.7% of estimated scampi catches (135 799 events). The main contributors to non-target catch of scampi were the hoki (38% of non-target total) and ling (11% of non-target total) bottom trawl fisheries. However, given the very low contribution compared with scampi targeted effort, non-target effort has not been considered further in this characterisation.

For TCEPR and ERS data, the raw records were groomed in the following manner. For each record, the reported data were used to estimate the duration of the trawl shot, the distance between the start and finish locations, and the midpoint between the start and finish locations. For records reported on Catch Effort Landing Return (CEL) forms (293 events) and Trawl Catch Effort Return (TCE) forms (2300 events) forms, no finish locations are recorded, and so fishing distance could not be calculated, and the trawl midpoint was set as the reported start position. All tows with tow durations unrecorded or less than 30 minutes (that caught scampi) were reset to the median tow duration for the trip (165 events). All tows without a recorded finish position (except records from CEL or TCE forms), or with a tow

distance greater than 50 km were reset to the median of the midpoint of tows on the same day, on adjacent days, or for the trip, depending on available data (3120 events). These edited events were included in the allocation of catch data to area and time step analysis, but not included in the CPUE standardisation analysis. Excluding fishing events with no scampi catch and removing additional events where the location could not be determined reduced the data set further, to 135 523 events, 2941 of which were those where the tow duration was not legitimate (165 events) or where start or end position was not legitimate (2776 events). This dataset accounts for over 99.8% of the estimated scampi catch taken by the New Zealand scampi target fishery, and over 99.5% of the estimated scampi catch taken by all New Zealand fisheries during 1989–90 to 2018–19. The SCI 6A data (36 911 records) were then extracted from this full data set on the basis of latitude and longitude. All analyses were conducted on the basis of the current management area boundaries.

Total annual landings for the fishery, and the percentage by the target scampi fishery, are presented in Table 1, and the distribution of fishing activity within the SCI 6A area over time is presented in Figure 5 and Figure 6. The area over which the assessment model is applied is defined as the survey strata (350–550 m depth range in the main area of the fishery) (Figure 3), where well over 90% of the reported targeted scampi catch from SCI 6A has been taken in most years (Table 1).

Table 1: Reported commercial landings (tonnes) from the 1990–91 to 2018–19 fishing years for SCI 6A, catch estimated from scampi target fishery, and estimated catch from modelled area (survey strata).

Fishing year	Landings (MHR)	Target catch (TCEPR + ERS)	% SCI target	Estimated catch (modelled area)	% catch (modelled area)
1990–91	2	2.95	147.50	0.85	28.81
1991–92	325	326.86	100.57	309.43	94.67
1992–93	279	255.75	91.67	190.26	74.39
1993–94	303	269.73	89.02	235.37	87.26
1994–95	239	217.46	90.99	216.11	99.38
1995–96	270	228.78	84.73	223.68	97.77
1996–97	275	281.95	102.53	236.48	83.87
1997–98	279	300.65	107.76	253.78	84.41
1998–99	325	319.09	98.18	261.24	81.87
1999–00	328	312.10	95.15	262.08	83.97
2000–01	264	287.81	109.02	258.12	89.68
2001–02	272	253.48	93.19	235.36	92.85
2002–03	255	251.28	98.54	231.16	91.99
2003–04	311	291.09	93.60	245.77	84.43
2004–05	295	281.65	95.47	281.53	99.96
2005–06	286	273.36	95.58	271.84	99.44
2006–07	302	288.22	95.44	285.31	98.99
2007–08	287	277.80	96.80	276.11	99.39
2008–09	264	250.51	94.89	238.02	95.01
2009–10	144	137.12	95.22	127.24	92.79
2010–11	198	185.01	93.44	179.06	96.79
2011–12	166	160.01	96.39	156.89	98.05
2012–13	146	137.04	93.86	133.89	97.70
2013–14	107	100.78	94.19	84.78	84.12
2014–15	102	95.55	93.68	71.87	75.22
2015–16	263	247.52	94.12	238.62	96.40
2016–17	300	285.21	95.07	275.18	96.48
2017–18	295	279.22	94.65	273.25	97.86
2018–19	257	242.41	94.32	241.33	99.55

The fishery initially developed in the shallower and western areas of the grounds, closest to the Auckland Islands, extending out to the full extent of the core area by the late 1990s. This area has been

consistently fished since the late 1990s, with smaller isolated patches (further to the east) fished up until 2004. These more easterly patches were outside the gazetted SCI 6A management area at the time (see Figure 4) and, as such, were subject to different catch constraints. The core (modelled) area has accounted for over 92% of scampi targeted catch over the history of the fishery. A box plot of the unstandardised CPUE (Figure 7) shows that catch rates initially declined from very high rates in the early 1990s, fluctuated without trend until the late 2000s, remained at the lower end of the observed range between 2011 and 2014, and have since increased to more mid-range levels in the most recent years.

The breakdown of catch by survey depth stratum and fishing year is presented in Figure 8. As evident from the spatial pattern (Figure 5), catches were focused in the shallower areas in the initial years of the fishery, but since the mid 1990s, the middle depth bands (400–450 m and 450–500 m) have dominated. No more than 3% of the overall catch has come from outside the 350–550 m depth range in any one year, and less than 1% in all years since 1993–94.

Monthly patterns of effort and catch are shown for SCI 6A in Figure 9 and Figure 10. Up until 1999–2000, fishing was focused between January and May, although there was some activity throughout the year (Figure 9). The fishery was managed with competitive catch limits between 2001–02 and 2003–04, and, during this period, effort and catches were focused in the first few months of the fishing year. Since the introduction of scampi into the QMS (2004–05), very little trawling has taken place between January and February (or in December in more recent years), which is the period during which there is a higher incidence of post moult (soft shell) animals. Fishing effort has been relatively evenly distributed through the rest of the year. The monthly catch data (Figure 10) show very similar patterns to the effort data.

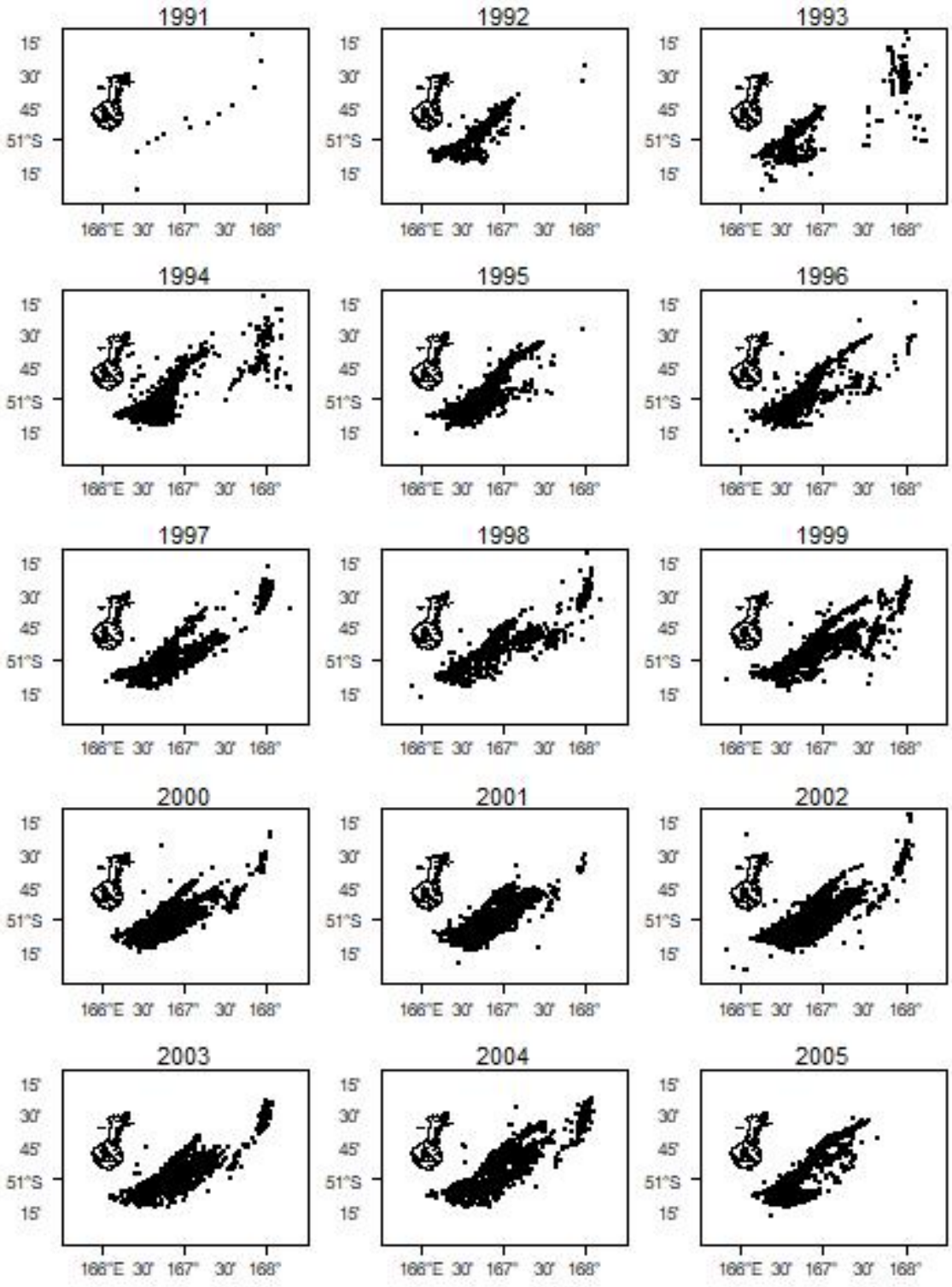

Figure 5: Spatial distribution of the main area of the SCI 6A scampi trawl fishery from 1990–91 to 2004–05. Each dot represents the midpoint of one or more tows reported by TCEPR and ERS. The general area covered by the plots is indicated within Figure 6.

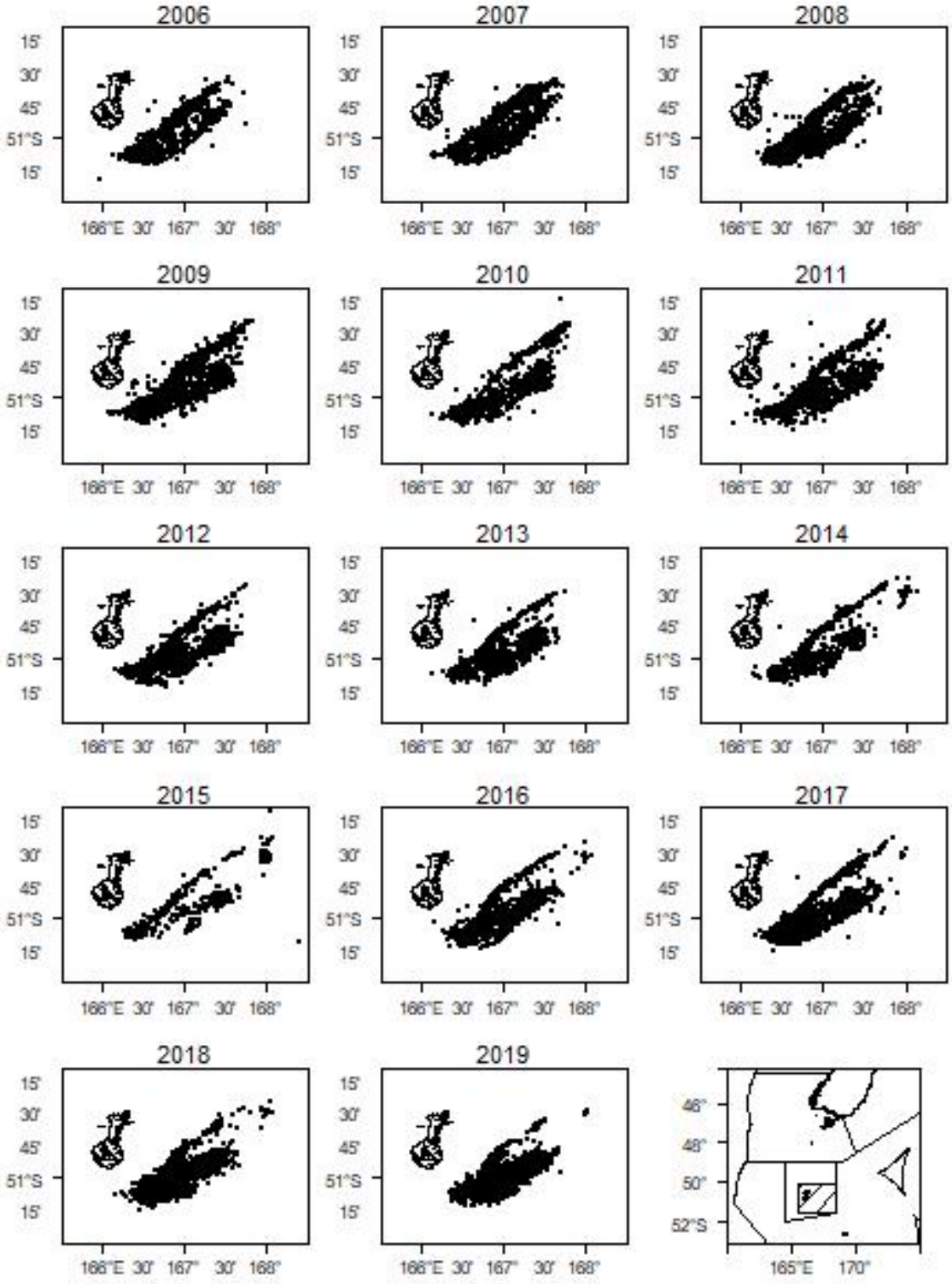

Figure 6: Spatial distribution of the main area of the SCI 6A scampi trawl fishery from 2005–06 to 2018–19. Each dot represents the midpoint of one or more tows reported by TCEPR and ERS. The general area covered by the plots is indicated by the hatched box in bottom right plot.

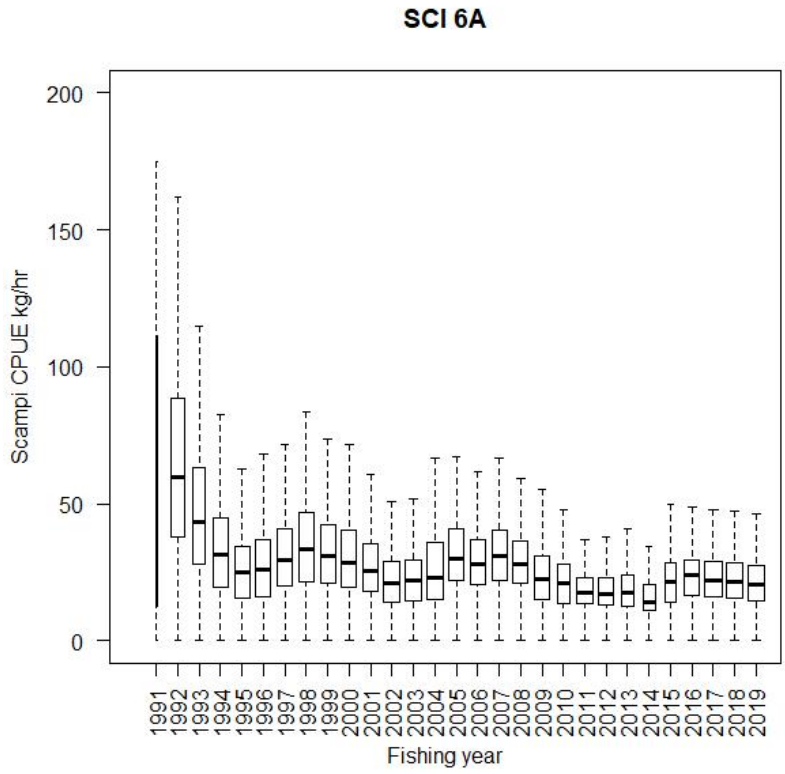

Figure 7: Box plots (with outliers removed) of unstandardised catch rate distributions (catch (kg) divided by tow effort (hours)) with tows of zero scampi catch excluded, by fishing year for the SCI 6A fishery. Box widths are proportional to square root of number of observations in each fishing year.

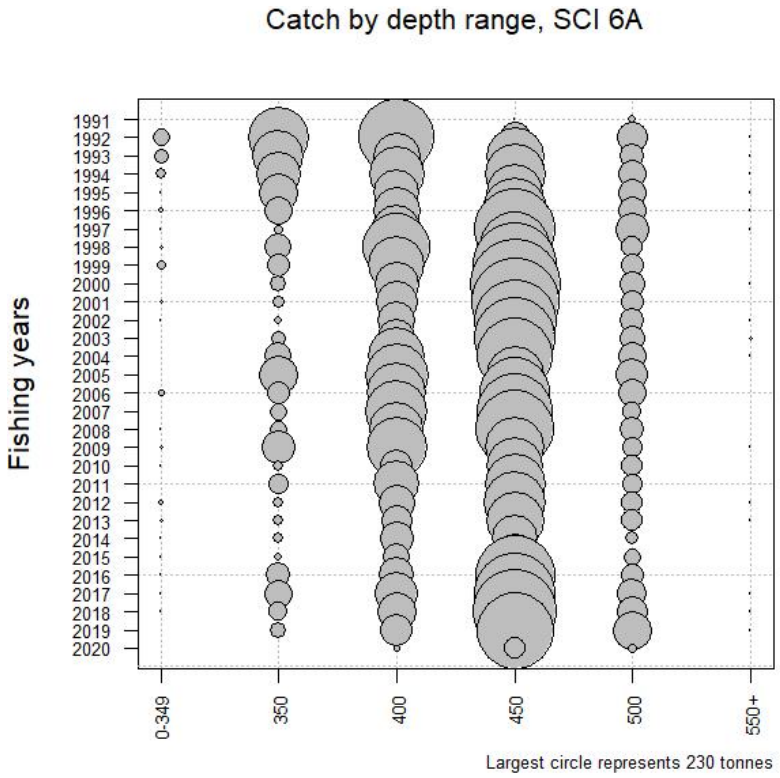

Figure 8: Annual catch breakdown by survey depth strata and fishing year for SCI 6A. Data were extracted to mid November 2019 (2019–20 fishing year) to align with the model year (see Table 3). Label '350' on x-axis indicates the 350–400 m stratum, etc.

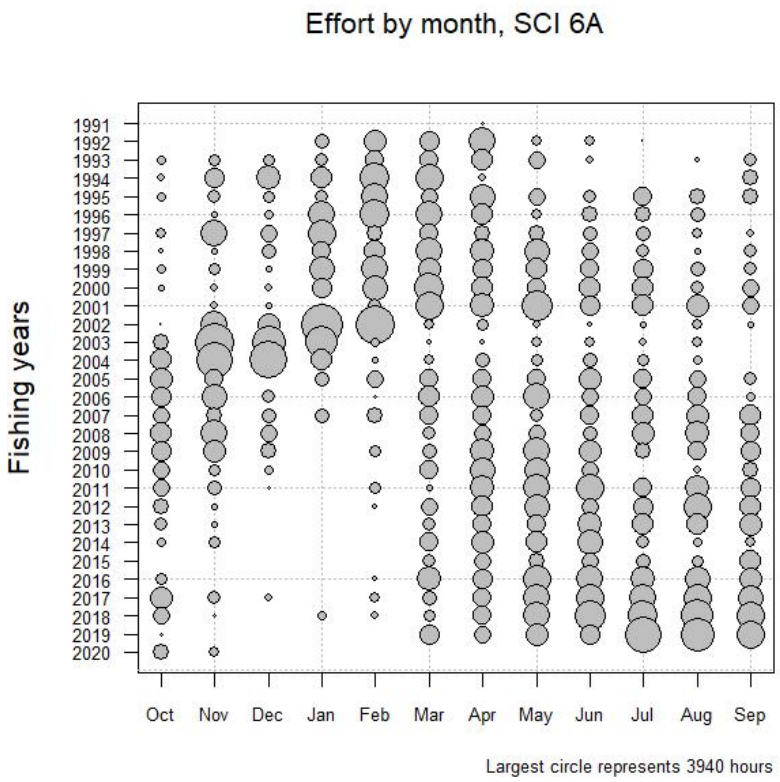

Figure 9: Monthly pattern of fishing effort in the scampi targeted fishery by fishing year for the core (modelled) area of SCI 6A. Data were extracted to mid November 2019 (2019–20 fishing year) to align with the model year (see Table 3).

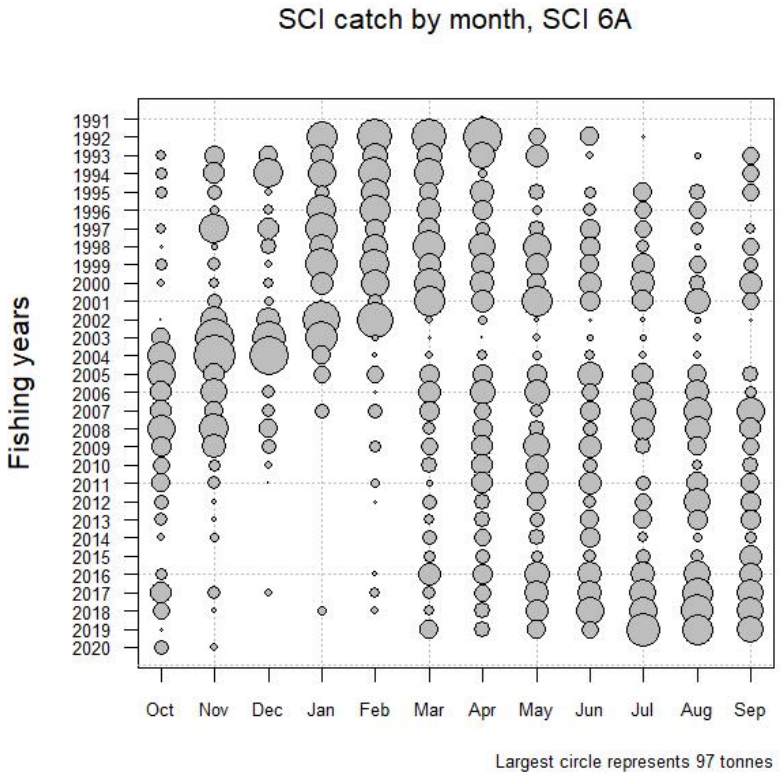

Figure 10: Monthly pattern of scampi catches in the scampi targeted fishery by fishing year for the core (modelled) area of SCI 6A. Data were extracted to mid November 2019 (2019–20 fishing year) to align with the model year (see Table 3).

2.2 Seasonal patterns in scampi biology

Previous development of the length-based model for scampi has shown that determination of appropriate time steps for the model is important when fitting to length and sex ratio data in particular (Tuck & Dunn 2006, Tuck & Dunn 2009, Tuck & Dunn 2012). Scampi inhabit burrows and are not usually vulnerable to trawling when they withdraw into their burrow. Catchability varies between the sexes on a seasonal basis as a result of sex specific moulting and reproductive behaviour, which leads to seasonal changes in the sex ratio of catches.

Current knowledge of the timing of scampi biological processes in SCI 6A is summarised in Table 2 (revised from Tuck 2010, Tuck & Dunn 2012). From patterns in the proportion of soft (post moult) animals (Figure 11), ovigerous females (Figure 12), and egg stages observed in commercial catches (Figure 13), mature female moulting appears to start in September and is focused around October and November, just after the hatching period (July-August). Hatching has been recorded at various times throughout the year and appears to vary between stocks (Wear 1976; K. Heasman, Cawthron, pers. com.). Mating occurs after the females have moulted, while the shell is still soft, and new eggs are spawned onto the pleopods in December-January. The main male moulting period occurs between December and March.

The combination of different biological processes for males and females leads to different relative availabilities of the two sexes through the year, resulting in the sex ratio pattern (displayed as proportion males) shown in Figure 14. This figure has been plotted on a half monthly basis, because some months appear to include a clear shift in sex ratio. Males are markedly less abundant than females in catches taken between December and March (male catches being reduced during their moulting period), whereas the ratio of the sexes in the catches is roughly equal between April and June, and also in November, and males are dominant from July to October.

On the basis of our understanding of the timing of biological processes for scampi in this area, and the seasonal pattern in sex ratios, the modelled year is defined as running from mid-November, with three time steps, mid-November to mid-April (when females dominate in catches), mid-April to June (when the sex ratio is about equal), and July to mid-November (when males dominate in catches) (Table 3).

Table 2: Summary of scampi biological processes for SCI 6A. Revised from Tuck (2010) and Tuck & Dunn (2012).

	Jan	Feb	Mar	Apr	May	Jun	Jul	Aug	Sep	Oct	Nov	Dec
Male moult	X	X	X									X
Female moult									X	X	X	
Mating										X	X	
Eggs spawn	X											X
Eggs hatch								X	X			

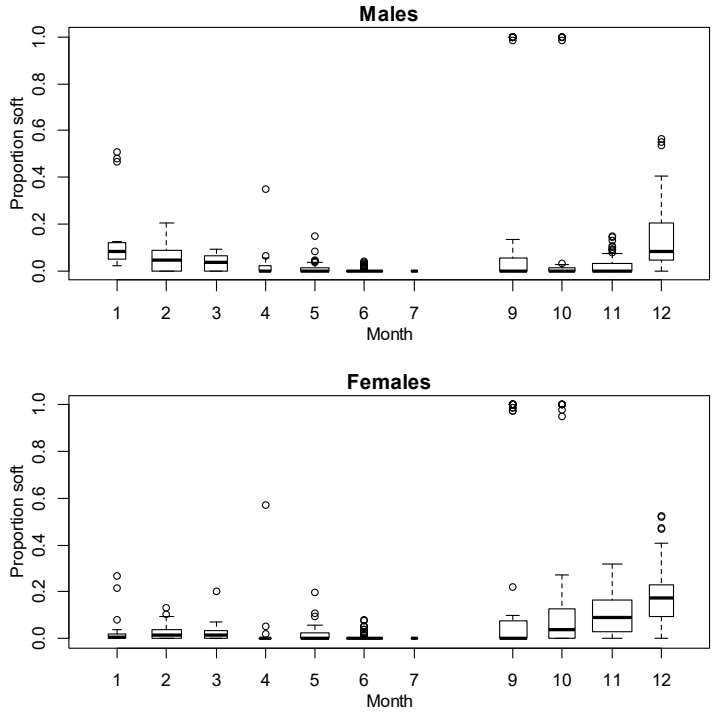

Figure 11: Box plots of proportions of soft animals (post moult) by sex and month, as recorded by observers. Box widths proportional to square root of number of observations for that month, where month 1 is January. No samples were available from August.

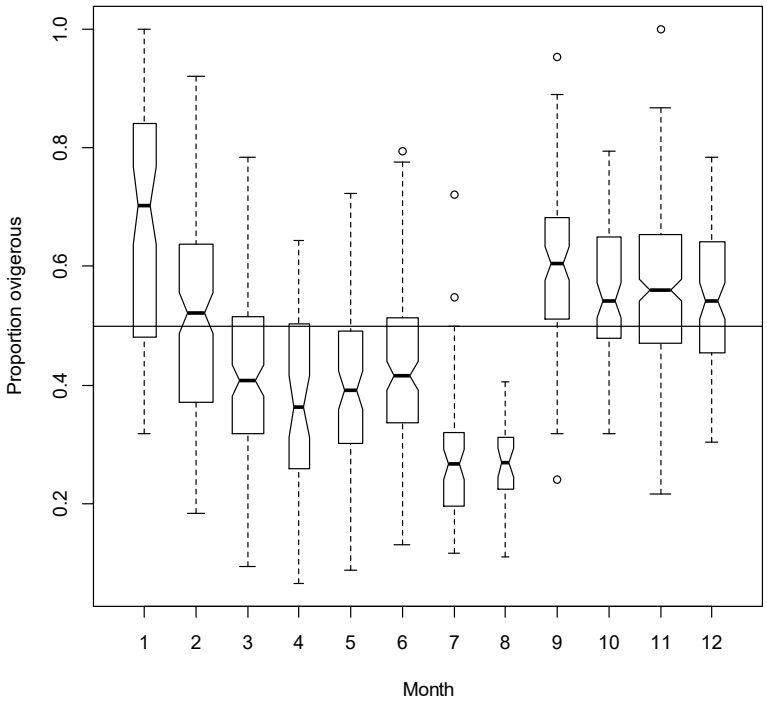

Figure 12: Box plots of proportions of ovigerous females by month, as recorded by observers. Box widths are proportional to square root of number of observations for that month, where month 1 is January.

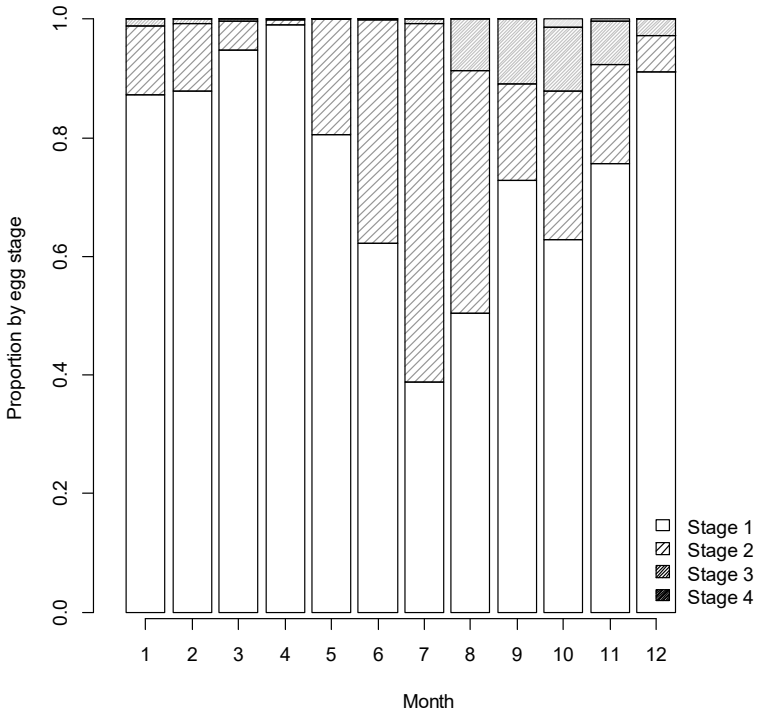

Figure 13: Bar plots of the proportion of ovigerous females by egg stage (as defined by Fenaughty (1989)) and month, where month 1 is January, from observer sampling in SCI 6A.

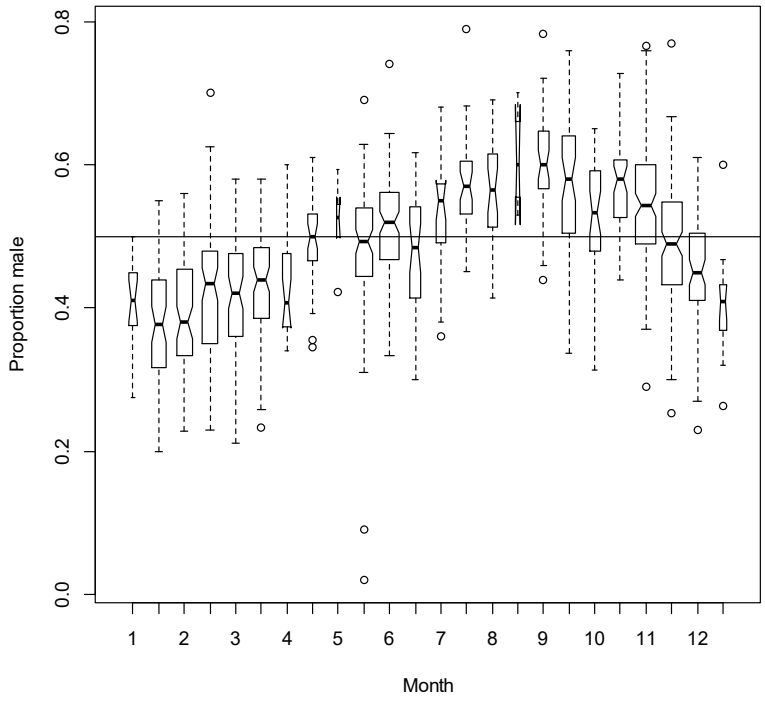

Figure 14: Box plots of proportion of males in catches by half month from observer sampling in the SCI 6A fishery. Box widths are proportional to square root of number of observations for that half month, where month 1 is January.

Table 3: Annual cycle of the population model for SCI 6A, showing the processes taking place at each time step, their sequence in each time step, and the available observations. Fishing and natural mortality that occur within a time step occur after all other processes, with 50% of the natural mortality for that time step occurring before and 50% after the fishing mortality.

Step	Period	Process	Proportion in time step
1	Mid Nov – Mid Apr	Maturation	1.0
		Growth (both sexes)	
		Natural mortality	0.42
		Fishing mortality	From TCEPR and ERS
2	Mid Apr – Jun	Recruitment	1.0
		Natural mortality	0.21
		Fishing mortality	From TCEPR and ERS
3	Jul – Mid Nov	Natural mortality	0.37
		Fishing mortality	From TCEPR and ERS

2.3 Standardised CPUE indices

Although the fishery started in the 1991 fishing year, this activity was very limited in extent, and over the next few years the fishery expanded into what is now considered to be the core area of the fishery (Figure 5). The standardised indices were therefore estimated from 1995 to provide data across the whole fishery area.

2.3.1 Core vessels

A plot of vessel activity since 1995 (number of scampi targeted tows recorded) over time is presented for SCI 6A in Figure 15. Seven vessels that were active for less than three years since 1995 have been excluded from this plot. Where a vessel has left and then returned to the fishery with a gap of more than 5 years, this has been considered a different vessel (i.e., vessel H and Ha). Eight vessels were active throughout most of the first decade of the fishery, but some of these dropped out of the fishery after 2003–04 (vessels D, G, I, O, and Q continuing to be active in most years), and a new vessel (U) started fishing at around this time, although this vessel left the fishery in 2012–13.

Figure 16 (upper plot) shows the proportion of the total catch (over the history of the fishery) in relation to the number of years that the vessels contributing that catch have been active in the fishery, and, on the basis of this, a cut-off of 5 years of activity has been selected to identify eleven core vessels. Over the fishery since 1995, these vessels caught about 90% of the scampi targeted catch taken from SCI 6A. The lower plot of Figure 16 shows the proportion of catch accounted for in each year by vessels active for at least 5 and 10 years. Other than the period of competitive catch limits (2002–03 and 2003–04), the core vessels (active for over 5 years) have accounted for over 80% of targeted scampi catches in each year, and mostly over 90%. The departure from the fishery of one of the main contributors in 2012–13 (vessel U), and the introduction of some new participants more recently, means that the contribution of the core vessels active for at least 5 years declined to below 90% in 2016–17 and 2017–18, but remains high. A 10 year cut-off has been used when characterising other scampi fisheries (Tuck 2019, Tuck 2020), but this would only provide around 60% coverage of the fishery over the first decade.

The pattern of activity for the selected core vessels is shown in Figure 17. Vessels D, G, I, and O have been active throughout the history of the fishery (albeit with some gaps for some vessels), whereas vessels E and F were only active up until 2002–03. Vessel H was also active in this early period and returned to the fishery in 2013–14 (designated Ha), vessel Q has been active since 1997–98, and vessel U was active from 2002–03 until 2012–13.

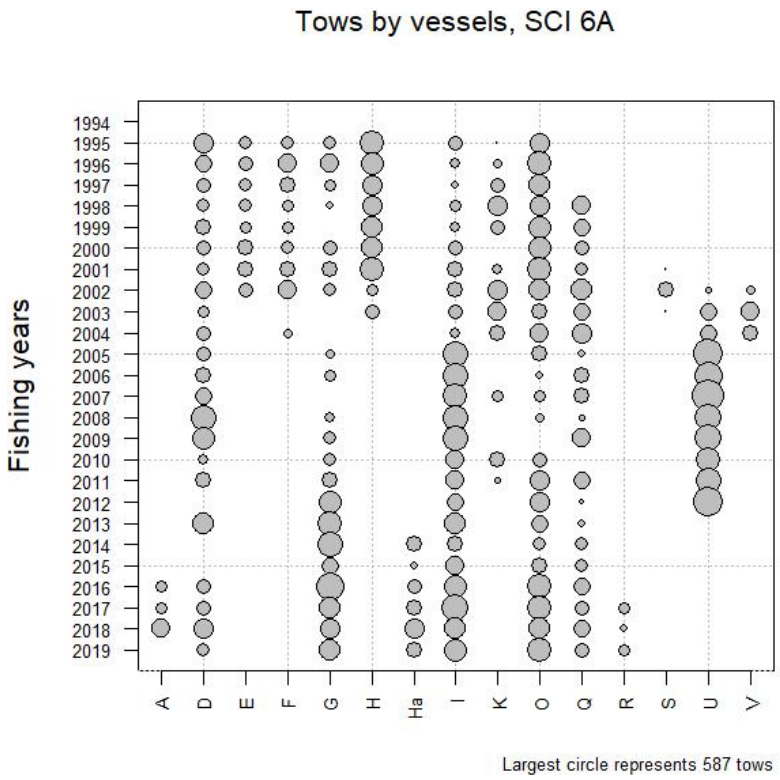

Figure 15: The temporal pattern of fishing activity by vessel and fishing year since 1995 for the modelled area of SCI 6A. The area of each circle is proportional to the number of tows recorded.

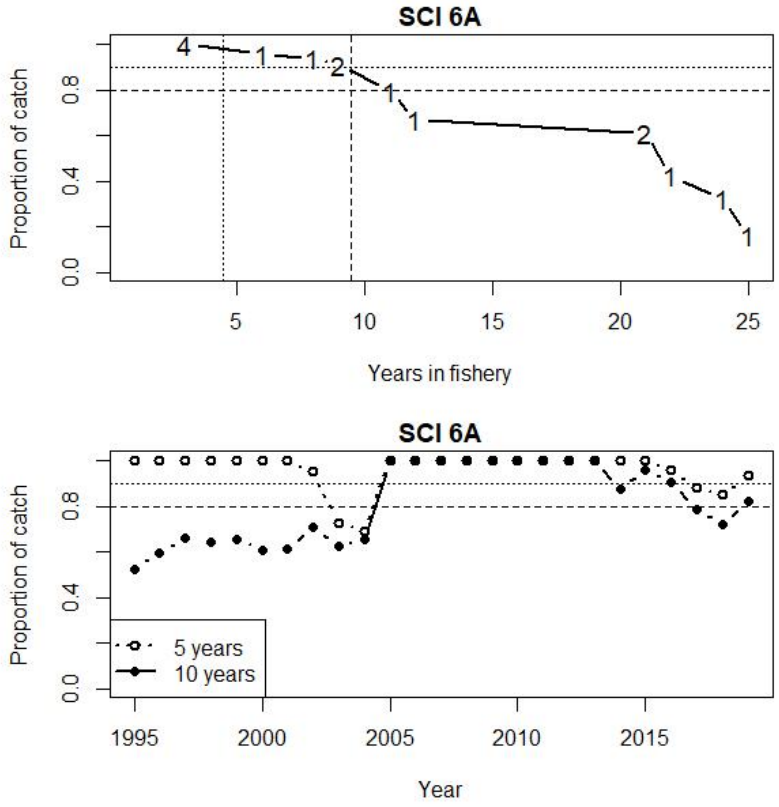

Figure 16: Catch breakdown by vessel. Upper plot - proportion of total scampi catch (all years) plotted against the number of years the vessels reporting that catch have been active in the fishery. Numbers indicate number of vessels active for that duration. Vertical dotted line represents cut off for core vessels. Lower plot – proportion of annual catch reported by vessels active in the fishery for at least 5 and 10 years.

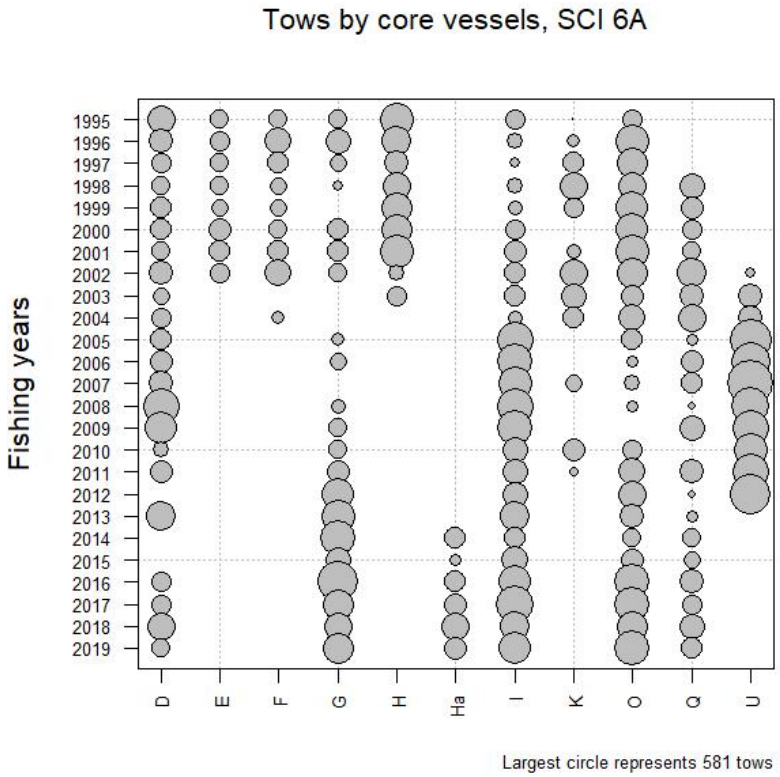

Figure 17: Core vessel pattern of fishing activity by vessel and fishing year for the modelled area of SCI 6A. The area of each circle is proportional to the number of tows recorded.

2.3.2 Exclusion of poorly sampled time periods

Following the approach developed for SCI 3 (Tuck 2013), time steps that were poorly sampled by the core vessels were excluded from the standardisation of the CPUE, on the basis that a small number of tows in a particular time step may not provide a good index of abundance. The number of records available for each time step was examined (Figure 18), and on the basis of a cut-off of 10 events, no time steps were excluded.

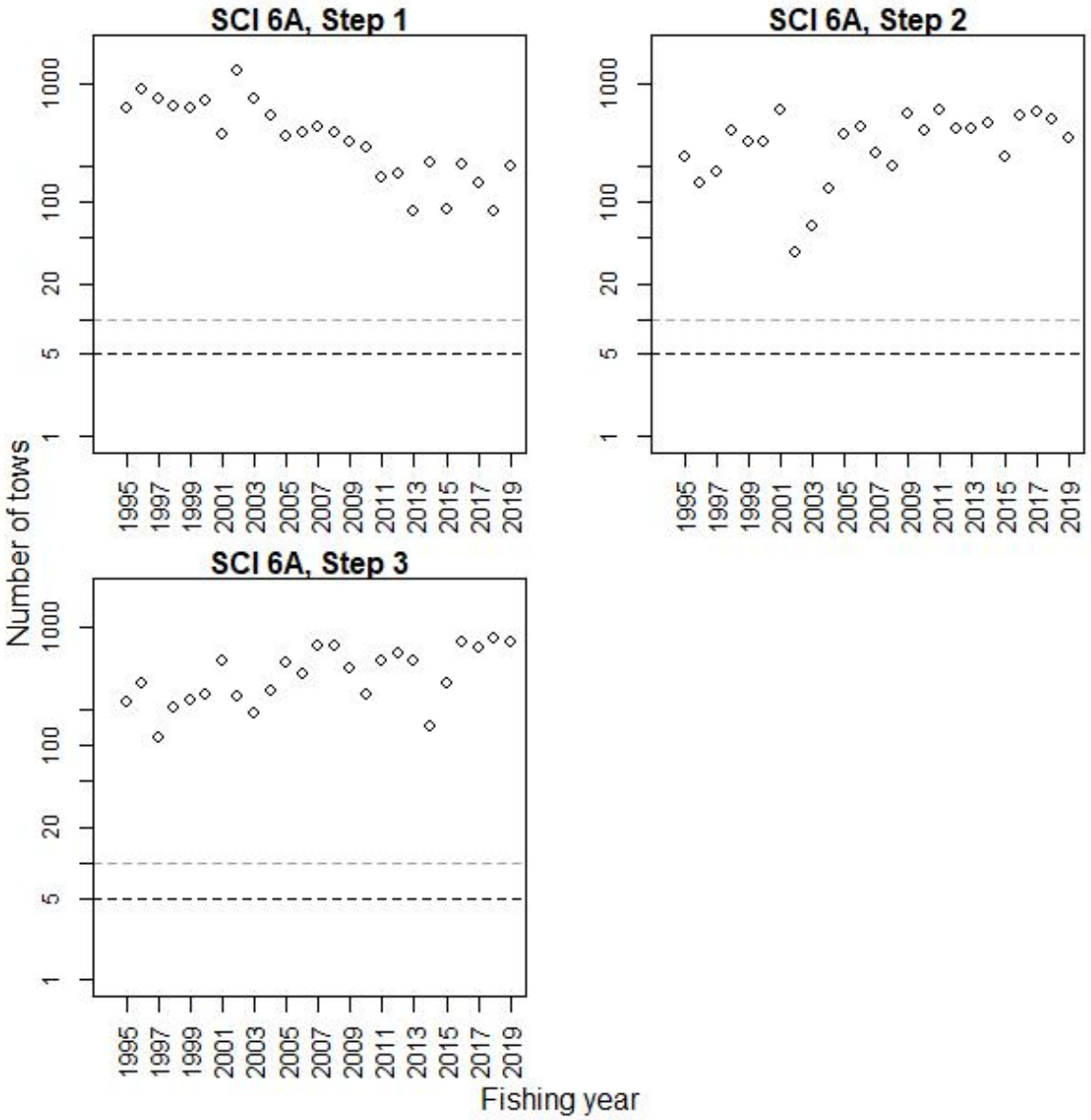

Figure 18: Number of commercial tows available within the core vessel dataset by time step and fishing year for SCI 6A. Dashed lines represent arbitrary cut-offs at 5 and 10 tows.

2.3.3 Calculation of abundance indices

For the first preliminary assessment of SCI 6A, separate abundance indices were fitted for different survey strata and time steps (Tuck & Dunn 2012), but, more recently, working groups have agreed on a simplification of the model structure (Tuck 2017). Therefore, an initial standardisation was conducted to generate an annual index (as applied in Tuck 2017), and this was compared with stratified indices where interaction terms were suggested by the data. Given the limited spatial coverage of the fishing activity in the early years (Figure 5), the standardised index was generated from the 1995 model year onwards. For each index examined, scampi catch rates reported by core vessels within the appropriate area and time step were modelled using a year index (forced), combined spatial and time step, vessel, time of day, state of moon, depth, and fishing duration terms. For the three time step indices, 'spatial strata' was included in the model as a term, whereas for the annual index, spatial strata and time step were included.

The indices were calculated from data for core vessels in the modelled area. Core vessels were selected as described above, by examining the scampi fleet's activity over the history of the fishery and selecting vessels that had consistently contributed over a number of years and, together, had contributed a significant proportion of the overall catches over the whole fishery, and in each year. This core vessel data set included 30 855 fishing events.

Of the core vessels identified, a number have changed gear configuration (twin rig to triple rig), and two have changed engine power over the history of the fishery. On the basis of previous investigations (Tuck 2013), engine power was fitted within the model (as a factor), and gear configuration as a two level factor (twin or triple rig). Gear configuration for a particular vessel and date was determined on the basis of information provided by the fishing industry as to when vessels changed from twin to triple rigs, and all tows after this date are defined as triple rig. These data were not reported on TCEPR forms until 2008. The recording of net width has varied over time within the data, but following discussions with some fishing companies, and grooming of data, a consistent net width (median over relevant time period) has been applied, changing over time where there is a clear change in the data. It is acknowledged that vessels may change gear configurations within a trip depending on gear damage or fishing conditions, but it is believed that this is not recorded consistently enough over the history of the fishery within the TCEPR records to be informative. Vessel and trawl gear configurations were offered to the model independently (vessel code as a factor, number of nets and net width as covariates) and as combined factors (vessel_number (of nets) and vessel_width (of nets)).

The time of day of each tow was calculated in relation to nautical dawn and dusk (time when the sun is 12 degrees below the horizon in the morning and evening), as calculated by the *crepescule* function of the *maptools* package in R. Individual tows were categorised on the basis of whether they occurred around Dawn (shot before dawn, hauled after dawn and before dusk), during the Day (shot after dawn, hauled before dusk), around Dusk (shot before dusk, hauled after dusk and before dawn), or at Night (shot after dusk and hauled before dawn). Longer tows including more than one period (i.e., shot before dusk and hauled after dawn) were excluded from this part of the analysis (excluding 106 records).

Individual hauls were also categorised in terms of moon state, on the assumption that tidal current strength at the sea floor will be related to the lunar cycle. Catch rates in *Nephrops* have been shown to vary with the lunar cycle (Bell et al. 2006). Tows were categorised by their date in relation to the lunar cycle, as Full moon (more than 26 days since full moon, or less than 3 days since full moon), Waning (4–11 days since full moon), New moon (12–18 days since full moon), and Waxing (19–26 days since full moon).

In addition, an examination of the data for SCI 3 (Tuck 2013) identified a distinct shift in trawl duration between 2002–03 and 2006–07 (from about 5 hours to 7 hours). This shift (in SCI 3) was fleet-wide and associated with a modification to the top of the trawl to reduce the finfish bycatch (John Finlayson, Sanford Ltd., pers. comm.), enabling vessels to fish for longer on each tow. The shift in haul duration is not apparent in data from other scampi management areas, but the vessels use the same trawl gear in all their scampi fishing. For each vessel, the timing of the gear modification was estimated from examination of tow durations in SCI 3 (see Tuck 2014) and fitted as a two level factor in the catch standardisations of the SCI 6A data.

The groomed SCI 6A dataset contained 30 855 fishing events, 611 of which had zero SCI catch, representing just under 2% of events. Previous scampi characterisations have only included positive catch events, excluding the small proportion of events with zero catch. Although the overall number of zero catch events is low, there is some evidence of decline in their incidence over time (Figure 19), and the implications of this were examined for the CPUE standardisation in preliminary analyses.

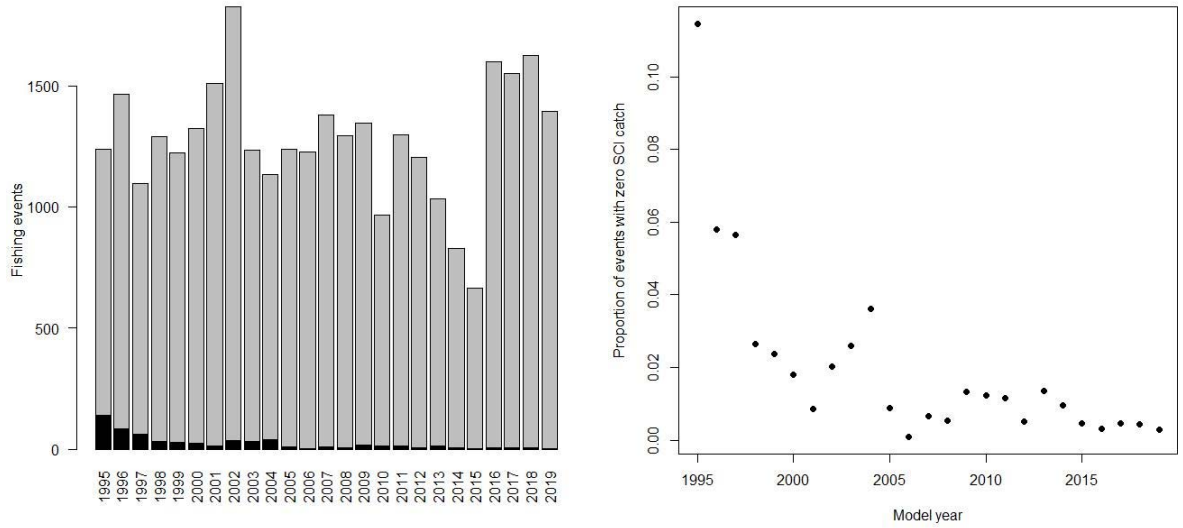

Figure 19: Stacked bar chart of SCI 6A fishing events with zero catch (black bar) and positive catch (grey bar) (left) and proportion of fishing events with zero catch (right) by model year.

A positive catch index was derived using generalised linear modelling (GLM) procedures (Vignaux 1994, Francis 1999), using the statistical software package R. The response variable in the GLM was the natural logarithm of scampi catch. The model-year was entered as a forced categorical covariate (explanatory) term on the right-hand side of the model. Standardised CPUE abundance indices (canonical) were derived from the exponential of the model-year covariate terms as described by Francis (1999).

To accommodate a non-linear relationship with the response variable (log catch), the continuous variables (effort and depth) were 'offered' to the GLMs as splines (using *bs*, the B-spline basis for polynomial splines in the R library *splines*). Vessel, time of day, state of tide (i.e., moon state), twin or triple rig, bycatch modification, and vessel power were 'offered' to the GLMs as factors. A forward fitting, stepwise, multiple-regression algorithm was used to fit GLMs to groomed catch, effort, and characterisation data. The stepwise algorithm generates a final regression model iteratively and uses a simple model with a single predictor variable, fishing year, as the initial model. The reduction in residual deviance relative to the null deviance is calculated for each additional term added to the initial model. The term that results in the greatest reduction in residual deviance is added to the initial model if this results in an improvement in residual deviance of more than 1%. The algorithm repeats this process, updating the model, until no new terms can be added. Diagnostic plots for the final models are presented in Appendix 1 (Bentley et al. 2012).

Preliminary investigations into different error distributions (comparing log normal, gamma, and Weibull) using a simple standardisation model

Log(catch)~fishing_year

identified that the gamma distribution provided a slight improvement in the distribution of residuals, and this error distribution was used for calculation of the indices reported below. Diagnostic plots for the three compared error distributions and the final standardisation model are presented in Appendix 1.

The GLM standardisation of the zero and positive catch ratios was structured in a similar fashion to that described above but used a binomial link function. The response variable in the binomial model was either '1' for a positive catch or '0' for a zero catch. Indices of abundance derived from the gamma and binomial models were combined into a unified index using the method described by Vignaux (1994).

Upon presentation to the Fisheries New Zealand Deepwater Working Group it was agreed that it was not necessary to include the zero catch events within the CPUE standardisation, and they were therefore excluded.

2.3.4 Final CPUE index

Single annual index

An initial single annual index was estimated, for consistency with the previous assessment (Tuck 2017) and to provide a baseline for comparison of other indices. Stepwise regression analysis of the dataset to estimate an annual CPUE index resulted in a final model with model year (forced), time of day, fishing duration, vessel_net_width, and time step retained (Table 4). Model diagnostics are presented in Appendix 1. The model explained 33.7% of the variation in the data. The vessel_net_width term was the most influential variable, at 8.8%, with time of day having an influence of 4.7%, and time step (2.2%) and vessel (1.5%) having less influence. The trend shown for the vessel_net_width term in the influence plot for this standardisation model (Figure 20) suggests that the scampi fleet steadily increased its fishing ability between the early 2000s and 2015. The standardised and unstandardised annual indices are shown in Figure 21. The two indices follow a similar pattern, although the standardised index is consistently above the unstandardised during the early part of the series, and below the unstandardised in later years. The relative effects of the explanatory variables (excluding model year) are shown in Figure 22. Expected catch rates are highest over dawn and during the day, and lowest (about 60% of daytime levels) at night. Expected catch increases for tow durations up to about 10 hours, but then declines. Catch rates varied between vessels but increased with net width for individual vessels. Catch rates are highest in time step 3, falling to about 85% of this level in time steps 1 and 2.

Table 4: Analysis of deviance table and overall influence for the standardisation model selected by a stepwise regression for an annual index for SCI 6A for positive catches. bs – B-spline.

	Df	Residual deviance	Deviance explained	Additional deviance explained (%)	Overall influence (%)*
NULL		8362.1			
model_year	24	7155.1	1206.9	14.43	
time of day	3	6470.9	684.2	8.18	4.74
bs(FishingDuration)	3	6053.2	417.7	4.99	1.52
Vessel_net_width	20	5727.5	325.8	3.90	8.80
step	2	5544.2	183.3	2.19	2.25

* Overall influence as in table 1 of Bentley et al. (2012).

Other standardised indices were also examined, including models with year:time step, year:depth band, and year:time step:depth band interactions. Although interactions with time step were retained by the model selection process, and improved AIC diagnostics, differences in the indices generated were minimal, and the Deepwater Working Group agreed that residual implied coefficient plots showed no concerning patterns for depth (Figure 23), and though correlations were not as good for time step 3 (Figure 24), this was largely related to poorer fits to the early part of the time series, when this time step was relatively less important for the fishery.

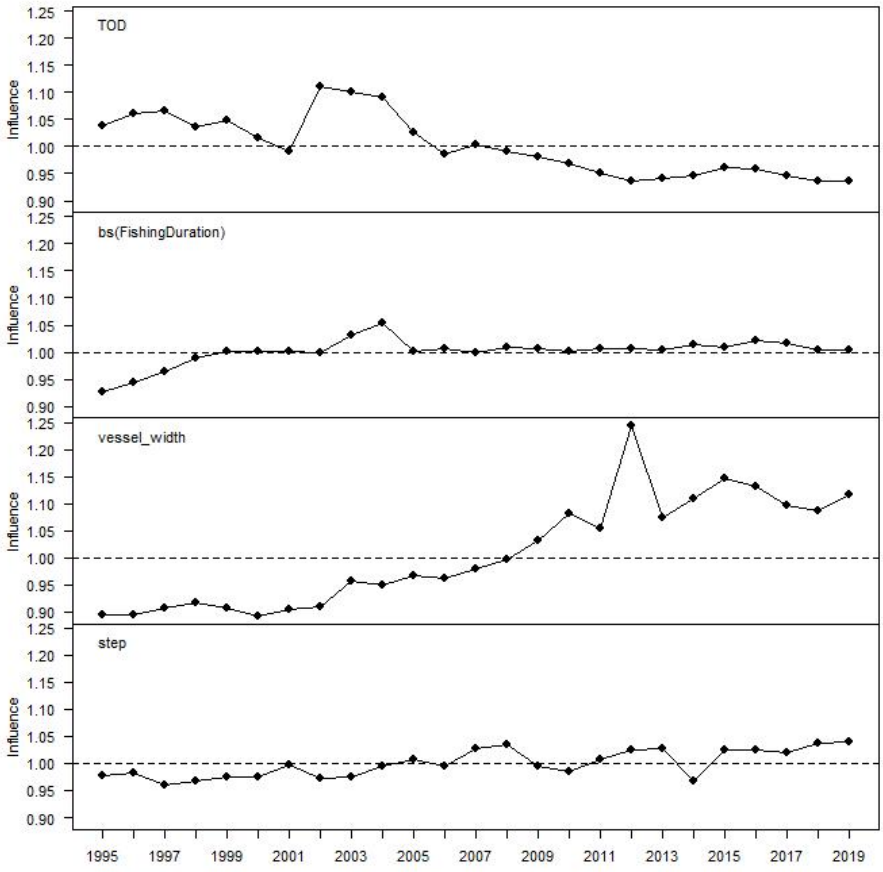

Figure 20: Year influence plots for each explanatory variable for annual SCI 6A CPUE standardisation model (Table 4).

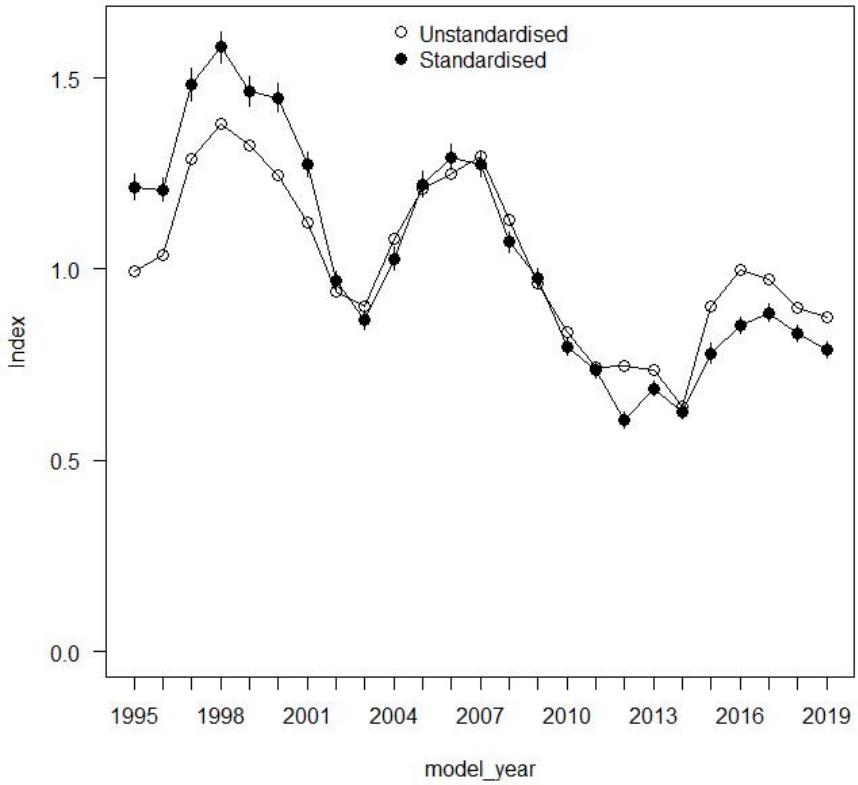

Figure 21: Comparison of standardised (Table 4) and unstandardised annual positive catch CPUE index for SCI 6A.

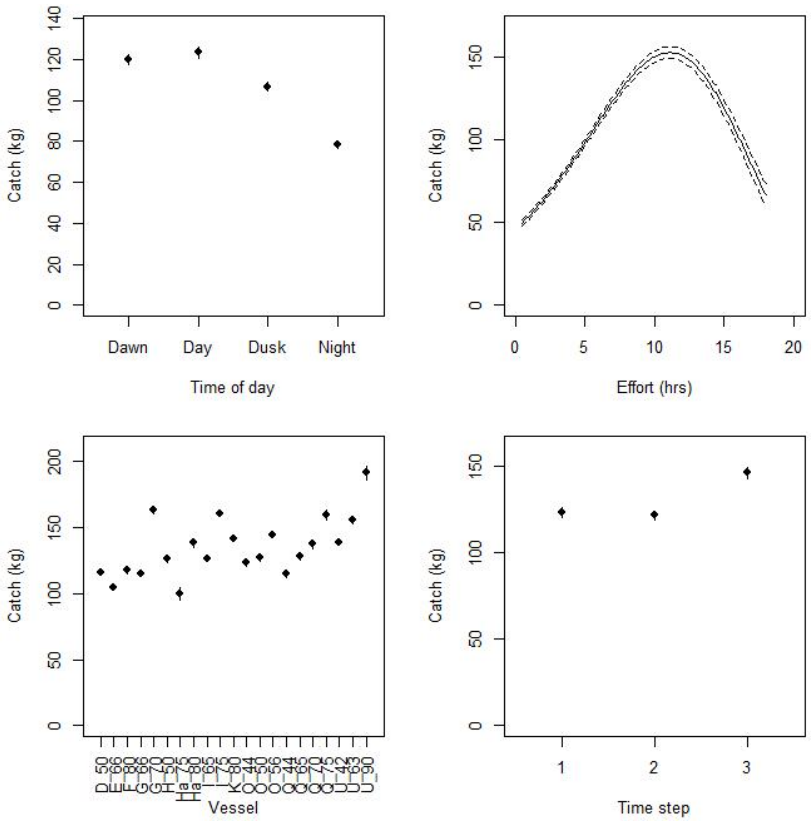

Figure 22: Termplot (in real space) for annual index standardisation model (Table 4), showing relative effects of time of day, effort (fishing duration), vessel_width, and time step.

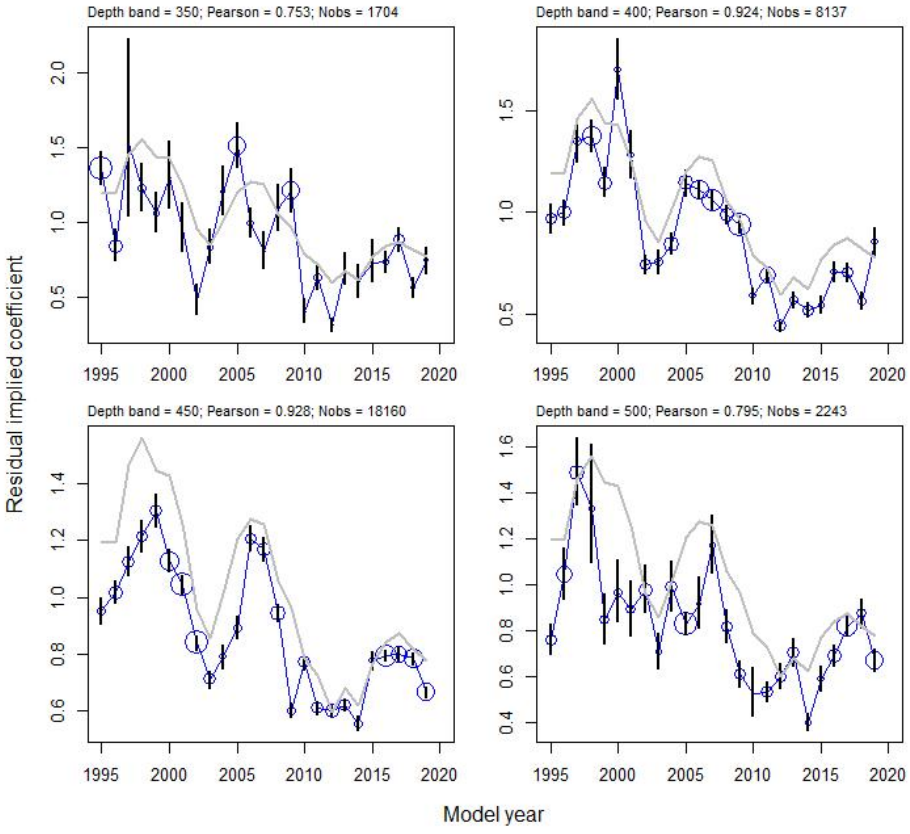

Figure 23: Residual implied coefficient plots for depth (split into four 50-m bands) for the annual index standardisation model (Table 4). Symbol size proportional to the relative number of fishing events.

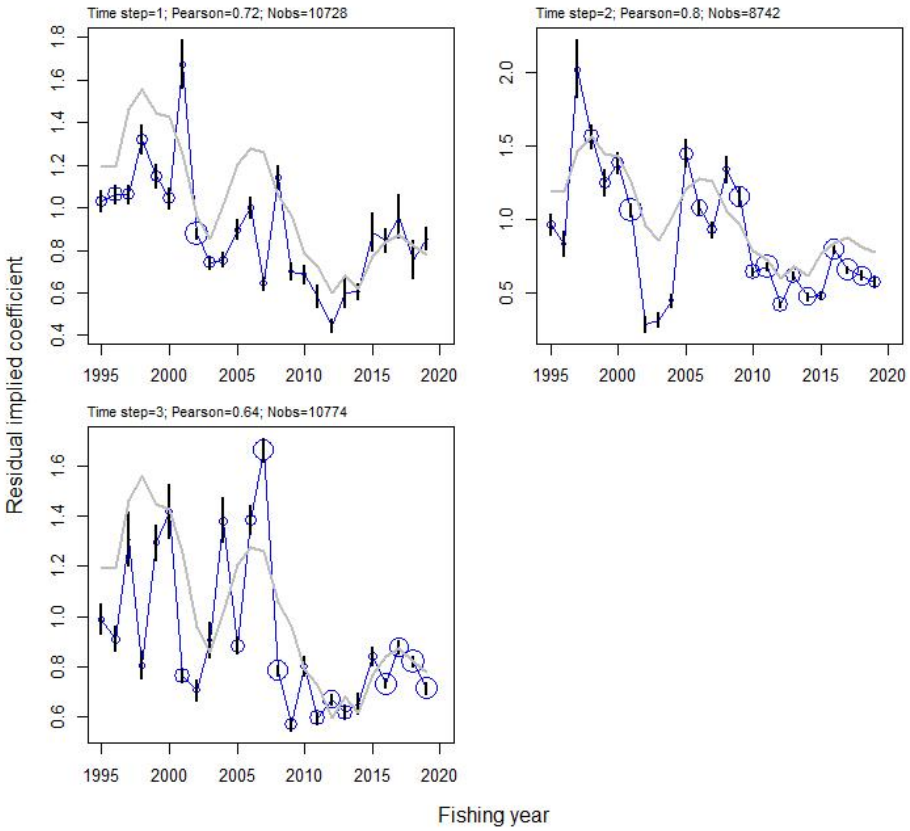

Figure 24: Residual implied coefficient plots for time step for the annual index standardisation model (Table 4). Symbol size proportional to the relative number of fishing events.

3. MODEL STRUCTURE AND INPUTS

3.1 Spatial and seasonal structure, and the model partition

The model partitions the SCI 6A scampi population by sex and length class. Growth between length classes is determined by sex-specific, length-based growth parameters. Individuals enter the partition by recruitment and are removed by natural mortality and fishing mortality. The model's annual cycle (starting in mid-November) is slightly offset from the fishing year to coincide with the moult cycle and is divided into the three time steps (see Table 2 and Table 3). The choice of three time steps was based on current understanding of scampi biology and sex ratio in catches. Note that model references to 'year' within this report refer to the modelled or fishing year and are labelled as the most recent calendar year, e.g., the fishing year 1998–99 is referred to as '1999' throughout. Previous models for SCI 6A have included spatial structure (Tuck & Dunn 2012), but following the characterisation and preliminary model investigation, the working group agreed to a single area model for the assessment.

The model uses capped logistic length-based selectivity curves for commercial fishing and research trawl surveys, which are allowed to vary with sex and time step (where necessary). Although the sex ratio data suggest that the relative catchability of the sexes varies throughout the year (hence the model time partitioning), there is no reason to suggest that, assuming equal availability, the relative change in selectivity across sizes would be different between the two sexes. Therefore the two sex selectivity implementation developed within CASAL for previous scampi assessments (Tuck & Dunn 2012) was applied. This allows the L_{50} (size at which 50% of individuals are retained) and a_{95} ($L_{50} + a_{95}$ gives size at which 95% of individuals are retained) selectivity parameters to be estimated as single values shared by both sexes in a particular time step, but allows for different availability between the sexes through estimation of different a_{max} (maximum level of selectivity) values for each sex. The change in the depth

distribution of the fishery catch in the early years (Figure 8), and the implication for selectivity (since mean size is larger in shallower areas), were allowed for using a shift parameter in the selectivity, related to the median depth of fishing in each year. Photographic survey abundance indices are not sex specific, and a double normal length-based selectivity curve is applied to allow for reduced availability of males (which grow to a larger size than females) at the time of the survey, related to moulting.

3.2 Biological inputs

3.2.1 Growth

Scampi growth has been investigated through field tagging exercises in SCI 6A in 2007, 2008, 2009, 2013, 2016, and 2019 (Tuck et al. 2007, Tuck et al. 2009a, Tuck et al. 2009b, Tuck et al. 2015a, Tuck et al. 2017, Tuck et al. 2020), with recaptures reported by the fishing industry. Growth data are fitted within the model. The tag recapture data for each release event have been split into year-time step combinations, and the numbers of recaptures per event are tabulated in Table 5.

Table 5: Numbers of scampi recaptured by release and recapture time step (SCI 6A). Releases and recaptures labelled by fishing year_time step.

Release / Recapture	2007_1	2008_1	2009_1	2013_1	2016_1	2019_1
2007_1	25					
2007_2	42					
2007_3	81					
2008_1	4	26				
2008_2	6	30				
2008_3	6	76				
2009_1	0	17	51			
2009_2	1	23	136			
2009_3	1	14	78			
2010_2	0	0	1			
2013_1	0	0	0	42		
2013_2	0	0	0	85		
2013_3	0	0	0	25		
2014_1	0	0	0	29		
2014_3	0	0	0	3		
2015_2	0	0	0	4		
2016_1	0	0	0	1	18	
2016_2	0	0	0	1	27	
2016_3	0	0	0	3	34	
2017_1	0	0	0	0	0	
2017_2	0	0	0	0	6	
2017_3	0	0	0	0	2	
2019_1	0	0	0	0	0	3

For the various combinations of release and recapture, the length increment is plotted by sex against initial length for each release in Figures 25–29. Growth for both sexes is thought to occur in time step 1.

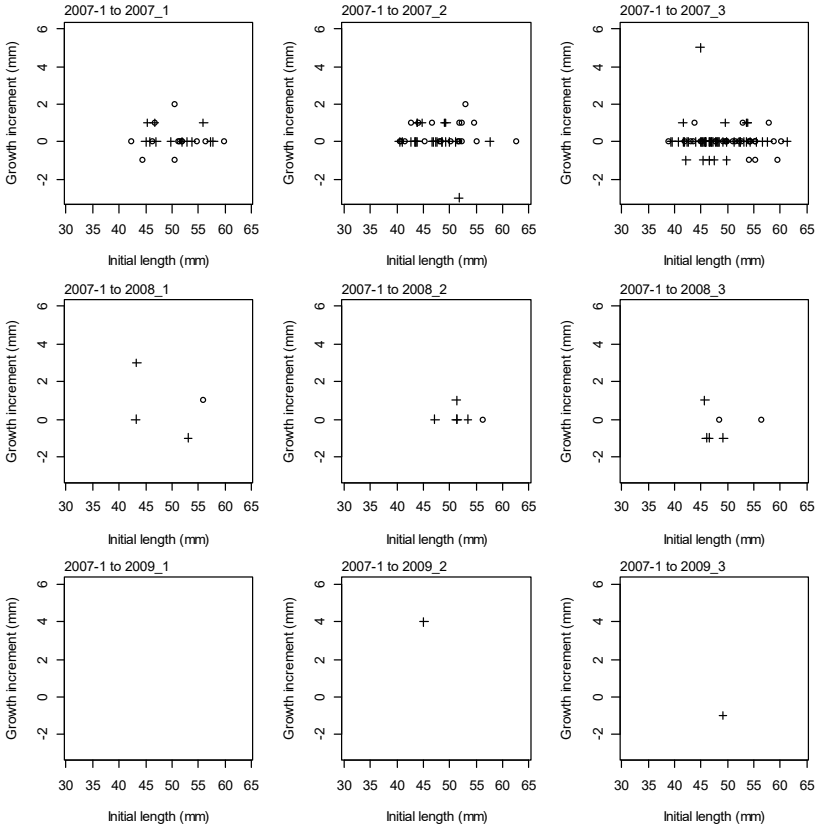

Figure 25: Plot of initial length against growth increment by combination of release and recapture time steps for 2007 releases. Males represented by hollow symbols, females represented by crosses.

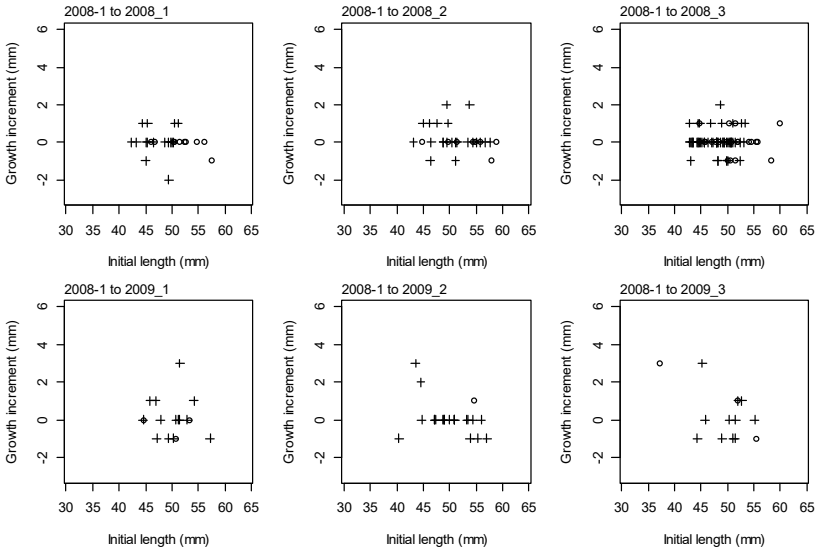

Figure 26: Plot of initial length against growth increment by combination of release and recapture time steps for 2008 releases. Males represented by hollow symbols, females represented by crosses.

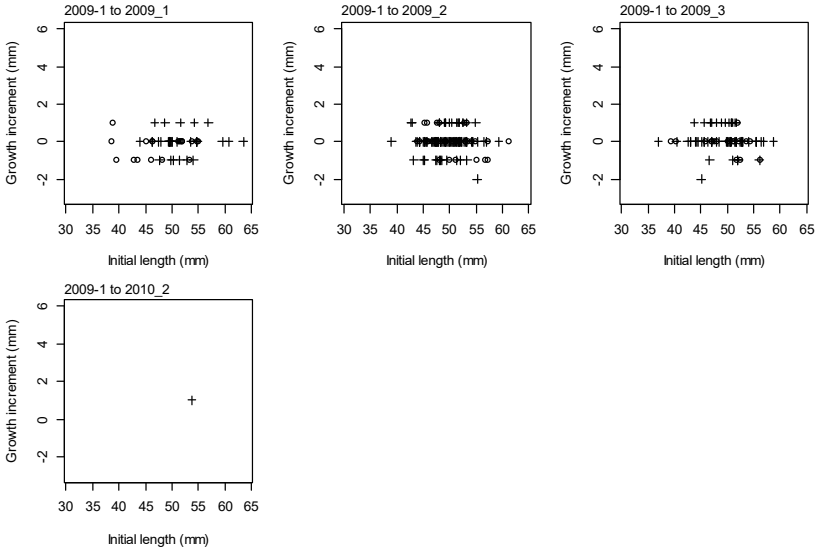

Figure 27: Plot of initial length against growth increment by combination of release and recapture time steps for 2009 releases. Males represented by hollow symbols, females represented by crosses.

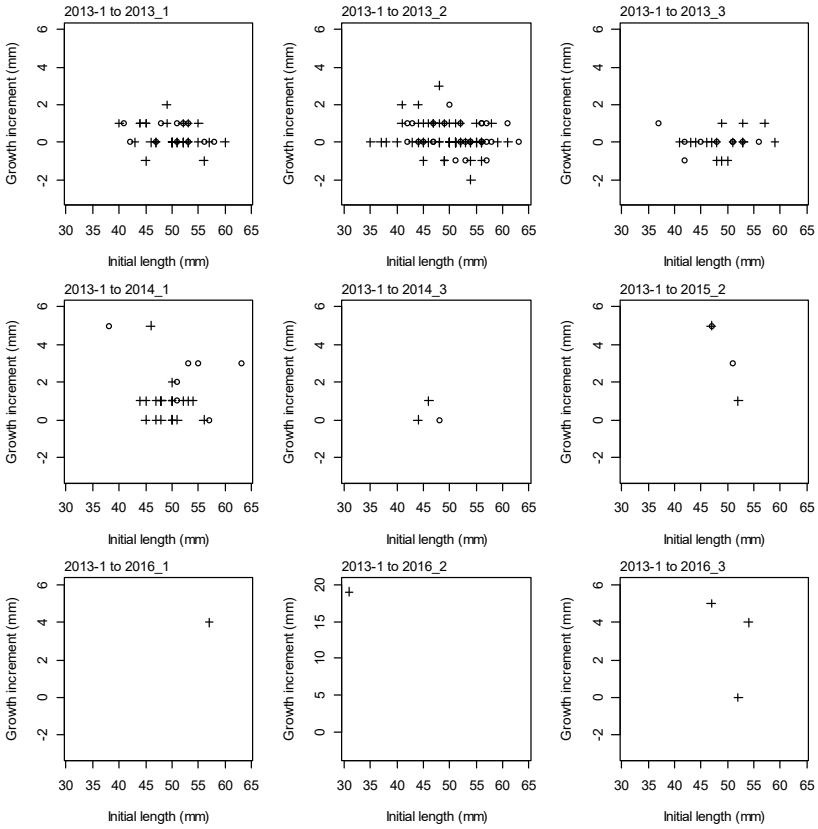

Figure 28: Plot of initial length against growth increment by combination of release and recapture time steps for 2013 releases. Males represented by hollow symbols, females represented by crosses.

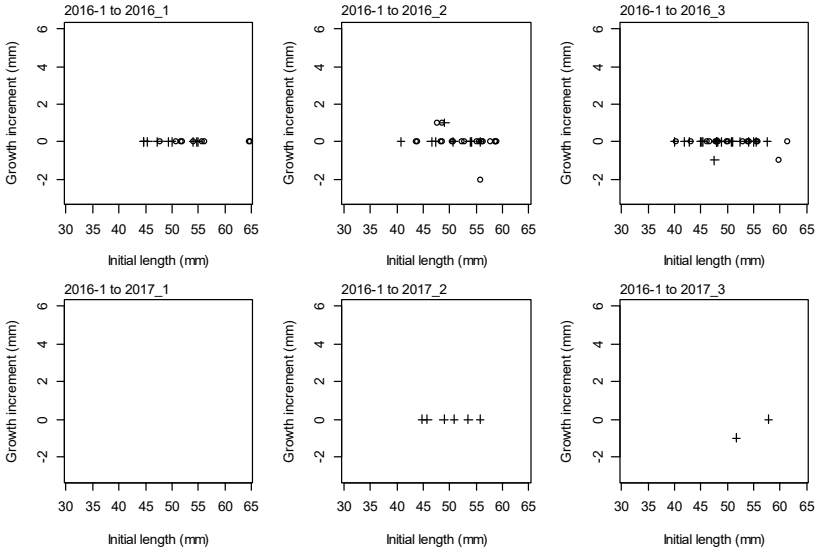

Figure 29: Plot of initial length against growth increment by combination of release and recapture time steps for 2016 releases. Males represented by hollow symbols, females represented by crosses.

3.2.2 Maturity

Female maturity can be estimated from gonad staging or the presence of eggs on the pleopods. Gonad stages are recorded from research survey catches (although only on scampi not tagged and released), and the presence and development stage of eggs on pleopods are recorded from research survey and observer sampling. No data are available for the maturity of male scampi in SCI 6A, so their maturity ogive was assumed to be identical to that of females, although studies on *Metanephrops* and *N. norvegicus* have suggested that male maturity may occur at a larger size (although possibly the same age) than females (Tuck et al. 2000, McCarthy et al. 2018). Maturity is not considered to be a part of the model partition, but the proportions of mature females in each length class were fitted within the model based on a logistic ogive with a binomial likelihood (Bull et al. 2008). Analysis of data collected during surveys on the proportion of mature females in each mm length bin was modelled as a function of length within a GLM framework, with a quasibinomial distribution of errors and a logit link (McCullagh & Nelder 1989),

$$P.mature = a + b * Length$$

which equates to the logistic model. The model was weighted by the number measured at each length. After obtaining estimates for the parameters a and b, the length at which 50% are mature (L_{50}) was calculated from:

$$L_{50} = -\frac{a}{b}$$

with selection range (SR) calculated from:

$$SR = \frac{(2.\ln(3))}{b}$$

Ovary stage at length data are presented in Figure 30. The L_{50} estimate for the SCI 6A data was 37.0 mm, with a selection range a_{25} to a_{75} of 5.8 mm.

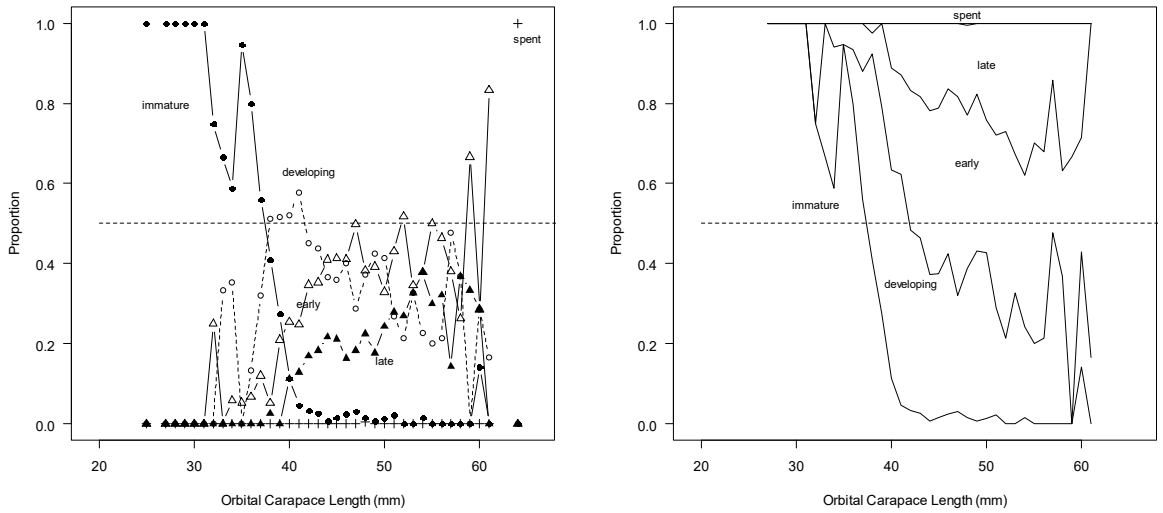

Figure 30: Proportions of female scampi at various developmental stages of internal ovaries. Left panel shows proportions of each stage separately, right panel shows combined proportions. Data are aggregated from research voyages in SCI 6A, all conducted in February/March.

3.2.3 Natural mortality

The instantaneous rate of natural mortality (*M*), has not been estimated directly for any scampi species, but estimates have been made (0.2–0.25) based on the estimate of the *K* parameter from a von Bertalanffy growth curve (Cryer & Stotter 1999) using a correlative method (Pauly 1980, Charnov et al. 1983). Morizur (1982) used length distributions from 'quasi-unexploited' *Nephrops* stocks to obtain estimates for annual *M* of 0.2–0.3. The values most commonly assumed for assessment of *Nephrops* stocks in the Atlantic is 0.3 for males and immature females, and 0.2 for mature females (assumed less vulnerable to predation during the ovigerous period) (Bell et al. 2006). For New Zealand scampi, *M* has previously been fixed at 0.2 (Tuck & Dunn 2012), or both 0.2 and 0.3 . Within the current assessment, preliminary models were explored where *M* was estimated, but the working group agreed that *M* should be fixed at 0.25 for the base model, with sensitivity to higher and lower fixed values (*M* = 0.2 and 0.3) examined.

3.3 Catch data

Data for the model were collated over the spatial and temporal strata as defined in the model structure (Tuck 2014). Catches in the modelled area represent over 90% of scampi catches from SCI 6A. Details of catches by fishing year and time step are provided in Table 6.

3.4 CPUE indices

The annual CPUE indices estimated within the standardisation (Tuck & Dunn 2009) were fitted within the model as abundance indices. There has been considerable discussion on whether CPUE is proportional to abundance for scampi (Tuck 2009), with rapid increases in both CPUE and trawl survey catch rates for a number of stocks in the early to mid 1990s (and changes in sex ratio in trawl survey catches) initially being considered related to changes in catchability. Later analysis suggested that the observed changes in sex ratio were related to slight changes in the survey timing in relation to the moult cycle. Similar increases in CPUE have been observed over the same period for rock lobster (Starr 2009, Starr et al. 2009) and scampi in SCI 3 (Tuck 2013), which may suggest broad scale environmental drivers influencing crustacean recruitment. The CPUE patterns for SCI 1 are mirrored by trawl survey catch rates, suggesting that they do not reflect fisher learning. Although not considered appropriate for use as an index in the assessment model (Tuck 2013), a scampi abundance index generated from the

middle depths (R.V. *Tangaroa*) trawl survey shows a very similar temporal pattern to the standardised CPUE indices for SCI 3, also supporting the suggestion that the increases in scampi catch rate observed during the 1990s reflect changes in scampi abundance, rather than fisher learning.

Table 6: Catch (t) breakdown by model year and time step for SCI 6A.

Model year	Step 1	Step 2	Step 3
1988	0.00	0.00	0.00
1989	0.00	0.00	0.00
1990	0.00	0.00	0.00
1991	0.89	0.00	0.00
1992	218.53	97.94	1.26
1993	118.34	59.23	30.39
1994	203.81	1.15	39.81
1995	162.77	39.76	66.33
1996	169.82	24.47	34.20
1997	130.28	47.63	69.53
1998	193.04	102.42	31.45
1999	168.70	70.63	89.18
2000	151.17	71.92	86.81
2001	82.84	108.49	86.50
2002	182.22	5.40	20.94
2003	126.45	6.65	74.57
2004	132.46	18.61	110.40
2005	200.57	80.40	128.80
2006	53.22	79.61	112.98
2007	87.80	47.11	166.83
2008	44.15	36.96	162.31
2009	85.05	98.65	93.80
2010	60.53	50.85	44.05
2011	25.86	75.91	88.27
2012	21.73	43.48	96.78
2013	9.63	45.58	80.85
2014	23.76	47.64	27.85
2015	14.80	28.23	54.17
2016	45.90	84.20	117.22
2017	24.78	78.84	176.29
2018	28.44	82.14	173.33
2019	31.67	45.41	165.21

The standardised CPUE index for SCI 6A was fitted using the approach of Clark & Hare (2006), as recommended by Francis (2011). This approach fits lowess smoothers with different degrees of smoothing (Figure 31) and uses the residuals from each fit to estimate the CV. From visual examination of the fits, the working group determined that a CV of 0.15 was appropriate for the CPUE, although sensitivity to narrower and wider CVs was also examined in preliminary model runs.

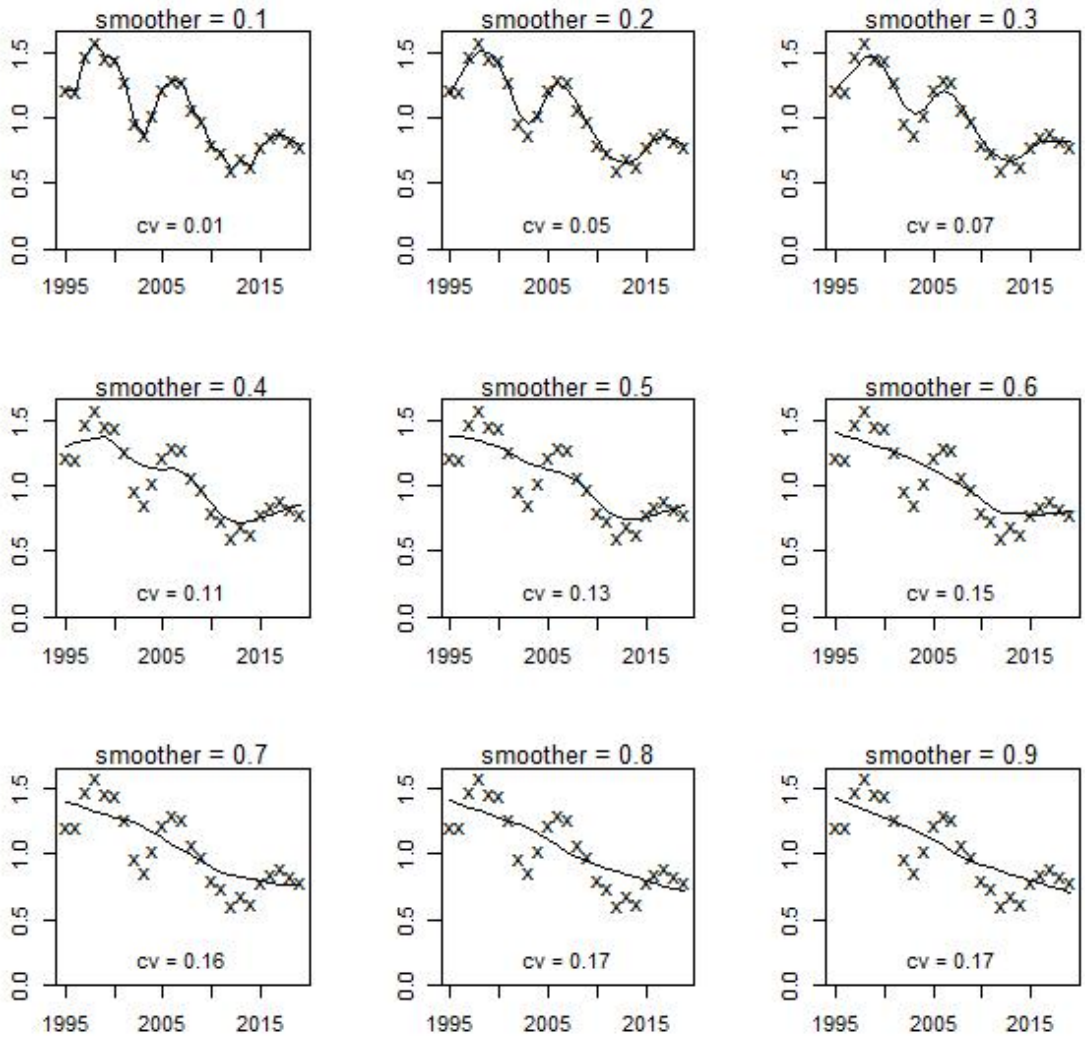

Figure 31: Fits of lowess smoothers to the standardised CPUE index.

3.5 Research survey indices

Trawl surveys were conducted annually in SCI 6A from the F.V. *San Tongariro*, between 2007 and 2009, with a fourth survey in 2013. The F.V. *San Tongariro* left the scampi fishery after 2013 and became unavailable for the survey after this. In 2016 and 2019 the survey was conducted from the R.V. *Kaharoa* using the standard trawl gear used on previous scampi surveys in SCI 1, SCI 2, and SCI 3. Details of the F.V. *San Tongariro* and R.V. *Kaharoa* scampi survey trawl gears are presented in Appendix 3. Each of these surveys was conducted (in conjunction with a photographic survey) between February and April.

3.5.1 Photographic surveys

Photographic surveys of SCI 6A were conducted in 2007–09, 2013, 2016, and 2019 (Tuck et al. 2007, Tuck et al. 2009a, Tuck et al. 2009b, Tuck et al. 2015a, Tuck et al. 2017, Tuck et al. 2020). These surveys provide three indices of scampi abundance, one based on major burrow openings, and two based on scampi; an index of all visible scampi and an index of scampi fully emerged from their burrows. Each index is subject to uncertainty, either from burrow detection and occupancy rates (for burrow based indices) or emergence patterns (for visible scampi based indices). The burrow index has been used to date within assessments for SCI 1, SCI 2, and SCI 3 (Tuck & Dunn 2012, Tuck 2013), but scampi in SCI 6A appear to spend less time in burrows, with animals frequently observed associated with 'trench features' (possibly collapsed burrows) (Tuck et al. 2007), and the total visible scampi index has also been used (Tuck & Dunn 2012). Recent sediment sample analyses (Tuck et al. in press) have

shown that the SCI 6A sediments contain more sand and less clay than other main scampi areas, and this may influence burrow cohesiveness. Survey estimates are provided in Table 7. Details of the estimation of the catchability priors are provided in Section 3.7.

Table 7: Time series of photographic survey indices (abundance in millions) and CV for SCI 6A.

	Major burrows		Visible scampi		Emerged scampi	
Survey	Abundance	CV	Abundance	CV	Abundance	CV
2007	366.71	0.08	60.45	0.14	40.34	0.12
2008	126.76	0.08	53.42	0.08	34.73	0.11
2009	287.61	0.10	36.59	0.14	23.35	0.18
2013	124.00	0.09	32.83	0.16	18.44	0.21
2016	167.20	0.12	48.72	0.14	27.70	0.14
2019	249.39	0.10	76.28	0.12	37.94	0.16

3.5.2 Trawl surveys

Stratified random trawl surveys of scampi in SCI 6A, 350–550 m depth, were conducted in conjunction with photographic surveys described above. The 2007–2013 surveys were conducted by the same vessel (*San Tongariro*), using the same trawl, but a gear loss just before the 2009 survey meant that slightly different trawl doors were used for that survey. Attempts have been made to scale catch rates appropriately for swept width to account for this (Tuck et al. 2009a), but concerns remain that catchability was different from other *San Tongariro* surveys, and the working group agreed the 2009 estimate should be excluded from the trawl survey time series within the assessment model. The working group also suggested that the trawl survey index be fitted as abundance rather than biomass, and this was also adopted.

The 2016 and 2019 surveys used a different vessel (*Kaharoa*), which appears to have a different catchability (Tuck et al. 2017). Comparison of photographic survey (which is expected to be independent of vessel) and trawl survey abundance estimates were used to provide estimates of the relative catchability of the *San Tongariro* and *Kaharoa* scampi trawl gear (Figure 32); this suggested that the *San Tongariro* caught over twice as much scampi as the *Kaharoa*. Survey biomass estimates are provided in Table 8. This relative catchability was explored as a potential q-ratio prior for the *San Tongariro* and *Kaharoa* surveys.

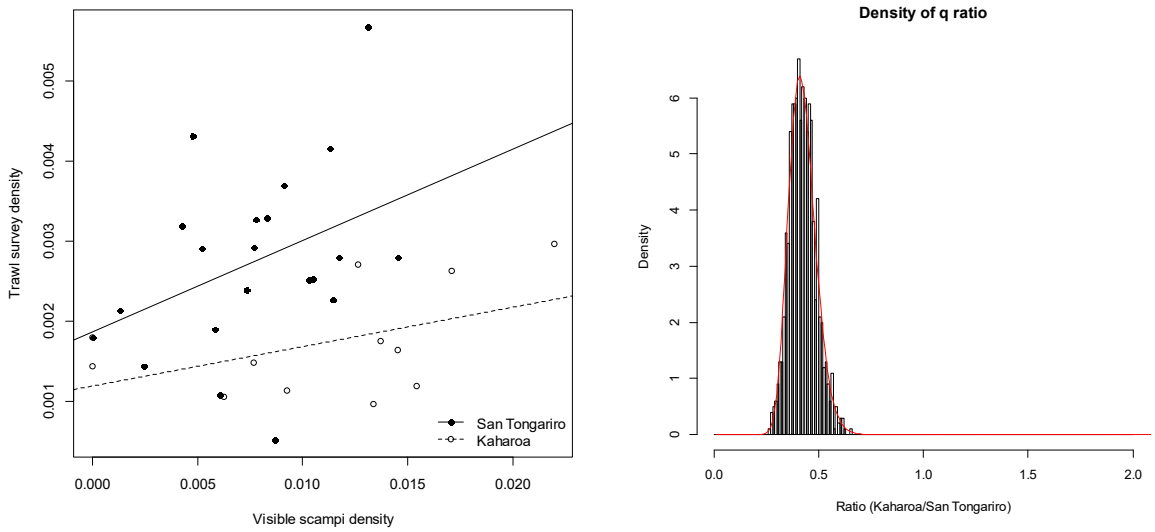

Figure 32: Plot of stratum level trawl survey scampi densities against photo survey scampi densities by vessel (left plot), and the distribution of the q-ratio (ratio between *q* values estimated for the two vessels for potential use as a prior). The red line represents the estimated log-normal distribution for the q-ratio prior, with mean of 0.42, and CV of 0.15.

Table 8: Time series of trawl survey scampi biomass (tonnes) and abundance (millions) and CV for SCI 6A.

Survey	Vessel	Biomass	CV	Abundance	CV
2007	*San Tongariro*	1 073.5	0.18	14.4	0.19
2008	*San Tongariro*	1 229.2	0.18	16.9	0.19
2009	*San Tongariro*	821.6	0.09	9.9	0.09
2013	*San Tongariro*	1 258.0	0.09	14.1	0.04
2016	*Kaharoa*	593.8	0.09	8.2	0.11
2019	*Kaharoa*	710.9	0.12	10.4	0.13

3.6 Length distributions

3.6.1 Commercial catch length distributions

Government Scientific Observers have collected scampi length frequency data from scampi targeted fishing on commercial vessels in SCI 6A since 1991–92. The numbers of tows for which length data are available are presented by model year, time step, and depth band in Table 9.

Detailed examination of the length distribution data identified some anomalous data that were excluded from further analyses. The median size of scampi in SCI 6A has generally varied between 44 mm and 55 mm, but a trip (10242) where the median size was 39 mm was removed, because the data suggest that the observer was not following measurement protocols correctly. Data from another trip (14096) where scampi were measured to the nearest whole centimetre (rather than millimetre) were also excluded.

Examination of the commercial catch length distributions as part of the previous characterisation of this fishery (Tuck 2015) identified depth related spatial structure in the length composition data (larger scampi in shallower water). Patterns in the sex ratio and mean size from the scampi observer length frequency data were examined using multivariate tree regression (using the R package *mvpart*). Data were analysed for each year separately at the observed tow level, with response variables regressed on the explanatory variables half_month and depth_bin. Pruning was conducted to determine the tree with the smallest cross-validated relative error. Depth splits were identified in over half of the years, with 450 m identified most frequently. The temporal splits identified were consistent with those already proposed for the model structure (Table 3).

On the basis of both the mean size and sex ratio (proportion males) within catches, it was considered appropriate to stratify the observer length data by depth, with separate strata for 350–450 m and 450–550 m (combined).

On the basis of the observer sampling within the two depth bands (350–450 m and 450–550 m) and the three time steps within each fishing year (Table 9), the proportion of scampi catch represented by the observer sampling (having at least one observer sample from that depth in that time step) has been examined (Table 10). This ranged from 20% (1998, time step 3) to 100%, with 40 of the 48 observed year_step combinations having over 90% of the catches represented by sampling. The working group agreed that 90% representation was an appropriate cut-off for inclusion in the assessment model, with the other data being excluded. For all the year_step combinations, proportional length distributions (and associated CVs) were calculated using CALA (Francis et al. 2016), using the approaches previously implemented by NIWA's *Catch-at-Age* software (Bull & Dunn 2002). Plots of the proportional length distribution are shown by year and time step in Figures 33–35.

Table 9: Numbers of scampi observer length frequency samples from SCI 6A, by model year, time step, and combined depth band.

	Step			Step 1		Step 2		Step 3	
Model year	1	2	3	350–450	450–550	350–450	450–550	350–450	450–550
1992	77	0	0	76	1	0	0	0	0
1993	53+	0	10	36	17	0	0	6	4
1994	91	0	35	37	54	0	0	7	28
1995	20	0	0	5	15	0	0	0	0
1996	32	0	18	13	19	0	0	0	18
1997	24	25	58	5	19	0	25	1	57
1998	87	6	1	65	22	0	6	1	0
1999	0	0	21	0	0	0	0	2	19
2000	24	0	0	1	23	0	0	0	0
2001	0	36	10	0	0	0	36	0	10
2002	15	0	54	0	15	0	0	38	16
2003	40	0	57	10	30	0	0	26	31
2004	7	0	0	1	6	0	0	0	0
2005	0	0	22*	0	0	0	0	2	20*
2006	19*	0	0	1*	18*	0	0	0	0
2007	34	0	12	29	5	0	0	0	12
2008	14	12	23	2	12	8	4	6	17
2009	16	0	0	2	14	0	0	0	0
2010	0	30	0	0	0	4	26	0	0
2011	42	28	59	15	27	18	10	1	58
2012	0	31	0	0	0	20	11	0	0
2013	0	89	0	0	0	8	81	0	0
2014	0	56	0	0	0	25	31	0	0
2016	0	16	84	0	0	1	15	5	79
2017	28	141	42	26	2	23	118	22	20
2018	0	84	24	0	0	11	73	3	21
2019	8	137	83	8	0	26	111	2	81

+ 35 tows in 1993_1 (observer trip 14096) measured scampi to the centimetre, rather than millimetre, and these have been excluded from further analysis.

* Exclusion of observer trip 10242 removes 8 samples from time step 3 in 2005 (all from the 450–550 m depth range, and all 17 samples from time step 1 in 2006.

Table 10: Estimated scampi catch (tonnes) in the modelled area by model year and time step, and the percentage of catch represented by the observer sampling.

	Estimated catch			% represented by sampling		
Model year	Step 1	Step 2	Step 3	Step 1	Step 2	Step 3
1991	0.89	0.00	0.00			
1992	218.53	97.94	1.26	100.00		
1993	118.34	59.23	30.39	100.00		100.00
1994	203.81	1.15	39.81	100.00		100.00
1995	162.77	39.76	66.33	100.00		
1996	169.82	24.47	34.20	100.00		88.61
1997	130.28	47.63	69.53	100.00	70.58	100.00
1998	193.04	102.42	31.45	100.00	61.98	20.93
1999	168.70	70.63	89.18			100.00
2000	151.17	71.92	86.81	100.00		
2001	82.84	108.49	86.50		83.63	91.94
2002	182.22	5.40	20.94	81.28		100.00
2003	126.45	6.65	74.57	100.00		100.00
2004	132.46	18.61	110.40	100.00		
2005	200.57	80.40	128.80			100.00*
2006	53.22	79.61	112.98	100.00*		
2007	87.80	47.11	166.83	100.00		70.41
2008	44.15	36.96	162.31	100.00	100.00	100.00
2009	85.05	98.65	93.80	100.00		
2010	60.53	50.85	44.05		100.00	
2011	25.86	75.91	88.27	100.00	100.00	100.00
2012	21.73	43.48	96.78		100.00	
2013	9.63	45.58	80.85		100.00	
2014	23.76	47.64	27.85		100.00	
2015	14.80	28.23	54.17			
2016	45.90	84.20	117.22		100.00	100.00
2017	24.78	78.84	176.29	100.00	100.00	100.00
2018	28.44	82.14	173.33		100.00	100.00
2019	31.67	45.41	165.21	64.42	100.00	100.00

* Exclusion of observer trip 10242 does not affect sample coverage for time step 3 in 2005 (because another trip also provides coverage) but removes all samples from time step 1 in 2006.

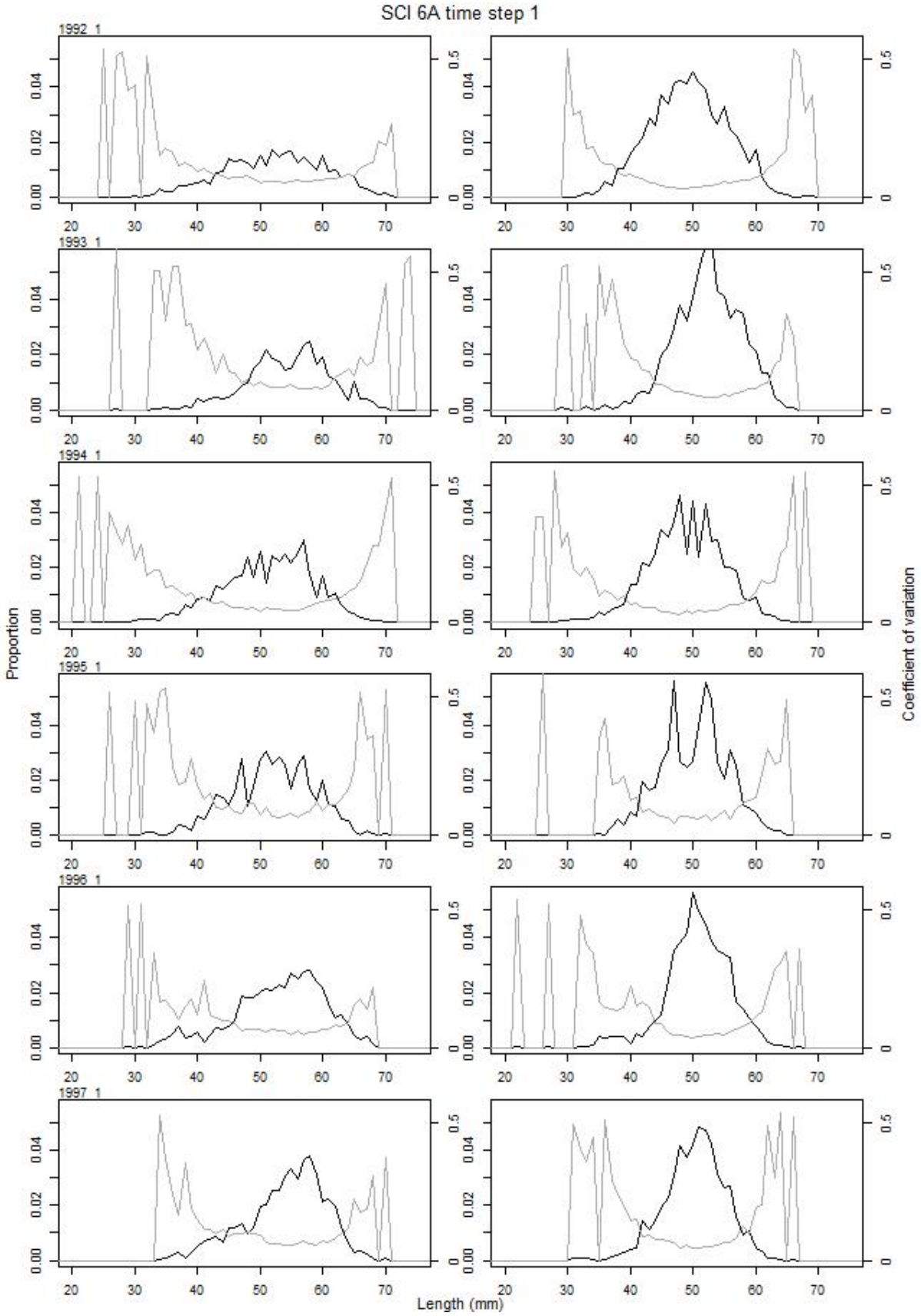

Figure 33: Proportional length frequency distributions (black line) and CVs (grey line) for commercial catches by model year and time step 1 for SCI 6A. Males plotted on left, females on right.

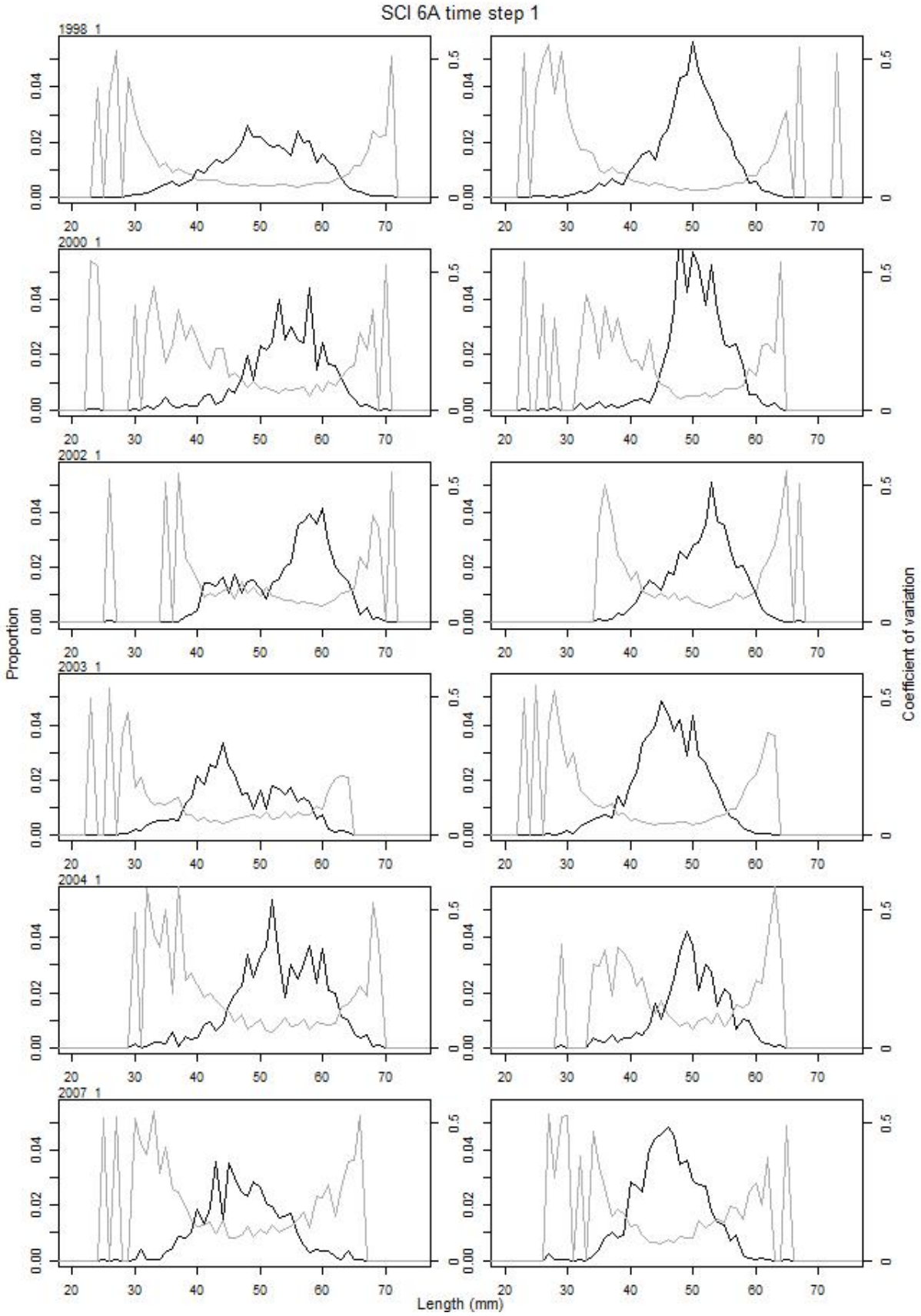

Figure 33 (continued): Proportional length frequency distributions (black line) and CVs (grey line) for commercial catches by model year and time step 1 for SCI 6A. Males plotted on left, females on right.

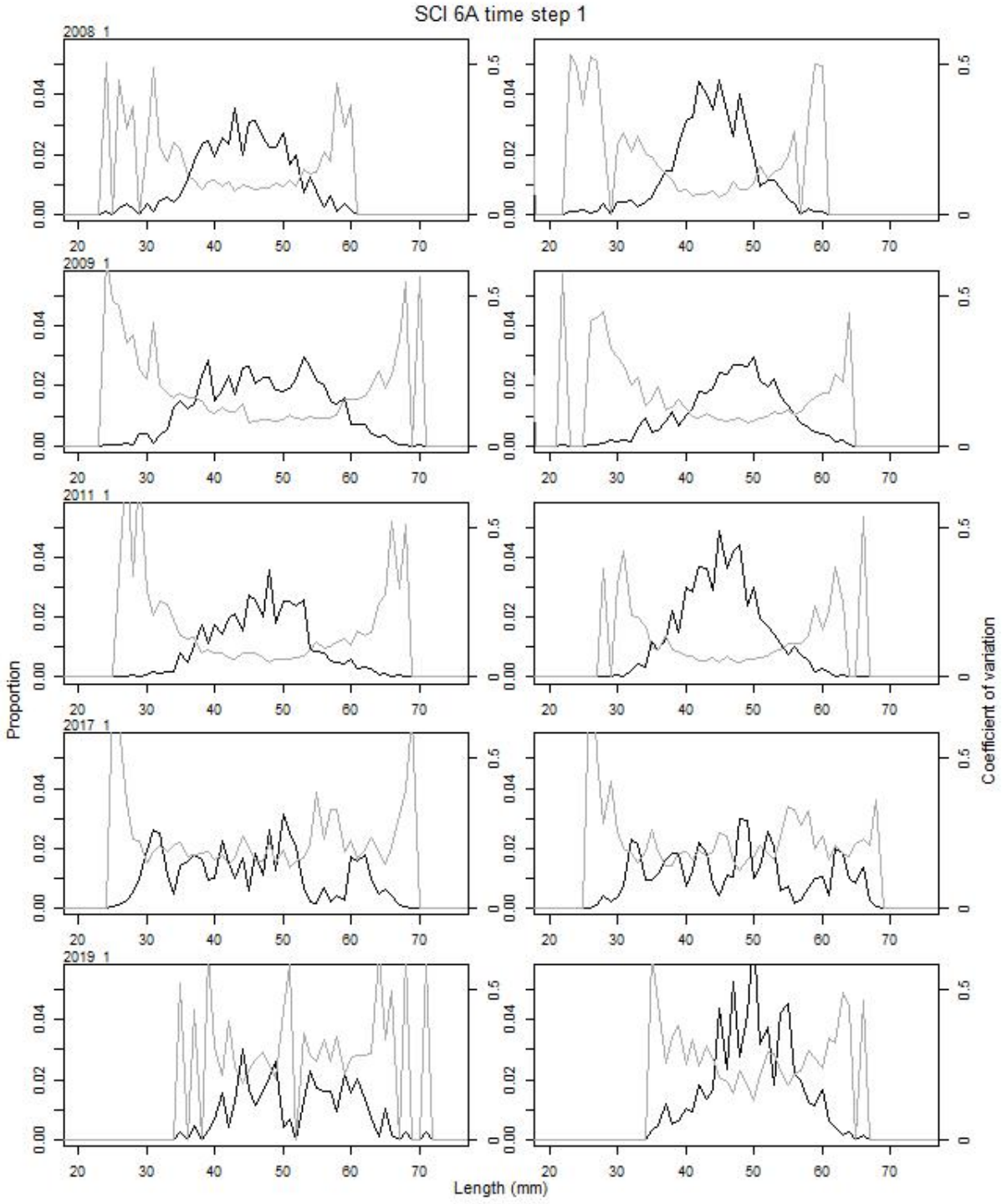

Figure 33 (continued): Proportional length frequency distributions (black line) and CVs (grey line) for commercial catches by model year and time step 1 for SCI 6A. Males plotted on left, females on right.

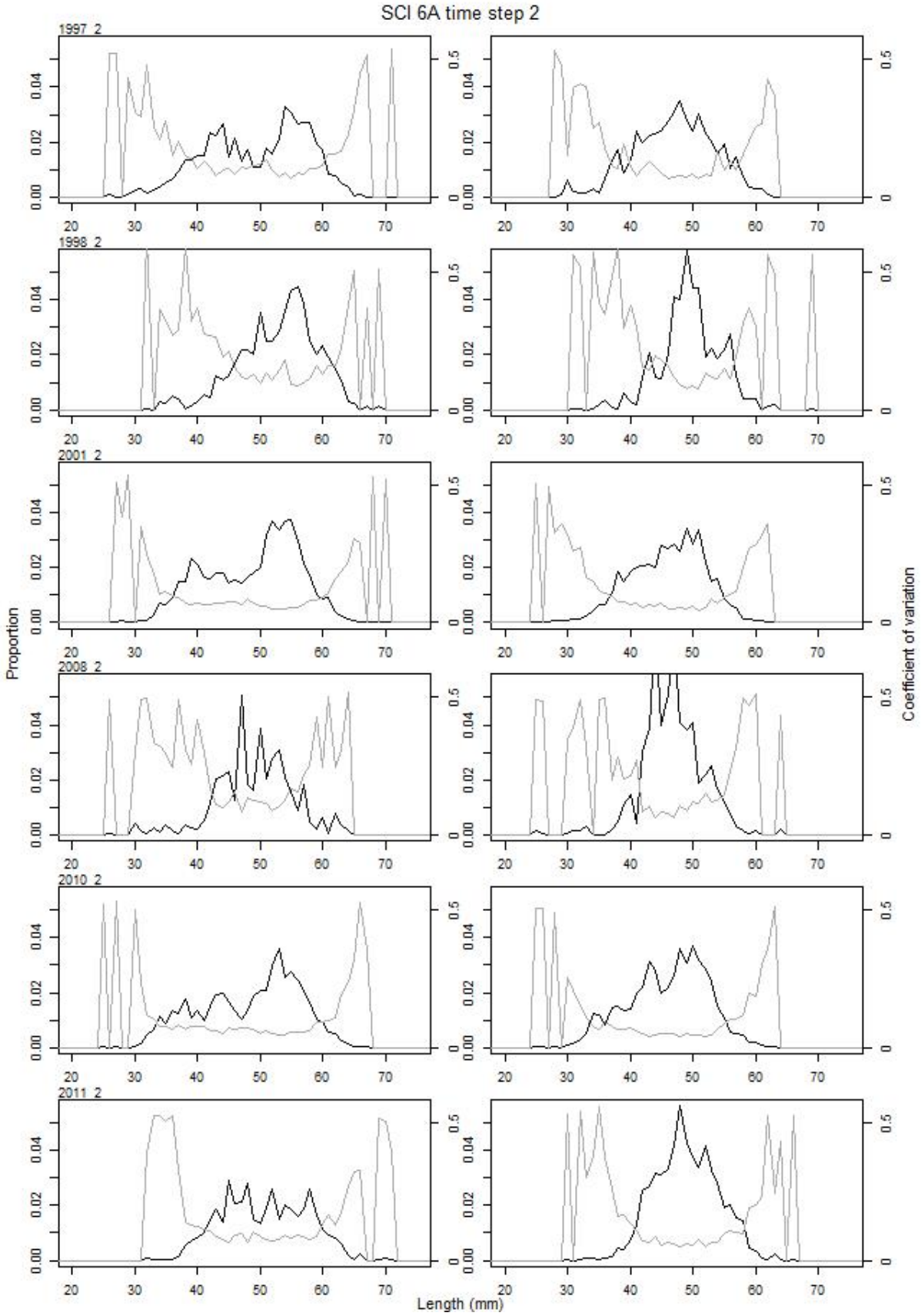

Figure 34: Proportional length frequency distributions (black line) and CVs (grey line) for commercial catches by model year and time step 2 for SCI 6A. Males plotted on left, females on right.

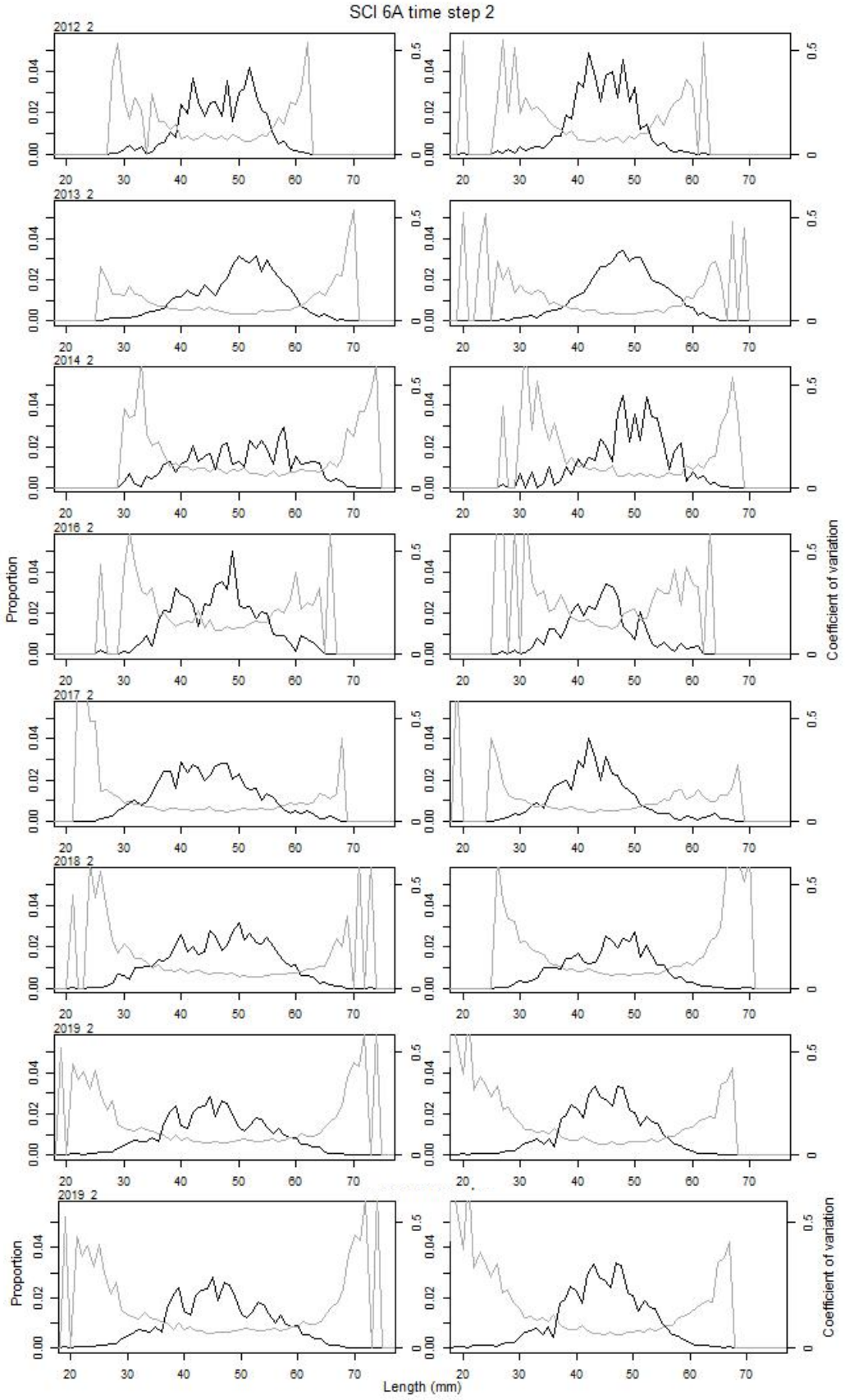

Figure 34 (continued): Proportional length frequency distributions (black line) and CVs (grey line) for commercial catches by model year and time step 2 for SCI 6A. Males plotted on left, females on right.

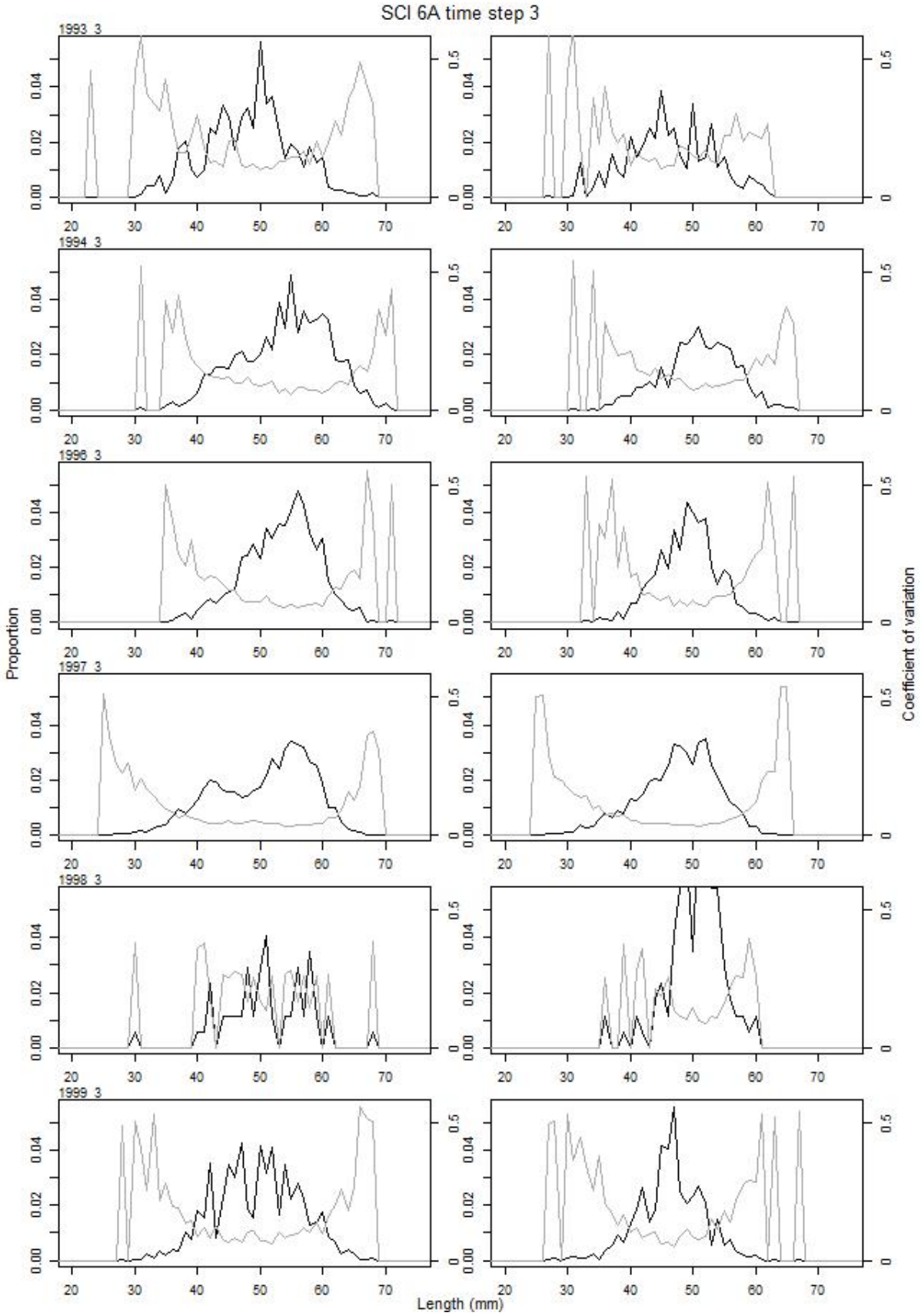

Figure 35: Proportional length frequency distributions (black line) and CVs (grey line) for commercial catches by model year and time step 3 for SCI 6A. Males plotted on left, females on right.

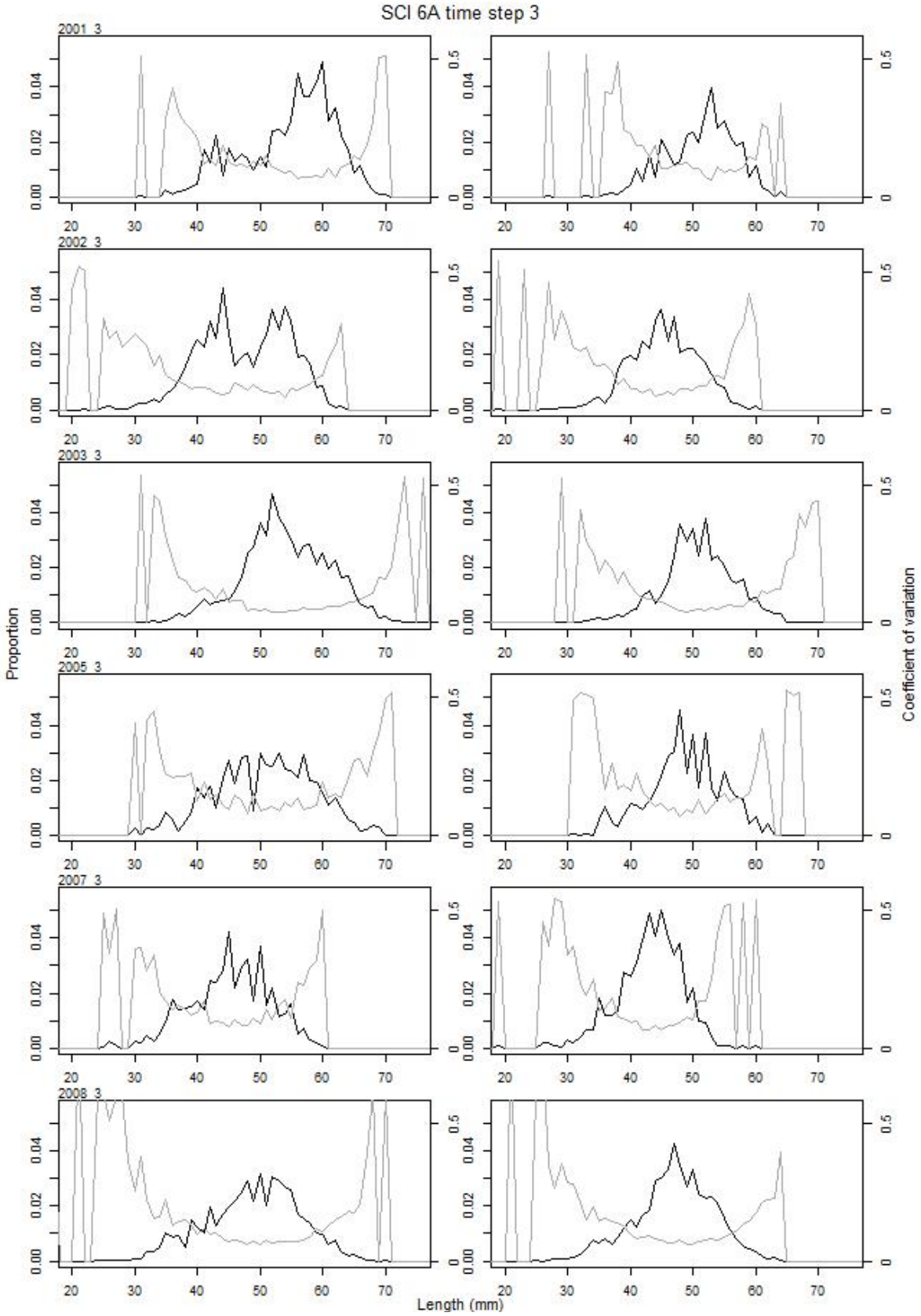

Figure 35 (continued): Proportional length frequency distributions (black line) and CVs (grey line) for commercial catches by model year and time step 3 for SCI 6A. Males plotted on left, females on right.

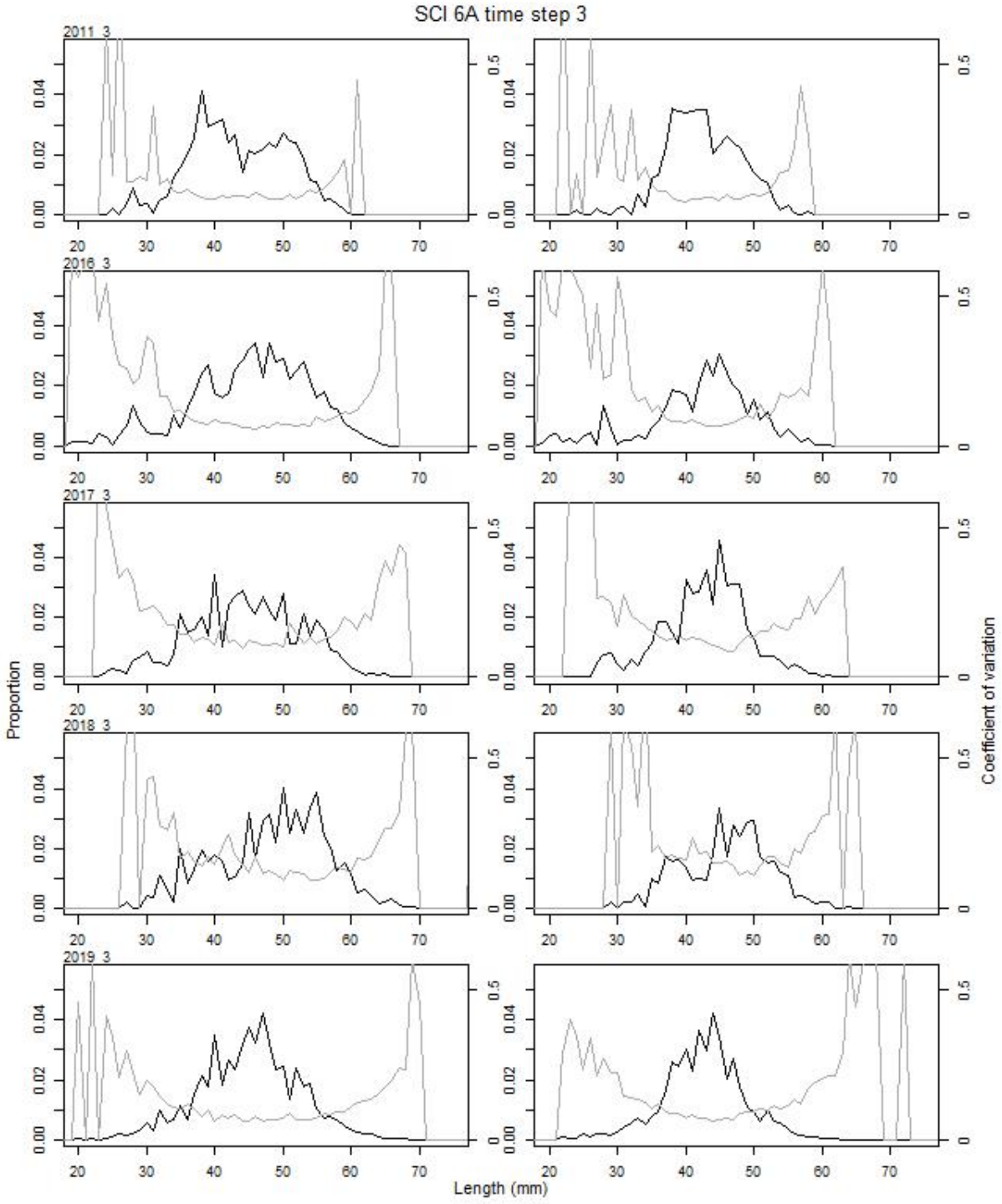

Figure 35 (continued): Proportional length frequency distributions (black line) and CVs (grey line) for commercial catches by model year and time step 3 for SCI 6A. Males plotted on left, females on right.

3.6.2 Trawl survey length distributions

Length frequency samples from research trawling were taken by scientific staff on all surveys (Table 8). Estimated length frequency distributions (with associated CVs) were derived using NIWA's CALA software (Francis et al. 2016), using 1-mm OCL (Orbital Carapace Length) length classes by sex, and are presented in Figure 36.

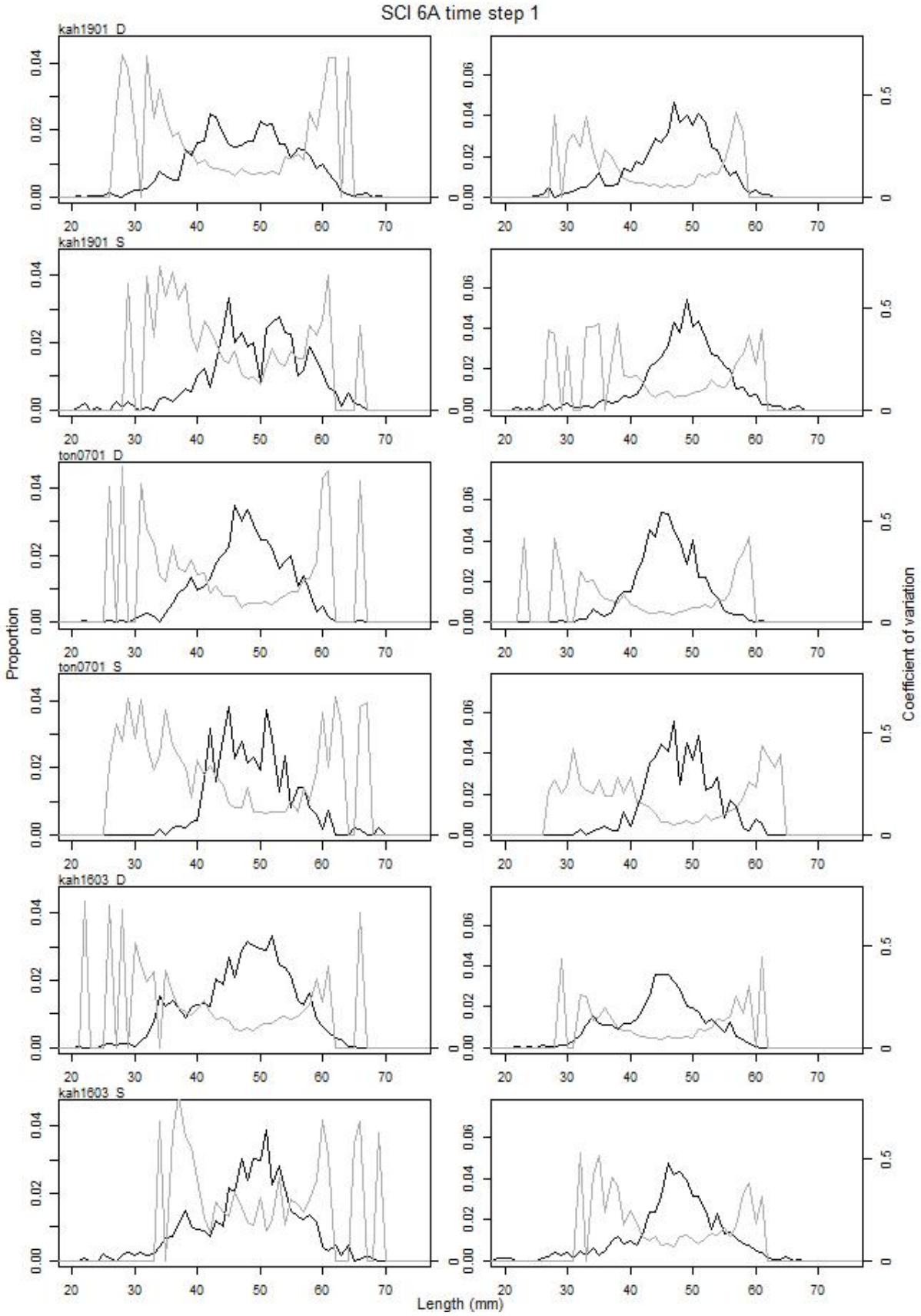

Figure 36: Proportional length frequency distributions (black line) and CVs (grey line) for research survey catches by model year for SCI 6A. Males plotted on left, females on right.

In preliminary model runs during the 2016 assessment (Tuck 2017), separate selectivity curves were estimated for commercial fishing in the three time steps, and the *San Tongariro* trawl survey (which occurred in time step 1 only). This led to L_{50} estimates that were considered to vary unrealistically between time steps. During the *San Tongariro* surveys, a commercial twin rig trawl was used with a research (42 mm) codend used on one net (providing the survey catches) and a commercial (80 mm) codend used on the other net (assumed to represent usual commercial selectivity). The length frequency distributions of survey and commercial net catches (examples provided in Figure 37) are considered to be similar enough to share selectivity parameters between the *San Tongariro* trawl survey and observer time step 1 data.

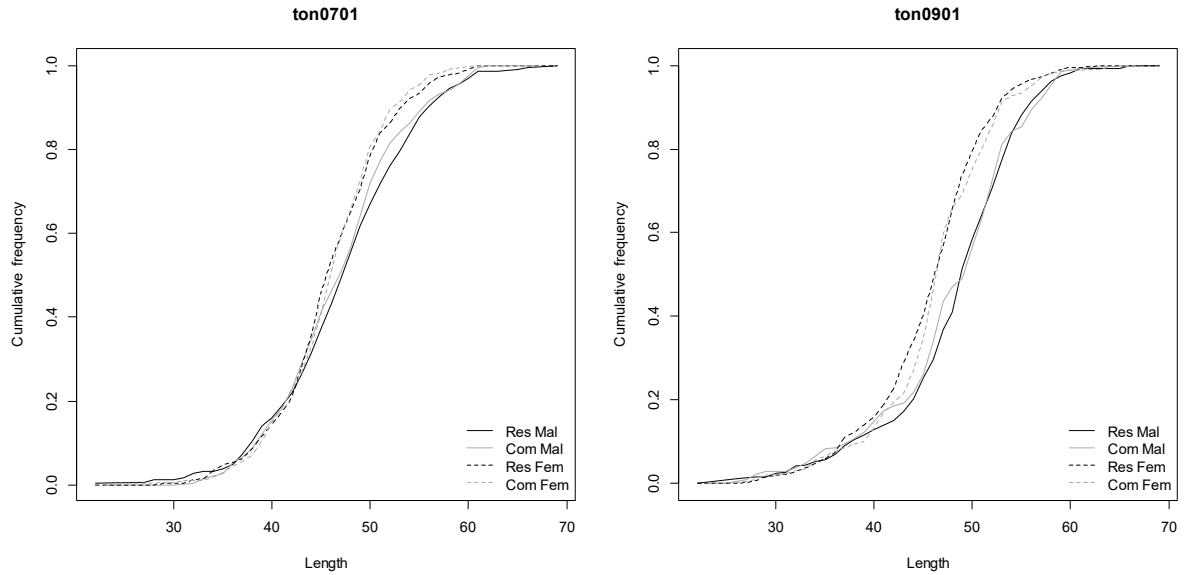

Figure 37: Cumulative frequency distributions of scampi length data (mm) for research survey and commercial nets from *San Tongariro* surveys by sex for time step 1.

3.6.3 Photographic survey length distributions

Length frequency distributions were estimated for the relative photographic abundance series, by measuring the abdomen width of those visible animals and converting abdomen width to orbital carapace length. Abdomen width is a measure considered to be less affected by foreshortening, when scampi are not orientated perpendicular to the plane of the camera, which is typically the case when they are viewed from above.

As with other scampi species (Tuck et al. 2000), the relationship between abdomen width and carapace length changes for *Metanephrops* females at maturity, with a wider abdomen providing more space to carry eggs on the pleopods (Figure 38).

It is not possible to confidently determine scampi sex from the survey photographs, but the pattern in sex ratio in relation to length appears quite consistent between surveys (Figure 39). Using the data from the trawl surveys on the proportion by sex at length, and the relationship between carapace length and abdomen width for males (and immature females), maturing females, and mature females (Figure 40), the proportion of males by abdomen width increment can be estimated (Figure 41).

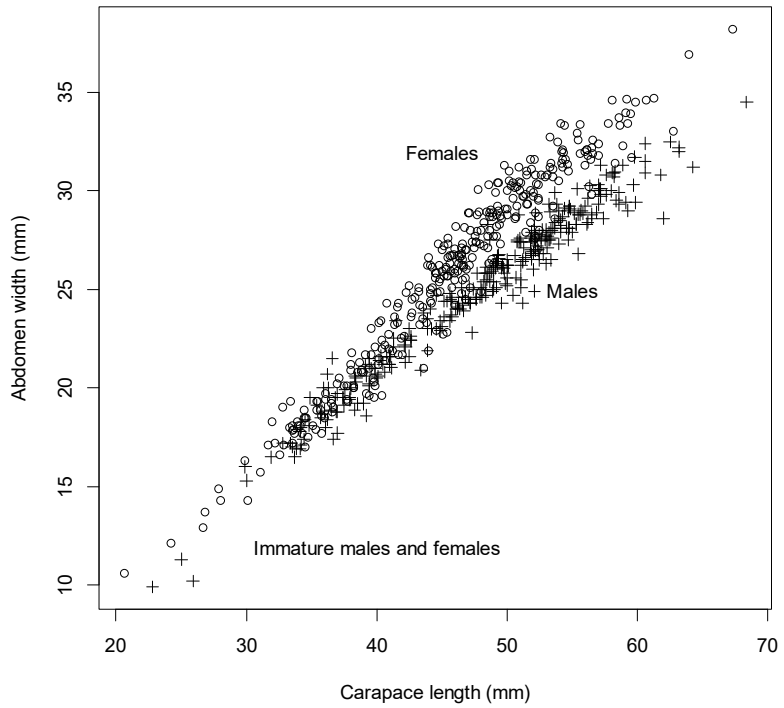

Figure 38: Relationship between abdomen width and carapace length for scampi in SCI 6A.

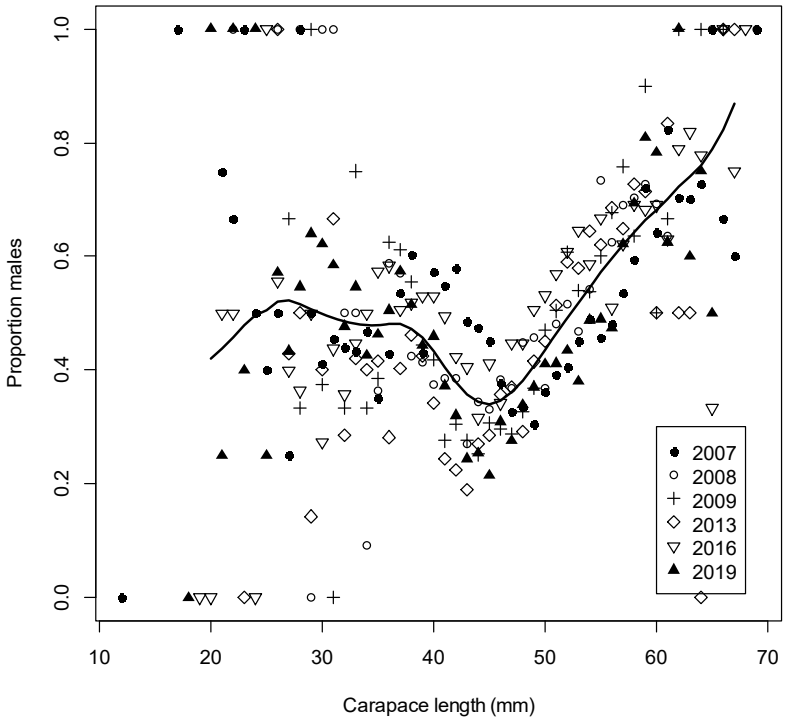

Figure 39: Plot of proportion of males in trawl survey catches against carapace length for each of the SCI 6A surveys, with an overall (lowess) smoother fitted through the data.

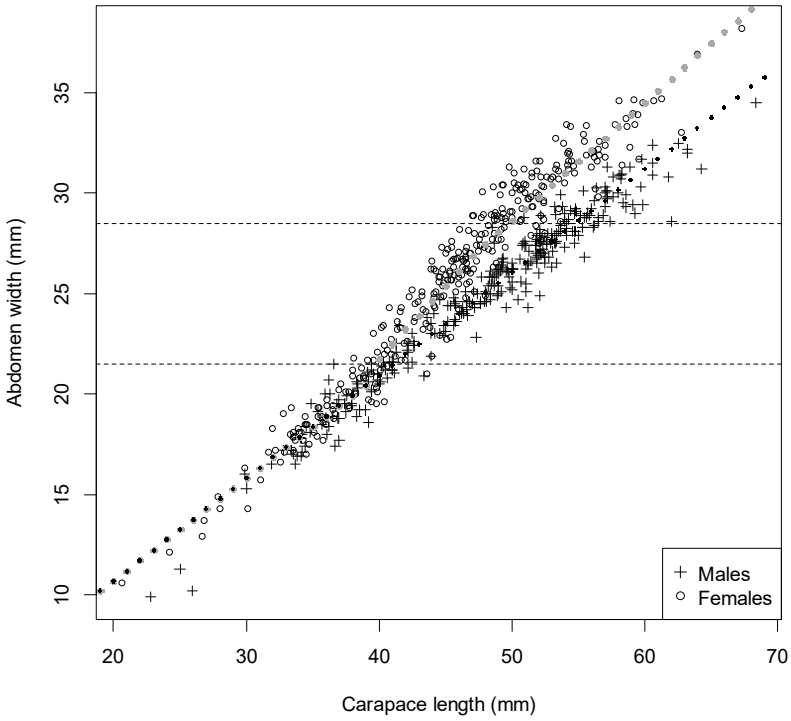

Figure 40: Relationship between abdomen width and carapace length for scampi in SCI 6A, with regression fits shown for different population components. Solid black symbols represent male regression estimates. Solid grey symbols represent female regression estimates, with horizontal dashed lines representing transition range between immature and mature female regression estimates.

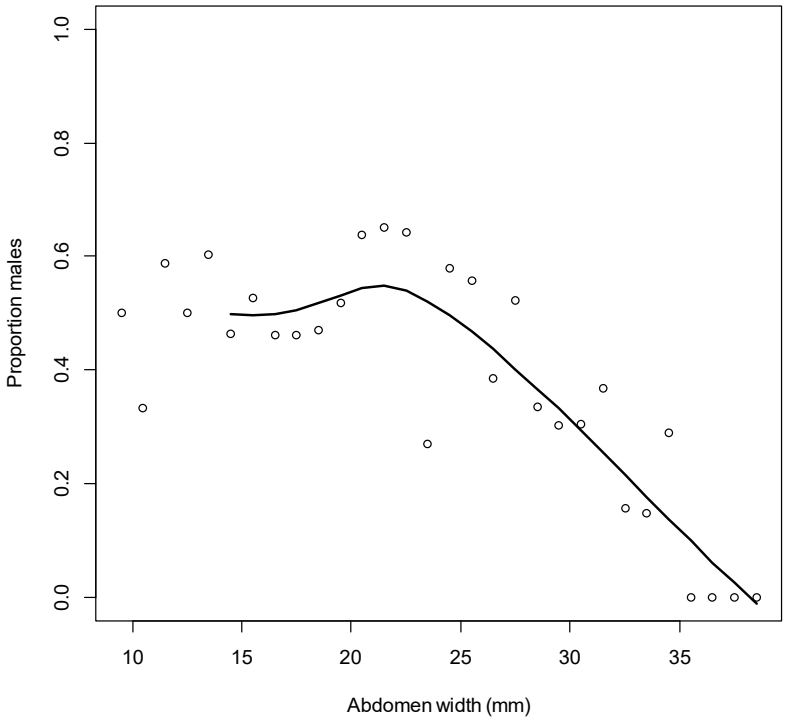

Figure 41: Overall plot of proportion of males in trawl survey catches against abdomen width for SCI 6A surveys, with an overall (lowess) smoother fitted through the data.

Each abdomen width measurement from each photographic survey was assigned a sex (on the basis of the probability observed in the trawl survey data shown in Figure 41), and then converted to a carapace length using the sex and abdomen width appropriate, abdomen width ~ carapace length relationship

(Figure 40). To estimate the CVs at length for each year, we used a bootstrapping procedure, resampling with replacement from the original observations. Compared with the length frequency distributions from trawl catches, this procedure gave very large CVs, but we think this is realistic given the uncertainties involved in generating a length frequency distribution from photographs and converting from abdomen width to carapace length. Estimates of the length frequency distributions (with associated CVs) for visible scampi are presented in Figure 42.

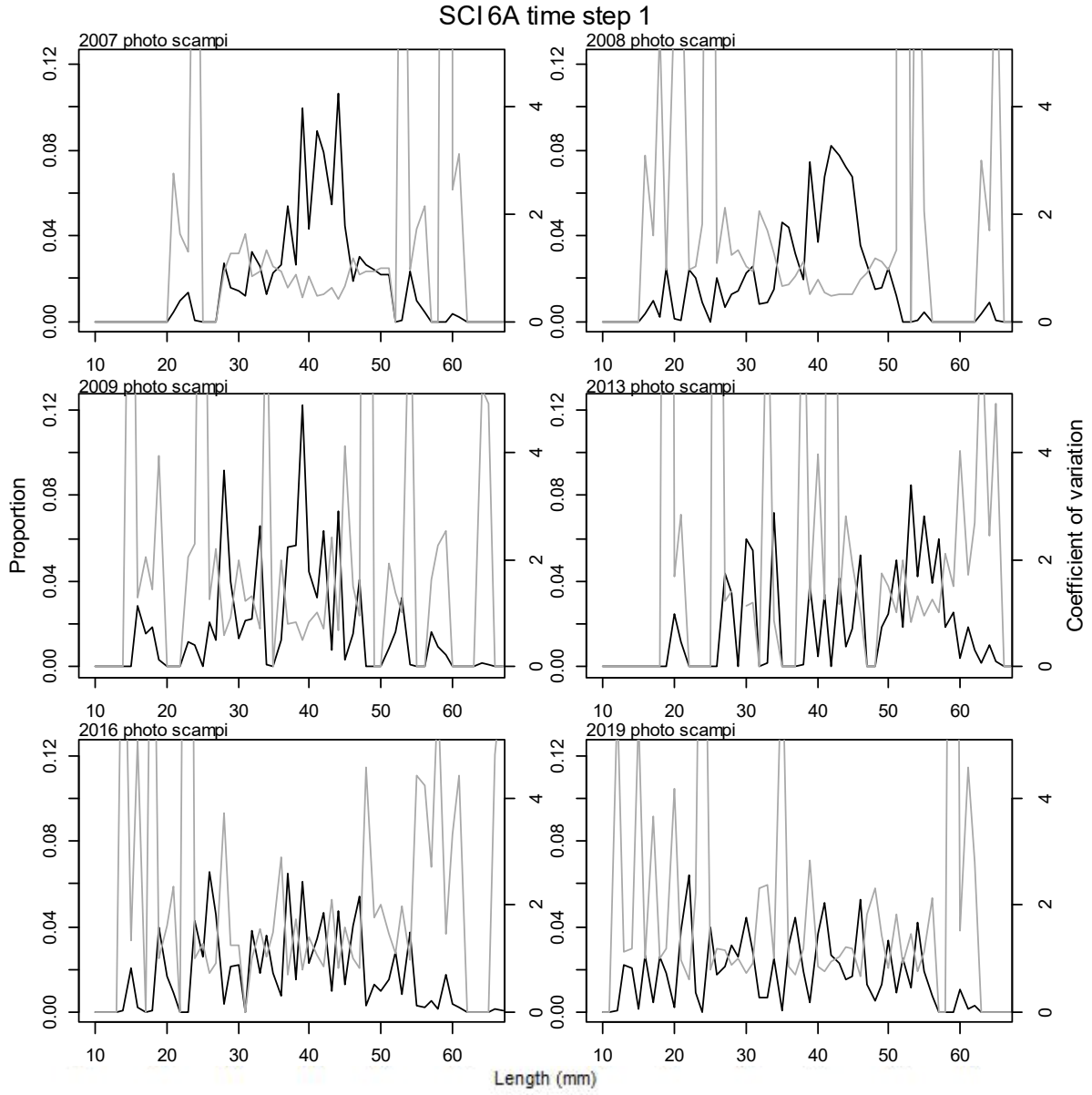

Figure 42: Proportional length frequency distributions (black line) and CVs (grey line) for photo survey observations of visible scampi by model year for SCI 6A.

3.7 Model assumptions and priors

Maximum Posterior Density (MPD) fits were found within CASAL using a quasi-Newton optimiser and the BETADIFF automatic differentiation package (Bull et al. 2012). Fitting was done inside the model except for the weighting of the CPUE indices and length frequency data. For the length frequency data, observation-error CVs were estimated using CALA, converted to equivalent observation-error multinomial *N*s, and used within the model. The appropriate multinomial *N*s to account for both

observation and process error were then calculated from the model residuals (method TA1.8 of (Francis 2011), and these final *N*s were used in all models reported. Generally, this process resulted in small *N*s for the commercial length frequency data in particular and were therefore given relatively low weighting within the model. For the CPUE indices, the approach proposed by Francis (2011) was initially investigated (estimating appropriate CVs by fitting a smoother to the index – see Figure 31), although sensitivities to this were examined, and in the final models CVs were fixed at the lower range of the sensitivities examined, with additional process error estimated within the model. CASAL was also used to run Markov chain Monte Carlo (MCMC) on the base and final sensitivity models. MPD output was analysed using the extract and plot utilities in the CASAL library running under the general analytical package R.

For all final models documented in this report, three independent MCMC chains were started a random step away from the MPD for each model and run for 2 million simulations, with every one thousandth sample saved, giving a set of 2000 samples. The three chains were examined for evidence of lack of convergence (trace plots provided in relevant appendices) and concatenated and systematically thinned to produce a 2000 sample chain. Posterior distributions of trawl and photo survey catchability were examined in relation to the prior distribution, and posterior trajectories of spawning stock biomass (*SSB*), stock status, and year class strength (YCS) provided.

The initial model was based on that described by Tuck (2017). The model inputs include catch data, abundance indices (CPUE, trawl and photo surveys) and associated length frequency distributions. The parameters estimated by the model include SSB_0 and R_0, a time series of SSBs and year class strengths, selectivity parameters for commercial and research trawling, and the photo survey, and associated catchability coefficients. Catchability coefficients (*q*s) for commercial fishing, research trawling, and photographic surveys were estimated as nuisance parameters. The only informative priors used in the initial model were for *q-Photo, q-Trawl*, the ratio of *q* values for the different trawl survey vessels (in some initial models), and the YCS vector (to constrain recruitment variability).

3.7.1 Scampi catchability

Previous priors for scampi catchability have been largely based on information on *Nephrops* emergence and occupancy rates from European studies conducted in shallower waters than *Metanephrops* populations inhabit (Tuck & Dunn 2012), but the acoustic tagging pilot study conducted at the Mernoo Bank in October 2010 offered an opportunity to estimate priors for occupancy and emergence from New Zealand data (Tuck et al. 2011, Tuck 2013). Acoustic tagging experiments were repeated successfully during the SCI 1 and SCI 2 surveys in 2012 (Tuck et al. 2013) and were also conducted within the SCI 6A and SCI 3 surveys in 2013 (although less successfully). The data collected within these studies have been used to estimate catchability priors (Tuck et al. 2015b).

Acoustic tags were fitted to scampi which were released with a moored hydrophone to record tag detections, and hence when animals were emerged from burrows. The tag detection hydrophones were deployed over a period of up to 21 days (Tuck et al. 2015a). Some tag detections showed distinct cyclical patterns (12.6 hour cycles), but most animals showed no clear behavioural pattern, and the proportion of scampi that were detectable during the daytime over the duration of the studies varied from 41 to 51% (95% confidence intervals), with a median detection rate of 46%.

In previous analyses, the density of all visible scampi (ranging from those walking free on the surface to those within burrows, where only the tips of claws can be seen) is scaled by emergence. Before conducting emergence trials with live scampi, scuba divers activated and placed tags in burrows in shallow waters to confirm whether the scampi became undetectable when they were acoustically obscured by the burrow. This showed that tags were detected on the surface of the seabed, and in the entrance to burrows, but not within a burrow.

Scampi are thought to spend a considerable amount of time within their burrow entrances, ‘door keeping’, and the classification of these individuals as visible scampi to be scaled up by the emergence

rate is likely to overestimate the population density. When 'door keeping', a scampi's position (and the inferred equivalent likelihood of a tagged scampi being acoustically detectable) can range from only just in the burrow (Figure 43, left, very likely to be detected), to about half in (Figure 43, centre, as likely or not to be detected), or almost fully in, with only the claws visible (Figure 43, right, very unlikely to be detected). Therefore, acoustically detectable scampi are considered those walking free on the surface (emerged), and a proportion of door keepers.

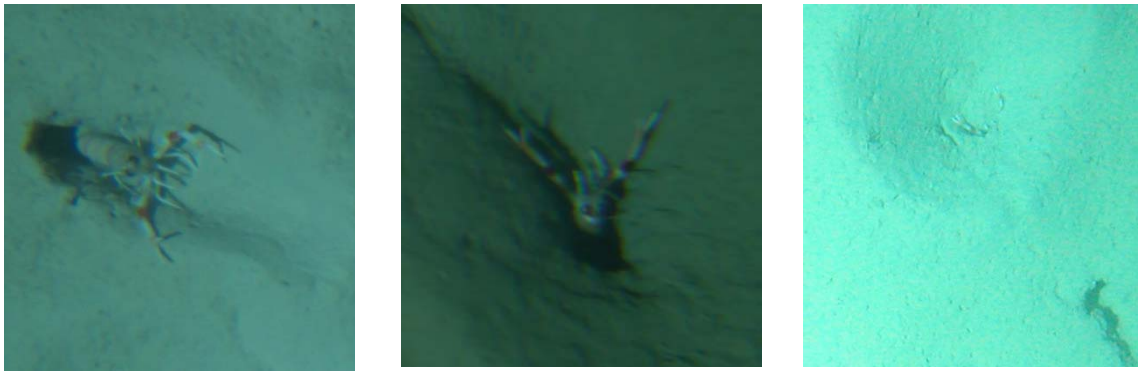

Figure 43: Examples of scampi within the entrance to burrows (door keeping). Only the tips of the claws can be seen in the right hand image.

From the combined SCI 6A photographic surveys, the 261 scampi observed door keeping were re-examined, to determine whether it was considered they would have been acoustically detectable, had they been acoustically tagged. It was estimated that 51% of the scampi would have been detectable, with a 95% confidence interval (estimated by resampling from the original data with replacement) of 45%–57%.

The process of using the emergence and photo survey data to estimate priors for *q-Photo* (the proportion of the scampi population represented by the count of major burrow openings) and *q-Scampi* (the proportion of the scampi population represented by the count of visible scampi) is summarised in Table 11. For each term in the process, a distribution was estimated by resampling from the original data with replacement. The proportion of visible scampi that would be acoustically detectable (if fitted with a tag) was estimated by summing the proportion of emerged scampi with the proportion of door keepers multiplied by the proportion of door keepers that were considered sufficiently out of their burrow to be acoustically detectable. The *q-Scampi* term (proportion of population represented by visible scampi index) was estimated by dividing the daytime emergence by the proportion of visible scampi that could be detected.

Table 11: Estimation of *qPhoto* prior for SCI 6A from emergence and photo data.

		Percentile			
		2.5%	50%	97.5%	Source
Door keeper detectability	(1)	45.0%	51.1%	57.3%	Seabed images (all years)
Daytime emergence	(2)	41.7%	46.1%	50.7%	Acoustic tagging (2013)
Proportion of visible scampi emerged	(3)	0.4042	0.5633	0.7066	Seabed images (all years)
Proportion of visible scampi door keeping	(4)	0.5958	0.4367	0.2934	Seabed images (all years)
Proportion of visible scampi detectable	(5)	0.7454	0.7866	0.8388	(3) + ((4) * (1))
q-Scampi	(6)	0.3577	0.5860	0.8050	(2) / (5)

Previous investigations into the relative abundance estimates of photographic and trawl approaches (Tuck 2017) have suggested a relative scaling value to adjust the *q_Scampi* prior distribution for use as a *q_Trawl* prior. Resampling the stratum level data for the *San Tongariro* surveys in SCI 6A provides a median estimate that trawl catch estimates are 57% of emerged scampi estimates (95% CI 40% – 88%). It is acknowledged that this approach does use survey stratum level abundance estimates from

the two surveys, which are combined to form the total survey abundance estimates used within the stock assessment model. In later model developments, the *q_Scampi* prior distribution was used as the prior distribution for the trawl surveys, though separate catchability terms were estimated.

Therefore, trawl survey catchability (*q-Trawl*) varies with both the percentage of door keepers that are acoustically detectable, and the percentage of emerged scampi that would be caught if within the path of a trawl. On the basis of the *q_Scampi* prior and details of relative catch rates, a *q_Trawl* prior for the *San Tongariro* was estimated at 0.36 (95% CI 0.14 – 0.71). For some preliminary models, a q-ratio prior was applied to the ratio between the survey *q* for *San Tongariro* and *Kaharoa*, as described in Section 3.5.2.

3.7.2 Priors for *q*s

q-Scampi

This is the proportion of the scampi population represented by the count of visible animals. The best estimate is 0.586 (daytime emergence divided by the proportion of visible scampi detectable, Table 11). Lower (0.358) and upper (0.805) estimates are taken as the 2.5th and 97.5th percentiles of the distribution.

q-Trawl

This is the proportion of the scampi population represented by the trawl survey catches. The best estimate is 0.36. Lower (0.14) and upper (0.71) estimates are taken as the 2.5th and 97.5th percentiles of the distribution.

Ratio *q-Trawl* (*San Tongariro*:*Kaharoa*)

The two survey vessels appear to have different catchabilities. The ratio of catches relative to photo survey abundances has been used to inform a *q* ratio prior. The best estimate is 0.42. Lower (0.31) and upper (0.56) estimates are taken as the 2.5th and 97.5th percentiles of the distribution. A q-ratio penalty was used in some initial models, but after these initial investigations the working group proposed that the same *q-Trawl* prior be applied to both trawl surveys, while still estimating separate *q*s.

3.7.3 Estimation of prior distributions

The bounds and best estimate were assumed to represent the 2.5th, 50th, and 97.5th percentiles of the prior distribution. These values were fitted within a binomial GLM (probit link) to estimate the slope and intercept of the cumulative frequency distribution, which in turn were used to estimate the mean and standard deviation of the lognormal distribution of the prior. The distributions of the priors are presented in Figure 44.

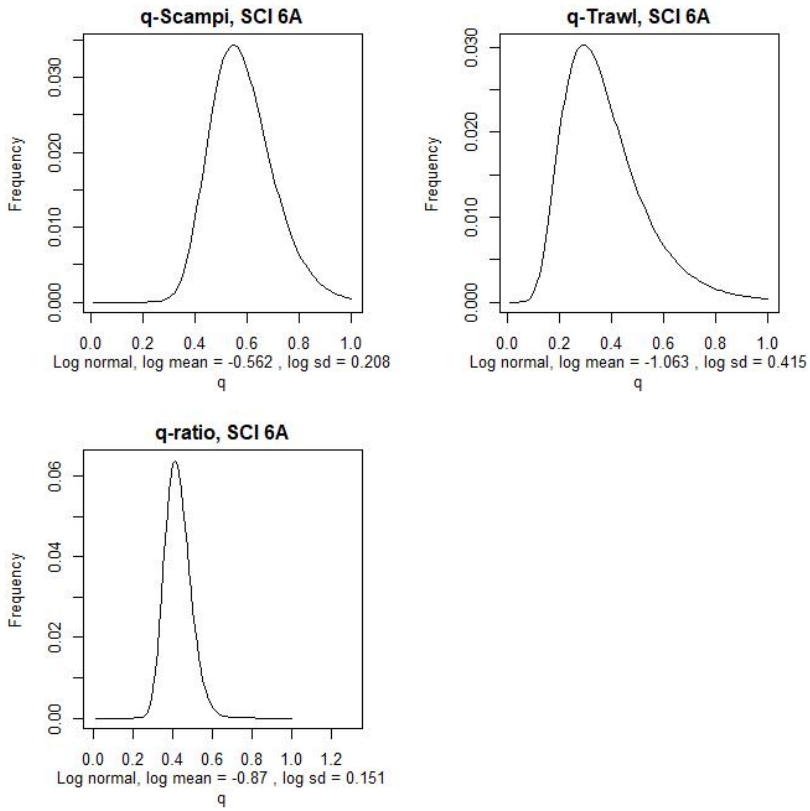

Figure 44: Estimated distribution of *q-Scampi*, *q-Trawl*, and the ratio of *q_Trawl* (between survey vessels) for SCI 6A.

3.7.4 Recruitment

Few data are available on scampi recruitment. Relative year class strengths were fixed at 1 for the two most recent years and were assumed to average to 1.0 over all other years. In the initial model development (Cryer et al. 2005), lognormal priors on relative year class strengths were assumed, with a mean of 1.0 and a CV of 0.2. The sensitivity of year class strength variation was examined in further developments (Tuck & Dunn 2006) and later increased to a CV of 1 (Tuck & Dunn 2012). Model explorations within the more recent SCI 6A assessments (Tuck 2017) suggested that extreme YCS values estimated by the model were related to model structure rather than data. The preliminary model, and those applied to other scampi stocks, used the Haist parameterisation of YCS (Bull et al. 2012) where

$$YCS_i = \frac{y_i}{\bar{y}}$$

with a lognormal prior on y_i with mean of 1 and CV of 1, and a small penalty to ensure that the mean of YCS does not drift away from 1 ('a YCS average to 1 penalty'). Sensitivity trials (Tuck 2017) with the Haist parameterisation showed that both individually removing the penalty, and tightening the CV on the YCS prior, reduced the final YCS estimated by the model, but only removing the penalty and tightening the CV (to 0.7) generated a final YCS estimate of similar magnitude to previous good years. Further investigations examined the sensitivity to the CV on the YCS prior for models with the Haist parameterisation without a penalty on YCS averaging to 1 and a YCS average to 1 penalty, and also without the Haist parameterisation but with a YCS average to 1 penalty (Tuck 2017).

On the basis of these sensitivity analyses, it was agreed to proceed with a model structure implementing the Haist parameterisation, without the YCS average to 1 penalty and with tighter CVs on the YCS prior (Tuck 2017). Preliminary examination of the implications of this parameterisation change to previously

accepted stock assessment models for SCI 1 and SCI 2 did not suggest that any change in perceived stock status, and this was confirmed when these assessments were updated (Tuck 2020).

The relationship between stock size and recruitment for scampi is unknown, and a Beverton-Holt relationship with a steepness of 0.8 has been assumed. New Zealand scampi have very low fecundity (Wear 1976, Fenaughty 1989) (in the order of tens to hundreds of eggs carried by each female), so high levels of recruitment are unlikely when abundance is low. Recruitment enters the model partition as a year class, with a normally distributed OCL with a mean of 10 mm and a CV of 0.4.

4. ASSESSMENT MODEL RESULTS

4.1 Preliminary investigations

Model developments since the last assessment have introduced new catchability priors, and so as a first step, the influence of these on the previous assessment, and the influence of three years additional data, were examined. Details of preliminary models examined are provided in Table 12.

Table 12: General details of preliminary models examined for SCI 6A.

Model name	Final year	*q* priors	Trawl survey included	*q* ratio
2016	2016	Old	San Ton 2007 - 2013	No
2019	2019	Old	San Ton 2007 - 2013	No
Kah survey	2019	Old	San Ton 2007 - 2013, Kah 2016 - 2019	No
New *q*	2019	New	San Ton 2007 - 2013, Kah 2016 - 2019	No
q ratio	2019	New	San Ton 2007 - 2013, Kah 2016 - 2019	Yes

Updating the catch, length frequencies, and photo survey index resulted in a revised model that estimated a slower increase in abundance at the end of the series, and slightly revised YCS patterns, potentially partly driven by the stock trajectory (Table 13, Figure 45). Including the *Kaharoa* survey (fitted with a separate *q* and selectivity) had minimal influence on model outputs. Revising the *q* priors led to estimation of a slightly lower SSB_0, and a slight change in the stock trajectory, but no effect on YCS patterns. Applying the *q*-ratio penalty slightly increased the SSB_0 and slightly improved the *SSB* trajectory at the end of the series, because the *q* for *Kaharoa* was reduced.

Table 13: Estimated key parameters and quantities from MPD fits for SCI 6A preliminary model runs.

	2016	2019	Kah survey	New *q*	*q* ratio
SSB_0	4078	4489	4476	4189	4448
SSB_{2016}	2876	2684	2724	2473	2753
SSB_{2016}/SSB_0	0.71	0.60	0.61	0.59	0.62
SSB_{2019}		2914	2933	2684	2965
SSB_{2019}/SSB_0		0.65	0.66	0.64	0.67
q-Photo	0.73	0.72	0.72	0.76	0.72
q-Trawl (ST)	0.53	0.50	0.51	0.64	0.62
q-Trawl (K)			0.37	0.43	0.29

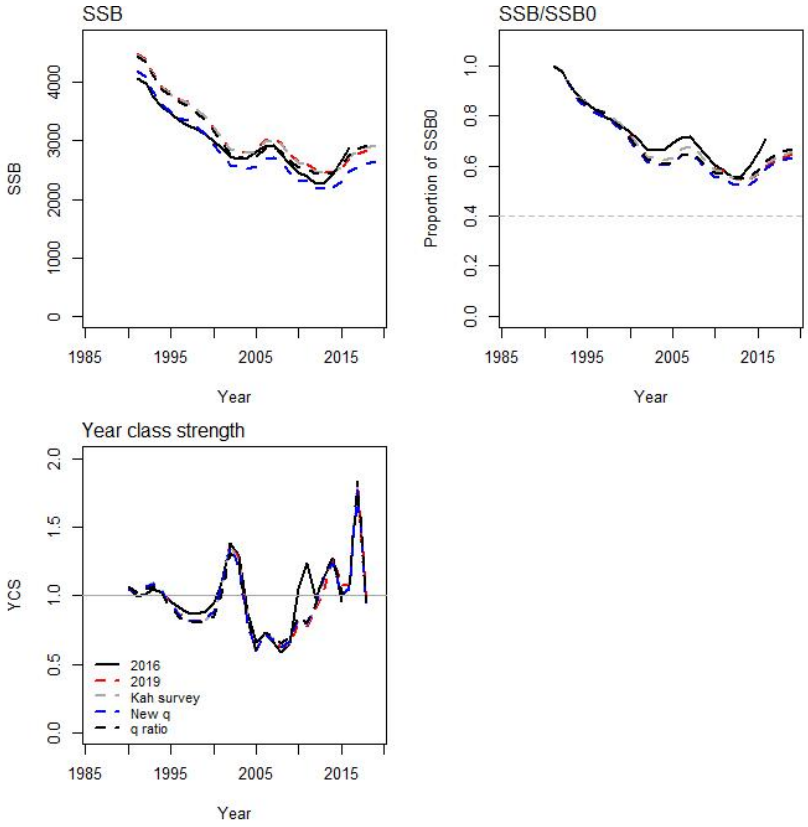

Figure 45: Plots of absolute SSB, SSB as a proportion of SSB_0, and year class strength (YCS) for MPD fits to the preliminary SCI 6A model runs.

The examination of preliminary assessment model runs identified a potential conflict between the commercial CPUE and survey (particularly the photo) indices. Although the CPUE index declines slightly in the most recent years, the trawl survey shows an increase in the point estimate between 2016 and 2019 but with an overlap in the confidence intervals (the vessel change makes comparison of trawl survey estimates with previous years more difficult) and the photo index of visible animals increases markedly since 2013 (Figure 46). Further examination of the photo survey data identified that much of the large increase in abundance between 2016 and 2019 was accounted for by an increase in the number of door keeper scampi observed. Although all sizes of scampi are observed door keeping, the smallest (recruit) animals are generally only seen in burrow entrances. The emerged scampi index is more representative of the population available to the commercial fishery or trawl surveys, and given the method used to estimate visible scampi size (see Section 3.6.3), the size distribution estimated from photographs is considered representative of emerged animals, but may provide an overestimate of the size of doorkeepers. On this basis the working group agreed that the emerged scampi index should be

used, rather than the visible scampi index. The significant increase in the doorkeeper index in 2019 may be an indication of good recruitment, and this will be explored further in the future. The emerged scampi index shows an increase between 2016 and 2019 more consistent with that observed in the trawl survey data. Although there is no evidence of strong recruitment from the 2019 trawl survey length compositions, the photo survey length composition data (while much more uncertain) do suggest an increase in the proportion of small scampi, consistent with recent recruitment.

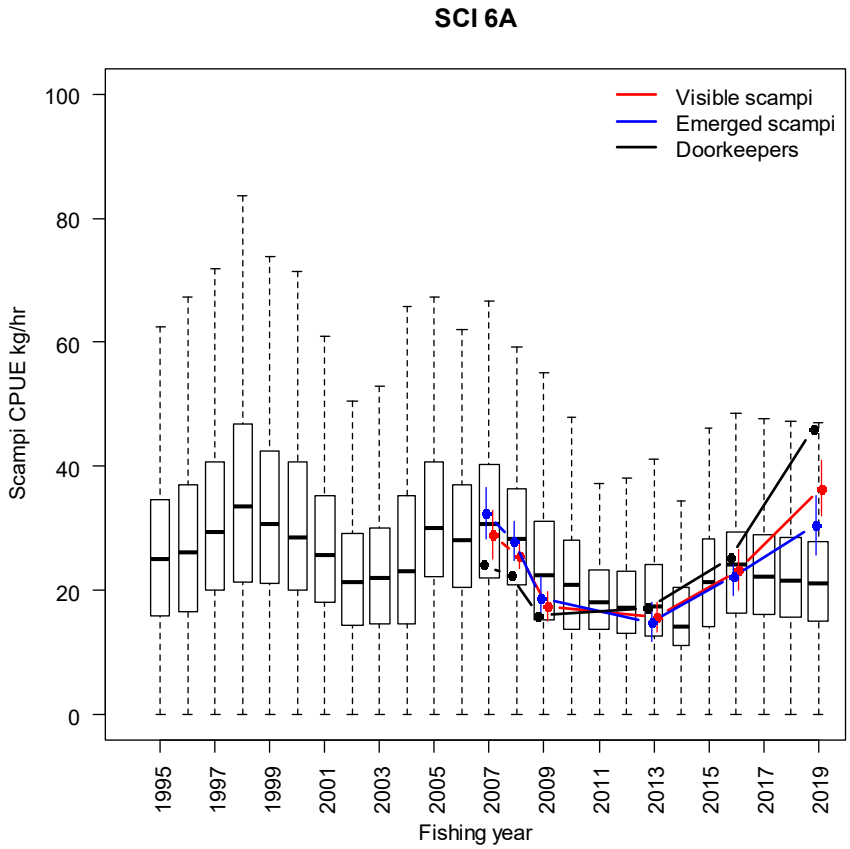

Figure 46: Boxplot of unstandardised CPUE by year overlaid with photo survey indices (scaled to the geometric mean of CPUE.

4.2 Initial models

Based on the previously accepted assessment for SCI 6A, a single area model was applied, with an annual CPUE index, and the photo and trawl survey data were fitted as separate indices, both in time step 1. The use of the *q*-ratio penalty was rejected by the working group, and so although separate *q*s were estimated for the two trawl survey series, both had the same prior distribution. Initial model explorations included sensitivities to CPUE process error, exclusion of one or other of the surveys and different assumed values for *M*. The working group also raised concerns over the representativeness of the observer sampling and the generation of an overall fishery catch composition, given the shift in size composition with depth. The development of a two area two stock model was not considered feasible within the time available, and so a preliminary test of the sensitivity of the model to shallow (less than 450 m) or deep (greater than 450 m) length composition and tag recapture data was proposed. Details of the exploratory models are provided in Table 14.

Table 14: General details of exploratory models examined for SCI 6A. LF is length frequency.

Model name	*M*	CPUE process error	LF & tag data	Surveys
Model 1	0.25	0.15	All	Trawl & Photo
Model 2	0.25	0.1	All	Trawl & Photo
Model 3	0.25	0.2	All	Trawl & Photo
Model 4	0.25	0.15	Shallow (<450m)	Trawl & Photo
Model 5	0.25	0.15	Deep (>450m)	Trawl & Photo
Model 6	0.25	0.15	All	Trawl only
Model 7	0.25	0.15	All	Photo only
Model 8	0.20	0.15	All	Trawl & Photo
Model 9	0.30	0.15	All	Trawl & Photo

Exploration of the effects of process error on the CPUE series (Figure 47, Table 15) found that though both the SSB_0 and stock trajectory were sensitive (higher SSB_0 and more optimistic current stock status with higher process error) to the process error and the lower process error model estimated more variable YCSs, there were only minimal differences in the fits to the data. Both the models fitted to the deep or shallow tag recapture and length data (but whole area abundance indices) produced higher SSB_0 estimates than the full data model (Model 1), and comparable or higher current stock status (Figure 48, Table 15). These models were examined as a sensitivity to the representativeness of observer sampling (rather than developing a two stock two area model). The different length composition data sets had considerably different weighting in the shallow and deep models, suggesting a conflict between the separate length data sets and the overall abundance indices. It was concluded that this may not be an appropriate approach to examine this sensitivity, and exploration of an area-based model was proposed for the next assessment of this stock.

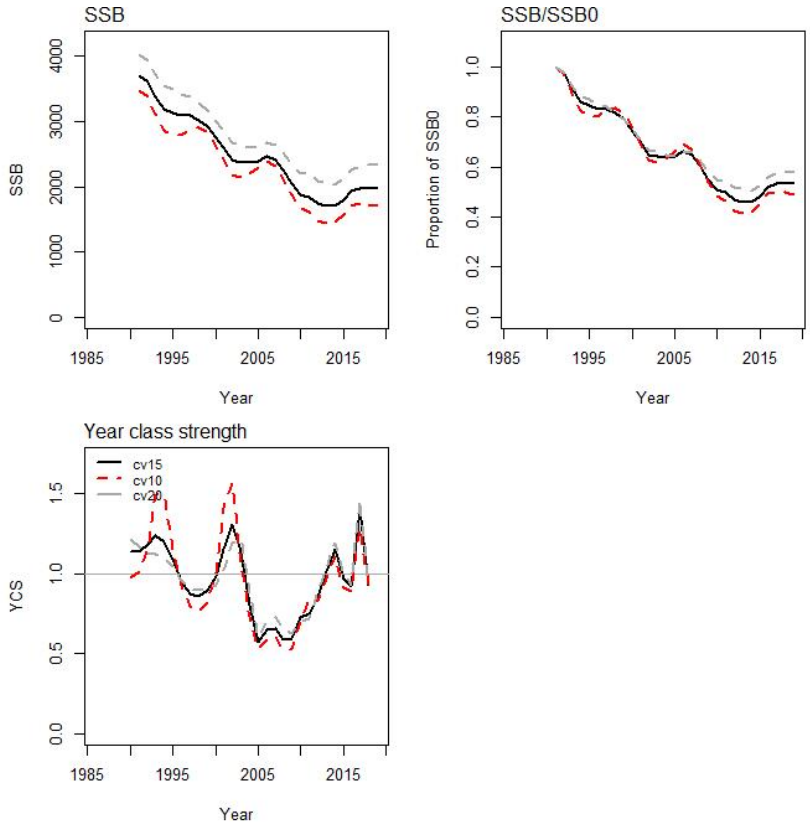

Figure 47: Plots of absolute *SSB*, *SSB* as a proportion of SSB_0, and year class strength (YCS) for MPD fits to the SCI 6A exploratory runs examining CPUE process error.

Table 15: Estimated key parameters and quantities from MPD fits for SCI 6A exploratory model runs described in Table 14. Italicised values indicate parameters that were fixed rather than estimated.

Model	1	2	3	4	5	6	7	8	9
SSB_0	3710	3478	4024	4287	3908	2833	3346	4001	3590
SSB_{2019}	1980	1708	2349	2612	2105	1170	1618	1935	2089
SSB_{2019}/SSB_0	0.53	0.49	0.58	0.61	0.54	0.41	0.48	0.48	0.58
q-Scampi	0.63	0.71	0.58	0.61	0.57		0.72	0.65	0.60
q-Trawl (ST)	0.71	0.73	0.65	0.66	0.60	1.00		0.71	0.69
q-Trawl (K)	0.45	0.52	0.38	0.40	0.43	0.61		0.44	0.44
Growth									
Male g20	10.52	11.34	10.56	11.29	10.73	15.16	10.35	9.96	10.99
Male g40	1.75	1.87	1.66	1.60	1.86	2.63	1.78	1.53	1.92
Female g20	12.61	13.13	12.75	14.46	11.48	16.03	12.01	11.50	13.53
Female g40	0.00	0.00	0.00	0.00	0.00	0.00	0.00	0.00	0.00
min_sigma	4.61	4.53	4.74	5.00	4.20	4.92	4.88	4.29	4.85
Selectivity									
step1 L50	42.93	41.86	43.38	44.34	41.01	41.37	45.76	42.43	43.30
step1 a95	11.96	11.96	11.98	12.01	10.39	12.51	11.78	11.92	11.97
step1 amax	0.88	0.86	0.89	0.76	0.81	0.89	0.81	0.84	0.91
step2 L50	43.85	44.68	42.37	42.92	43.33	48.36	44.09	42.96	44.65
step2 a95	14.60	15.78	13.34	13.51	14.33	20.53	14.14	14.43	14.75
step2 amax	1.29	1.28	1.27	1.12	1.10	1.34	1.26	1.24	1.32
step3 L50	*42.00*	*42.00*	*42.00*	*42.00*	*42.00*	*42.00*	*42.00*	*42.00*	*42.00*
step3 a95	12.14	12.68	12.18	11.21	12.34	14.47	11.46	12.74	11.69
step3 amax	1.78	1.82	1.70	1.53	1.31	2.03	1.73	1.66	1.87
trawl L50	44.40	45.04	43.72	45.20	43.81	42.76		43.78	44.94
trawl a95	13.02	13.68	12.90	12.64	12.90	13.82		13.01	13.02
trawl amax	1.19	1.17	1.15	1.07	1.05	1.23		1.14	1.22
photo a1	41.10	38.09	40.64	33.19	42.85		43.90	39.45	42.64
photo aL	30.00	30.00	29.94	29.95	30.00		30.00	30.00	30.00
photo aR	28.61	28.06	25.68	26.45	29.61		29.08	28.12	27.61

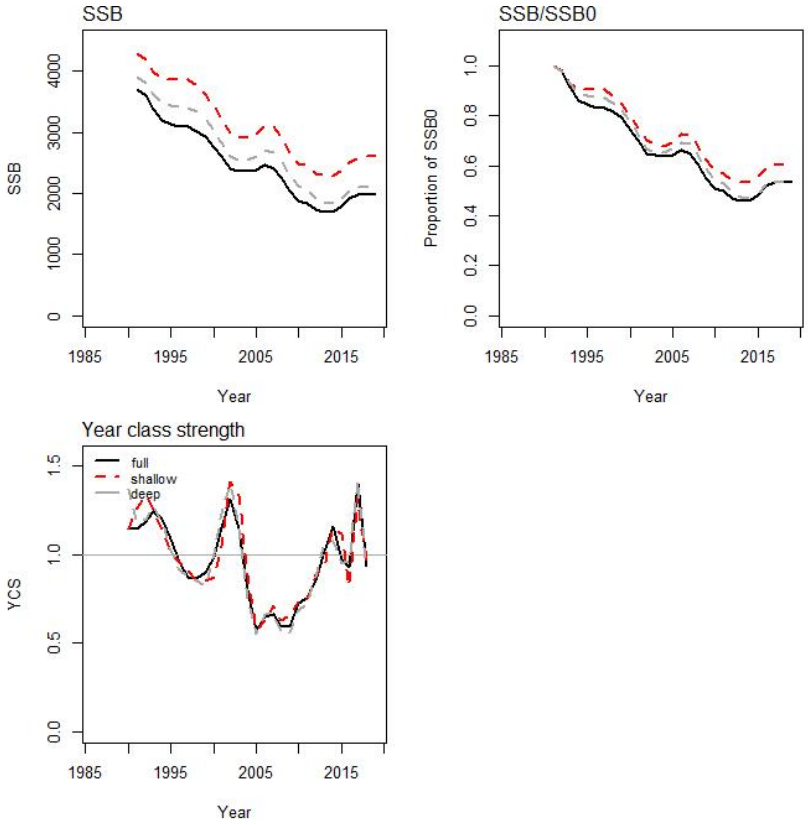

Figure 48: Plots of absolute *SSB*, *SSB* as a proportion of SSB_0, and year class strength (YCS) for MPD fits to the SCI 6A exploratory runs examining the influence of deep and shallow length frequency and tag data.

Exclusion of either of the survey indices (Figure 49, Table 15) resulted in more influence of the CPUE series, with a lower SSB_0 estimated and a steeper stock trajectory and lower current stock status, although, as with previous model comparisons, there were minimal effects to the fits to indices or length data. The final initial exploration examined sensitivity to M (Figure 50, Table 15), observing relatively small effects (SSB_0 estimates being lower and current stock status estimates being higher when higher estimates of M were assumed).

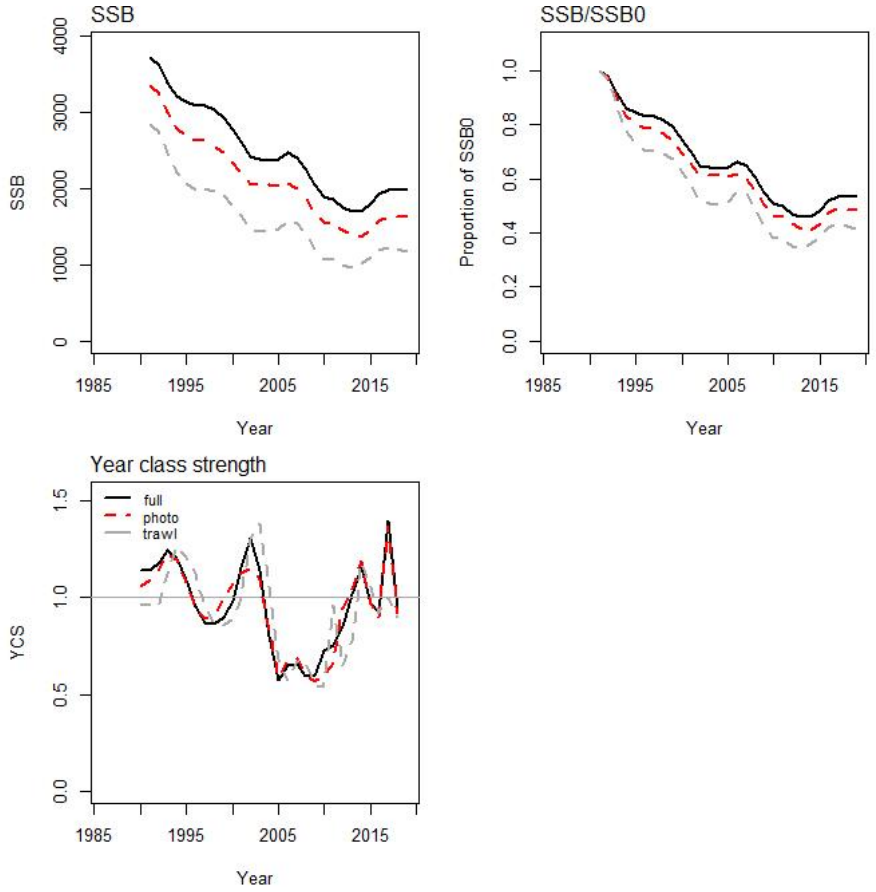

Figure 49: Plots of absolute *SSB*, *SSB* as a proportion of SSB_0, and year class strength (YCS) for MPD fits to the SCI 6A exploratory runs examining the influence of excluding each of the surveys.

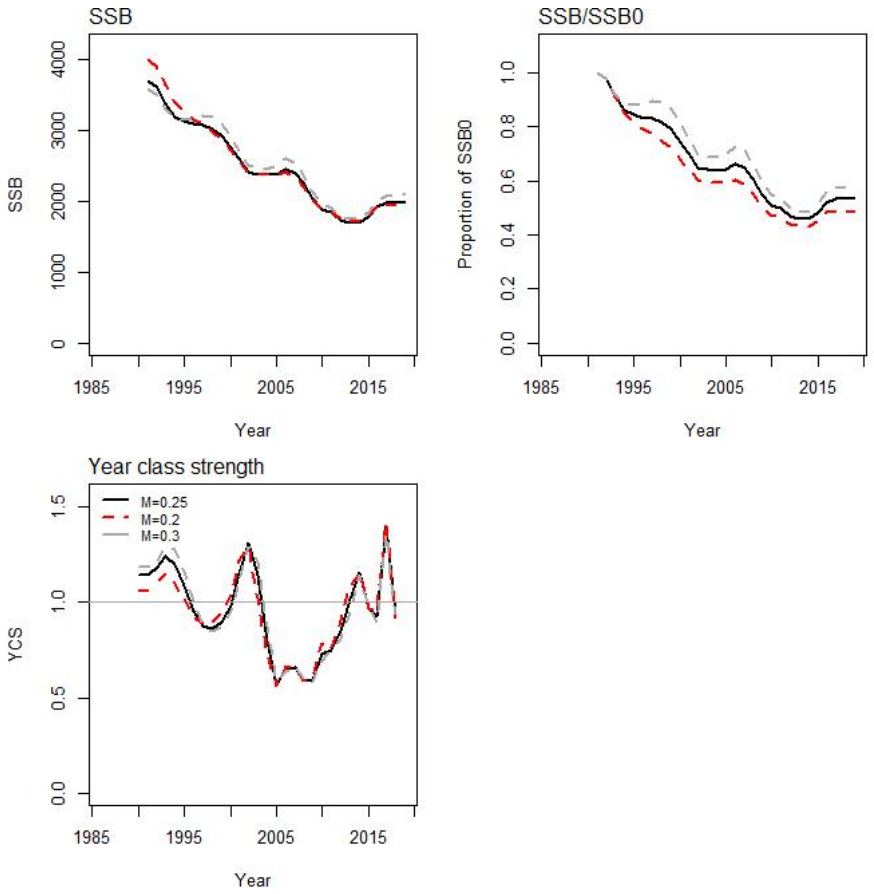

Figure 50: Plots of absolute *SSB*, *SSB* as a proportion of SSB_0, and year class strength (YCS) for MPD fits to the SCI 6A exploratory runs examining the influence of *M*.

Based on these initial explorations, the Deepwater Working Group recommended further exploration of process error on the CPUE series and sensitivity to prior distributions for survey *q* parameters (Table 16). Models described above have used the prior distributions described in Section 3.7. Sensitivities were examined using approximately halved and doubled prior *mu* values. The working group agreed that the *q-Scampi* prior distribution (representing the proportion of scampi emerged on the seabed) may also be appropriate for the trawl survey *q*, and so a wider range of values were considered for *q-Trawl*. Model 1b represents the equivalent of Model 1 in Table 14, but with a fixed selectivity parameter now estimated.

Table 16: General details of further models examined for SCI 6A. The label refers to model label with the relevant plots of *SSB* trajectory below (Figures 51–53).

Model name	CPUE process error	*q-Scampi* prior *mu* (CV)	*q-Trawl* prior *mu* (CV)	Label
Model 1b	0.15	0.58 (0.21)	0.36 (0.41)	p58t36
Model 1c	0.05	0.58 (0.21)	0.36 (0.41)	
Model 10	0.15	0.58 (0.21)	0.18 (0.41)	p58t18
Model 11	0.15	0.58 (0.21)	0.58 (0.21)	p58t58
Model 12	0.15	0.58 (0.21)	0.80 (0.21)	p58t80
Model 13	0.15	0.30 (0.21)	0.36 (0.41)	p30t36
Model 14	0.15	0.80 (0.21)	0.36 (0.41)	p80t36
Model 15	0.15	0.30 (0.21)	0.58 (0.21)	p30t58
Model 16	0.15	0.80 (0.21)	0.58 (0.21)	p80t58

Fixing the CPUE process error at 0.05 (Table 17) continued the pattern observed in Figure 47 of estimating a lower SSB_0 and steeper decline in stock trajectory and was consistent with dropping the surveys and putting more weight onto the CPUE data.

A range of combinations of prior distributions for *q-Scampi* and *q-Trawl* were examined (Table 17, Figures 51–53). The working group agreed that though there was sensitivity to extreme values, model outputs were not particularly sensitive to plausible *q-Trawl* priors when *q-Scampi* priors were set at informed levels. It was also agreed that because both the photographic survey of emerged scampi and the trawl survey sampled the same group of animals, it was appropriate to use the *q-Scampi* prior distribution for *q-Trawl*.

Table 17: Estimated key parameters and quantities from MPD fits for SCI 6A exploratory model runs described in Table 16.

Model	1	1a	10	11	12	13	14	15	16
SSB_0	3589	3142	4665	3558	3319	4926	3256	4415	3285
SSB_{2019}	1909	1396	2884	1870	1653	3197	1575	2737	1591
SSB_{2019}/SSB_0	0.53	0.44	0.62	0.53	0.50	0.65	0.48	0.62	0.48
q-Scampi	0.63	0.85	0.52	0.64	0.69	0.37	0.78	0.41	0.77
q-Trawl (ST)	0.81	0.80	0.44	0.78	1.00	0.54	0.93	0.67	0.84
q-Trawl (K)	0.48	0.64	0.27	0.59	0.79	0.36	0.53	0.55	0.60
Growth									
Male g20	9.39	12.54	10.82	9.32	9.17	8.59	10.05	8.07	10.04
Male g40	1.66	2.06	1.57	1.67	1.75	1.32	1.86	1.35	1.86
Female g20	11.58	13.98	13.16	11.48	11.22	10.34	12.35	9.85	12.34
Female g40	0.00	0.00	0.00	0.00	0.00	0.00	0.00	0.00	0.00
min_sigma	4.49	4.59	4.63	4.47	4.46	4.19	4.65	4.12	4.62
Selectivity									
step1 L50	44.22	40.65	41.58	44.08	44.97	44.33	43.97	45.17	43.58
step1 a95	12.14	11.50	11.63	12.00	12.27	12.03	12.20	12.08	12.00
step1 amax	0.90	0.85	0.89	0.91	0.89	0.85	0.91	0.86	0.92
step2 L50	47.22	46.47	40.97	47.47	50.35	45.19	48.09	47.48	47.80
step2 a95	15.93	17.68	12.88	16.01	17.12	14.34	16.80	15.12	16.70
step2 amax	1.29	1.29	1.25	1.29	1.28	1.21	1.32	1.23	1.32
step3 L50	49.44	50.10	44.66	49.72	50.50	49.16	49.33	50.91	49.50
step3 a95	16.49	18.87	15.43	16.53	16.37	16.19	16.68	16.31	16.86
step3 amax	1.66	1.73	1.61	1.65	1.65	1.50	1.70	1.53	1.70
trawl L50	45.11	45.93	42.59	46.47	48.06	46.10	44.56	48.51	45.56
trawl a95	12.72	14.79	12.62	13.40	13.95	13.12	12.60	13.88	13.19
trawl amax	1.26	1.15	1.19	1.20	1.17	1.10	1.31	1.08	1.25
photo a1	47.34	36.44	36.52	47.77	48.82	46.57	46.00	47.98	45.89
photo aL	30.00	30.00	29.29	29.97	29.90	27.60	30.00	26.61	30.00
photo aR	29.72	29.23	24.54	29.73	29.75	27.31	29.27	27.48	29.30

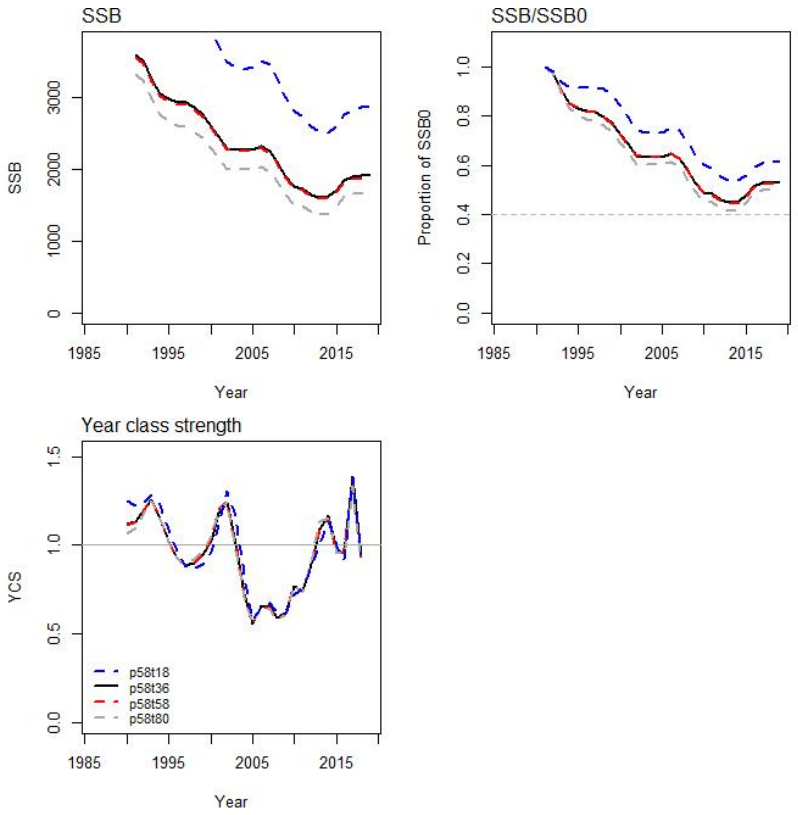

Figure 51: Plots of absolute *SSB*, *SSB* as a proportion of SSB_0, and year class strength (YCS) for MPD fits to the SCI 6A sensitivity runs examining the prior for *q-Trawl* when *q_Photo* prior at 0.58 (CV=0.21).

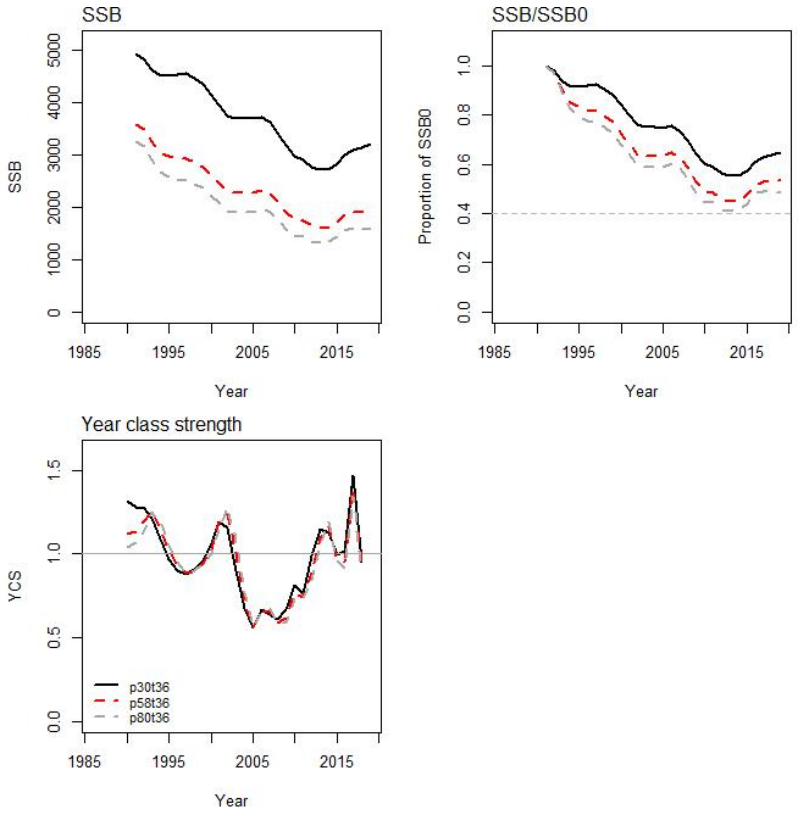

Figure 52: Plots of absolute *SSB*, *SSB* as a proportion of SSB_0, and year class strength (YCS) for MPD fits to the SCI 6A sensitivity runs examining the prior for *q-Photo* when *q_Trawl* prior at 0.36 (CV=0.41).

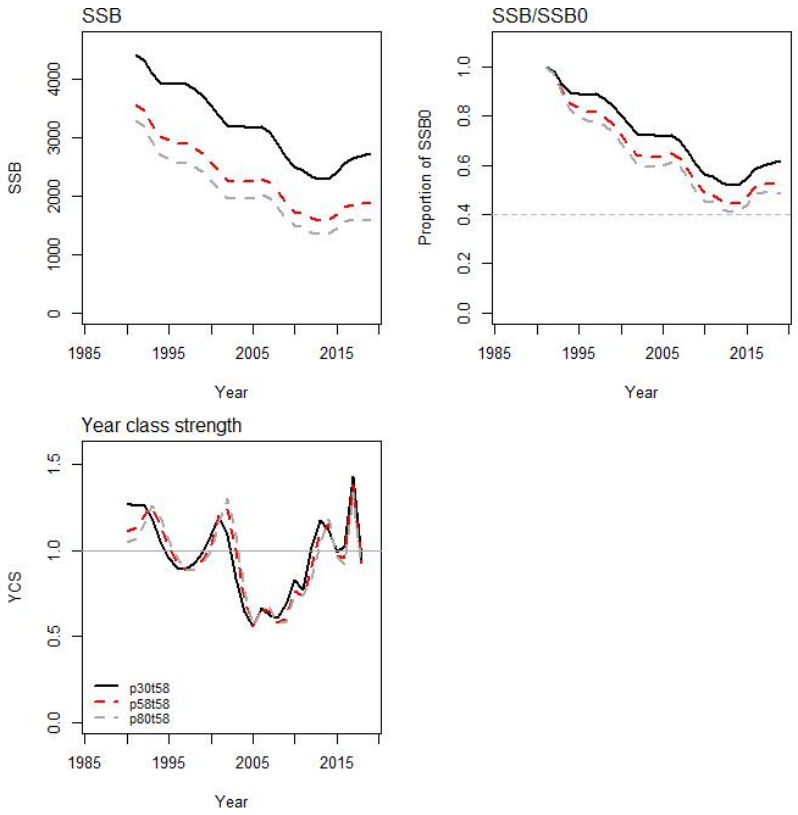

Figure 53: Plots of absolute *SSB*, *SSB* as a proportion of SSB_0, and year class strength (YCS) for MPD fits to the SCI 6A sensitivity runs examining the prior for *q-Photo* when *q_Trawl* prior at 0.58 (CV=0.21).

4.3 Final models

Based on the model exploration and sensitivity runs described above, the working group agreed on a set of final models to be presented, documented, and taken to MCMC. The base case included the CPUE and trawl and photo survey abundance indices, with *M* fixed at 0.25, and survey catchability priors informed by our best estimate of scampi emergence (fully out of burrows). Sensitivities were based on this model, individually examining the effect of low *M*, a low *q* prior distribution, and excluding the CPUE abundance index. Although the base case is considered the most plausible (and is the model described in the WG report (Fisheries New Zealand 2020), and for which the fishing pressure and projections are provided), this set of models is considered to represent the range of sensitivities previously examined (Figure 54). Diagnostic plots associated with the final models are provided in Appendices 3–6.

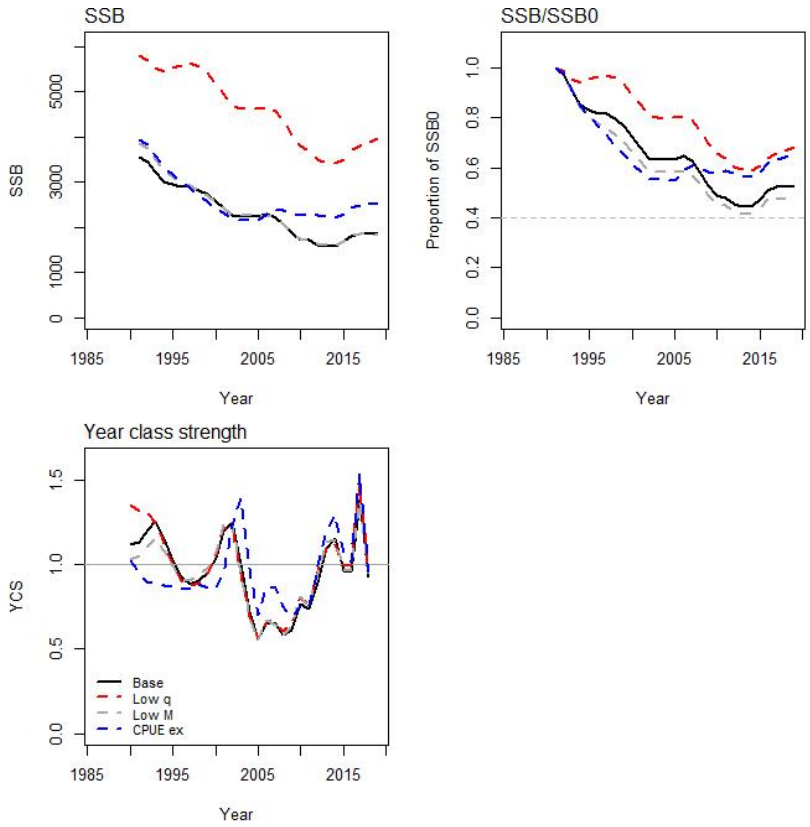

Figure 54: Plots of absolute *SSB*, *SSB* as a proportion of SSB_0, and year class strength (YCS) for MPD fits to the SCI 6A final model runs.

4.3.1 Base model (see Appendix 3)

The base model included CPUE and survey (trawl and photo) indices, had *M* fixed at 0.25, and an informed lognormal prior distribution for all survey *q*s (mu=0.58, CV=0.21). The MPD fit to the base model estimated SSB_0 to be 3558 t with SSB_{2019} at 1870 t, 53% of SSB_0. Fits to the abundance indices and normalised residuals (A3. 1 in Appendix 3) show that the model followed the overall trend in CPUE well but smoothed through the broader fluctuations. Fits to the trawl and photographic survey indices were reasonable, although the model does not show the same magnitude of decline in abundance between 2007 and 2013 as the photographic survey. The *SSB* is estimated to have declined steadily from the start of the fishery in 1990 to 2013, and increased by 2016, remaining stable after this (A3. 2). Above average year class strengths were estimated in 1992, 1993, 2001, 2002, 2014, and 2017 (A3. 2). Estimated selectivity curves (A3. 3) were consistent with our expectation of changes in sex ratio in relation to model time step. MPD estimates of trawl and photo survey catchability were within the prior distribution (A3. 4), and the *San Tongariro* survey catchability was greater than that of the *Kaharoa*. Model fits to the individual observer length frequency distributions were variable (e.g., A3. 5), but overall residual plots by length or year (e.g., A3. 6) showed that overall fits were reasonable. Annual length distributions from trawl surveys showed less variability, and individual model fits were better (A3. 14 and 17), although residual plots did show a small but consistent pattern (A3. 15). The length frequency distributions of scampi observed emerged from burrows in the photographic survey are variable with high levels of uncertainty (Figure 42). Individual fits were variable (A3. 20) but overall residuals were acceptable (A3. 21).

The likelihood profiles when B_0 was fixed were strongly U shaped (A3. 22), with the greatest contribution to the location of the overall minimum (SSB_0 estimate) coming from the abundance indices and priors (and particularly *q-Scampi*).

MCMC runs

MCMC diagnostics provided reasonable evidence the model converged (A3. 23–A3. 25). Posterior distributions of the survey catchability estimates showed some divergence from the median for the prior (A3. 26). The posterior trajectory of the *SSB* (Figure 55) suggests small fluctuations around a steadily declining trend from the start of the fishery until 2013, followed by a slight increase and stabilisation. In 2013, the median estimate of stock status (SSB_{2013}/SSB_0) was 45% (95% confidence interval 38%–53%). The median estimate of current stock status (SSB_{2019}/SSB_0) is 53% (95% confidence interval 43%–65%), with 0% probability that SSB_{2019} is below 40% SSB_0.

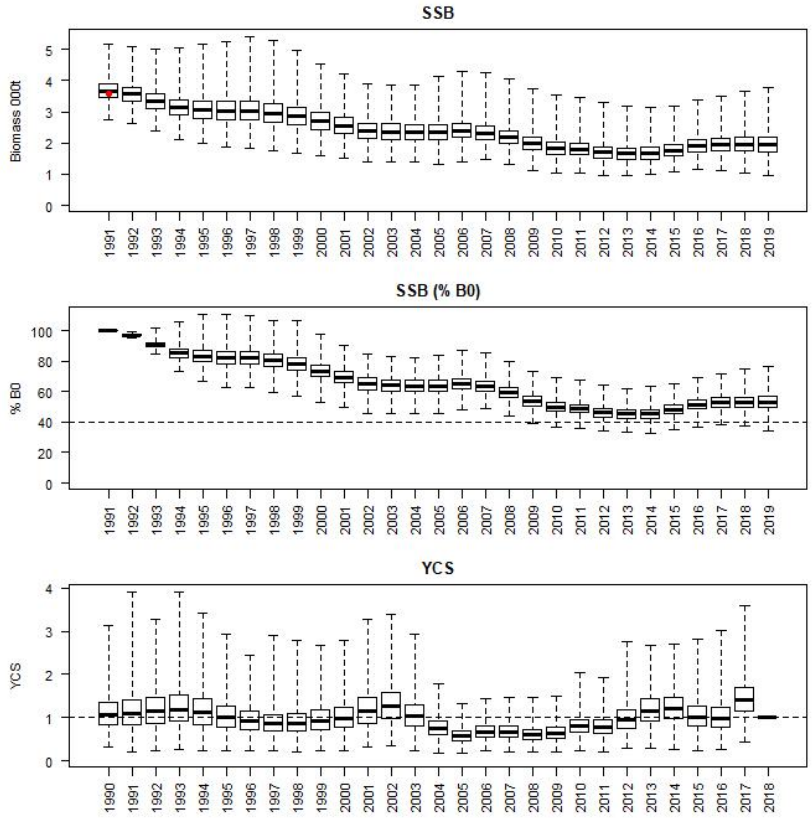

Figure 55: Posterior trajectories of *SSB*, SSB/SSB_0, and YCS from the MCMC run for the SCI 6A base model. Red dot represents MPD estimate of SSB_0.

4.3.2 Low *q* sensitivity model (see Appendix 4)

This low *q* model only deviated from the base model in terms of the prior distribution for all survey *q*s, which was set at roughly half the base level (*mu*=0.30, CV=0.21).

The MPD fit to the base model estimated SSB_0 to be 5802 t with SSB_{2019} at 3958 t, 68% of SSB_0. Fits to the abundance indices and normalised residuals (A4. 1), show that the model followed the overall trend in CPUE, but smoothed through the broader fluctuations. Fits to the trawl and photographic survey indices were reasonable but, as with the other models, did not show the same magnitude of decline in abundance between 2007 and 2013 as the photographic survey. *SSB* is estimated to have declined steadily from the start of the fishery in 1990 to 2013 and increased after this (A4. 2). Above average year class strengths were estimated before 1994, and then in 2001, 2002, 2014, and 2017 (A4. 2). Estimated selectivity curves (A4. 3) were consistent with our expectation of changes in sex ratio in relation to model time step. MPD estimates of trawl and photo survey catchability were within the prior distribution (A4. 4), and the *San Tongariro* survey catchability was greater than that of the *Kaharoa*. As with the other models, fits to the individual observer length frequency distributions were variable

(e.g., A4. 5), but overall residual plots by length or year (e.g., A4. 6) were acceptable. Annual length distributions from trawl surveys showed less variability, and individual model fits were better (A4. 14 and 17), although residual plots showed similar patterns to those observed in other models (A4. 15). The length frequency distributions of scampi observed emerged from burrows in the photographic survey are variable with high levels of uncertainty (Figure 42). As with the other models, individual fits were variable (A4. 20) but overall residuals were acceptable (A4. 21).

The overall likelihood profile when B_0 is fixed was U shaped (A4. 22), although not to the extent seen with the base model, with a signal appearing to come from the priors (and particularly *q-Scampi*), with some signal away from lower biomass values from the abundance indices and proportions at length.

MCMC runs

MCMC diagnostics provided reasonable evidence the model converged (A4. 23–A4. 25). Posterior distributions of the survey catchability estimates showed some divergence from the median for the prior (A4. 26). The posterior trajectory of the *SSB* (Figure 56) suggests small fluctuations around a steadily declining trend from the start of the fishery until 2014, followed by a slight increase to 2019. In 2014 the median estimate of stock status (SSB_{2014}/SSB_0) was 59% (95% confidence interval 51%–67%). The median estimate of current stock status (SSB_{2019}/SSB_0) is 68% (95% confidence interval 57%–79%), with 0% probability that SSB_{2019} is below 40% SSB_0.

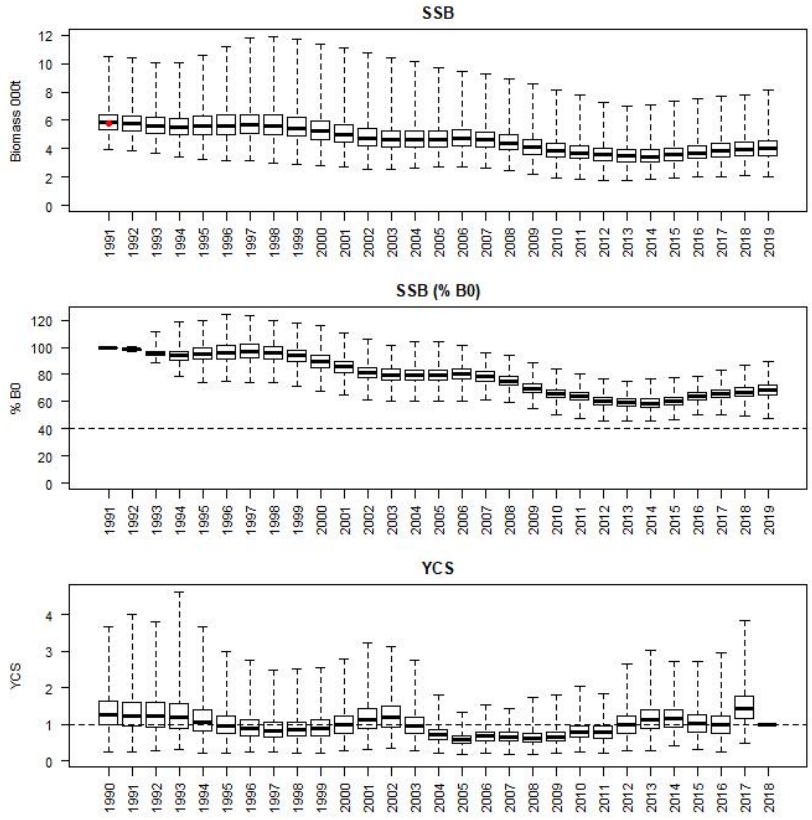

Figure 56: Posterior trajectories of *SSB*, SSB/SSB_0, and YCS from the MCMC run for the SCI 6A low *q* model. Red dot represents MPD estimate of SSB_0.

4.3.3 Low *M* sensitivity model (see Appendix 5)

This low *M* model only deviated from the base model in terms M, which was fixed at 0.2.

The MPD fit to the base model estimated SSB_0 to be 3865 t with SSB_{2019} at 1824 t, 47% of SSB_0. Fits to the abundance indices and normalised residuals (A5. 1), show that the model followed the overall decline in CPUE well, but smoothed through the broader fluctuations. Fits to the trawl and photographic survey indices were reasonable, although as previously seen, the model does not show the same magnitude of decline in abundance between 2007 and 2013 as the photographic survey. *SSB* was estimated to have declined steadily from the start of the fishery in 1990 to 2013, and increased by 2016, but declined slightly after this (A5. 2). Above average year class strengths were estimated in 1993, 2001, 2002, 2013, 2014, and 2017 (A5. 2). Estimated selectivity curves (A5. 3) were consistent with our expectation of changes in sex ratio in relation to model time step. MPD estimates of trawl and photo survey catchability were within the prior distribution (A5. 4), and, as with the other models, the *San Tongariro* survey catchability was greater than that of the *Kaharoa*. As previously noted, model fits to the individual observer length frequency distributions were variable (e.g., A5. 5), but overall residual plots by length or year (e.g., A5. 6) were reasonable. Annual length distributions from trawl surveys showed less variability, and individual model fits were better (A5. 14 and 17), although residual plots showed some patterns (A5. 15). Individual fits to length frequency distributions of scampi observed emerged from burrows were variable (A5. 20) but overall residuals were acceptable (A5. 21).

The overall likelihood profile when B_0 is fixed was strongly U shaped (A5. 22), with signal appearing to come from abundance indices and priors (and particularly *q-Scampi*).

MCMC runs

MCMC diagnostics provided reasonable evidence the model converged (A5. 23–A5. 25). Posterior distributions of the survey catchability estimates showed some divergence from the median for the prior (A5. 26). The posterior trajectory of the *SSB* (Figure 57) suggests small fluctuations around a steadily declining trend from the start of the fishery until 2013, followed by a slight increase and a very slight decline. In 2013 the median estimate of stock status (SSB_{2013}/SSB_0) was 42% (95% confidence interval 35%–50%). The median estimate of current stock status (SSB_{2019}/SSB_0) is 47% (95% confidence interval 38%–57%), with 6% probability that SSB_{2019} is below 40% SSB_0.

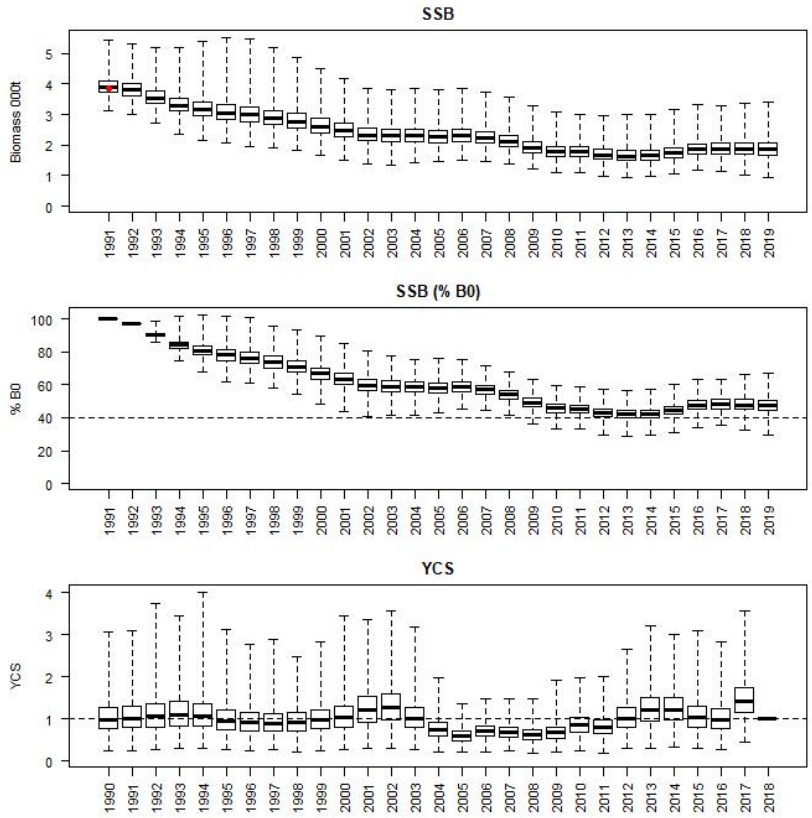

Figure 57: Posterior trajectories of *SSB*, *SSB*/*SSB*$_0$, and YCS from the MCMC run for the SCI 6A low *M* model. Red dot represents MPD estimate of *SSB*$_0$.

4.3.4 CPUE excluded sensitivity model (see Appendix 6)

With the CPUE abundance index removed, the CPUE excluded model only included the trawl and photo surveys as abundance indices.

The MPD fit to the base model estimated SSB_0 to be 3934 t with SSB_{2019} at 2549 t, 65% of SSB_0. Fits to the trawl survey indices were reasonable (A6. 1), but the model did not replicate the decline and increase in abundance observed in the photo abundance index. *SSB* was estimated to have declined steadily from the start of the fishery in 1990 to about 2002, increased slightly by about 2006, remained stable until around 2015, and increased slightly after this (A6. 2). This increase in *SSB* since the early 2000s is quite different from the stock trends estimated by the other models examined. Above average year class strengths were estimated in 2002, 2003, 2013, 2014, and 2017 (A6. 2). Estimated selectivity curves (A6. 3) were consistent with our expectation of changes in sex ratio in relation to model time step. MPD estimates of trawl and photo survey catchability were within the prior distribution (A6. 4), and the *San Tongariro* survey catchability was greater than that of the *Kaharoa*. As with the other models, fits to the individual observer length frequency distributions were variable (e.g., A6. 5), but overall residual plots by length or year (e.g., A6. 6) were reasonable. Fits to length distributions from trawl surveys were better (A6. 14 and 17), although residuals showed some patterns (A6. 15). Individual fits to the length frequency distributions of scampi observed emerged from burrows in the photographic survey were variable (A6. 20) but overall residuals were acceptable (A6. 21).

The overall likelihood profile when B_0 is fixed was quite U shaped (A6. 22), with some signal appearing to come from abundance indices and priors (and particularly *q-Scampi*).

MCMC runs

MCMC diagnostics provided reasonable evidence the model converged (A6. 23–A6. 25), although some of the individual parameter traces were not as stable as for the other models. Posterior distributions of the survey catchability estimates showed some divergence from the median for the prior (A6. 26). The posterior trajectory of the *SSB* (Figure 58) suggests a steadily declining trend from the start of the fishery until 2003, a slight increase after 2005, followed by a slight decline to 2013, followed by an increase to 2019. In 2004 the median estimate of stock status (SSB_{2004}/SSB_0) was 54% (95% confidence interval 42%–69%). In 2013 the median estimate of stock status (SSB_{2013}/SSB_0) was 57% (95% confidence interval 44%–69%). The median estimate of current stock status (SSB_{2019}/SSB_0) is 66% (95% confidence interval 51%–81%), with 0% probability that SSB_{2019} is below 40% SSB_0.

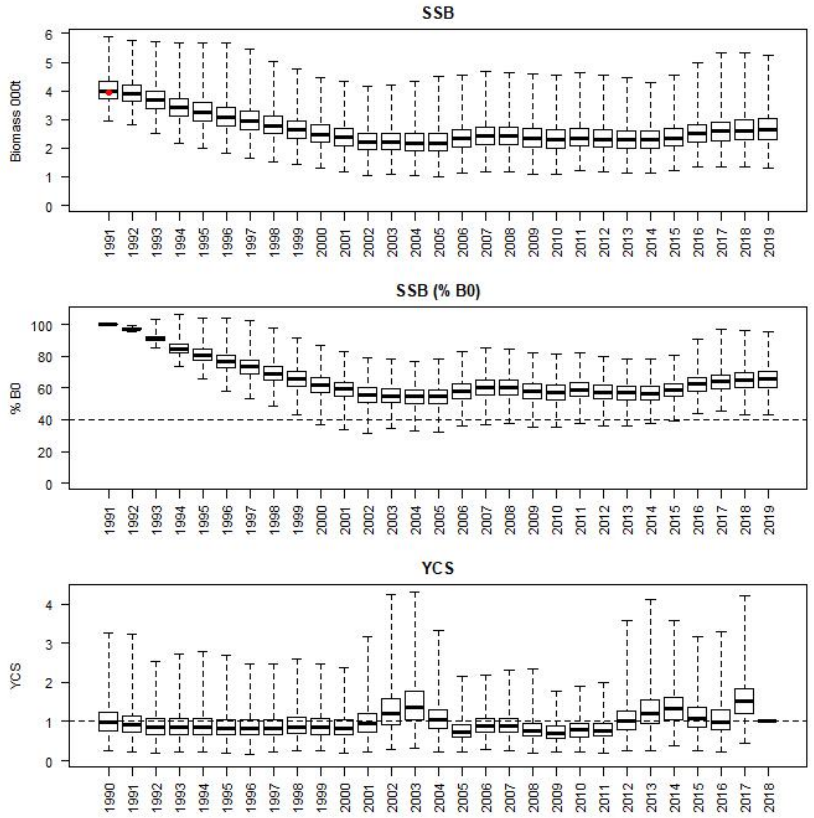

Figure 58: Posterior trajectories of *SSB*, SSB/SSB_0, and YCS from the MCMC run for the SCI 6A CPUE excluded model. Red dot represents MPD estimate of SSB_0.

4.4 Fishing Pressure (Base model)

Annual fishing intensity (equivalent annual *F*) and the level of fishing that, if applied for ever, would result in an equilibrium biomass of 40% SSB_0 (*F* 40% B_0) were calculated using methods described by Cordue (2012). Plots of annual fishing intensity against proportion SSB_0 (Figure 59) show that *SSB* declined steadily from the start of the fishery to 2012 but has increased slightly since this time. Over the same period, fishing intensity increased to 2008, declined to about half the 2008 level by 2015, but then increased significantly to 2017 and declined slightly by 2019. Throughout the fishery, the *SSB* (median of the MCMC estimates) has remained above the 40% SSB_0 target, and though fishing intensity is currently at the higher end of estimated values for this stock, it remains below *F* 40% SSB_0.

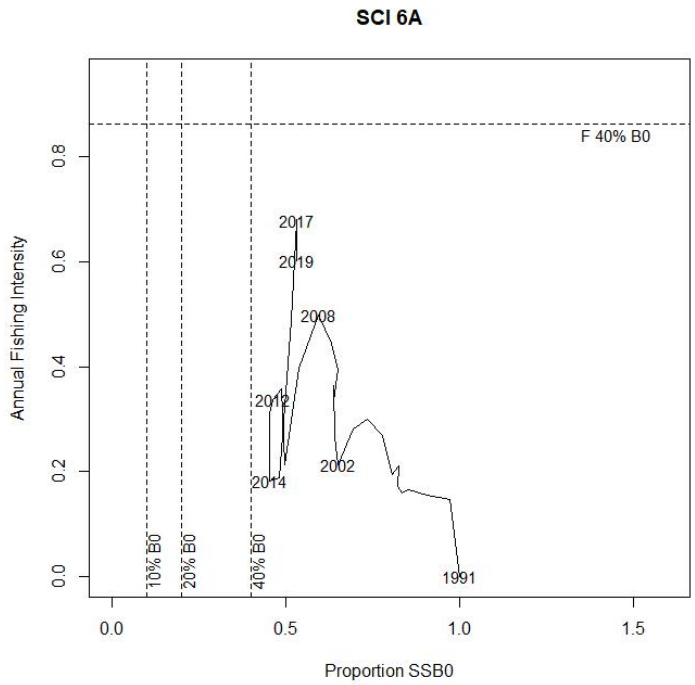

Figure 59: Trajectory of annual fishing intensity (equivalent annual *F*) plotted against proportion SSB_0 for the SCI 6A base model, in relation to Harvest Strategy Standard target and limit reference points.

4.5 Projections (Base model)

This assessment reported SSB_0 and SSB_{2019} estimates and used the ratio of current and projected *SSB* to SSB_0 as preferred indicators. Projections were conducted up until 2025, on the basis of catch scenarios proposed by Fisheries New Zealand (recent average landings (278 t) and current TACC (306 t)) (Table 18). Future catches were allocated to time steps on the basis of averages over the last 5 years. Projections have been conducted by randomly resampling year class strengths from the last decade estimated within the model (2008–17). The probabilities of exceeding the default Harvest Strategy Standard target and limit reference points are reported (Table 19). Projected stock trajectories are shown in Figure 60.

Under both future catch scenarios, the median stock status is projected to remain above 40% SSB_0 through to 2025 (Figure 60). The estimated probability of *SSB* being below either of the limits is zero, and the probability of remaining above the 40% B_0 target remains high through to 2025 (Table 19).

Table 18: Results from MCMC runs showing SSB_0, SSB_{2019}, and *SSB* projection estimates for future years at varying catch levels for the base model for SCI 6A.

	Status quo (278 t)		TACC (306 t)	
SSB_0	3 661		3 661	
SSB_{2019}	1 950		1 950	
SSB_{2019}/SSB_0	0.53		0.53	
	Status (proportion of SSB_0)	Status (proportion of SSB_{2019})	Status (proportion of SSB_0)	Status (proportion of SSB_{2019})
SSB_{2020}	0.55	1.03	0.55	1.03
SSB_{2021}	0.56	1.06	0.56	1.04
SSB_{2022}	0.56	1.05	0.55	1.03
SSB_{2023}	0.55	1.04	0.54	1.00
SSB_{2024}	0.54	1.02	0.52	0.98
SSB_{2025}	0.53	1.00	0.51	0.95

Table 19: Results from MCMC runs for the base for SCI 6A, showing probabilities of projected spawning stock biomass exceeding the default Harvest Strategy Standard target and limit reference points.

	Status quo (278 t)				TACC (306 t)			
	Pr < 10% SSB_0	Pr < 20% SSB_0	Pr > 40% SSB_0	Pr > SSB_{2019}	Pr < 10% SSB_0	Pr < 20% SSB_0	Pr > 40% SSB_0	Pr > SSB_{2019}
2020	0.00	0.00	1.00	0.84	0.00	0.00	1.00	0.82
2021	0.00	0.00	0.99	0.76	0.00	0.00	0.99	0.69
2022	0.00	0.00	0.98	0.68	0.00	0.00	0.96	0.60
2023	0.00	0.00	0.95	0.61	0.00	0.00	0.92	0.52
2024	0.00	0.00	0.93	0.55	0.00	0.00	0.88	0.45
2025	0.00	0.00	0.89	0.49	0.00	0.00	0.83	0.39

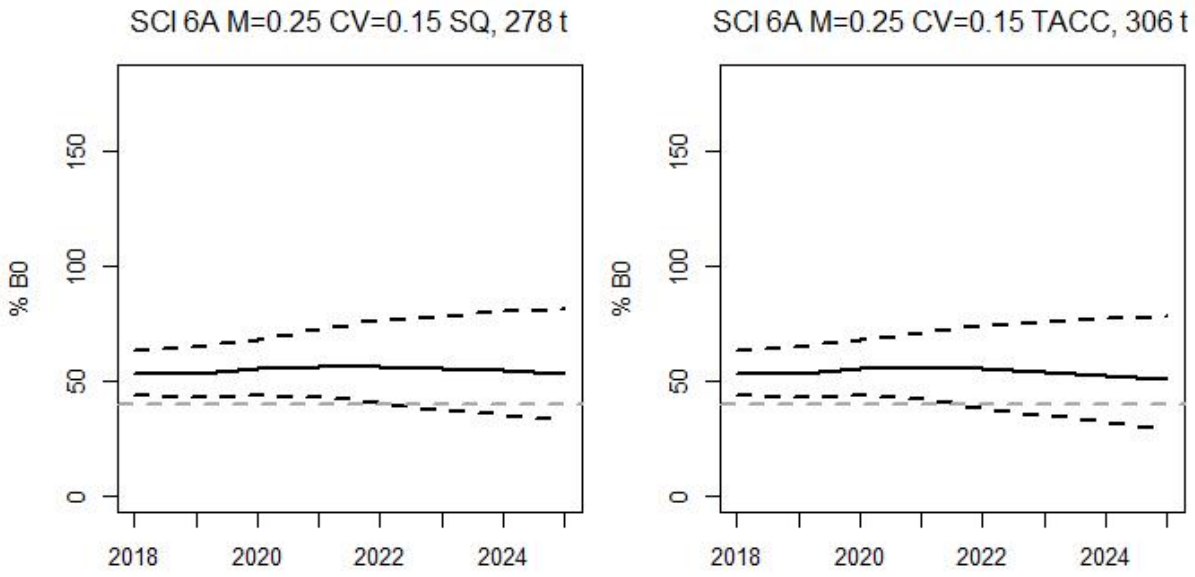

Figure 60: Projected stock trajectory (as a % of SSB_0) for SCI 6A from the base model for recent average landings (left) and the TACC (right). Solid black line represents median of projections, and dashed black lines represent 2.5th and 97.5th quantiles. Horizontal dashed grey line represents 40% SSB_0.

5. DISCUSSION

An assessment of the SCI 6A stock was last conducted in 2017 (Tuck 2017), and the current study has progressed this assessment by updating the catchability priors. The assessment was accepted.

A base model was developed with *M* fixed at 0.25 and lognormal prior distributions for survey catchability *q*s were informed by analysis of acoustic tagging of scampi to track emergence rates (Tuck et al. 2015b) and seabed observations that recorded the ratio of visible scampi in and out of burrows. Sensitivity to catchability priors, *M*, and inclusion of abundance indices were examined in the model development, and a subset of the sensitivities have been described in more detail, representing the range examined. Projections were conducted up until 2025 on the basis of recent average landings and the TACC as future constant catch scenarios.

Although SSB_0 and stock status estimates were sensitive to the assumed value of *M*, halving the catchability priors had a greater effect on SSB_0, and though the stock status followed a higher trajectory, it followed a similar fluctuating declining trend and more recent increase to the base and *M* sensitivity models. The model excluding the CPUE series showed a markedly different pattern, declining in the

first decade of the fishery, but remaining more stable after this. The CPUE series provides the longest abundance index for this stock (1995–2019) whereas the surveys only started in 2007, and the longer-term trends in the other models are largely driven by the CPUE data.

The median estimates of SSB_{2019}/SSB_0 from the base model was 53% (95% confidence interval 43%–65%), whereas the sensitivities estimated SSB_{2019}/SSB_0 between 47% and 68% (median values). Patterns of estimated YCS were similar between the models including CPUE data (the differences relating to YCS estimates at the start of the series), and all models estimated a strong year class in 2017. Projections out to 2025 suggested that *SSB* would remain above 40% SSB_0 with future catches at the level of the TACC (83% probability of SSB_{2025} exceeding 40% SSB_0, and 39% probability of SSB_{2025} exceeding SSB_{2019}).

6. ACKNOWLEDGMENTS

This work was funded by Fisheries New Zealand under project SCI201902 and builds on a series of scampi assessment projects funded by the predecessors of Fisheries New Zealand (e.g., Ministry of Fisheries, Ministry for Primary Industries). We thank the many NIWA and Ministry of Fisheries and Ministry for Primary Industries staff who measured scampi over the years, and the members of the NIWA scampi image reading team. Model progress this year benefitted considerably from the constructive comments of the Deepwater Working Group. This report was reviewed by Bruce Hartill (NIWA).

7. REFERENCES

Bell, M.C.; Redant, F.; Tuck, I.D. (2006). Nephrops species. In: B. Phillips (Ed). *Lobsters: Biology, Management, Aquaculture and Fisheries*. Blackwell Publishing, Oxford: 412–461.

Bentley, N.; Kendrick, T.H.; Starr, P.J.; Breen, P.A. (2012). Influence plots and metrics: tools for better understanding fisheries catch-per-unit-effort standardisations. *ICES Journal of Marine Science 69*: 84–88.

Bull, B.; Dunn, A. (2002). Catch-at-age: User manual v 1.06.2002/09/12. *NIWA Internal Report 114*. 23 p.

Bull, B.; Francis, R.I.C.C.; Dunn, A.; McKenzie, A.; Gilbert, D.J.; Smith, M.H.; Bian, R. (2008). CASAL (C++ algorithmic stock assessment laboratory): CASAL user manual v2.20-2008/02/14. *NIWA Technical Report No. 130*. 276 p.

Bull, B.; Francis, R.I.C.C.; Dunn, A.; McKenzie, A.; Gilbert, D.J.; Smith, M.H.; Bian, R.; Fu, D. (2012). CASAL (C++ algorithmic stock assessment laboratory): CASAL user manual v2.30-2012/03/21. *NIWA Technical Report No. 135*. 280 p.

Carter, D. (2003). Inquiry into the administration and management of the scampi fishery. New Zealand House of Representatives Report to the Primary Production Committee. 226 p.

Charnov, E.L.; Berrigan, D.; Shine, R. (1983). The M/*k* ratio is the same for fish and reptiles. *American Naturalist 142*: 707–711.

Clark, W.G.; Hare, S.R. (2006). Assessment and management of Pacific halibut: data, methods, and policy. *International Pacific Halibut Commission Scientific Report No. 83*. 104 p.

Cordue, P.L. (2012). Fishing intensity metrics for use in overfishing determination. *ICES Journal of Marine Science: Journal du Conseil 69(4)*: 61–-623. 10.1093/icesjms/fss036.

Cryer, M. (2000). A consideration of current management areas for scampi in QMAs 3, 4, 6A and 6B. Final Research Report for Ministry of Research Project MOF199904K Objective 1. 52 p. (Unpublished report held by Fisheries New Zealand.)

Cryer, M.; Coburn, R. (2000). Scampi stock assessment for 1999. *New Zealand Fisheries Assessment Report 2000/7*. 61 p.

Cryer, M.; Dunn, A.; Hartill, B. (2005). Length-based population model for scampi (Metanephrops challengeri) in the Bay of Plenty (QMA 1). *New Zealand Fisheries Assessment Report 2005/27*. 56 p.

Cryer, M.; Stotter, D.R. (1999). Movement and growth rates of scampi inferred from tagging, Alderman Islands, western Bay of Plenty. *NIWA Technical Report 49*. 36 p.

Fenaughty, C. (1989). Reproduction in *Metanephrops challengeri*. Unpubl. Rep. MAF Fisheries, Wellington. 46 p. (Unpublished report held by NIWA library, Wellington.)

Fisheries New Zealand (2020). Fisheries Assessment Plenary, May 2020: stock assessments and stock status. Compiled by the Fisheries Science and Information Group, Fisheries New Zealand, Wellington, New Zealand. 1746 p.

Francis, R.I.C.C. (1999). The impact of correlations in standardised CPUE indices. New Zealand Fisheries Assessment Research Document 99/42. 31 p. (Unpublished report held by NIWA library, Wellington.)

Francis, R.I.C.C. (2011). Data weighting in statistical fisheries stock assessment models. *Canadian Journal Fisheries and Aquatic Science 68*: 1124–1138.

Francis, R.I.C.C.; Rasmussen, S.; Fu, D.; Dunn, A. (2016). CALA: Catch-at-length and -age user manual, CALA v1.00. National Institute of Water & Atmospheric Research Ltd. 92 p. (Unpublished report held by NIWA library, Wellington.)

McCarthy, A.; Tuck, I.; Jeffs, A. (2018). Estimates for the size at onset of maturity for New Zealand scampi (*Metanephrops challengeri*). *Bulletin of Marine Science 94(3)*: 699–718. doi.org/10.5343/bms.2017.1122.

McCullagh, P.; Nelder, J.A. (1989). *Generalised Linear Models*. Chapman and Hall, London: 511 p.

Morizur, Y. (1982). Estimation de la mortalité pour quelques stocks de langoustine, *Nephrops norvegicus*. ICES CM, 1982/K:10. 19 p.

Pauly, D. (1980). On the interrelationships between natural mortality, growth parameters, and mean environmental temperature in 175 fish stocks. *Journal du Conseil International pour l'Exloration du Mer 39*: 1751–92.

Starr, P.J. (2009). Rock lobster catch and effort data: summaries and CPUE standardisations, 1979–80 to 2007–08. *New Zealand Fisheries Assessment Report 2009/38.* 72 p.

Starr, P.J.; Breen, P.A.; Kendrick, T.H.; Haist, V. (2009). Model and data used for the 2008 stock assessment of rock lobsters (*Jasus edwardsii*) in CRA 3. *New Zealand Fisheries Assessment Report 2009/22*. 62 p.

Tuck, I.D. (2009). Characterisation of scampi fisheries and the examination of catch at length and spatial distribution of scampi in SCI 1, 2, 3, 4A and 6A. *New Zealand Fisheries Assessment Report 2009/27*. 102 p.

Tuck, I.D. (2010). Scampi burrow occupancy, burrow emergence and catchability. *New Zealand Fisheries Assessment Report 2010/13*. 58 p.

Tuck, I.D. (2013). Characterisation and length-based population model for scampi (*Metanephrops challengeri*) on the Mernoo Bank (SCI 3). *New Zealand Fisheries Assessment Report 2013/24*. 165 p.

Tuck, I.D. (2014). Characterisation and length-based population model for scampi (*Metanephrops challengeri*) in the Bay of Plenty (SCI 1) and Hawke Bay/Wairarapa (SCI 2). *New Zealand Fisheries Assessment Report 2014/33*. 172 p.

Tuck, I.D. (2015). Characterisation and length-based population model for scampi (*Metanephrops challengeri*) at the Auckland Islands (SCI 6A). *New Zealand Fisheries Assessment Report 2015/21*. 164 p.

Tuck, I.D. (2016a). Characterisation and length-based assessment model for scampi (*Metanephrops challengeri*) in the Bay of Plenty (SCI 1) and Hawke Bay– Wairarapa (SCI 2). *New Zealand Fisheries Assessment Report 2016/51*. 194 p.

Tuck, I.D. (2016b). Characterisation and length-based population model for scampi (*Metanephrops challengeri*) on the Mernoo Bank (SCI 3). *New Zealand Fisheries Assessment Report 2016/55*. 221 p.

Tuck, I.D. (2017). Characterisation and length-based population model for scampi (*Metanephrops challengeri*) at the Auckland Islands (SCI 6A). *New Zealand Fisheries Assessment Report 2017/56*. 180 p.

Tuck, I.D. (2019). Characterisation and a length-based assessment model for scampi (*Metanephrops challengeri*) on the Mernoo Bank (SCI 3). *New Zealand Fisheries Assessment Report 2019/61*. 246 p.

Tuck, I.D. (2020). Characterisation and length-based population model for scampi (*Metanephrops challengeri*) in the Bay of Plenty (SCI 1) and Hawke Bay/Wairarapa (SCI 2) for 2018. *New Zealand Fisheries Assessment Report 2020/06*. 299 p.

Tuck, I.D.; Atkinson, R.J.A.; Chapman, C.J. (2000). Population biology of the Norway lobster, *Nephrops norvegicus* (L.) in the Firth of Clyde, Scotland. II. Fecundity and size at onset of maturity. *ICES Journal of Marine Science 57*: 1222–1237.

Tuck, I.D.; Dunn, A. (2006). Length based population model for scampi (*Metanephrops challengeri*) in the Bay of Plenty (SCI 1) and Wairarapa / Hawke Bay (SCI 2). Final Research Report for Ministry of Research Project SCI200501 (Objectives 2 & 3). 42 p. (Unpublished report held by Fisheries New Zealand, Wellington,)

Tuck, I.D.; Dunn, A. (2009). Length-based population model for scampi (*Metanephrops challengeri*) in the Bay of Plenty (SCI 1) and Wairarapa / Hawke Bay (SCI 2). Final Research Report for Ministry of Fisheries Research Projects SCI2006-01 & SCI2008-03W Obj 1. 30 p. (Unpublished report held by Fisheries New Zealand, Wellington.)

Tuck, I.D.; Dunn, A. (2012). Length-based population model for scampi (*Metanephrops challengeri*) in the Bay of Plenty (SCI 1), Wairarapa / Hawke Bay (SCI 2) and Auckland Islands (SCI 6A). *New Zealand Fisheries Assessment Report 2012/01*. 125 p.

Tuck, I.D.; Hartill, B.; Parkinson, D.; Drury, J.; Smith, M.; Armiger, H. (2009a). Estimating the abundance of scampi - Relative abundance of scampi, *Metanephrops challengeri*, from a photographic survey in SCI 6A (2009). Final Research Report for Ministry of Fisheries research project SCI2008-01 Objectives 1 & 2. 26 p. (Unpublished report held by Fisheries New Zealand, Wellington.)

Tuck, I.D.; Hartill, B.; Parkinson, D.; Harper, S.; Drury, J.; Smith, M.; Armiger, H. (2009b). Estimating the abundance of scampi - Relative abundance of scampi, *Metanephrops challengeri*, from a photographic survey in SCI 1 and SCI 6A (2008). Final Research Report for Ministry of Fisheries Research Project SCI2007-02 Objectives 1 & 2. 37 p. (Unpublished report held by Fisheries New Zealand, Wellington.)

Tuck, I.D.; Hartill, B.; Parkinson, D.; Smith, M.; Armiger, H.; Rush, N.; Drury, J. (2011). Estimating the abundance of scampi – Relative abundance of scampi, *Metanephrops challengeri*, from photographic surveys in SCI 3 (2009 & 2010). Final Research Report for Ministry of Fisheries research projects SCI2009-01 & SCI2010-01. 29 p. (Unpublished report held by Fisheries New Zealand, Wellington.)

Tuck, I.D.; Parkinson, D.; Armiger, H.; Smith, M.; Miller, A.; Drury, J.; Spong, K. (2020). Estimating the abundance of scampi in SCI 6A (Auckland Islands) in 2019. *New Zealand Fisheries Assessment Report 2020/13*. 50 p.

Tuck, I.D.; Parkinson, D.; Armiger, H.; Smith, M.; Miller, A.; Drury, J.; Spong, K. (in press). Estimating the abundance of scampi in SCI 3 (Mernoo Bank) in 2019. Draft New Zealand Fisheries Assessment Report.

Tuck, I.D.; Parkinson, D.; Armiger, H.; Smith, M.; Miller, A.; Rush, N.; Spong, K. (2015a). Estimating the abundance of scampi in SCI 6A (Auckland Islands) in 2013. *New Zealand Fisheries Assessment Report 2015/10*. 52 p.

Tuck, I.D.; Parkinson, D.; Armiger, H.; Smith, M.; Miller, A.; Rush, N.; Spong, K. (2017). Estimating the abundance of scampi in SCI 6A (Auckland Islands) in 2016. *New Zealand Fisheries Assessment Report 2017/06*. 40 p.

Tuck, I.D.; Parkinson, D.; Drury, J.; Armiger, H.; Miller, A.; Rush, N.; Smith, M.; Hartill, B. (2013). Estimating the abundance of scampi - Relative abundance of scampi, *Metanephrops challengeri*, from a photographic survey in SCI 1 and SCI 2 (2012). Final Research Report for Ministry of Fisheries Research Project SCI201002A. 54 p. (Unpublished report held by Fisheries New Zealand, Wellington.)

Tuck, I.D.; Parkinson, D.; Hartill, B.; Drury, J.; Smith, M.; Armiger, H. (2007). Estimating the abundance of scampi - relative abundance of scampi, *Metanephrops challengeri*, from a photographic survey in SCI 6A (2007). Final Research Report for Ministry of Fisheries Research Project SCI2006/02 Objectives 1 & 2. 29 p. (Unpublished report held by Fisheries New Zealand, Wellington.)

Tuck, I.D.; Parsons, D.M.; Hartill, B.W.; Chiswell, S.M. (2015b). Scampi (*Metanephrops challengeri*) emergence patterns and catchability. *ICES Journal of Marine Science 72 (Supplement 1)*: i199-i210. http://icesjms.oxfordjournals.org/content/early/2015/01/08/icesjms.fsu244.abstract.

Vignaux, M. (1994). Catch per unit effort (CPUE) analysis of west coast South Island and Cook Strait spawning hoki fisheries, 1987–93. New Zealand Fisheries Assessment Research Document 94/11. 29 p. (Unpublished report held by NIWA library, Wellington.)

Wear, R.G. (1976). Studies on the larval development of *Metanephrops challengeri* (Balss, 1914) (Decapoda, Nephropidae). *Crustaceana* 30: 113–122.

APPENDIX 1. CPUE standardisation diagnostics

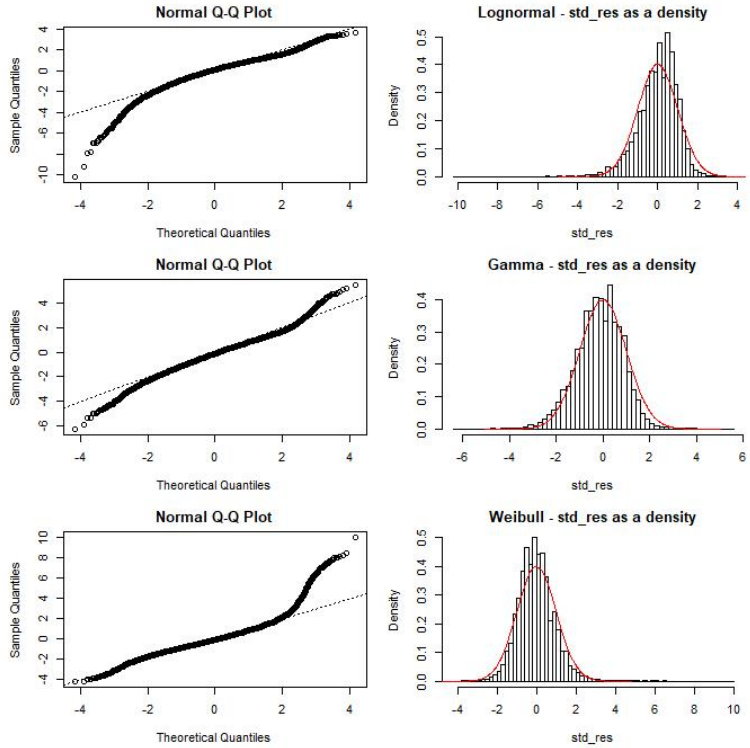

A1. 1: Plots of the distributions of standardised residuals for simple standardised CPUE models of positive catch for SCI 6A with log normal (top panel), gamma (middle panel), and Weibull (bottom panel) error distributions.

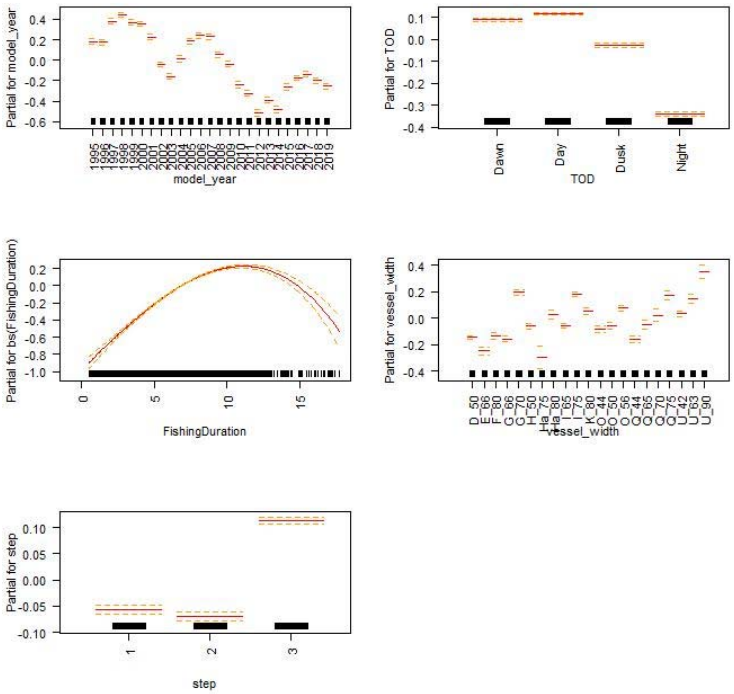

A1. 2: Termplot for annual SCI 6A positive catch CPUE standardisation model (Table 4).

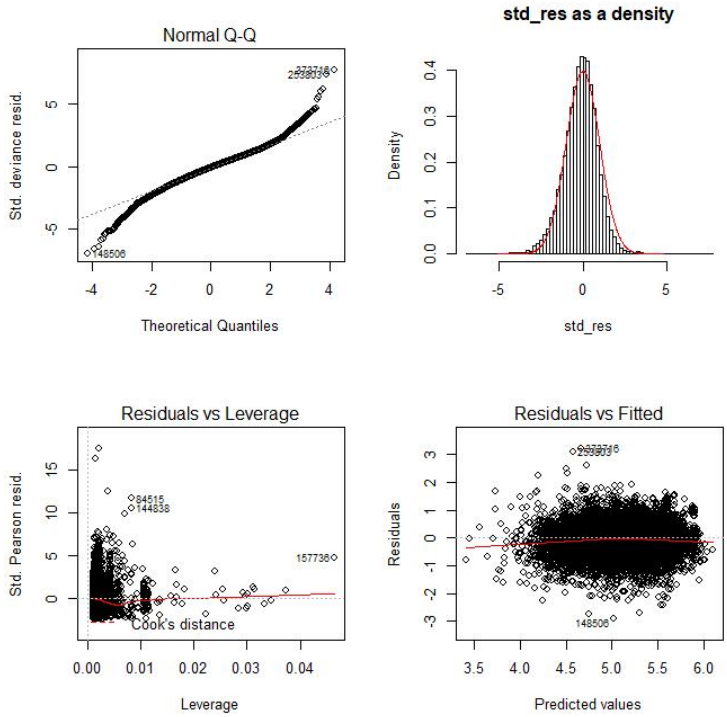

A1. 3: Diagnostic plots for final SCI 6A positive catch CPUE standardisation model (Table 4).

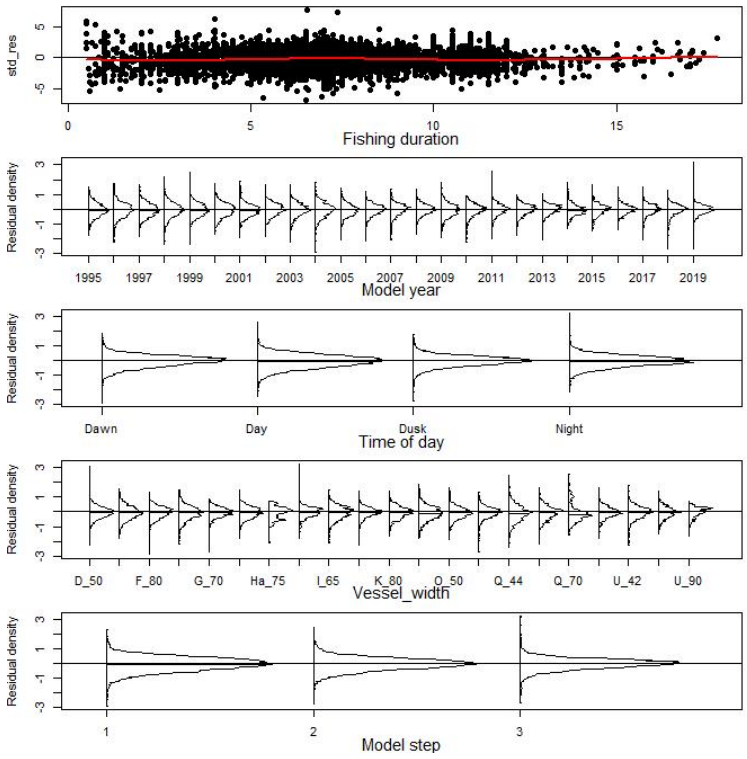

A1. 4: Distributions of residuals for annual SCI 6A positive catch CPUE standardisation model (Table 4).

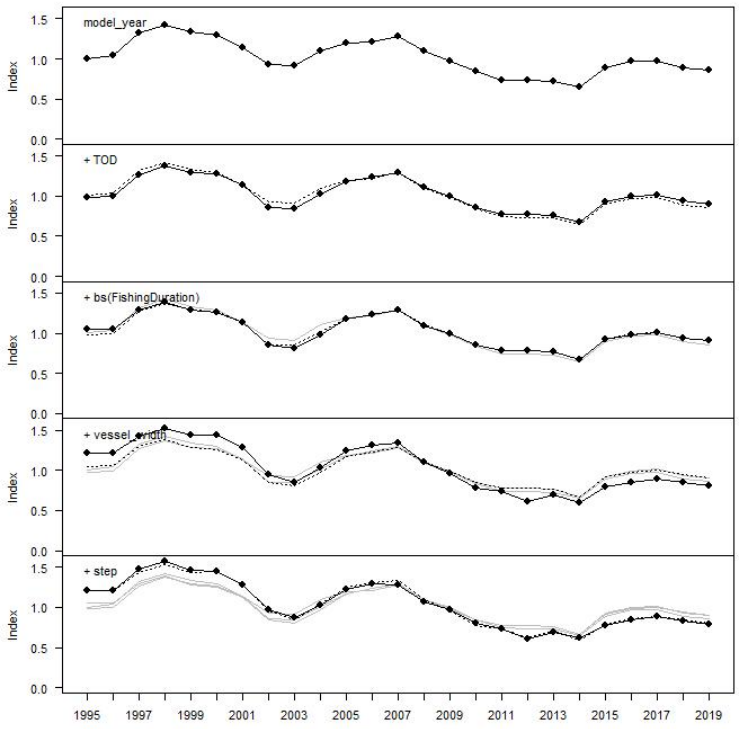

A1. 5: Step influence plot for annual SCI 6A positive catch CPUE standardisation model (Table 4).

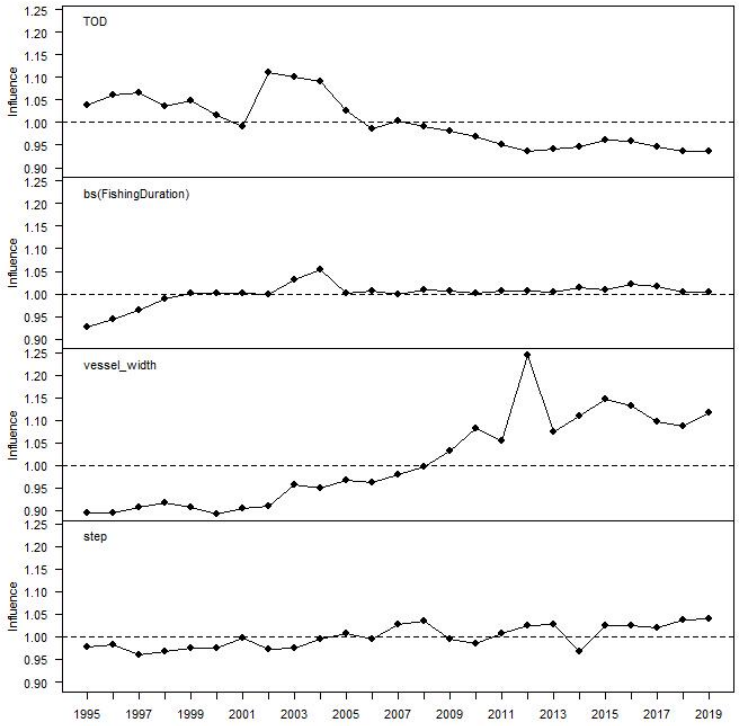

A1. 6: Year influence plots for each explanatory variable for annual SCI 6A CPUE standardisation model (Table 4).

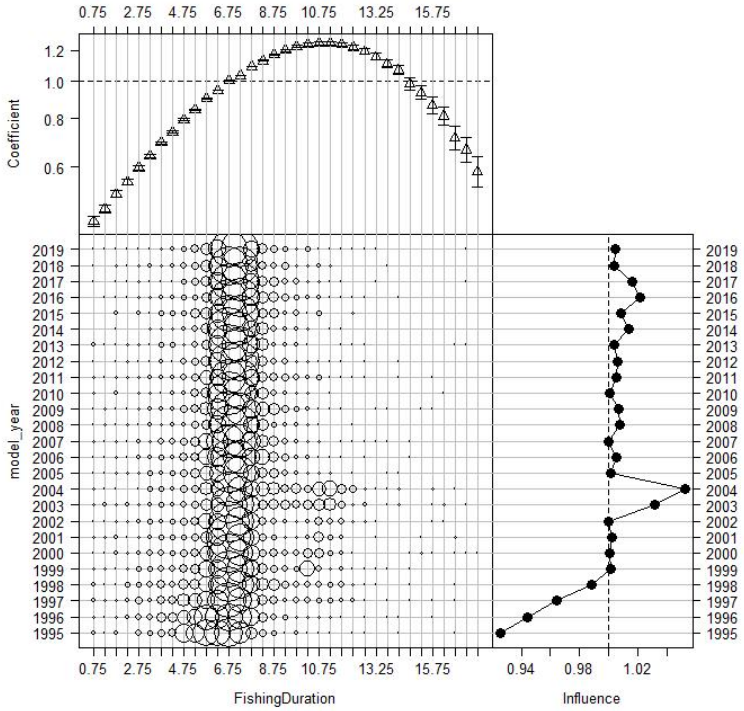

A1. 7: Coefficient-distribution influence plot for effort (fishing duration) for annual SCI 6A CPUE standardisation model (Table 4).

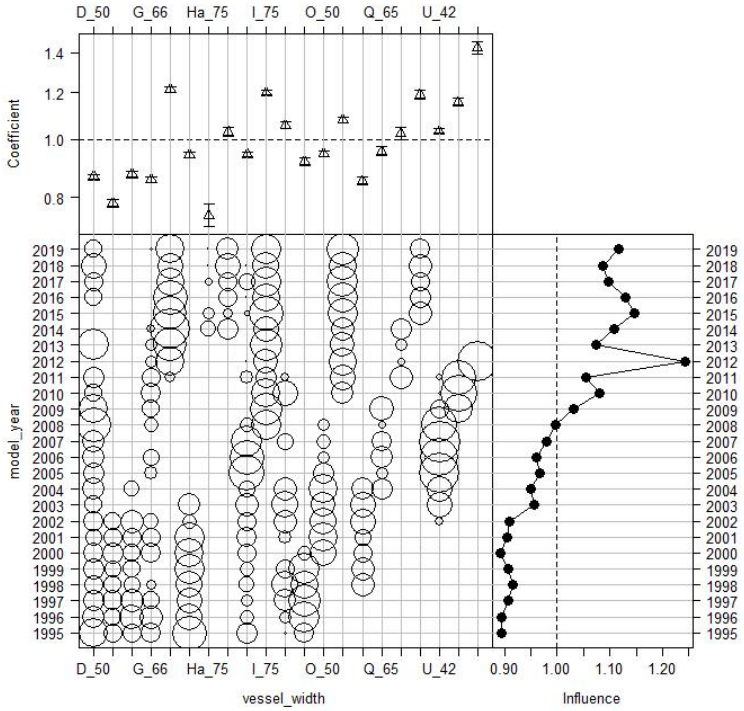

A1. 8: Coefficient-distribution influence plot for vessel_width for annual SCI 6A CPUE standardisation model (Table 4).

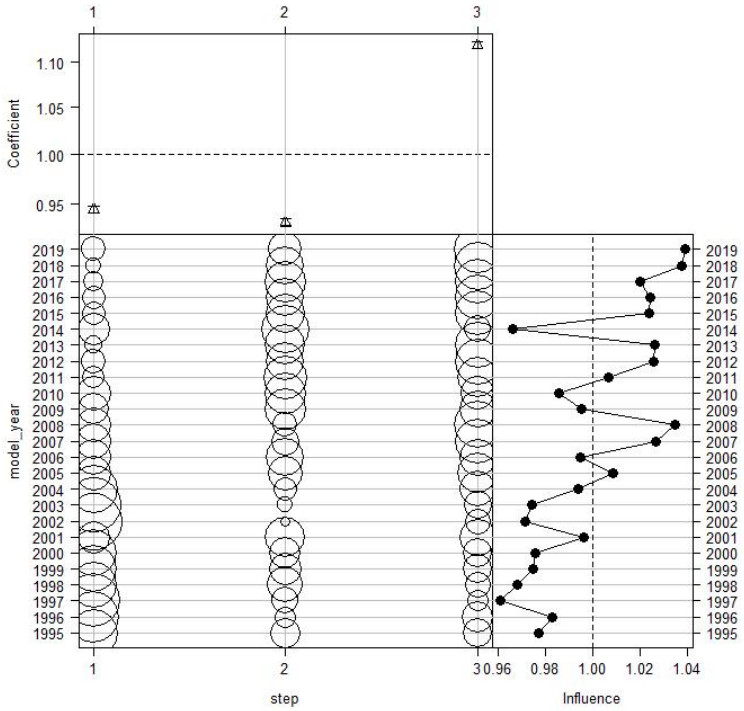

A1. 9: Coefficient-distribution influence plot for time step for annual SCI 6A positive catch CPUE standardisation model (Table 4).

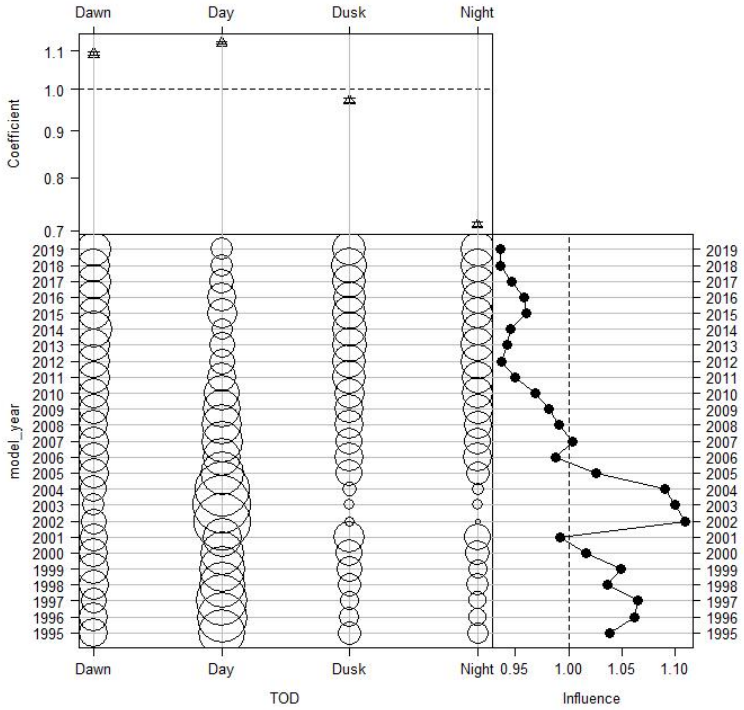

A1. 10: Coefficient-distribution influence plot for time of day for annual SCI 6A positive catch CPUE standardisation model (Table 4).

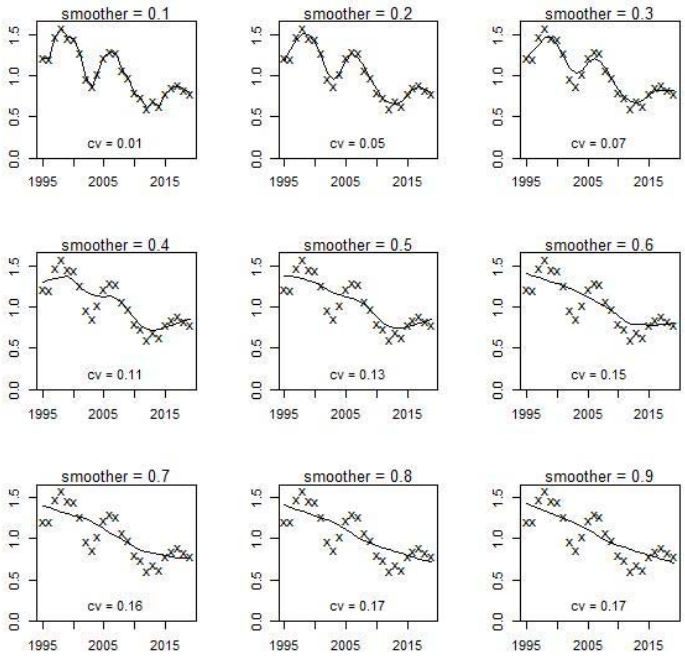

A1. 11: Range of smoothers fitted to index from the annual SCI 6A CPUE standardisation model (Table 4).

APPENDIX 2. Analysis of length composition data

Trawl survey length frequency

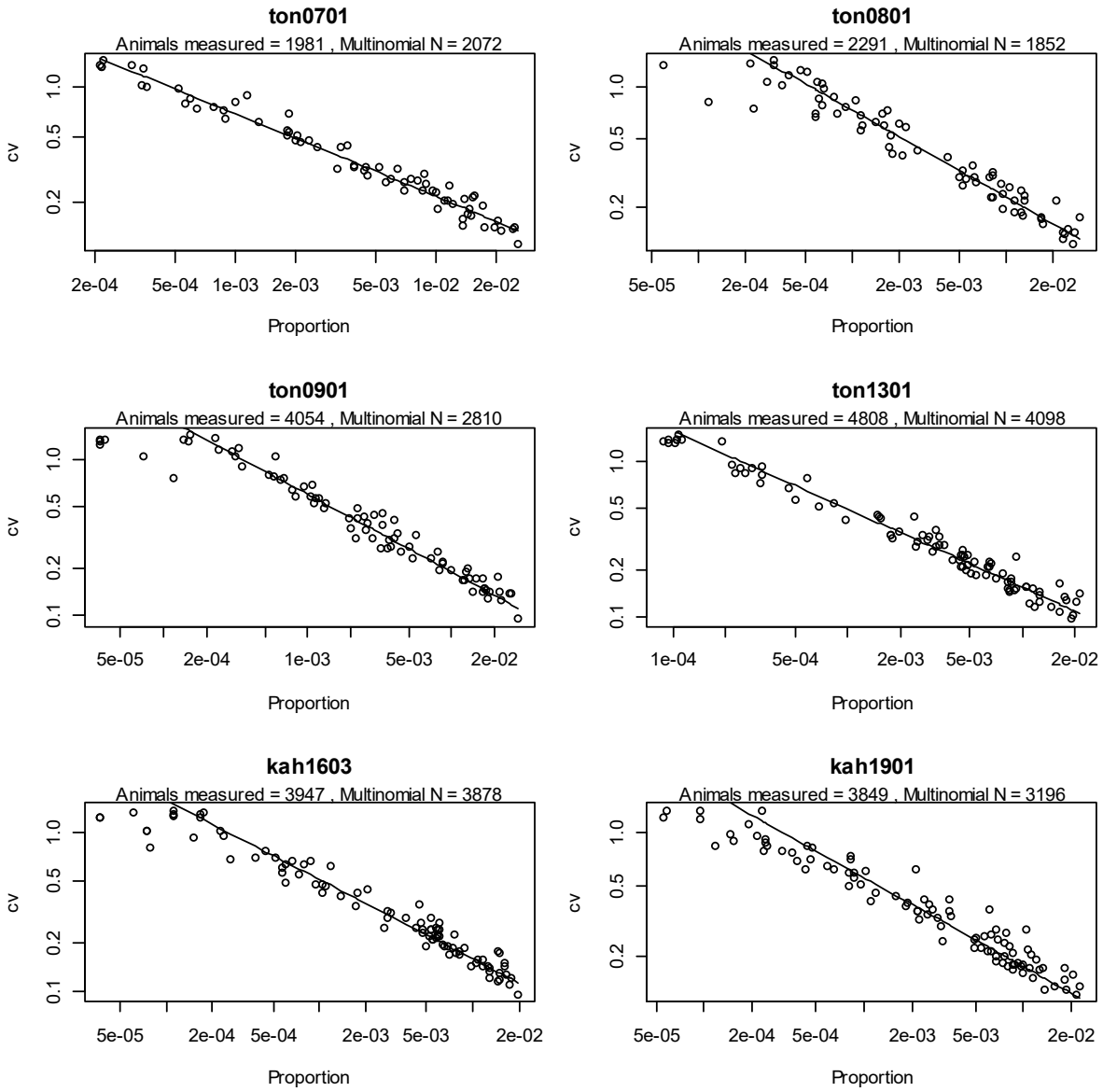

A2. 1: Observation-error CVs for the trawl survey proportions-at-length data sets. Each point represents a proportion at a specific length and sex for a given year. The diagonal line, which is the same in each panel, is added to aid comparison between panels; it shows the relationship between proportion and CV that would hold with simple multinomial sampling with sample size 500.

Observer length frequency

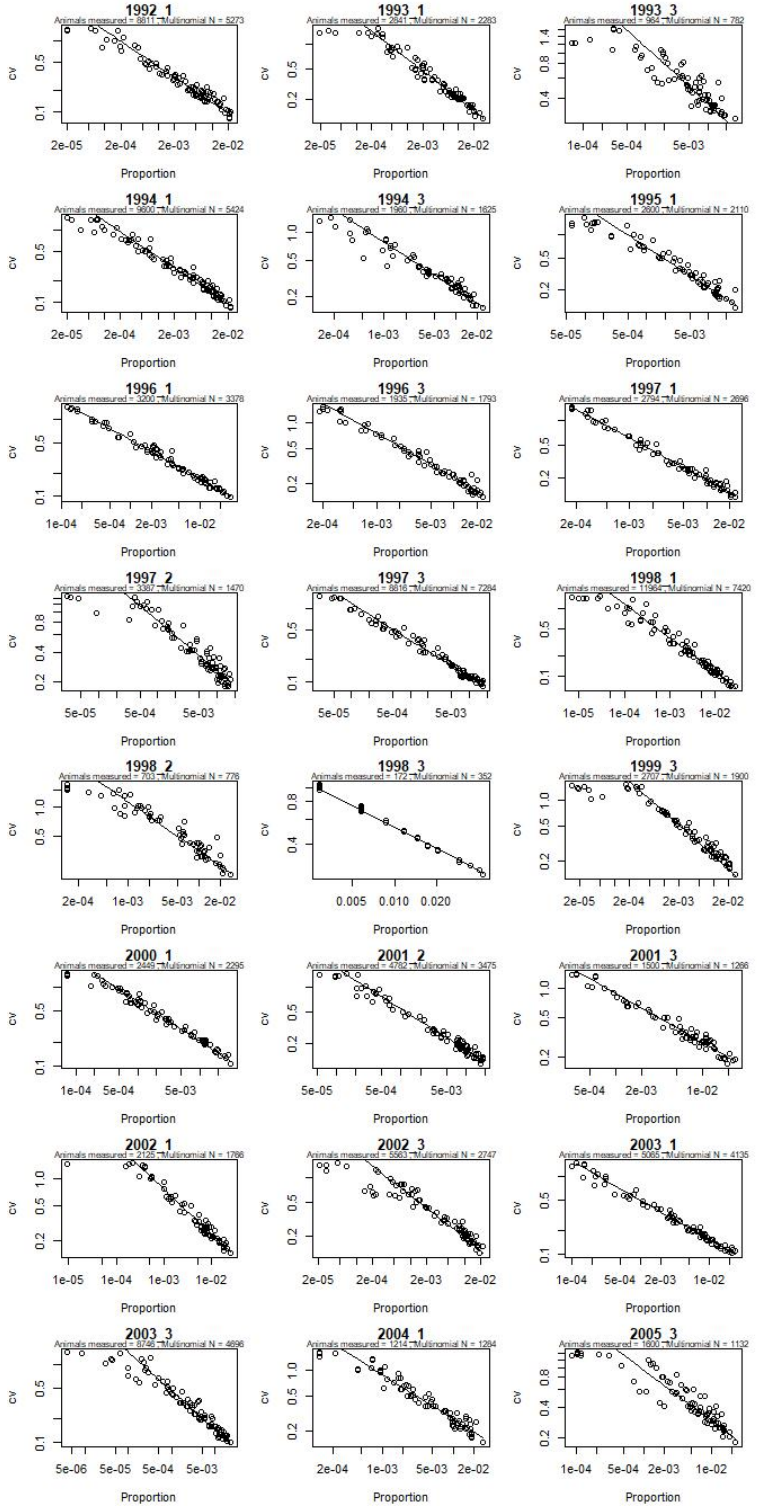

A2. 2: Observation-error CVs for the observer proportions-at-length data sets. Each point represents a proportion at a specific length and sex for a given year. The diagonal line, which is the same in each panel, is added to aid comparison between panels; it shows the relationship between proportion and CV that would hold with simple multinomial sampling with sample size 500.

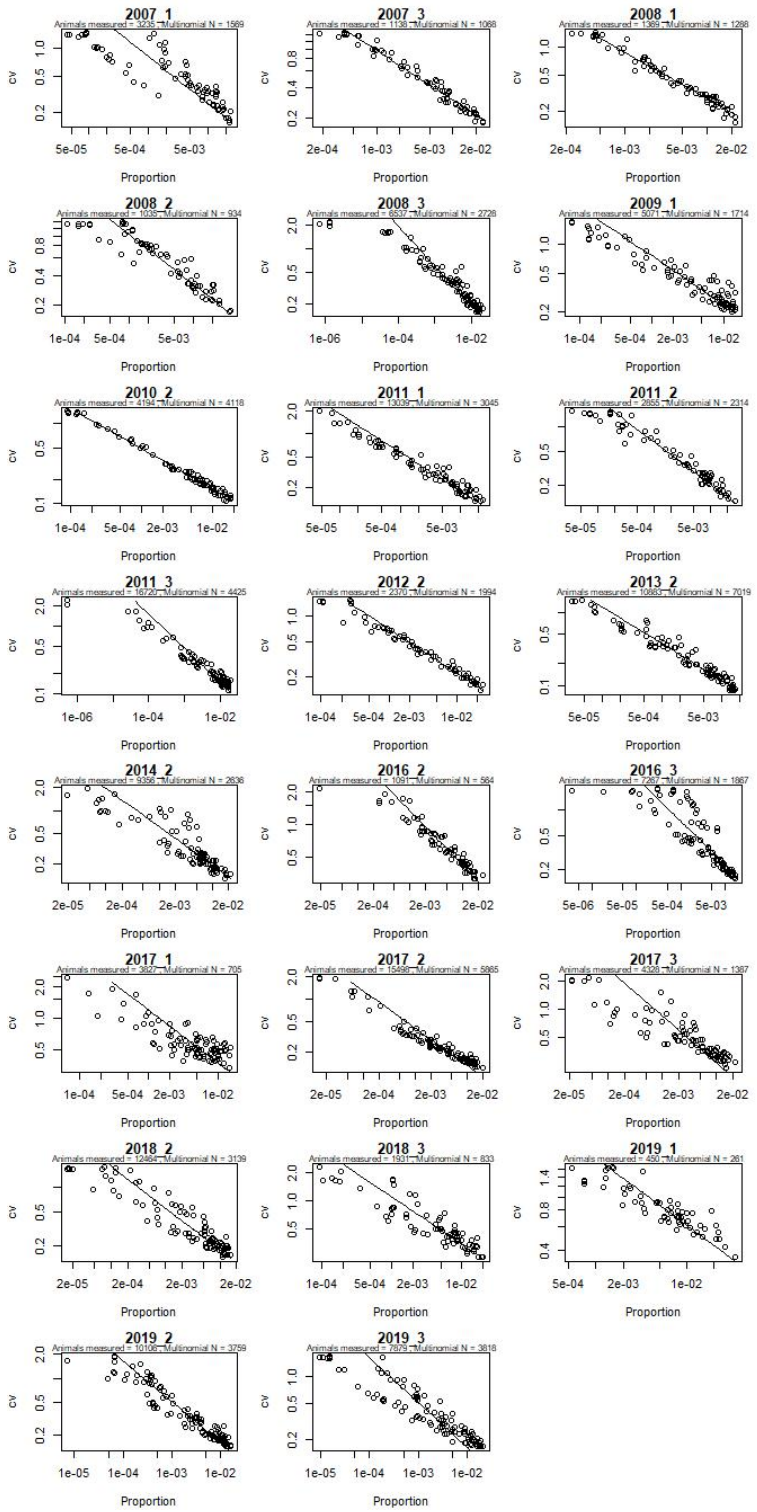

A2. 2(continued): Observation-error CVs for the observer proportions-at-length data sets. Each point represents a proportion at a specific length and sex for a given year. The diagonal line, which is the same in each panel, is added to aid comparison between panels; it shows the relationship between proportion and CV that would hold with simple multinomial sampling with sample size 500.

Photo survey

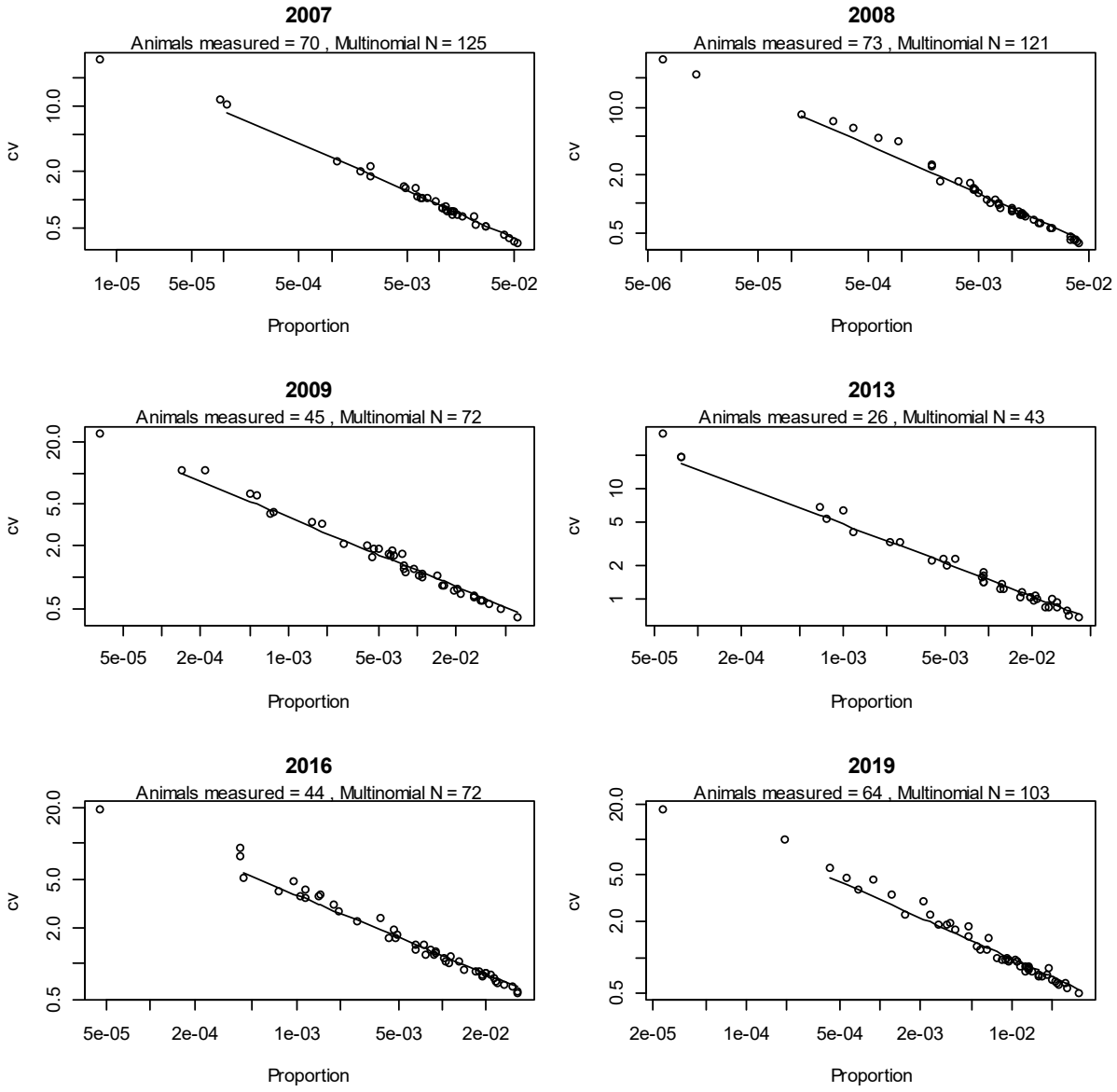

A2. 3: Observation-error CVs for the photo survey proportions-at-length data sets. Each point represents a proportion at a specific length for a given year. The diagonal line, which is the same in each panel, is added to aid comparison between panels; it shows the relationship between proportion and CV that would hold with simple multinomial sampling with sample size 500.

APPENDIX 3. SCI 6A Base model plots

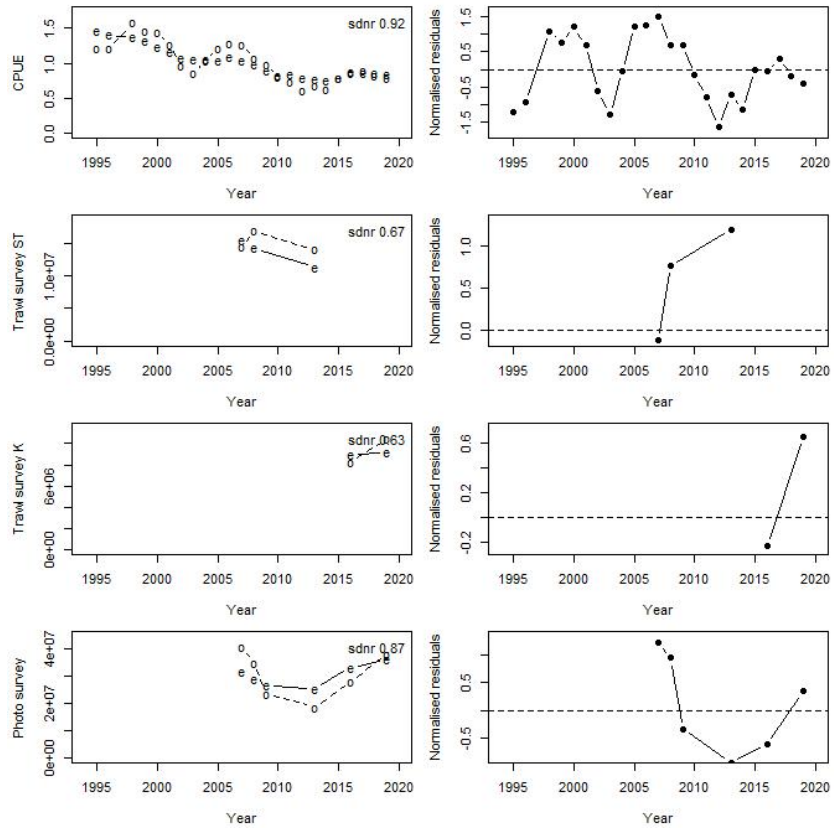

A3. 1: Fits to abundance indices (left column) and normalised residuals (right column) for standardised CPUE index (top row) *San Tongariro* (ST) trawl survey abundance index (second row), *Kaharoa* (K) trawl survey abundance index (third row), and photo survey emerged scampi abundance index for the SCI 6A base model.

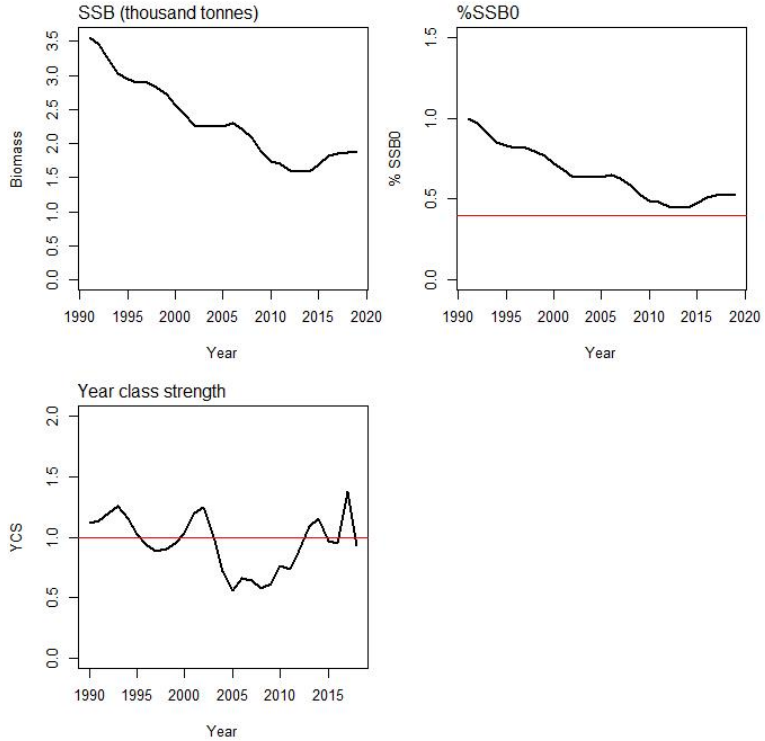

A3. 2: Spawning stock biomass trajectory (upper left), stock status (upper right), and year class strength (lower left) for the SCI 6A base model.

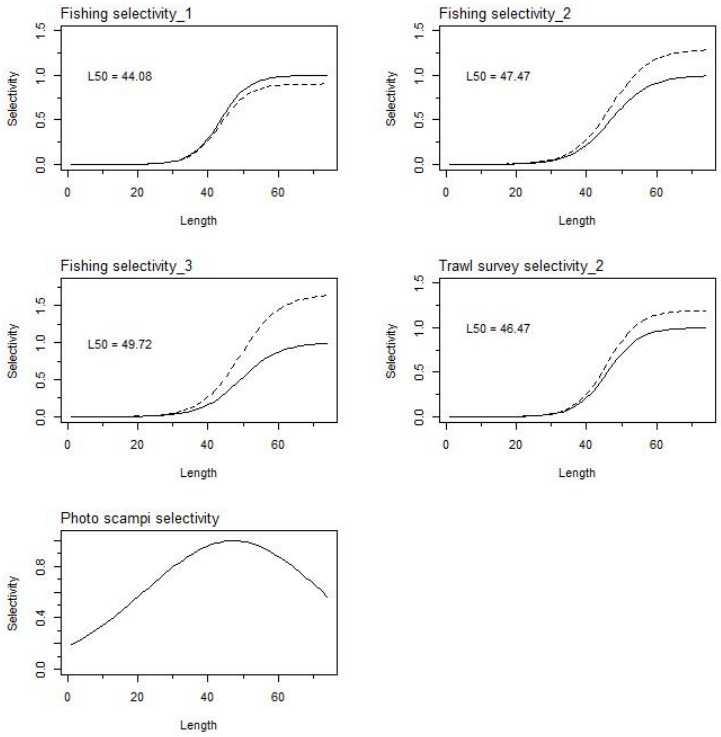

A3. 3: Fishery and survey selectivity curves for SCI 6A base model. Solid line – females, dotted line – males. The scampi photo index is not sexed, and a single selectivity applies.

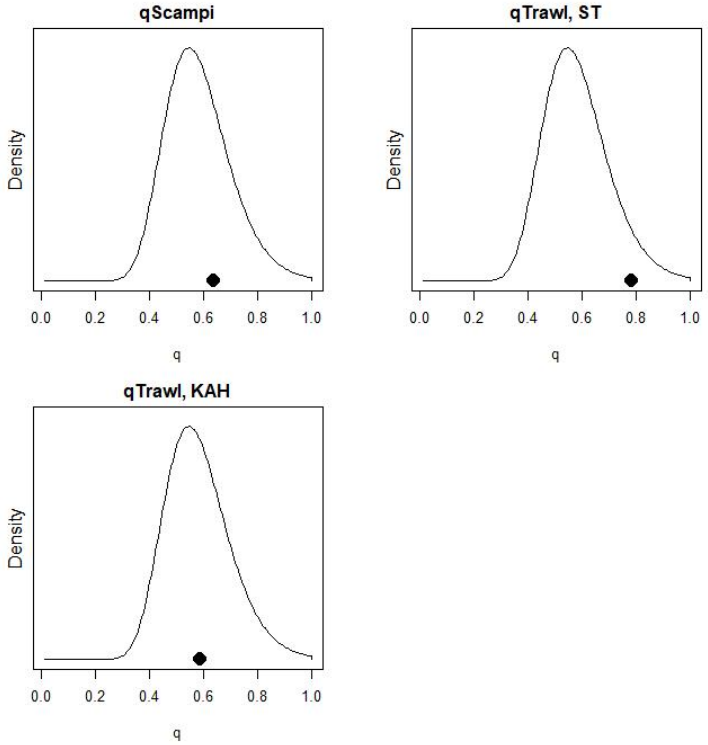

A3. 4: Catchability estimates from MPD model run, plotted in relation to prior distribution for SCI 6A base model.

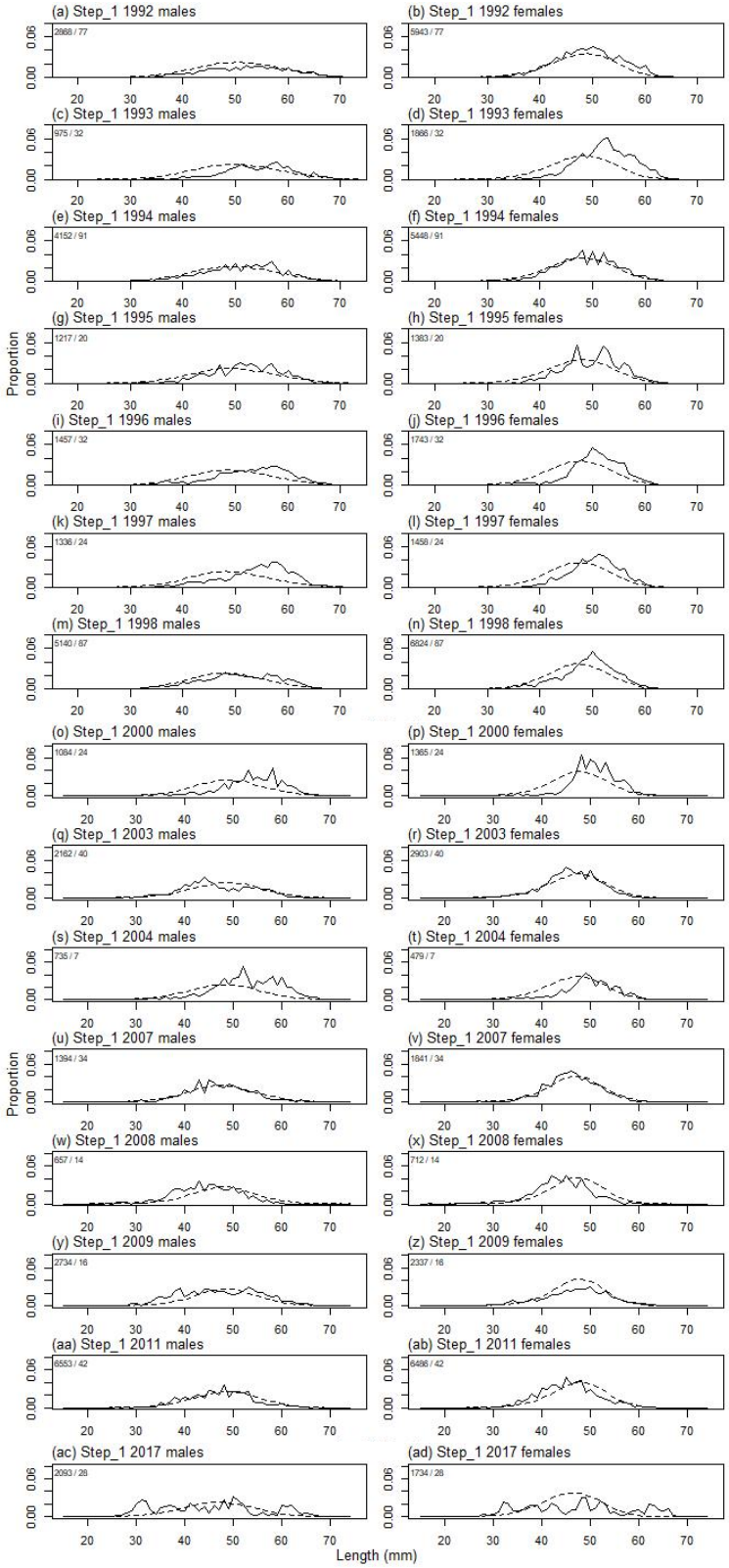

A3. 5: Observed (solid line) and fitted (dashed line) length frequency distributions from observer samples, time step 1 for the SCI 6A base model. Numbers in top left corner of each plot represent number of scampi measured / number of events sampled.

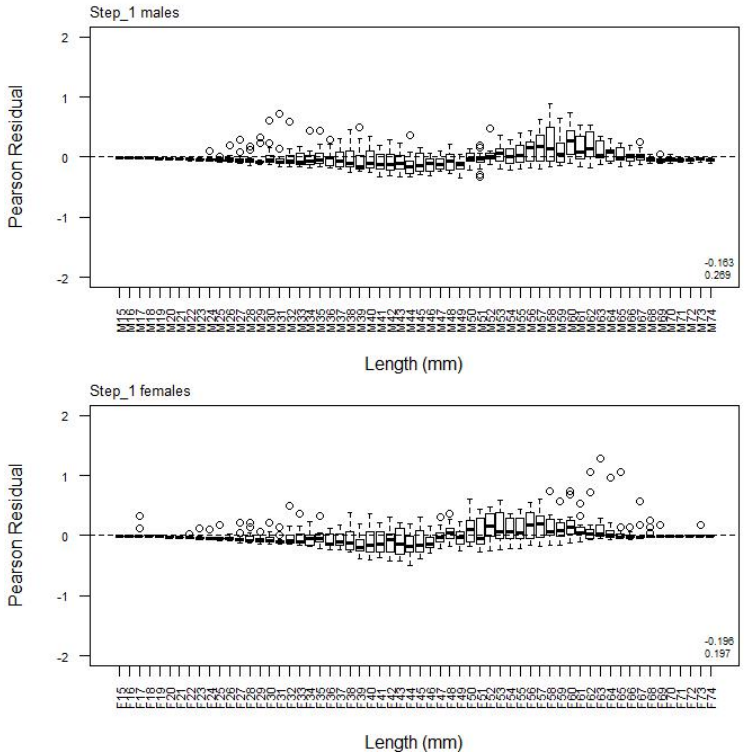

A3. 6: Box plots of Pearson residuals from the fit to length frequency distributions by length from observer sampling by sex for time step 1 for the SCI 6A base model.

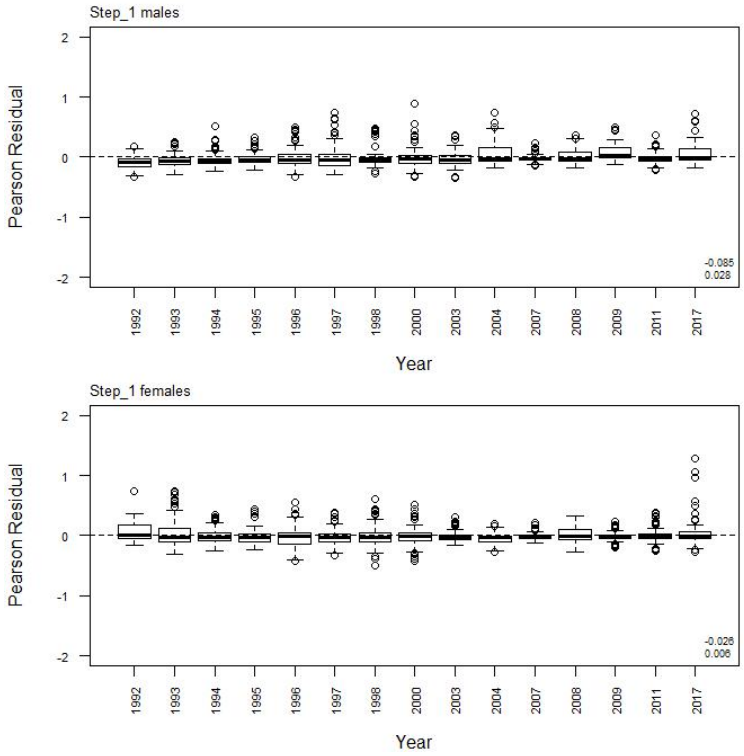

A3. 7: Box plots of Pearson residuals from the fit to length frequency distributions by year from observer sampling by sex for time step 1 for the SCI 6A base model.

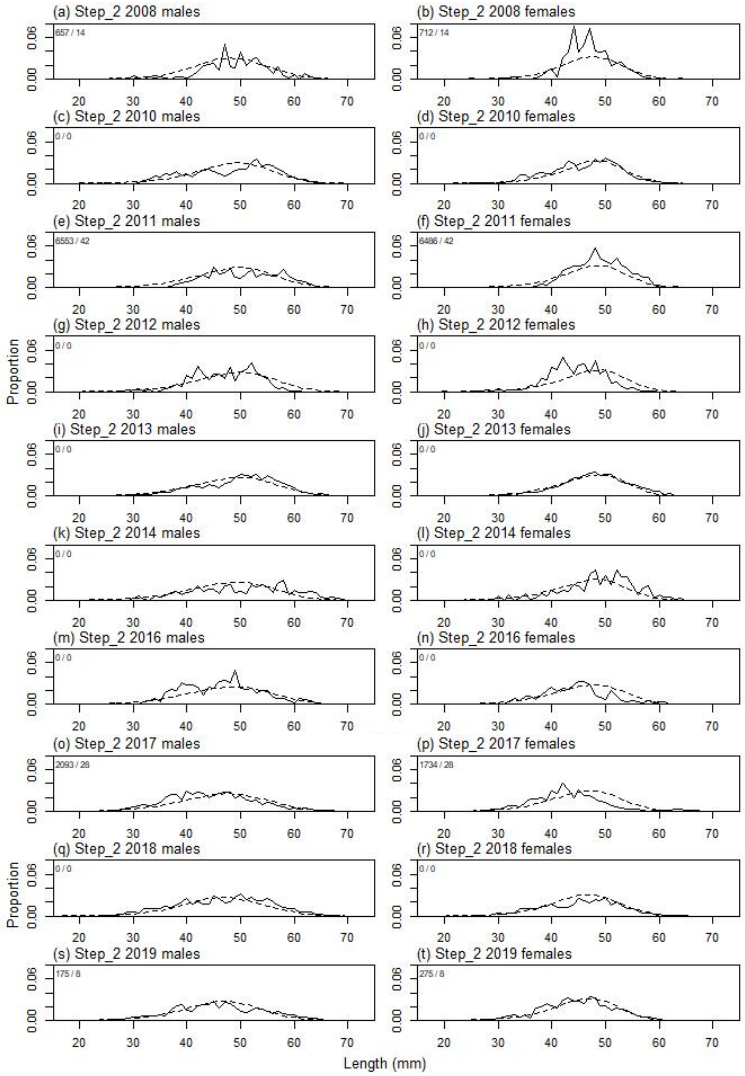

A3. 8: Observed (solid line) and fitted (dashed line) length frequency distributions from observer samples, time step 2 for the SCI 6A base model. Numbers in top left corner of each plot represent number of scampi measured / number of events sampled.

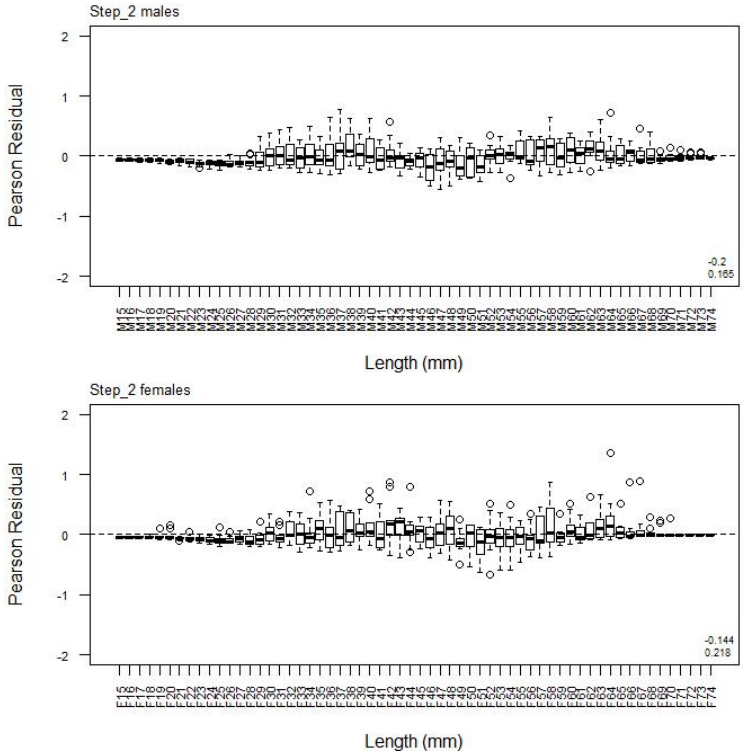

A3. 9: Box plots of Pearson residuals from the fit to length frequency distributions by length from observer sampling by sex for time step 2 for the SCI 6A base model.

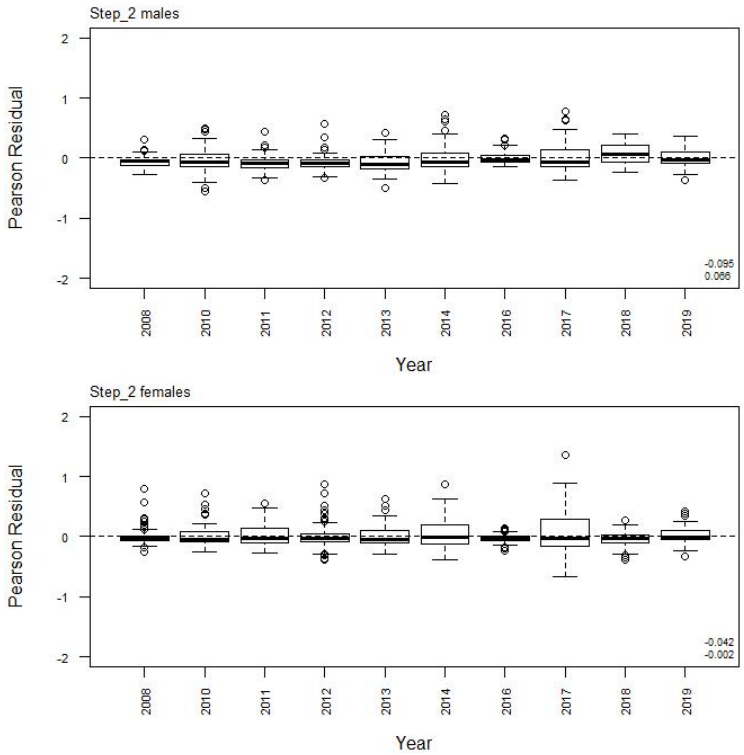

A3. 10: Box plots of Pearson residuals from the fit to length frequency distributions by year from observer sampling by sex for time step 2 for the SCI 6A base model.

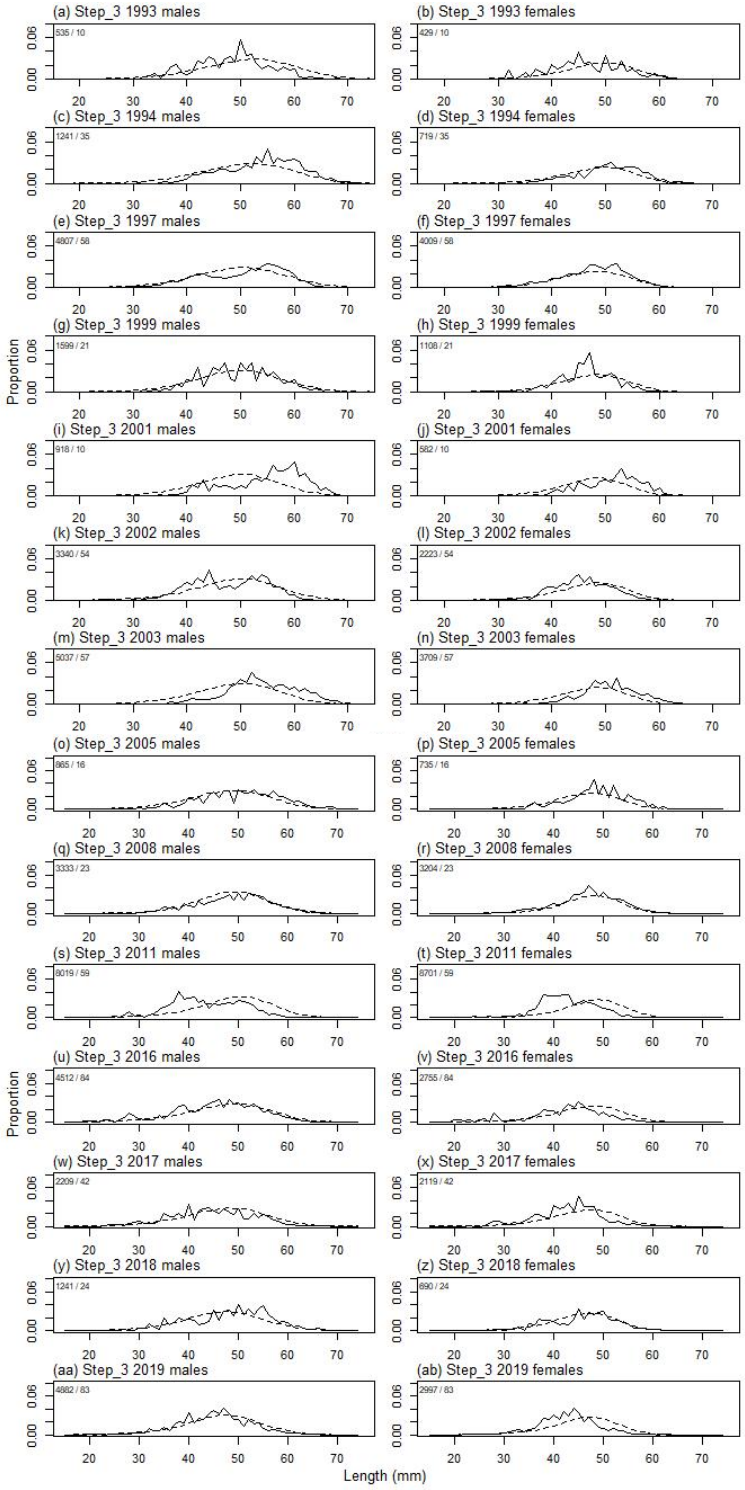

A3. 11: Observed (solid line) and fitted (dashed line) length frequency distributions from observer samples, time step 3 for the SCI 6A base model. Numbers in top left corner of each plot represent number of scampi measured / number of events sampled.

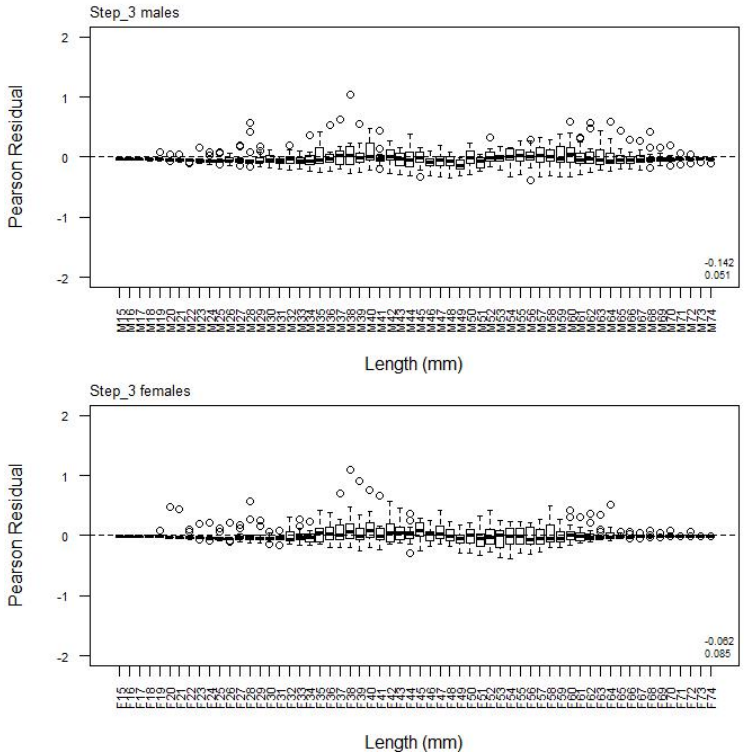

A3. 12: Box plots of Pearson residuals from the fit to length frequency distributions by length from observer sampling by sex for time step 3 for the SCI 6A base model.

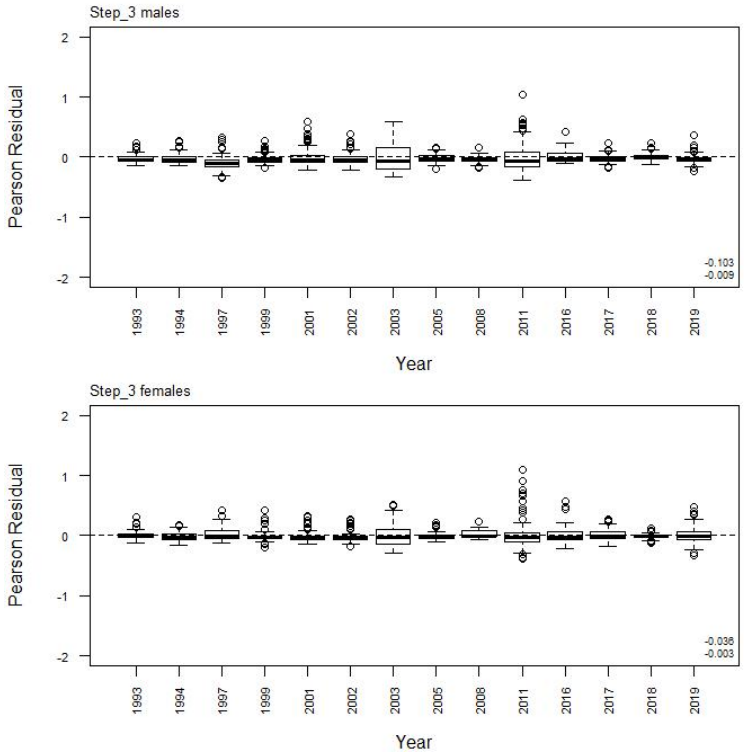

A3. 13: Box plots of Pearson residuals from the fit to length frequency distributions by year from observer sampling by sex for time step 3 for the SCI 6A base model.

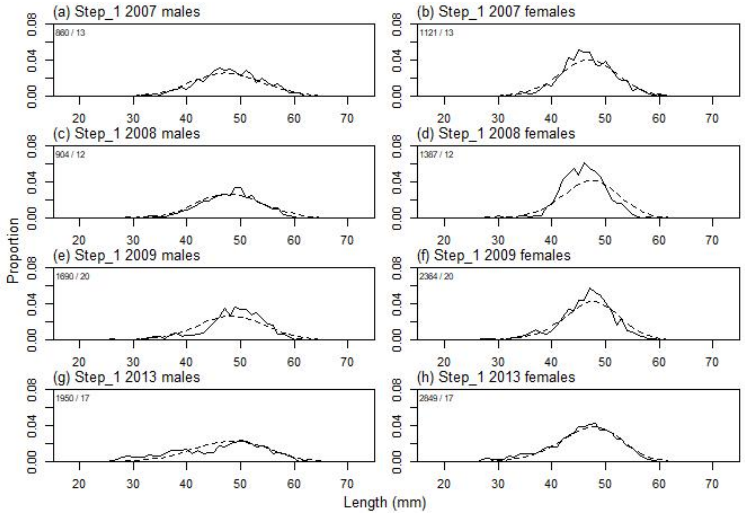

A3. 14: Observed (solid line) and fitted (dashed line) length frequency distributions from *San Tongariro* trawl survey samples for SCI 6A base model. Numbers in top left corner of each plot represent number of scampi measured / number of events sampled.

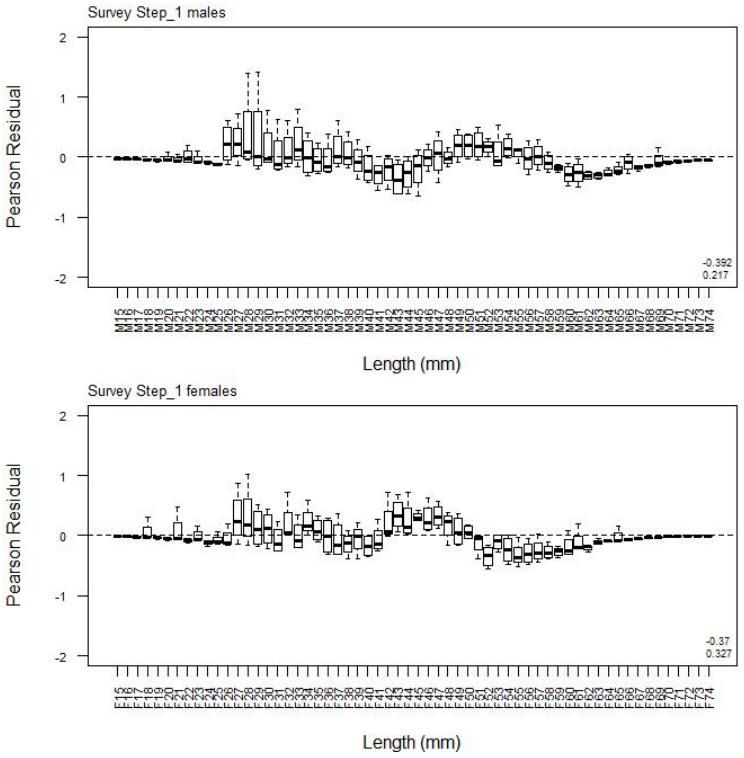

A3. 15: Box plots of Pearson residuals from the fit to length frequency distributions by length from *San Tongariro* trawl survey by sex for the SCI 6A base model.

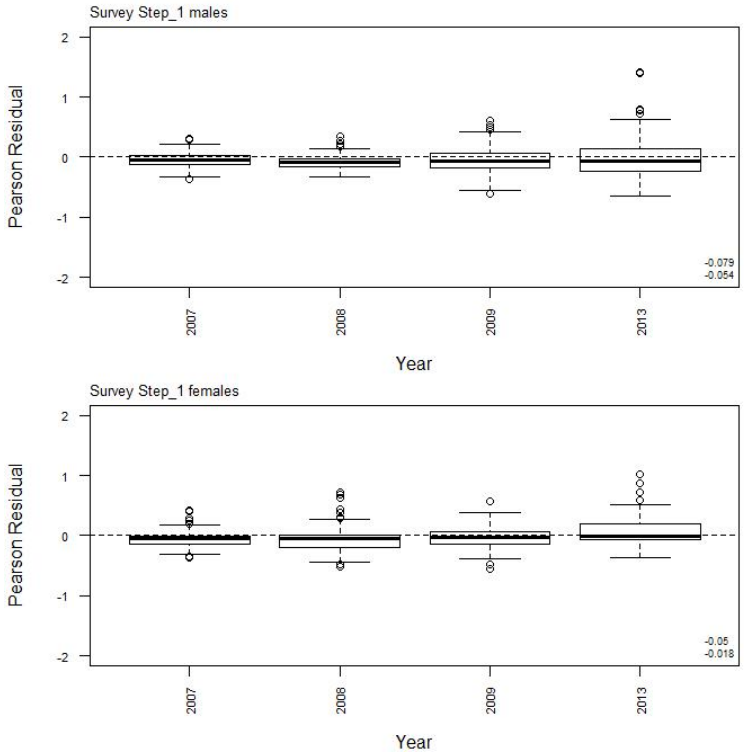

A3. 16: Box plots of Pearson residuals from the fit to length frequency distributions by year from *San Tongariro* trawl survey by sex for the SCI 6A base model.

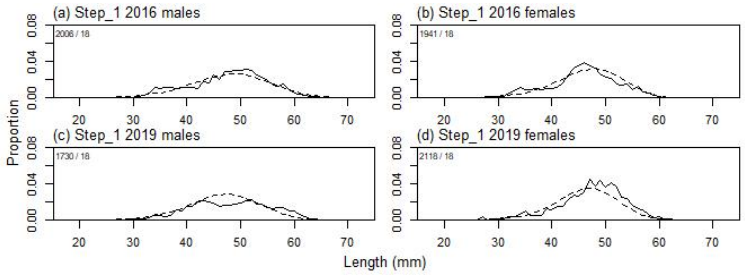

A3. 17: Observed (solid line) and fitted (dashed line) length frequency distributions from *Kaharoa* trawl survey samples for SCI 6A base model. Numbers in top left corner of each plot represent number of scampi measured / number of events sampled.

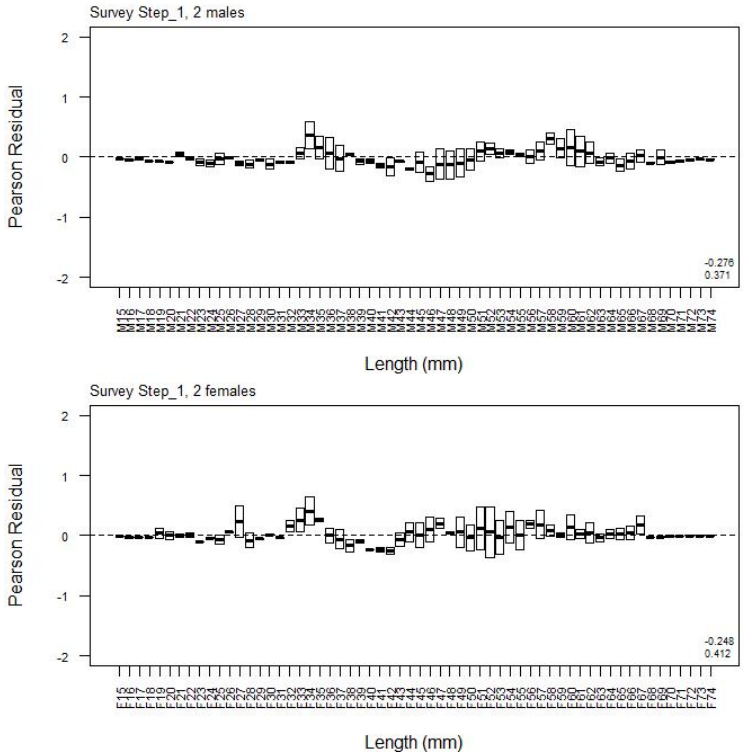

A3. 18: Box plots of Pearson residuals from the fit to length frequency distributions by length from *Kaharoa* trawl survey by sex for the SCI 6A base model.

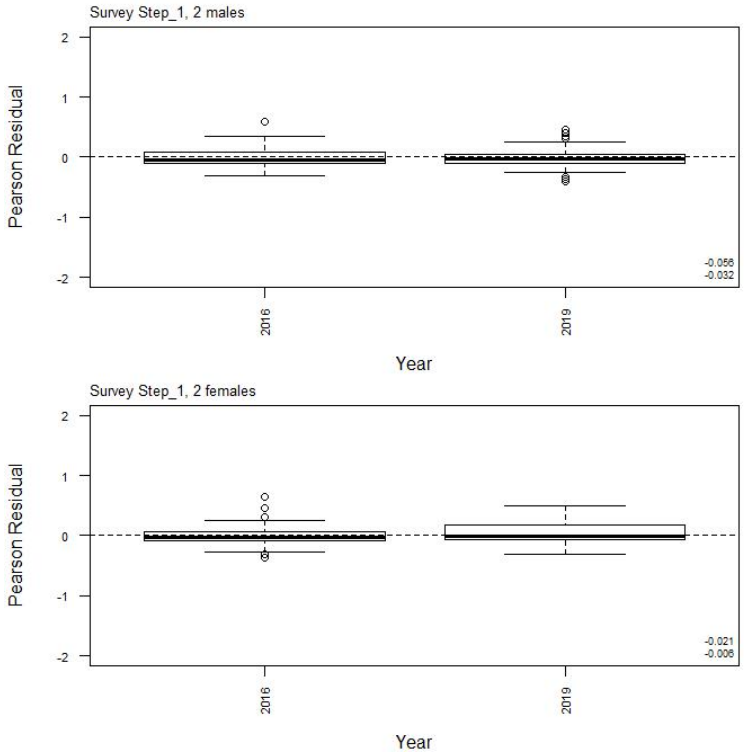

A3. 19: Box plots of Pearson residuals from the fit to length frequency distributions by year from *Kaharoa* trawl survey by sex for the SCI 6A base model.

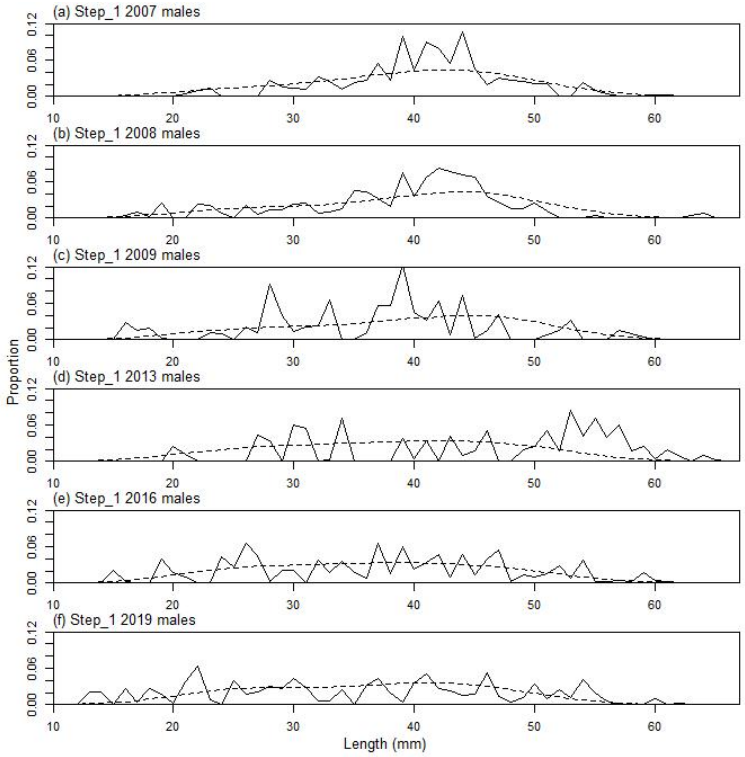

A3. 20: Observed (solid line) and fitted (dashed line) length frequency distributions from photo survey samples for the SCI 6A base model.

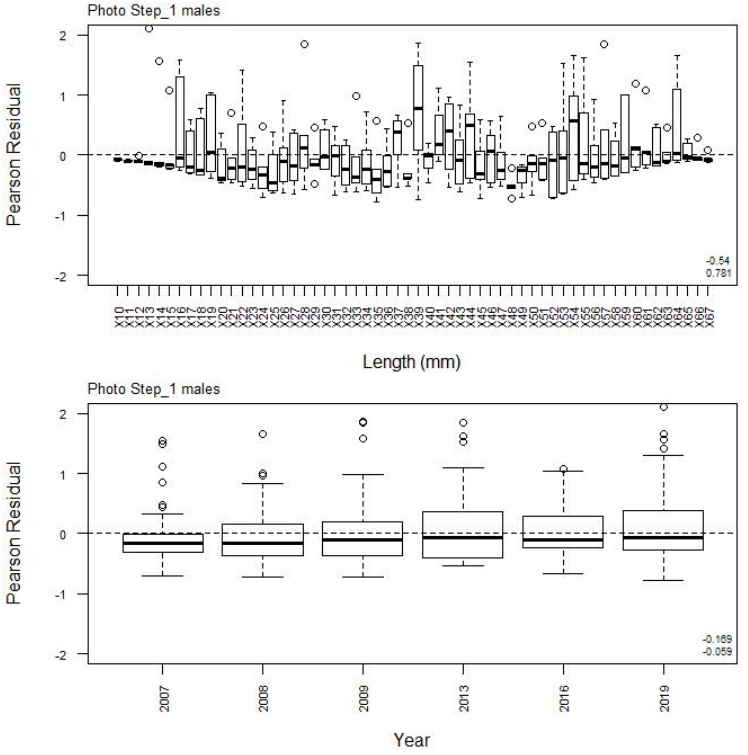

A3. 21: Box plots of Pearson residuals from the fit to length frequency distributions by length (top plot) and year (bottom plot) from photo survey sampling by sex for the SCI 6A base model.

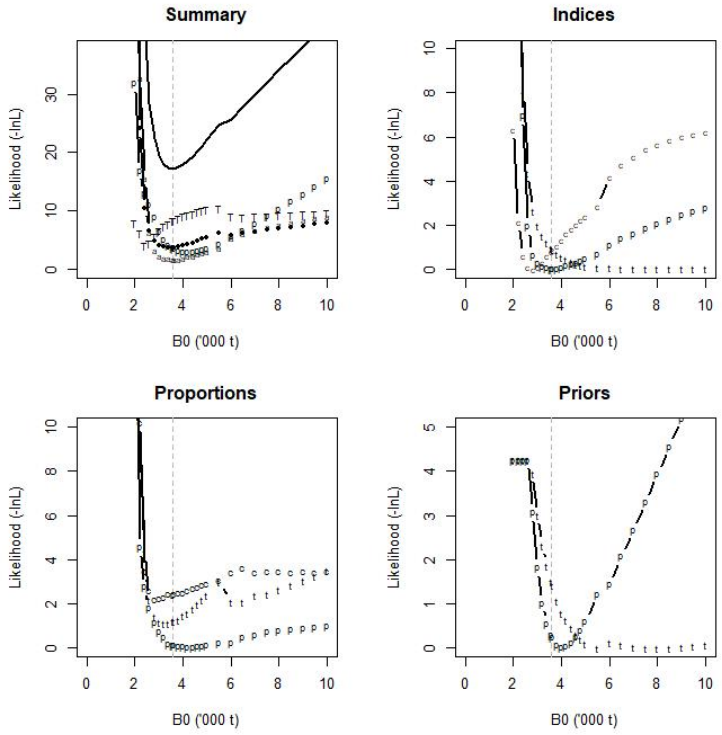

A3. 22: Likelihood profiles for the SCI 6A base model when B_0 is fixed in the model. Figures show profiles for main priors (top left, p – priors, a – abundance indices, • – proportions at length, T – tag recaptures), abundance indices (top right, t – trawl survey step, c – CPUE, p – photo survey), proportion at length data (bottom left, p-photo, t – trawl, c – observer), and priors (bottom right, p – *q-Scampi*, t – *q-Trawl*).

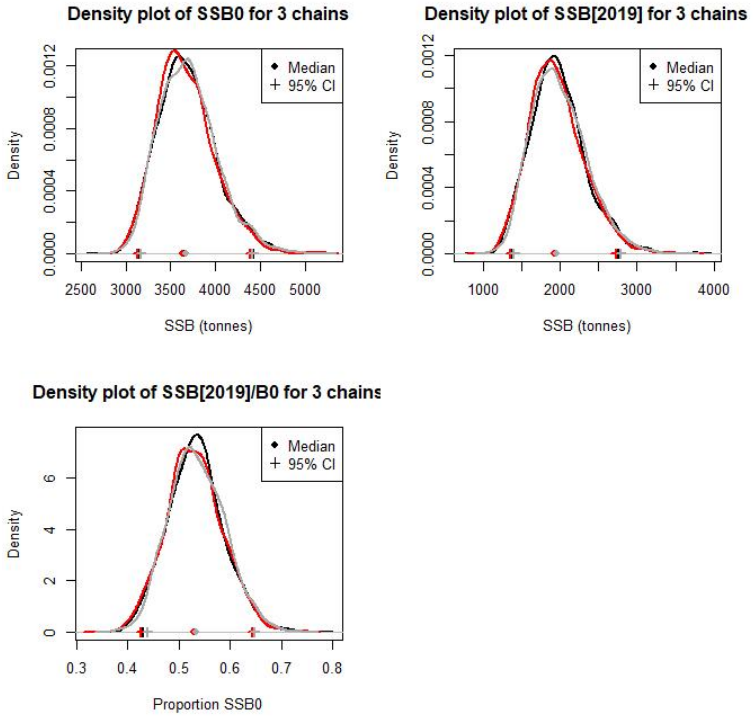

A3. 23: Density plots for SSB_0, SSB_{2019} and SSB_{2019}/SSB_0 for the SCI 6A base model for three independent MCMC chains, with median and 95% confidence intervals.

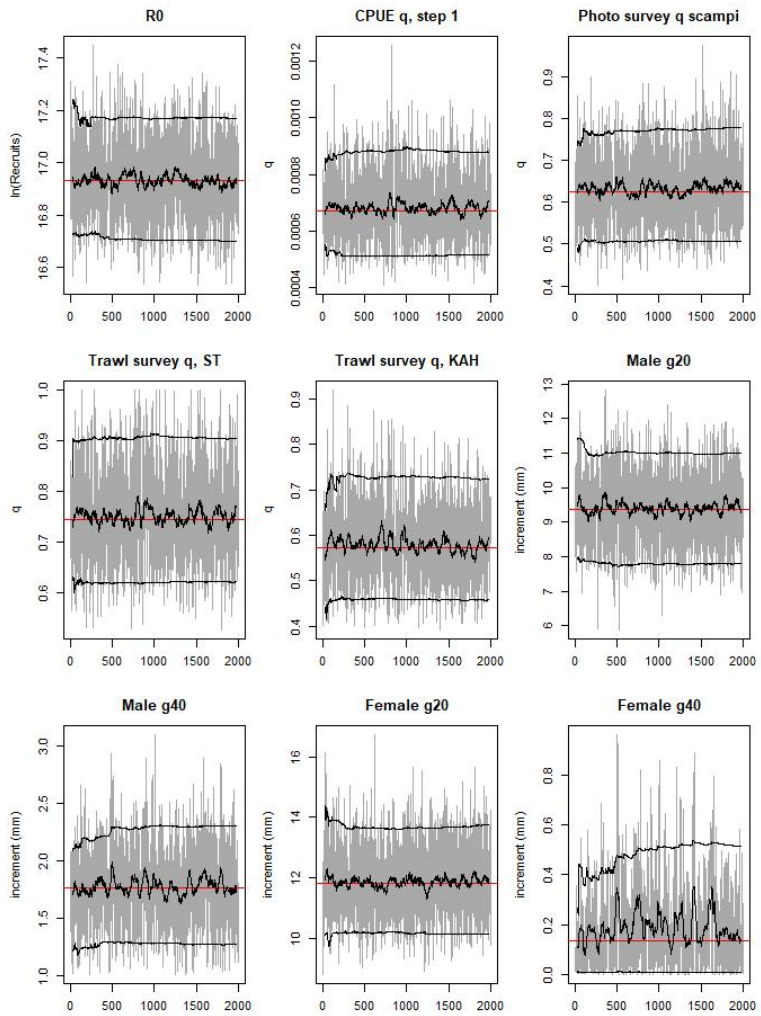

A3. 24: MCMC traces for R_0, catchability, and growth terms for the SCI 6A base model.

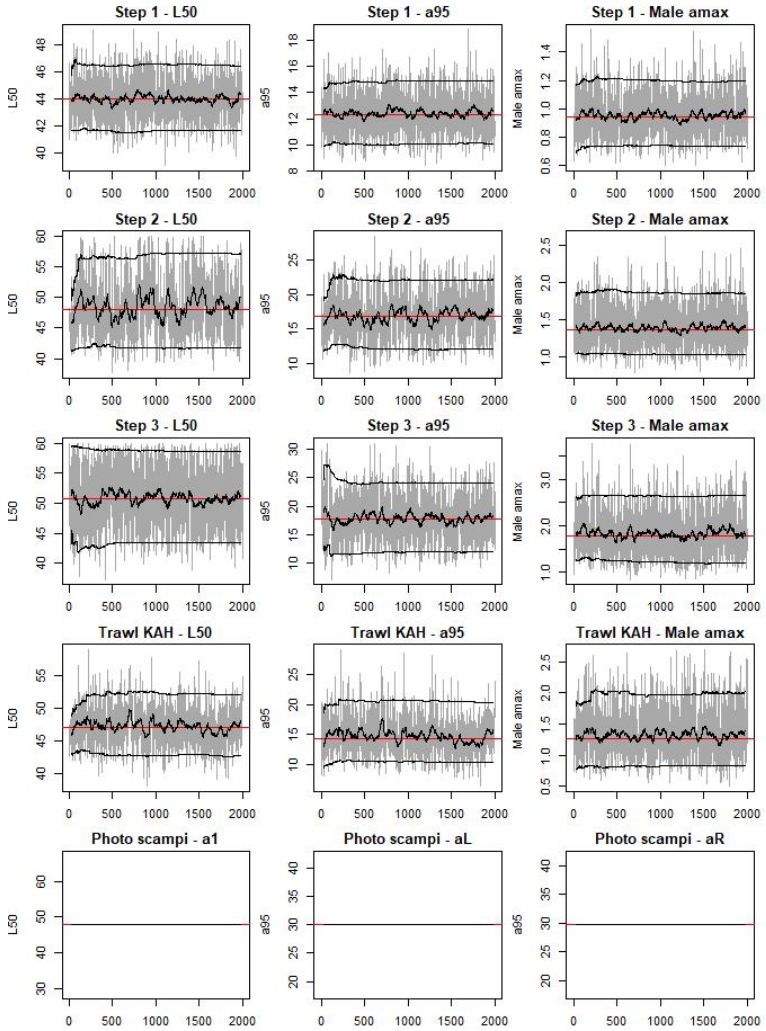

A3. 25: MCMC traces for selectivity terms for the SCI 6A base model. Photo scampi selectivity fixed at MPD estimate within the MCMC.

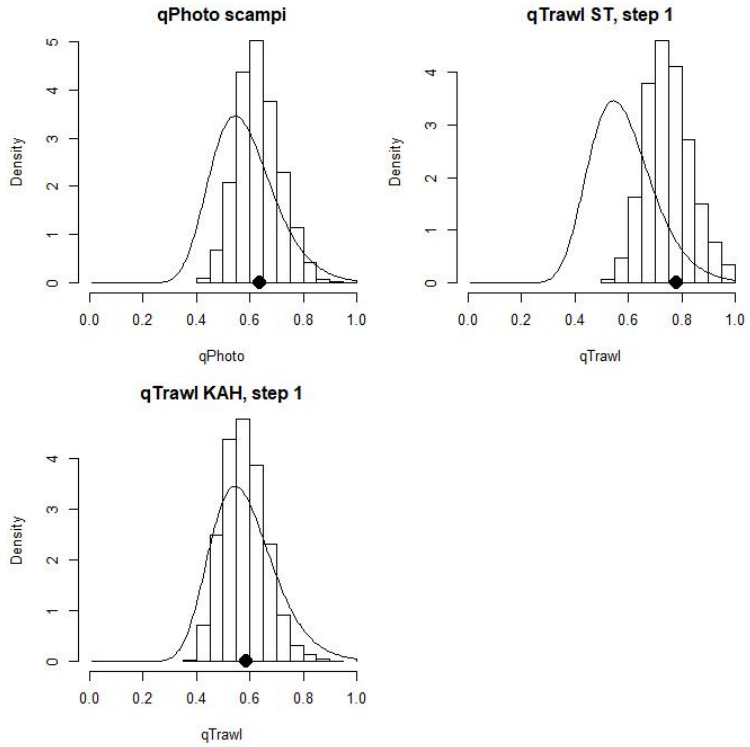

A3. 26: Marginal posterior distributions (histograms), MPD estimates (solid symbols), and distributions of priors (lines) for catchability terms for the SCI 6A base model.

APPENDIX 4. SCI 6A Low *q* model plots

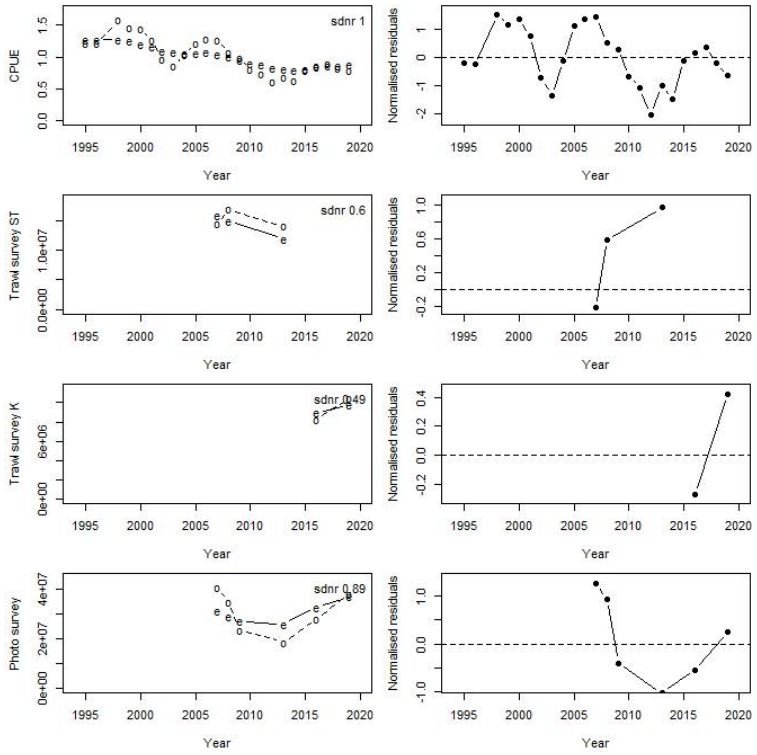

A4. 1: Fits to abundance indices (left column) and normalised residuals (right column) for standardised CPUE index (top row) *San Tongariro* (ST) trawl survey abundance index (second row), *Kaharoa* (K) trawl survey abundance index (third row), and photo survey emerged scampi abundance index for the SCI 6A low *q* model.

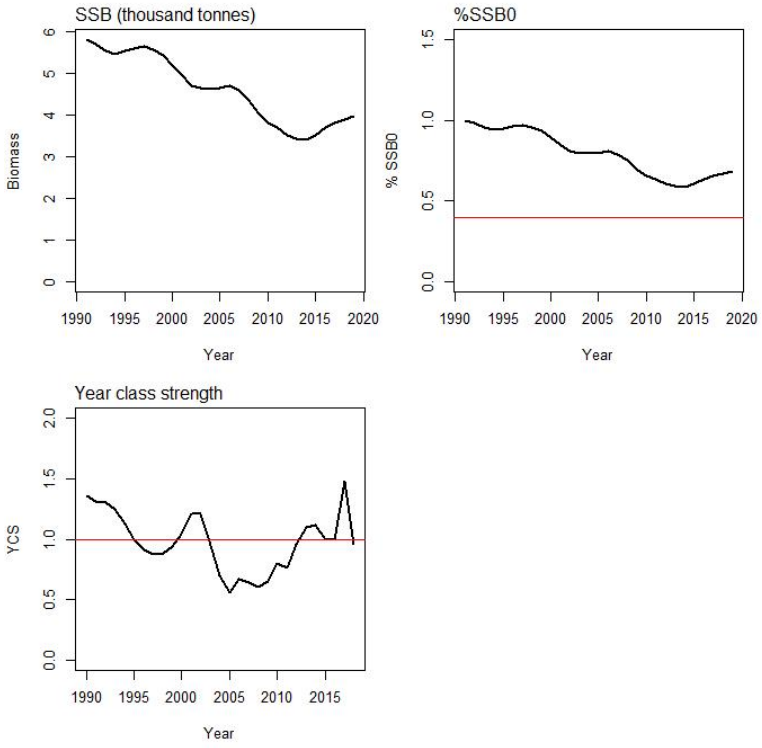

A4. 2: Spawning stock biomass trajectory (upper left), stock status (upper right), and year class strength (lower left) for the SCI 6A low *q* model.

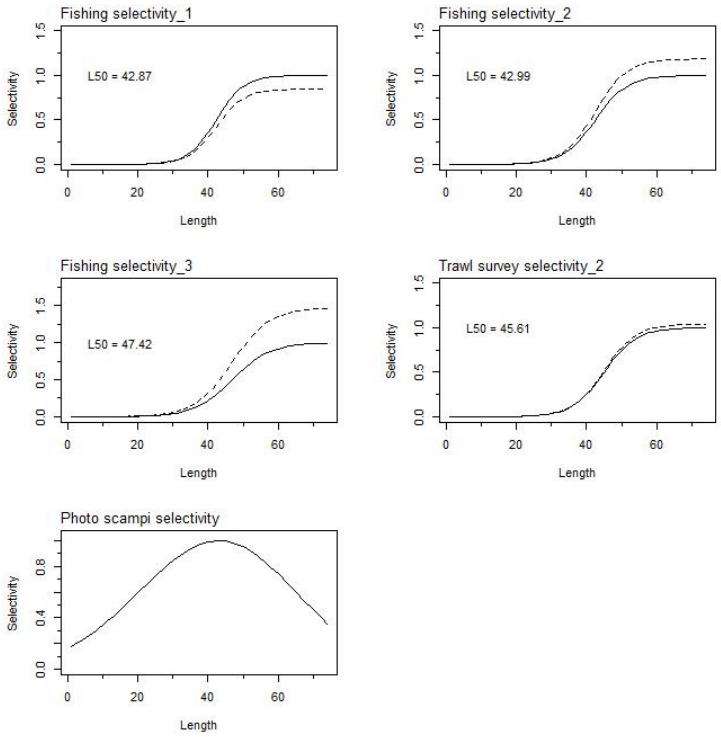

A4. 3: Fishery and survey selectivity curves for SCI 6A low *q* model. Solid line – females, dotted line – males. The scampi photo index is not sexed, and a single selectivity applies.

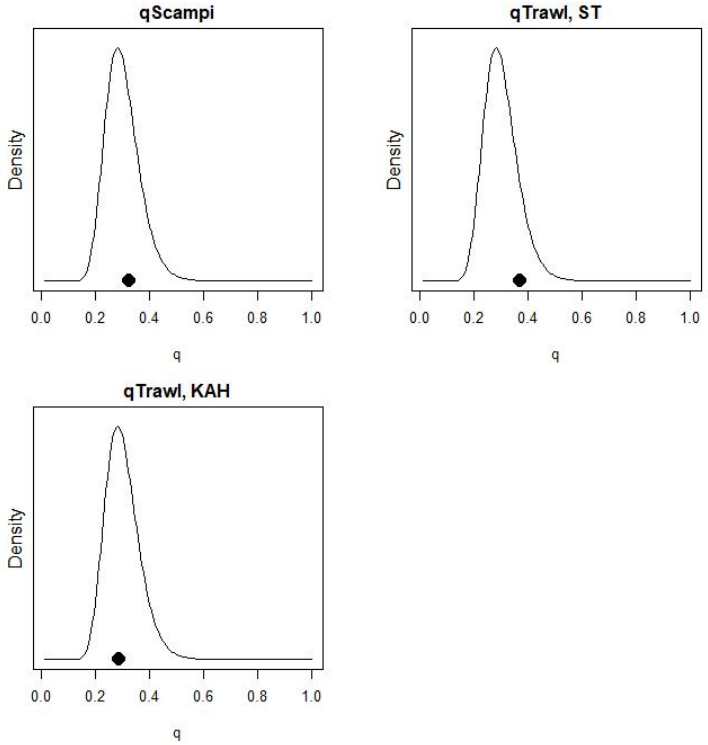

A4. 4: Catchability estimates from MPD model run, plotted in relation to prior distribution for SCI 6A low *q* model.

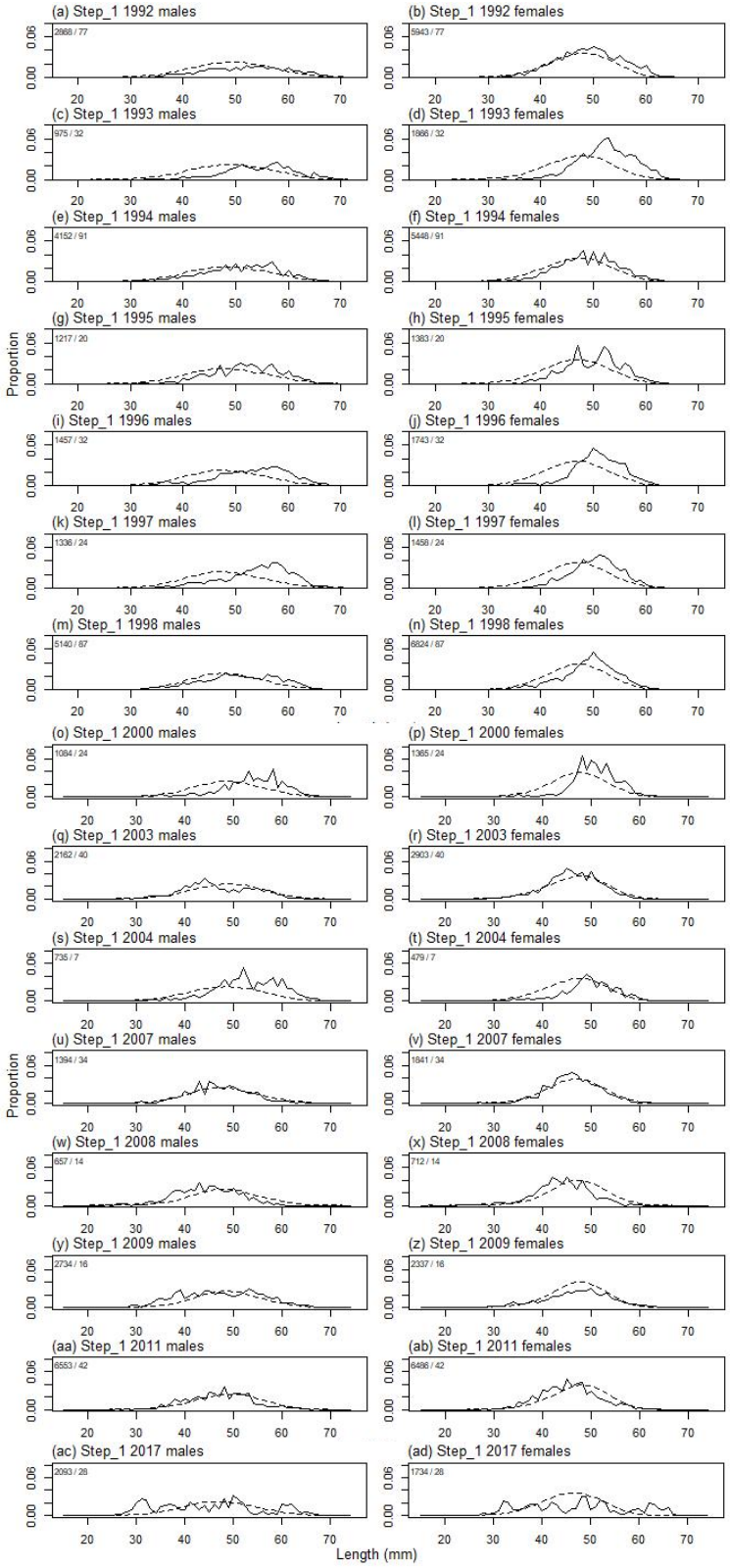

A4. 5: Observed (solid line) and fitted (dashed line) length frequency distributions from observer samples, time step 1 for the SCI 6A low *q* model. Numbers in top left corner of each plot represent number of scampi measured / number of events sampled.

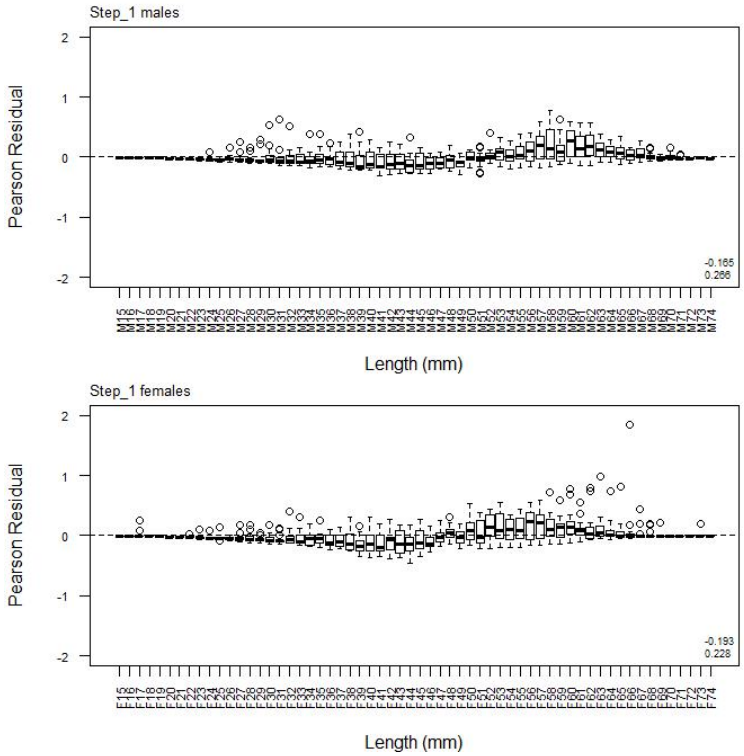

A4. 6: Box plots of Pearson residuals from the fit to length frequency distributions by length from observer sampling by sex for time step 1 for the SCI 6A low *q* model.

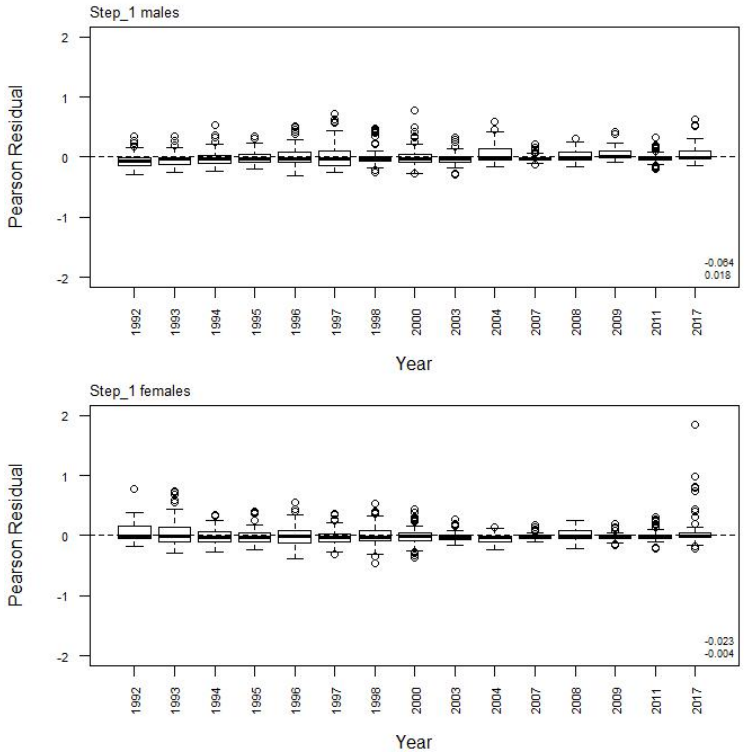

A4. 7: Box plots of Pearson residuals from the fit to length frequency distributions by year from observer sampling by sex for time step 1 for the SCI 6A low *q* model.

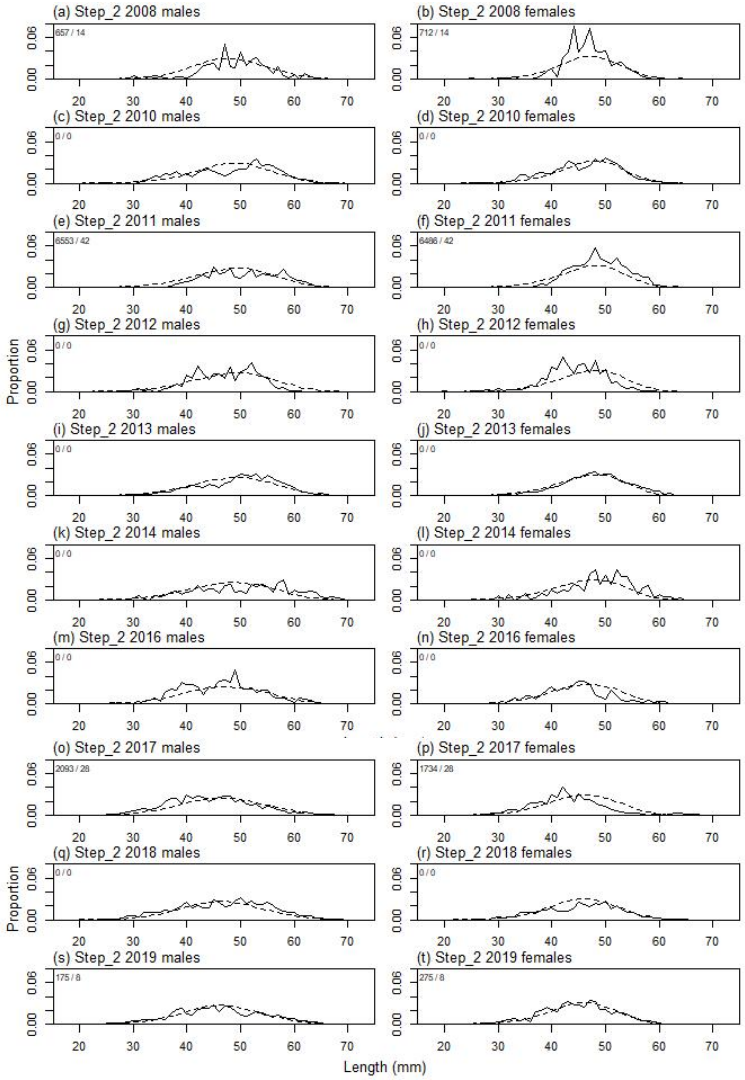

A4. 8: Observed (solid line) and fitted (dashed line) length frequency distributions from observer samples, time step 2 for the SCI 6A low *q* model. Numbers in top left corner of each plot represent number of scampi measured / number of events sampled.

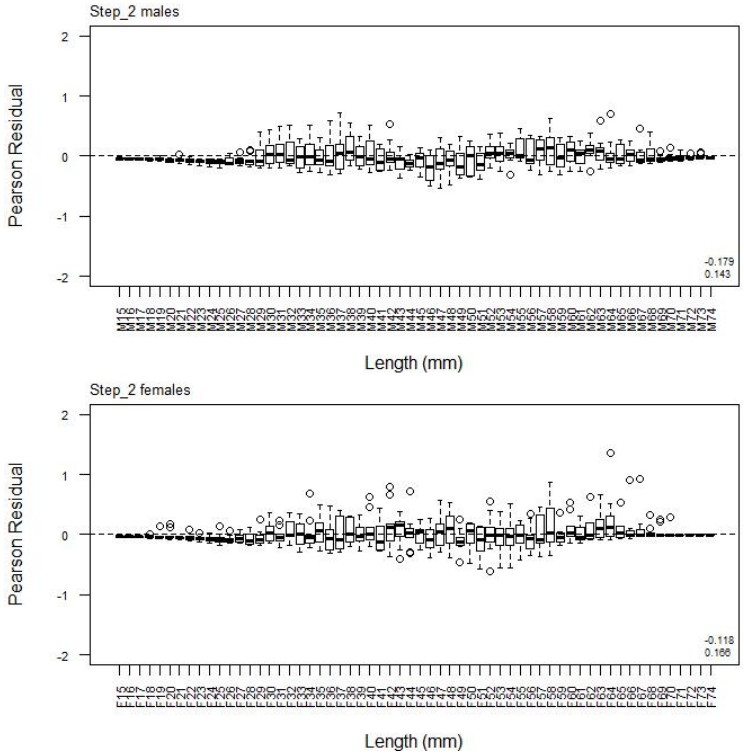

A4. 9: Box plots of Pearson residuals from the fit to length frequency distributions by length from observer sampling by sex for time step 2 for the SCI 6A low *q* model.

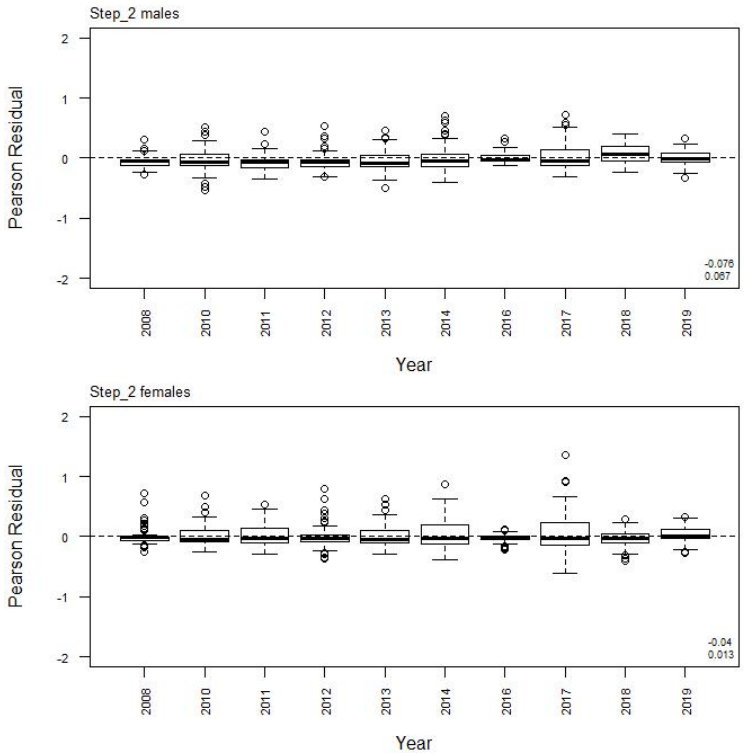

A4. 10: Box plots of Pearson residuals from the fit to length frequency distributions by year from observer sampling by sex for time step 2 for the SCI 6A low *q* model.

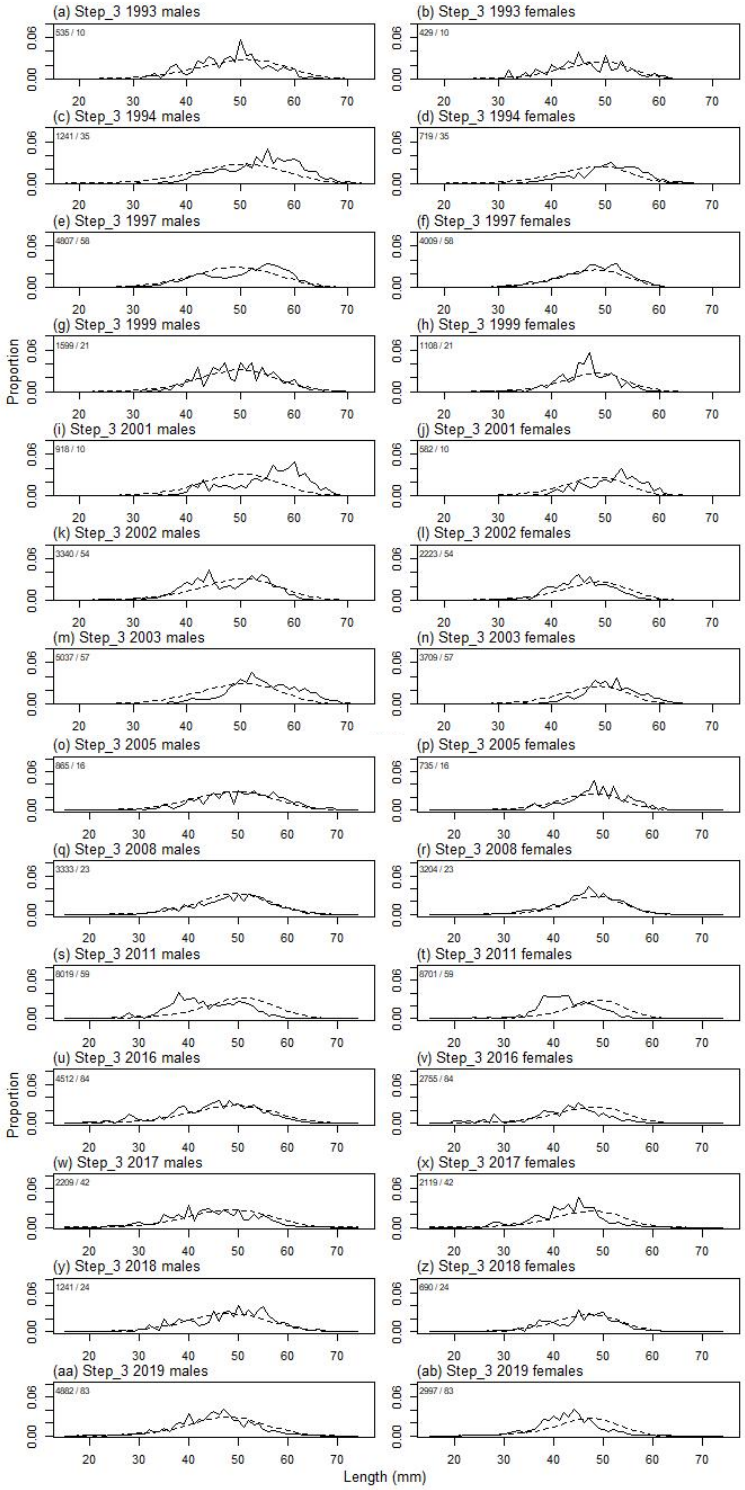

A4. 11: Observed (solid line) and fitted (dashed line) length frequency distributions from observer samples, time step 3 for the SCI 6A low *q* model. Numbers in top left corner of each plot represent number of scampi measured / number of events sampled.

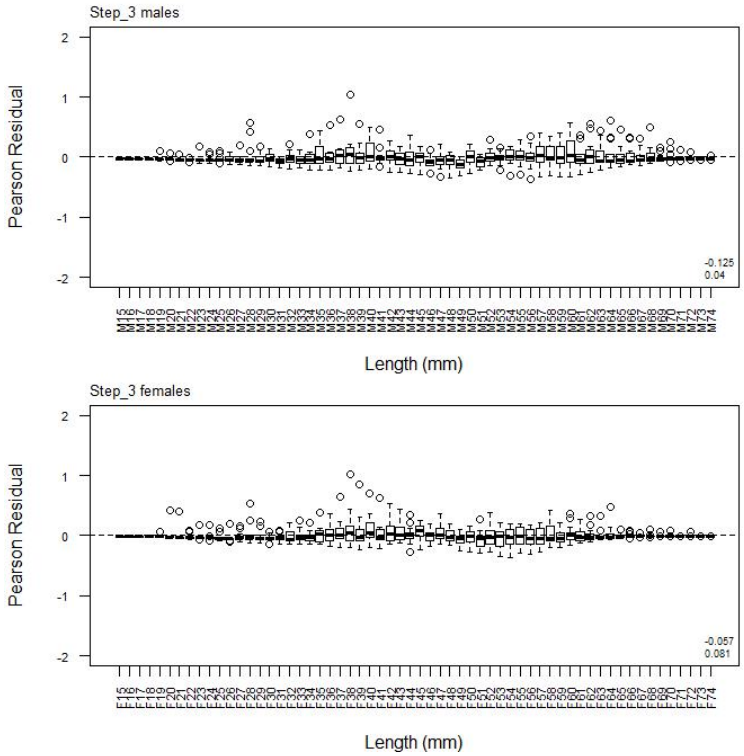

A4. 12: Box plots of Pearson residuals from the fit to length frequency distributions by length from observer sampling by sex for time step 3 for the SCI 6A low *q* model.

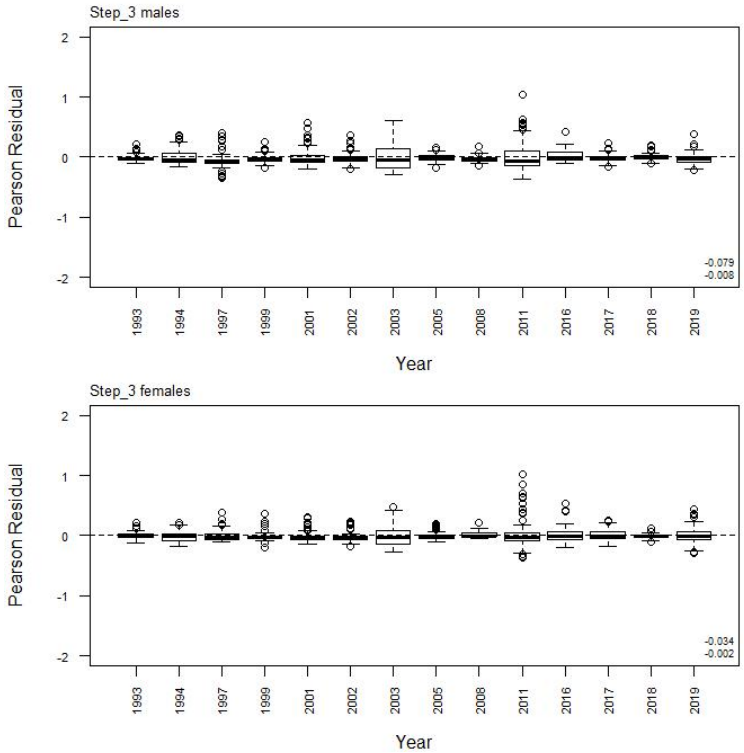

A4. 13: Box plots of Pearson residuals from the fit to length frequency distributions by year from observer sampling by sex for time step 3 for the SCI 6A low *q* model.

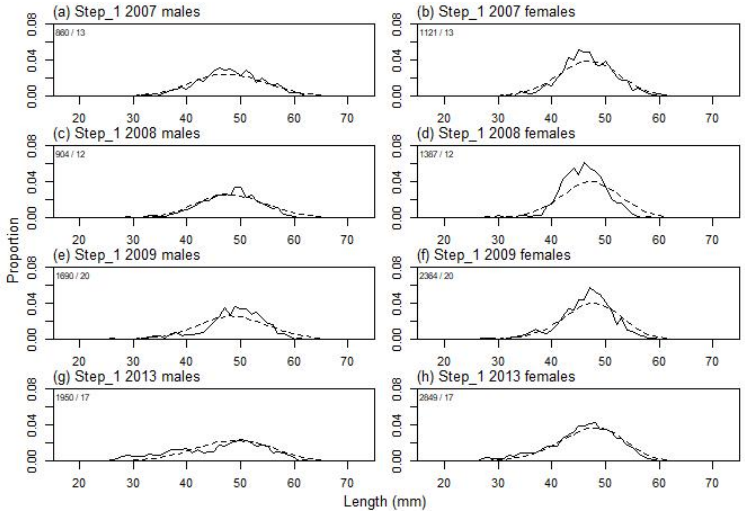

A4. 14: Observed (solid line) and fitted (dashed line) length frequency distributions from *San Tongariro* trawl survey samples for SCI 6A low *q* model. Numbers in top left corner of each plot represent number of scampi measured / number of events sampled.

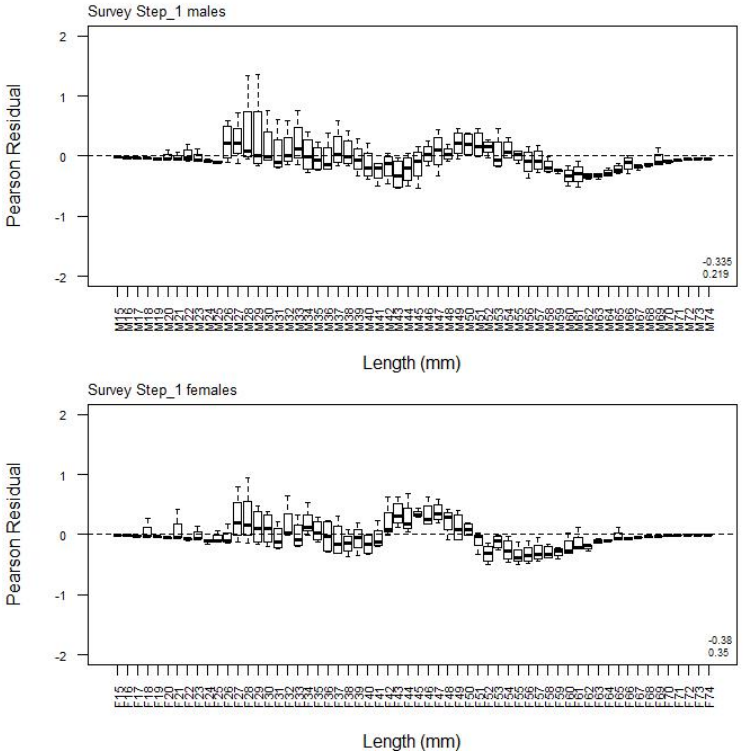

A4. 15: Box plots of Pearson residuals from the fit to length frequency distributions by length from *San Tongariro* trawl survey by sex for the SCI 6A low *q* model.

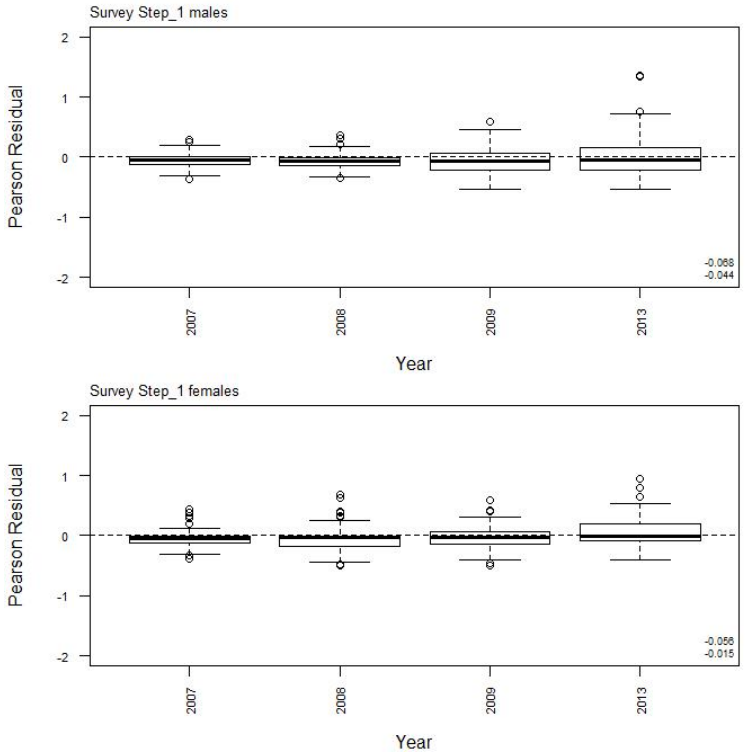

A4. 16: Box plots of Pearson residuals from the fit to length frequency distributions by year from *San Tongariro* trawl survey by sex for the SCI 6A low *q* model.

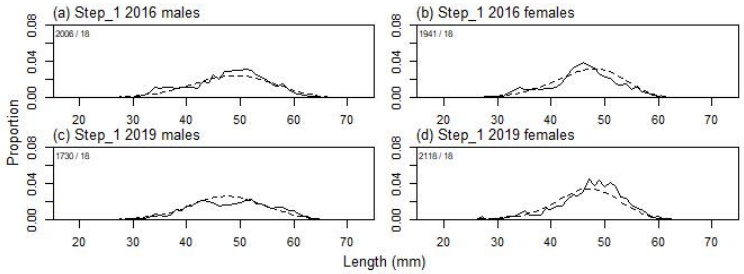

A4. 17: Observed (solid line) and fitted (dashed line) length frequency distributions from *Kaharoa* trawl survey samples for SCI 6A low *q* model. Numbers in top left corner of each plot represent number of scampi measured / number of events sampled.

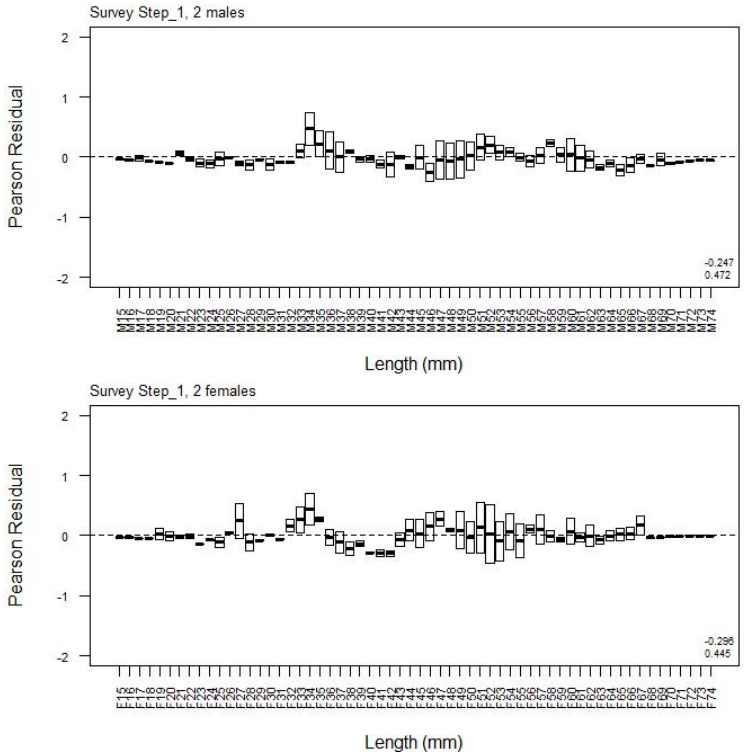

A4. 18: Box plots of Pearson residuals from the fit to length frequency distributions by length from *Kaharoa* trawl survey by sex for the SCI 6A low *q* model.

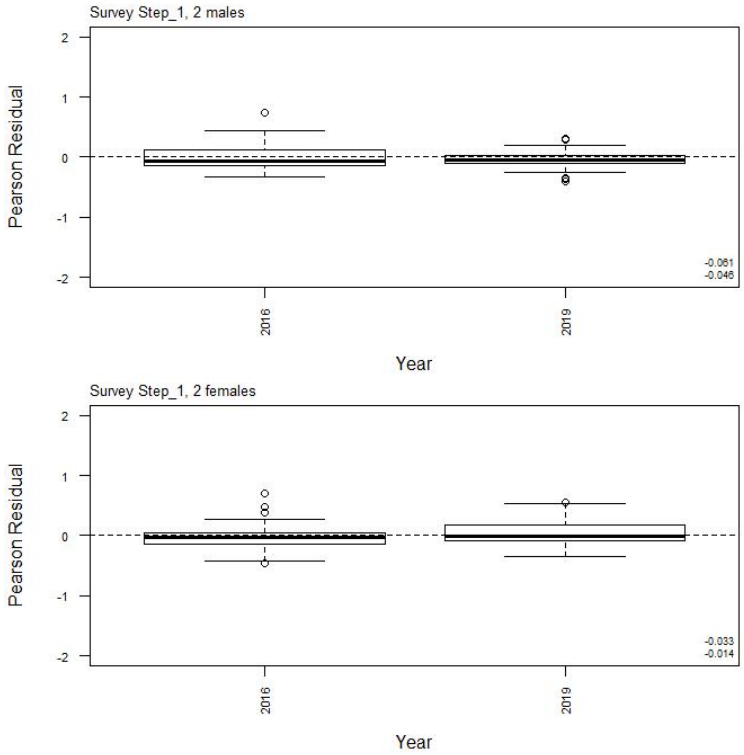

A4. 19: Box plots of Pearson residuals from the fit to length frequency distributions by year from *Kaharoa* trawl survey by sex for the SCI 6A low *q* model.

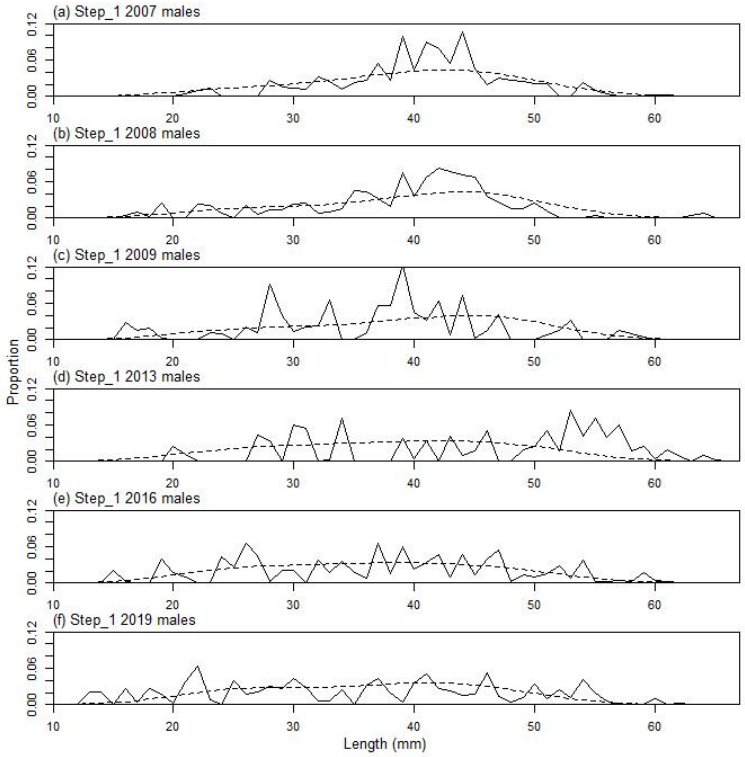

A4. 20: Observed (solid line) and fitted (dashed line) length frequency distributions from photo survey samples for the SCI 6A low *q* model.

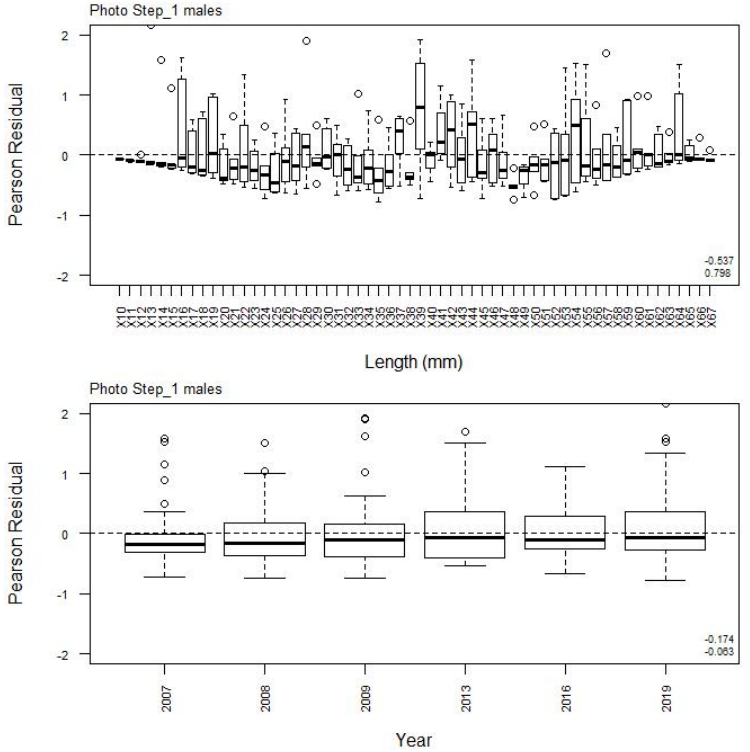

A4. 21: Box plots of Pearson residuals from the fit to length frequency distributions by length (top plot) and year (bottom plot) from photo survey sampling by sex for the SCI 6A low *q* model.

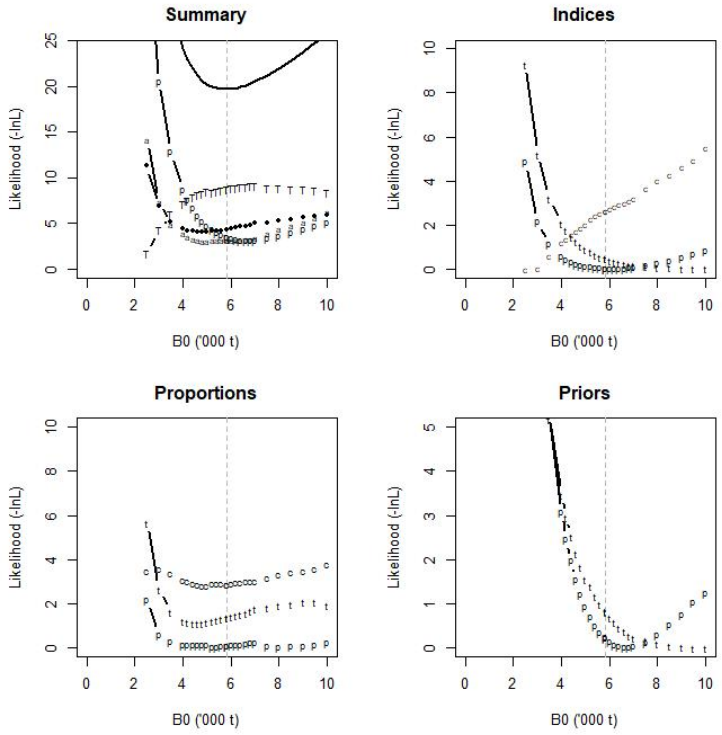

A4. 22: Likelihood profiles for the SCI 6A low *q* model when B_0 is fixed in the model. Figures show profiles for main priors (top left, p – priors, a – abundance indices, • – proportions at length, T – tag recaptures), abundance indices (top right, t – trawl survey step, c – CPUE, p – photo survey), proportion at length data (bottom left, p-photo, t – trawl, c – observer), and priors (bottom right, p – *q-Scampi*, t – *q-Trawl*).

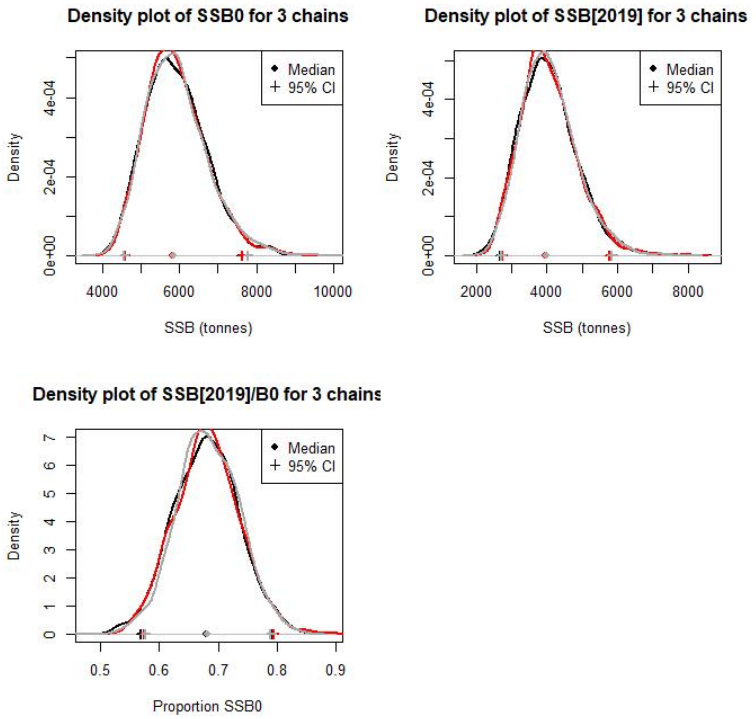

A4. 23: Density plots for SSB_0, SSB_{2019}, and SSB_{2019}/SSB_0 for the SCI 6A low *q* model for three independent MCMC chains, with median and 95% confidence intervals.

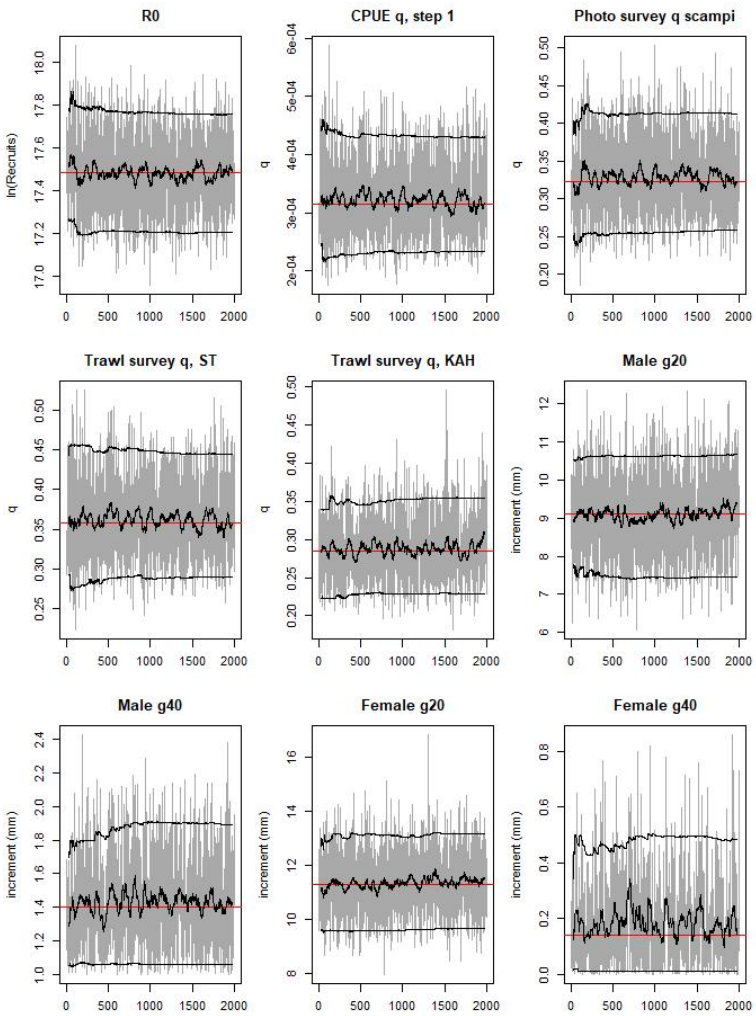

A4. 24: MCMC traces for R_0, catchability, and growth terms for the SCI 6A low q model.

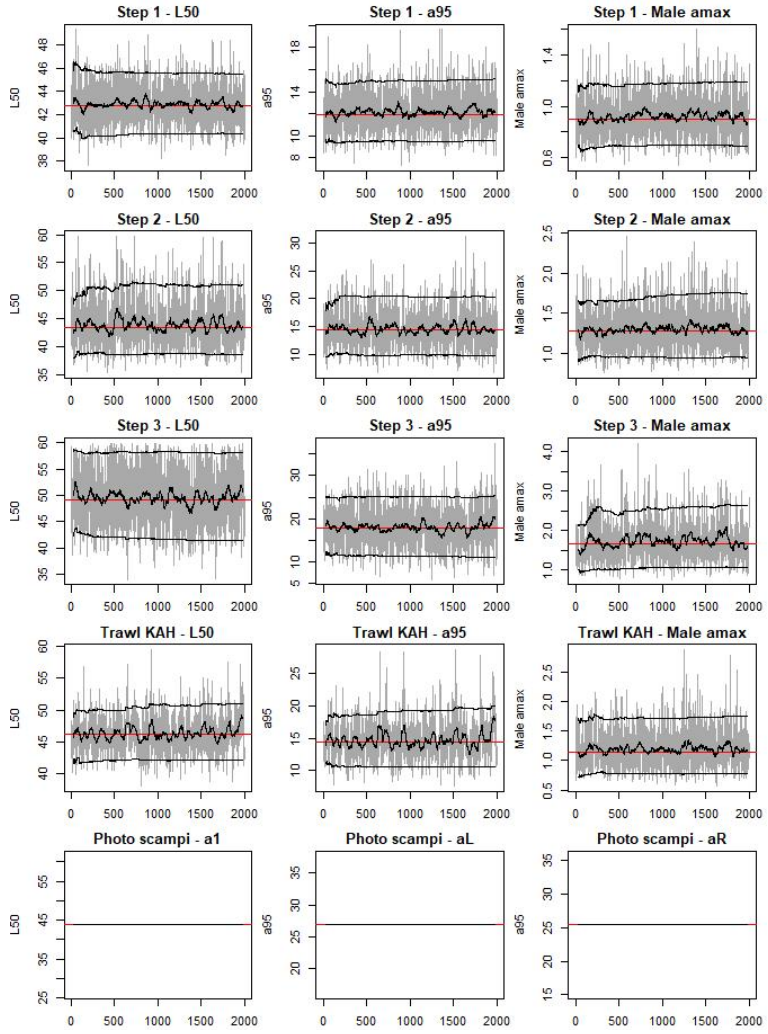

A4. 25: MCMC traces for selectivity terms for the SCI 6A low *q* model. Photo scampi selectivity fixed at MPD estimate within the MCMC.

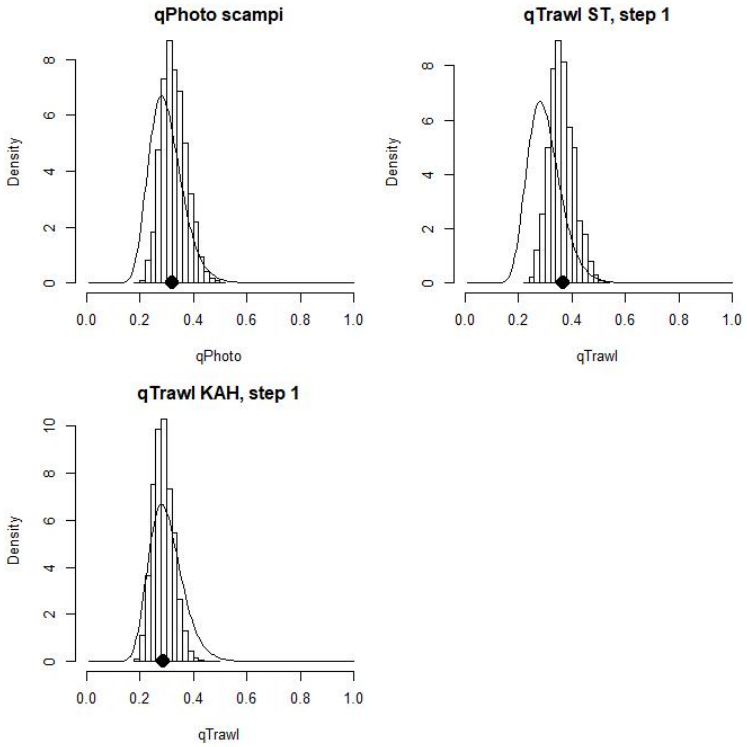

A4. 26: Marginal posterior distributions (histograms), MPD estimates (solid symbols), and distributions of priors (lines) for catchability terms for the SCI 6A low *q* model.

APPENDIX 5. SCI 6A Low *M* model plots

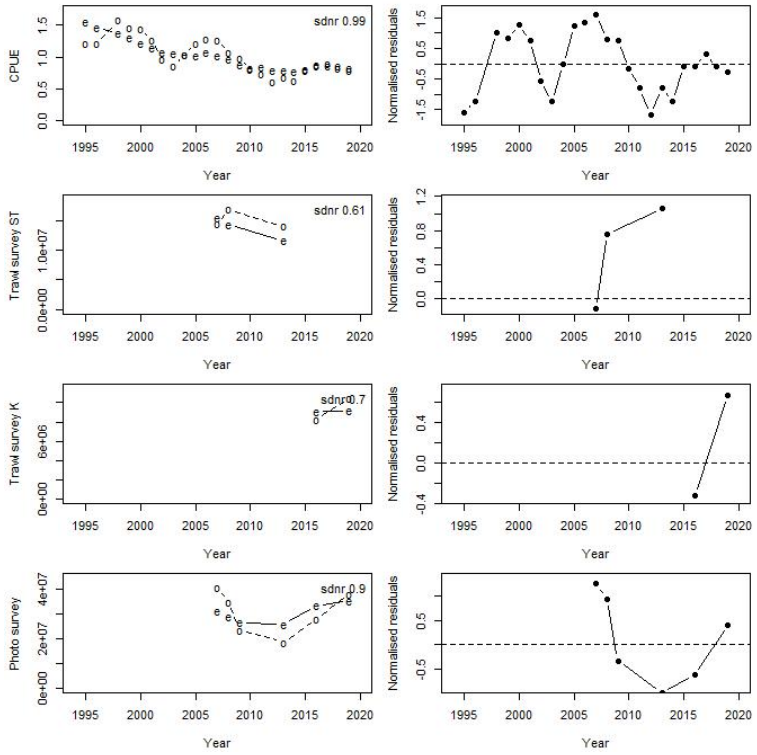

A5. 1: Fits to abundance indices (left column) and normalised residuals (right column) for standardised CPUE index (top row) *San Tongariro* (ST) trawl survey abundance index (second row), *Kaharoa* (K) trawl survey abundance index (third row), and photo survey emerged scampi abundance index for the SCI 6A low *M* model.

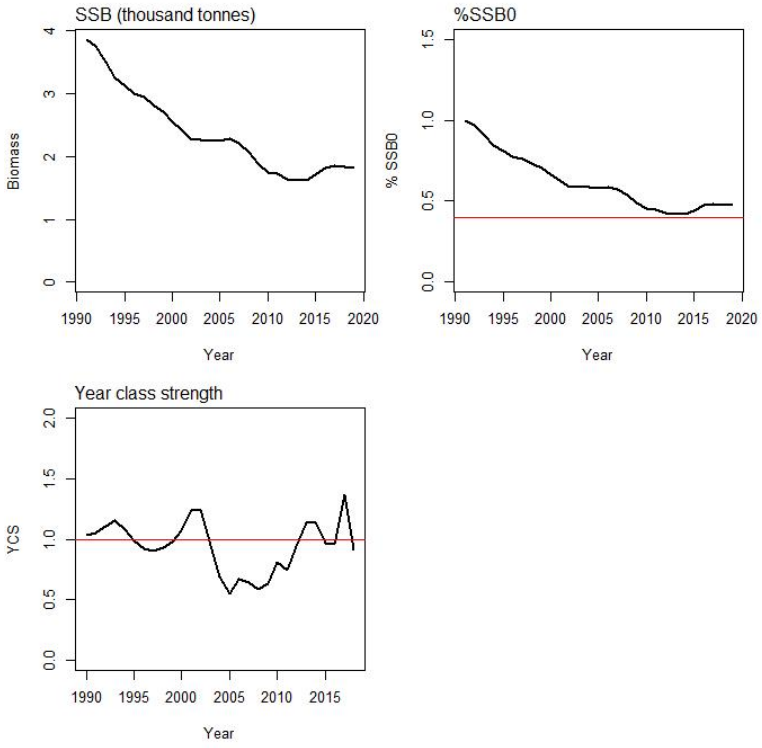

A5. 2: Spawning stock biomass trajectory (upper left), stock status (upper right), and year class strength (lower left) for the SCI 6A low *M* model.

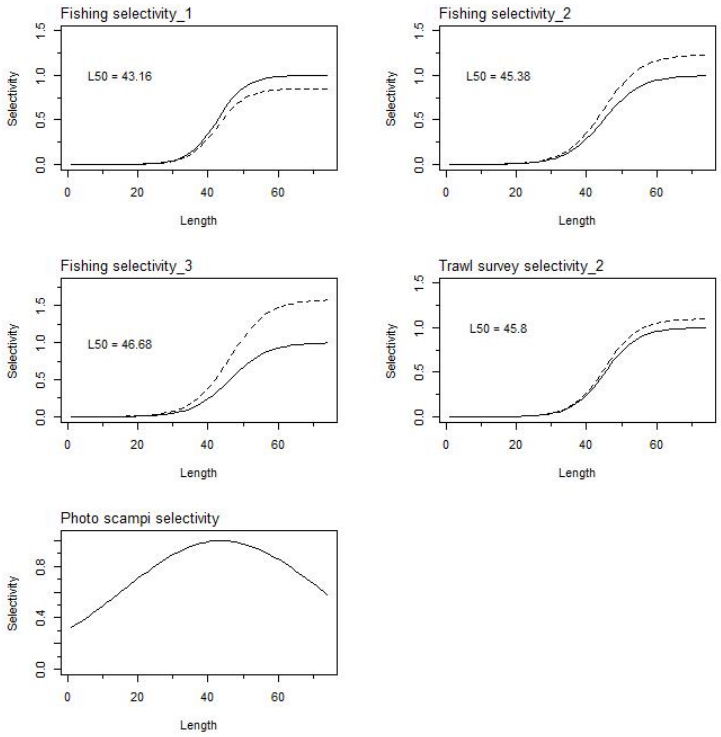

A5. 3: Fishery and survey selectivity curves for SCI 6A low *M* model. Solid line – females, dotted line – males. The scampi photo index is not sexed, and a single selectivity applies.

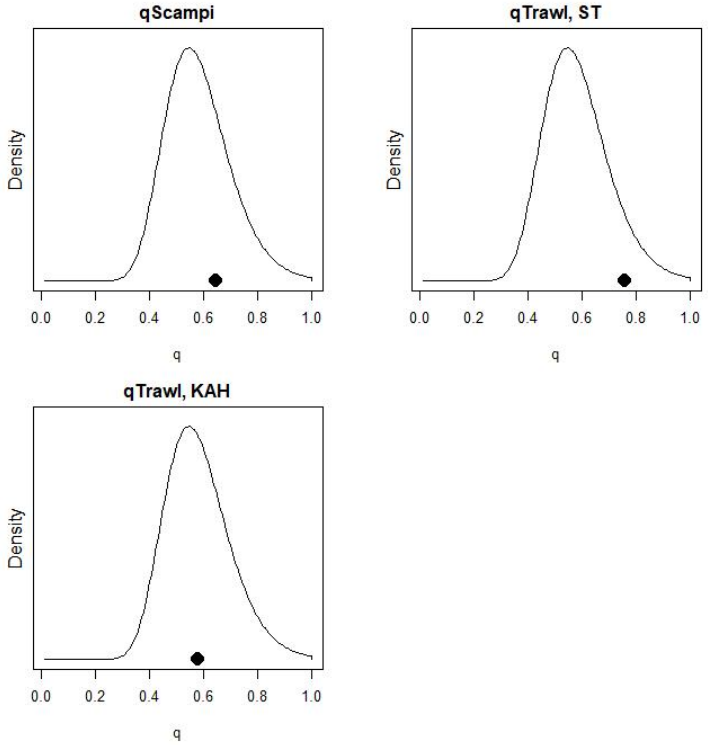

A5. 4: Catchability estimates from MPD model run, plotted in relation to prior distribution for SCI 6A low *M* model.

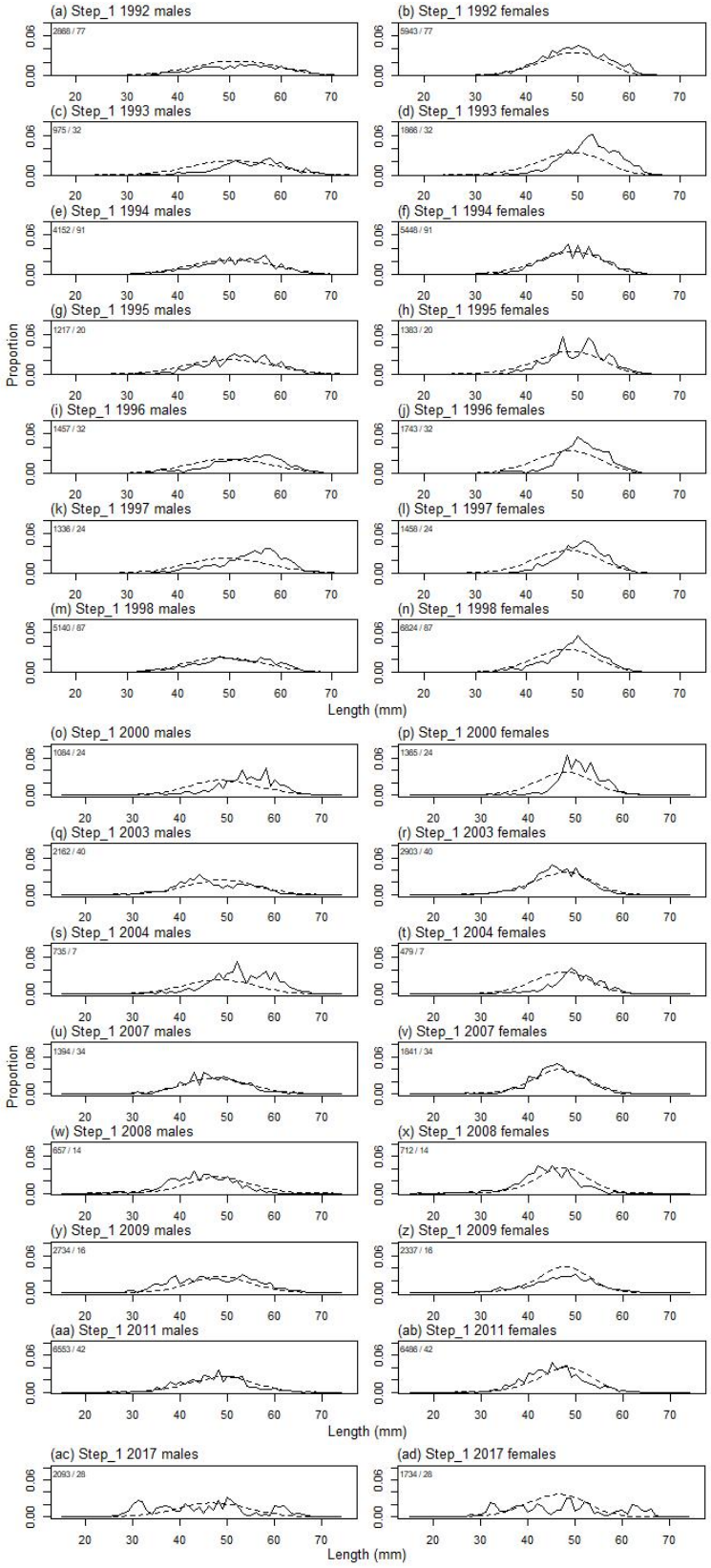

A5. 5: Observed (solid line) and fitted (dashed line) length frequency distributions from observer samples, time step 1 for the SCI 6A low *M* model. Numbers in top left corner of each plot represent number of scampi measured / number of events sampled.

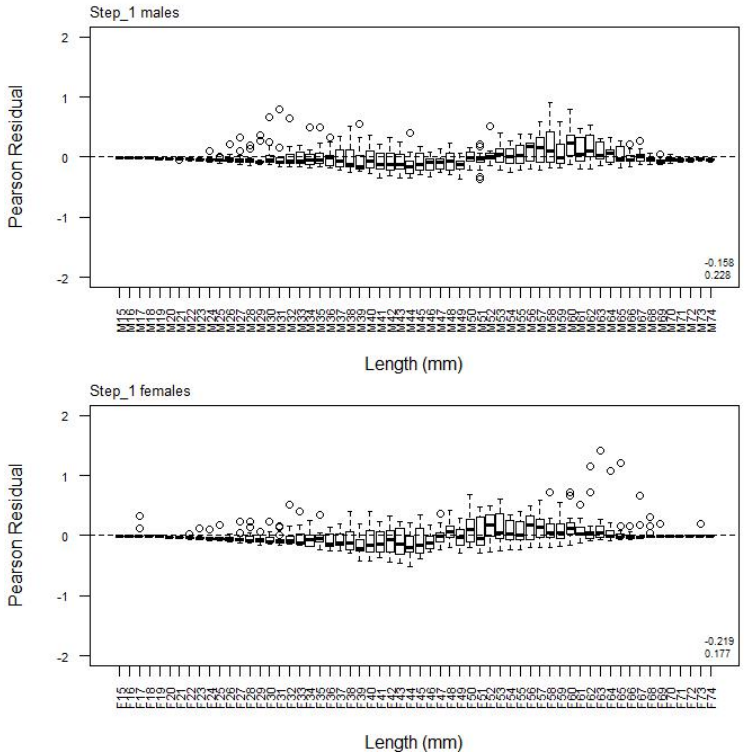

A5. 6: Box plots of Pearson residuals from the fit to length frequency distributions by length from observer sampling by sex for time step 1 for the SCI 6A low *M* model.

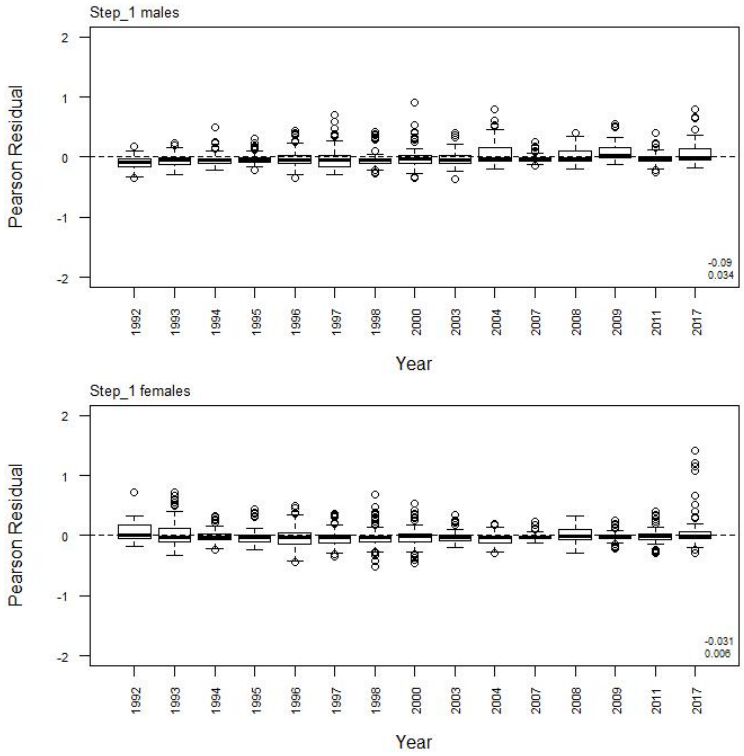

A5. 7: Box plots of Pearson residuals from the fit to length frequency distributions by year from observer sampling by sex for time step 1 for the SCI 6A low *M* model.

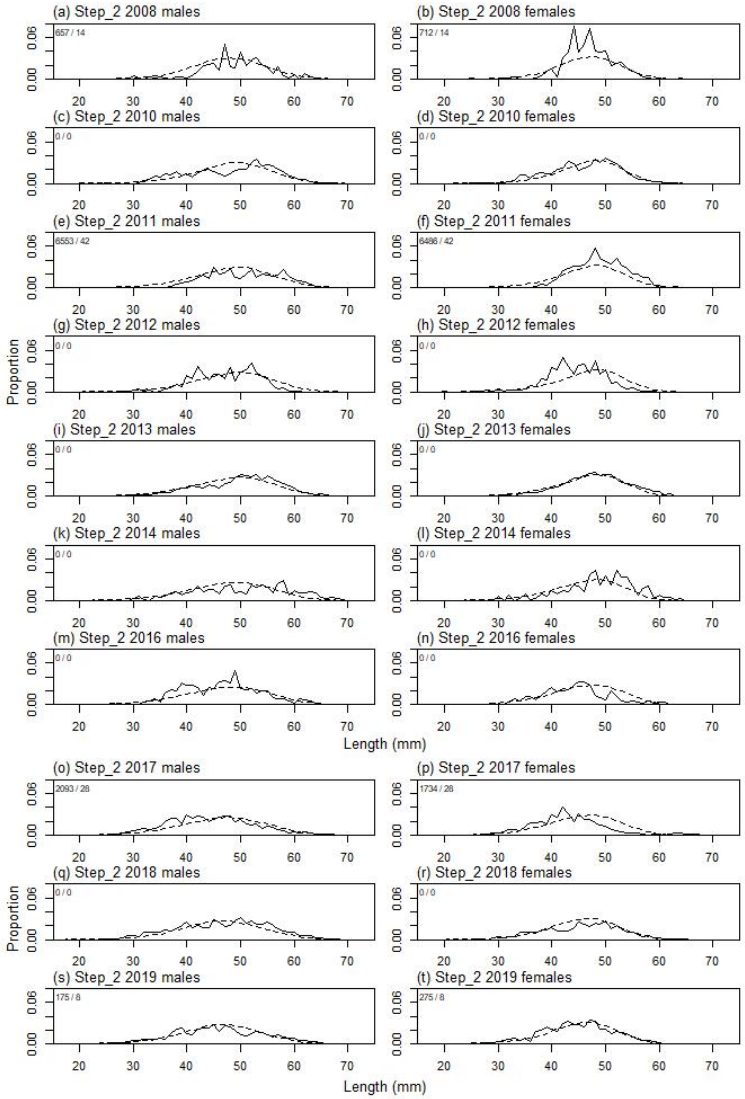

A5. 8: Observed (solid line) and fitted (dashed line) length frequency distributions from observer samples, time step 2 for the SCI 6A low *M* model. Numbers in top left corner of each plot represent number of scampi measured / number of events sampled.

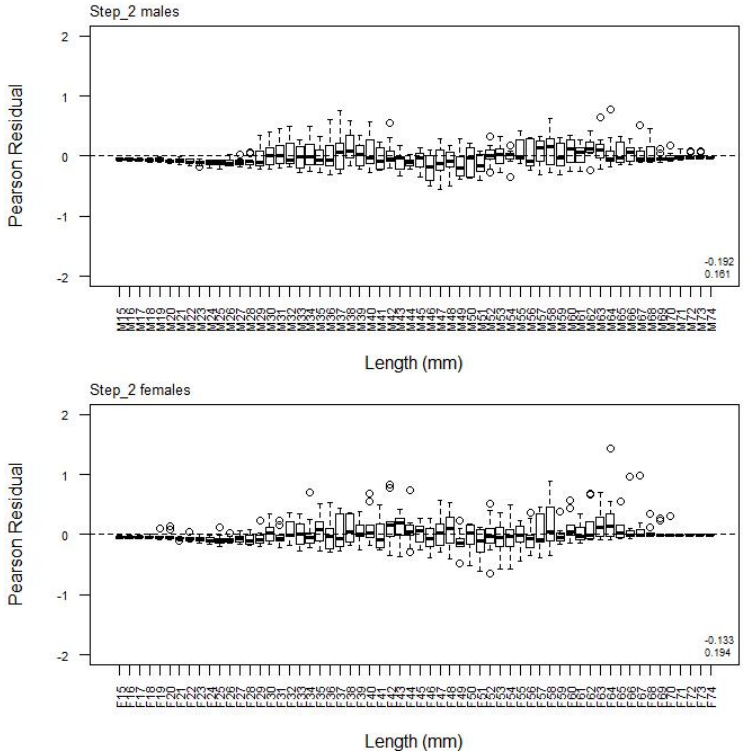

A5. 9: Box plots of Pearson residuals from the fit to length frequency distributions by length from observer sampling by sex for time step 2 for the SCI 6A low *M* model.

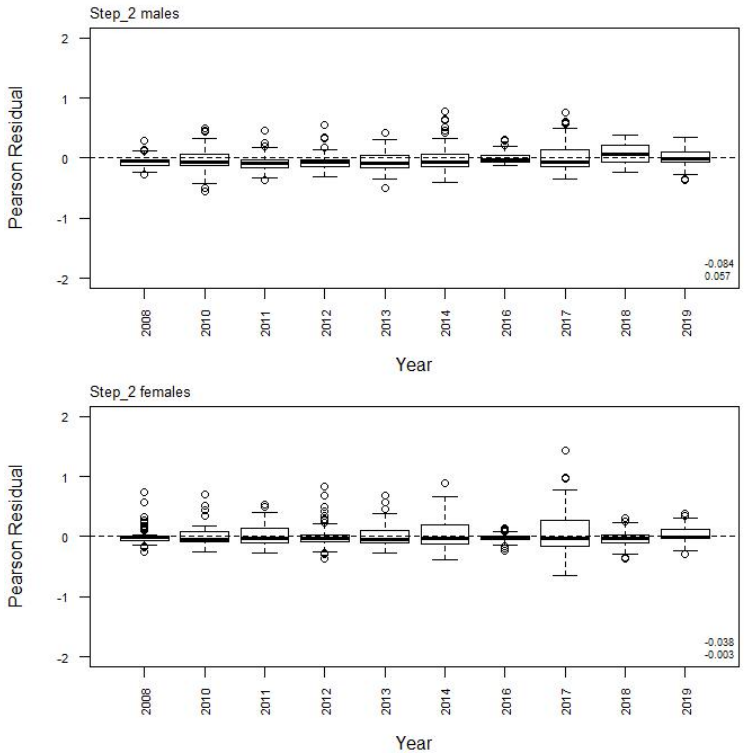

A5. 10: Box plots of Pearson residuals from the fit to length frequency distributions by year from observer sampling by sex for time step 2 for the SCI 6A low *M* model.

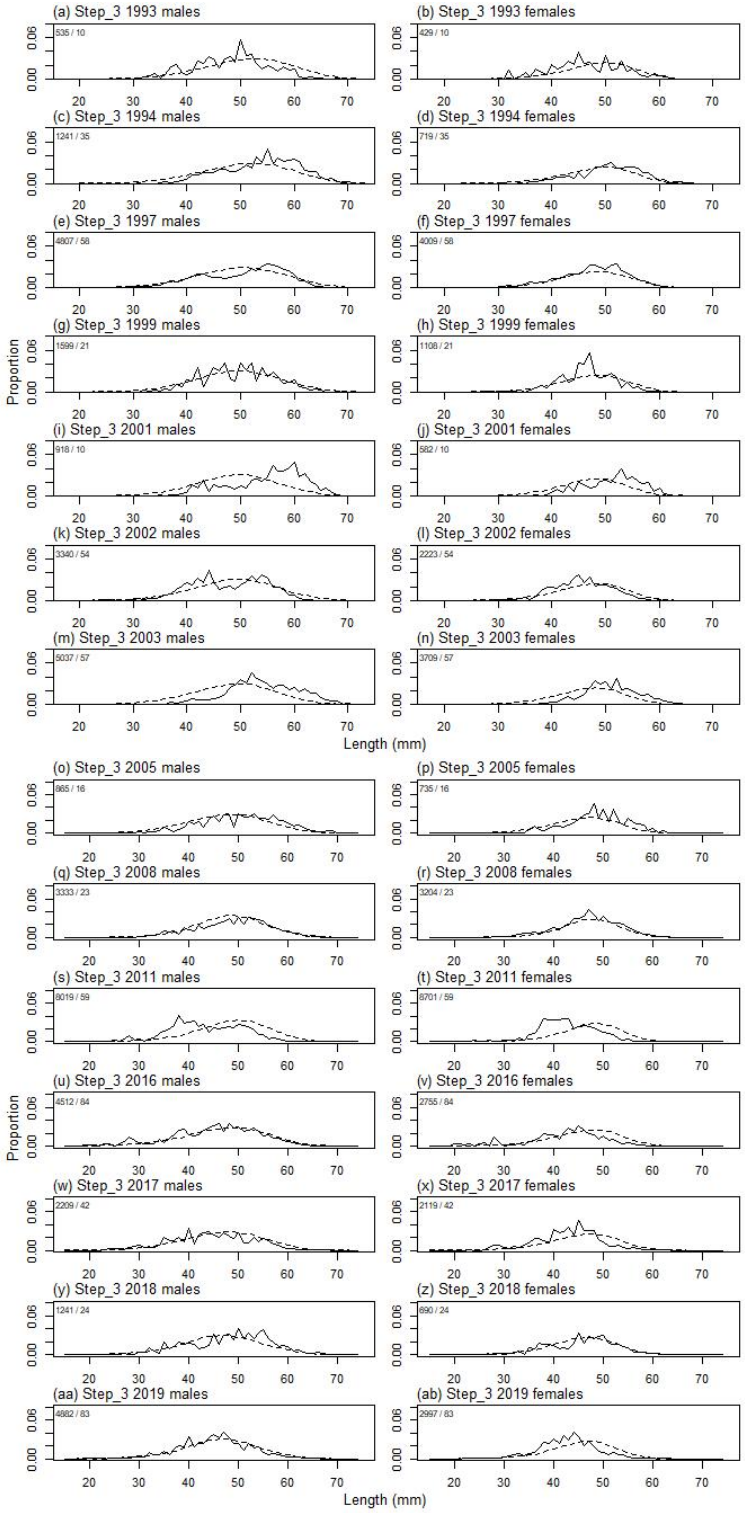

A5. 11: Observed (solid line) and fitted (dashed line) length frequency distributions from observer samples, time step 3 for the SCI 6A low *M* model. Numbers in top left corner of each plot represent number of scampi measured / number of events sampled.

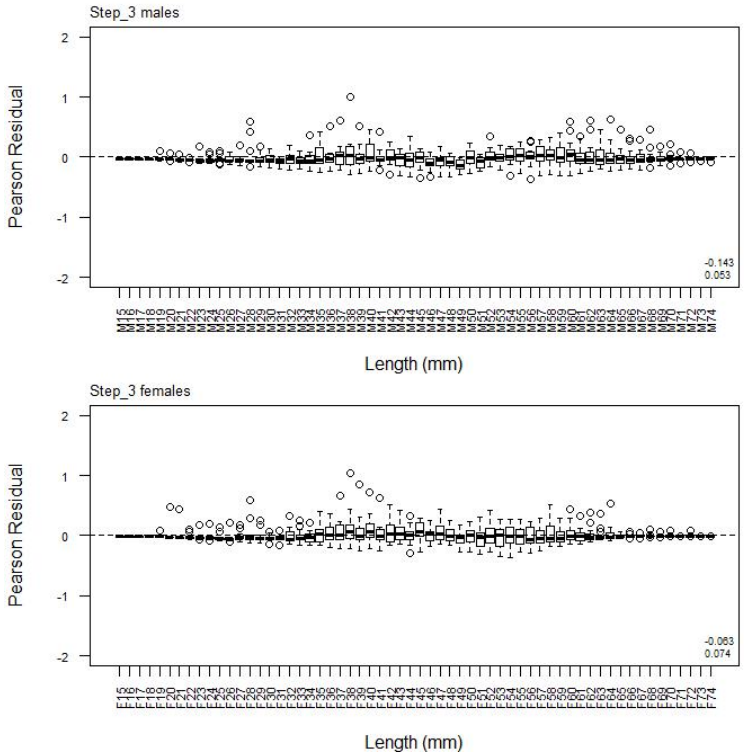

A5. 12: Box plots of Pearson residuals from the fit to length frequency distributions by length from observer sampling by sex for time step 3 for the SCI 6A base model.

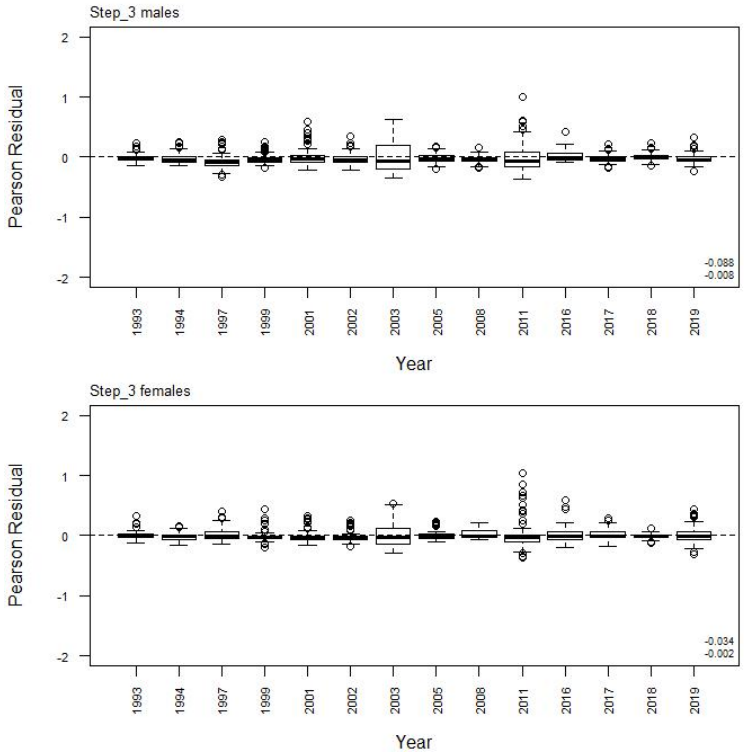

A5. 13: Box plots of Pearson residuals from the fit to length frequency distributions by year from observer sampling by sex for time step 3 for the SCI 6A low *M* model.

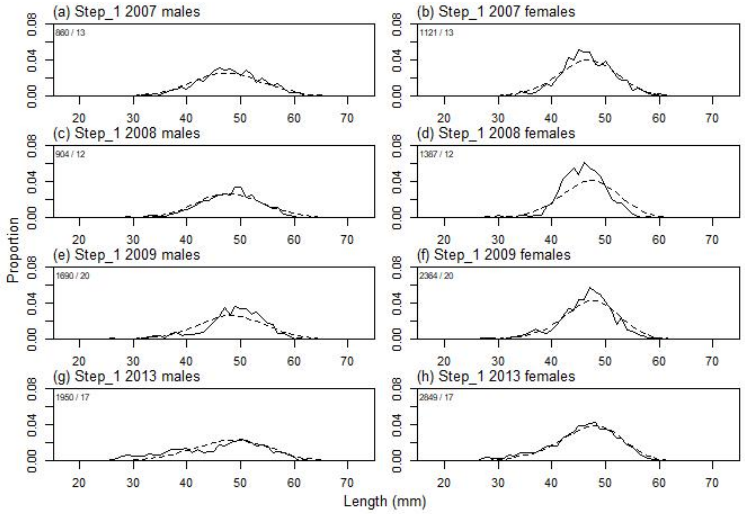

A5. 14: Observed (solid line) and fitted (dashed line) length frequency distributions from *San Tongariro* trawl survey samples for SCI 6A low *M* model. Numbers in top left corner of each plot represent number of scampi measured / number of events sampled.

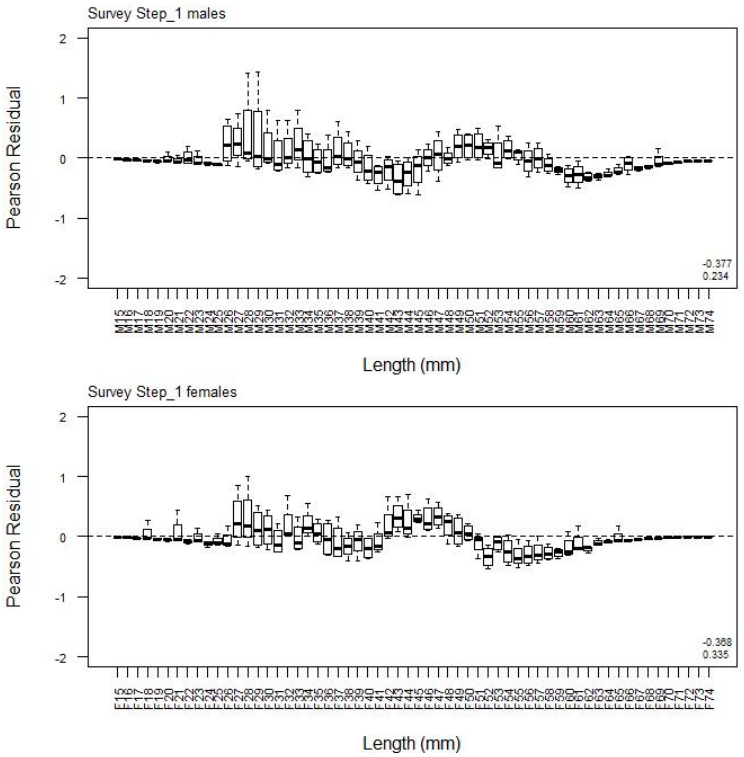

A5. 15: Box plots of Pearson residuals from the fit to length frequency distributions by length from *San Tongariro* trawl survey by sex for the SCI 6A low *M* model.

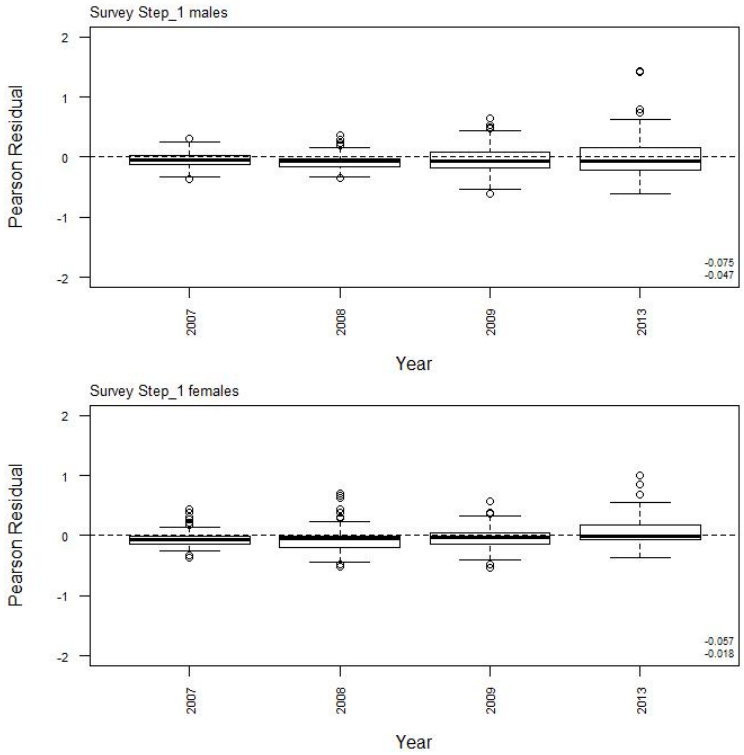

A5. 16: Box plots of Pearson residuals from the fit to length frequency distributions by year from *San Tongariro* trawl survey by sex for the SCI 6A low *M* model.

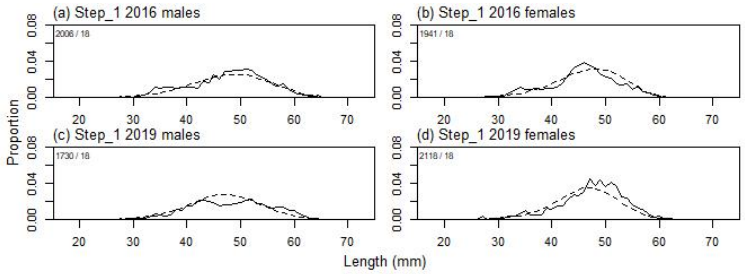

A5. 17: Observed (solid line) and fitted (dashed line) length frequency distributions from *Kaharoa* trawl survey samples for SCI 6A low *M* model. Numbers in top left corner of each plot represent number of scampi measured / number of events sampled.

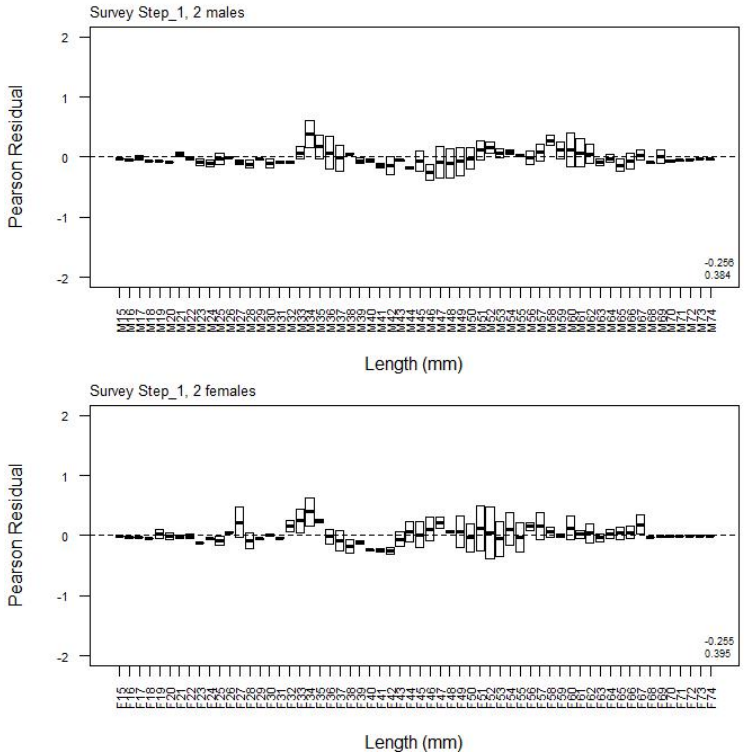

A5. 18: Box plots of Pearson residuals from the fit to length frequency distributions by length from *Kaharoa* trawl survey by sex for the SCI 6A low *M* model.

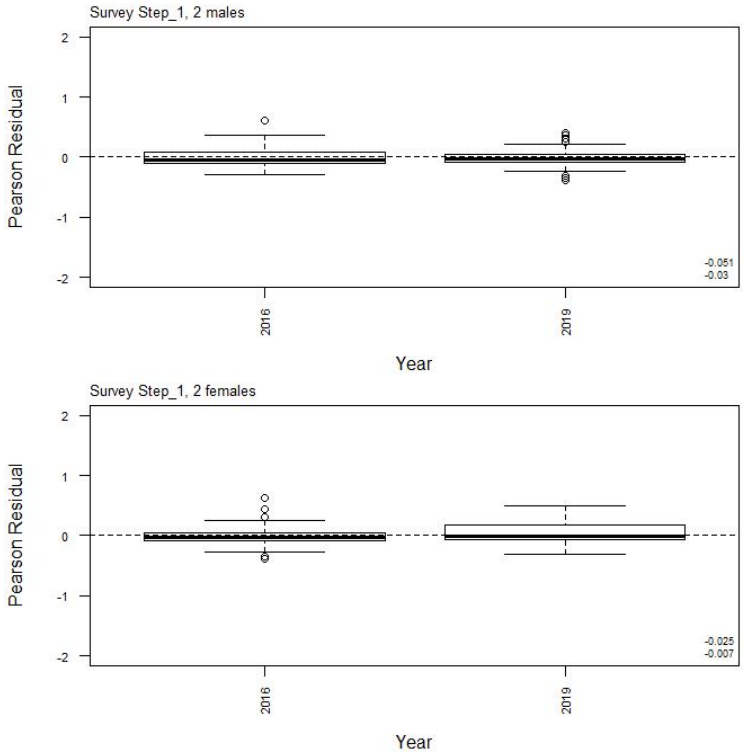

A5. 19: Box plots of Pearson residuals from the fit to length frequency distributions by year from *Kaharoa* trawl survey by sex for the SCI 6A low *M* model.

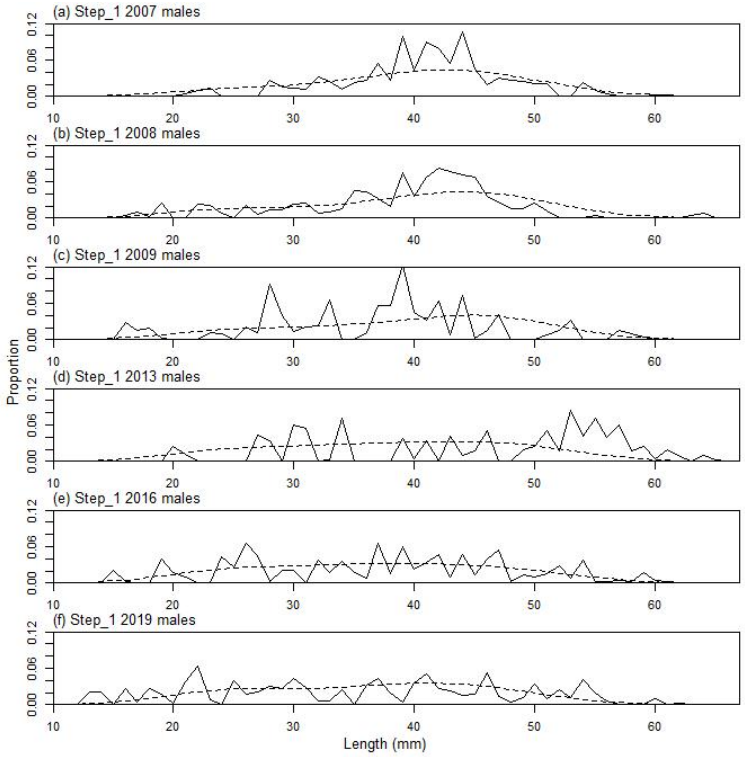

A5. 20: Observed (solid line) and fitted (dashed line) length frequency distributions from photo survey samples for the SCI 6A low *M* model.

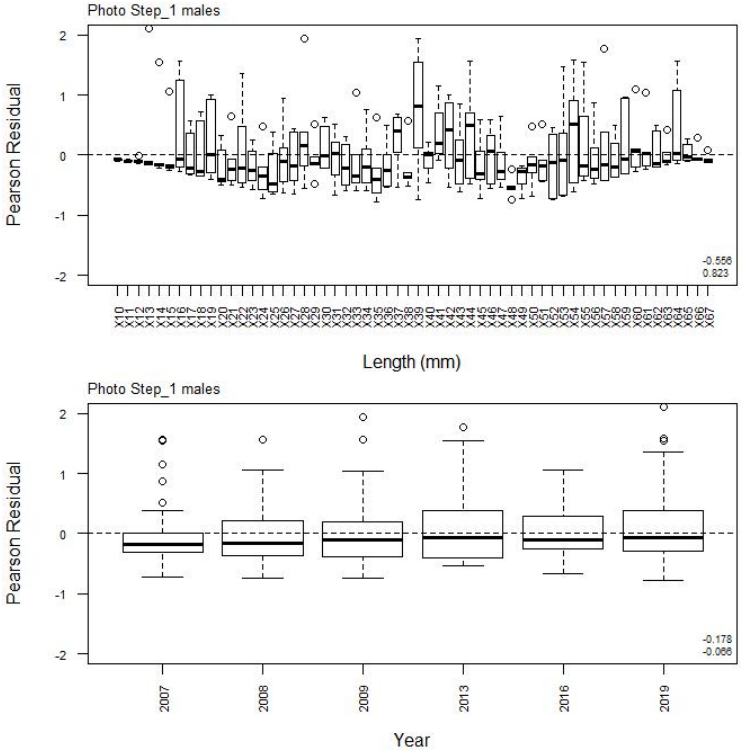

A5. 21: Box plots of Pearson residuals from the fit to length frequency distributions by length (top plot) and year (bottom plot) from photo survey sampling by sex for the SCI 6A low *M* model.

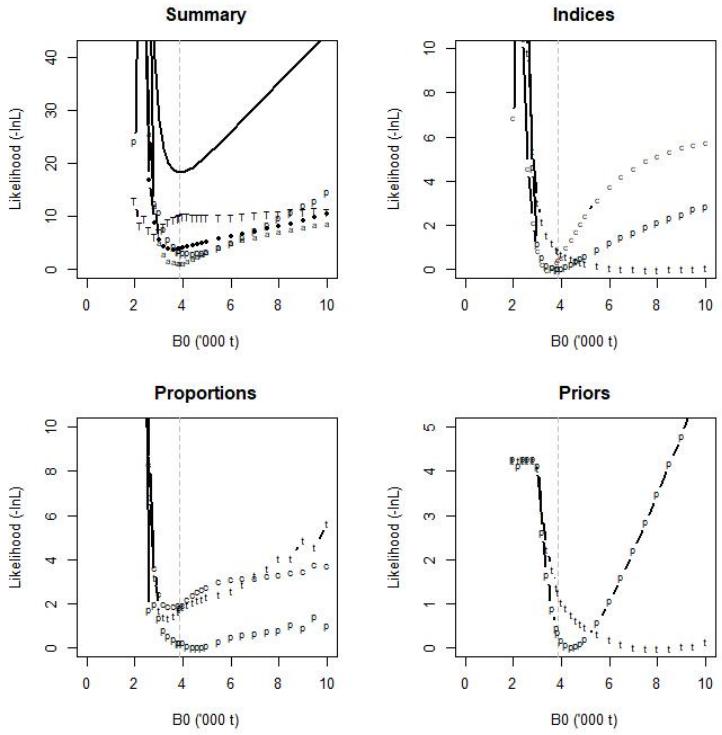

A5. 22: Likelihood profiles for the SCI 6A low *M* model when B_0 is fixed in the model. Figures show profiles for main priors (top left, p – priors, a – abundance indices, • – proportions at length, T – tag recaptures), abundance indices (top right, t – trawl survey step, c – CPUE, p – photo survey), proportion at length data (bottom left, p-photo, t – trawl, c – observer), and priors (bottom right, p – *q-Scampi*, t – *q-Trawl*).

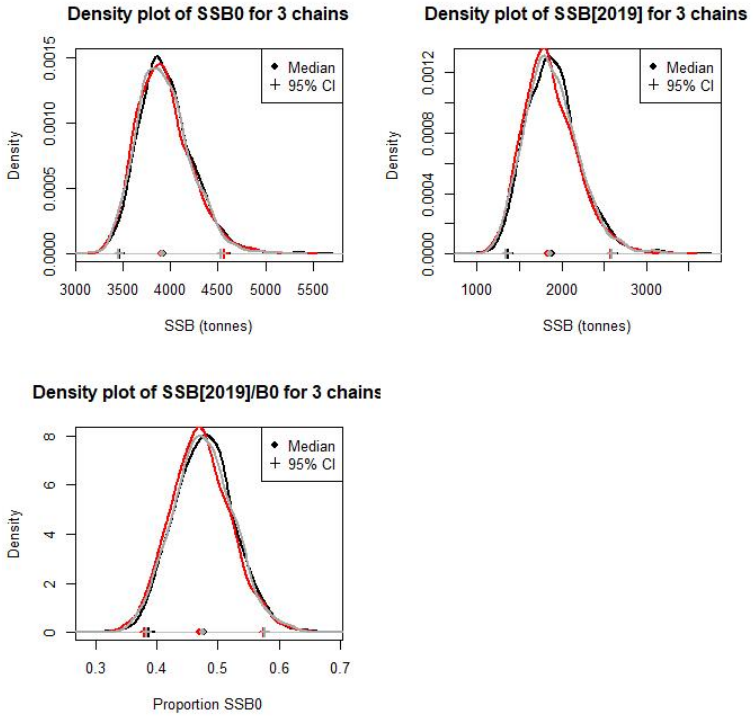

A5. 23: Density plots for SSB_0, SSB_{2019}, and SSB_{2019}/SSB_0 for the SCI 6A low *M* model for three independent MCMC chains, with median and 95% confidence intervals.

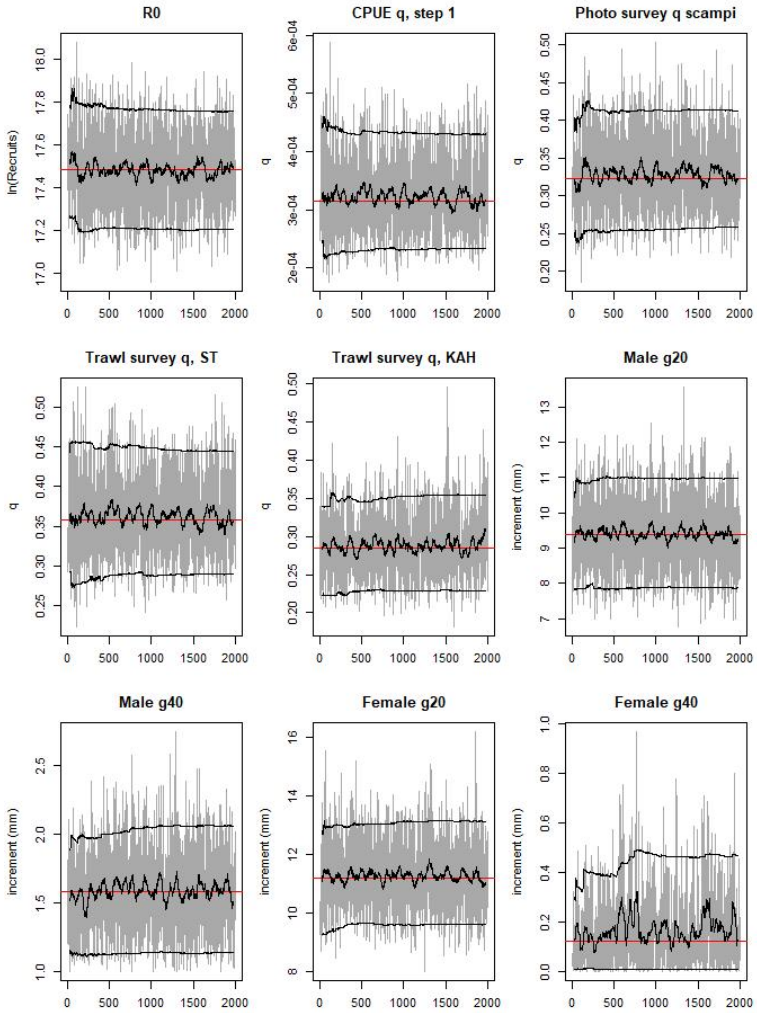

A5. 24: MCMC traces for R_0, catchability, and growth terms for the SCI 6A low *M* model.

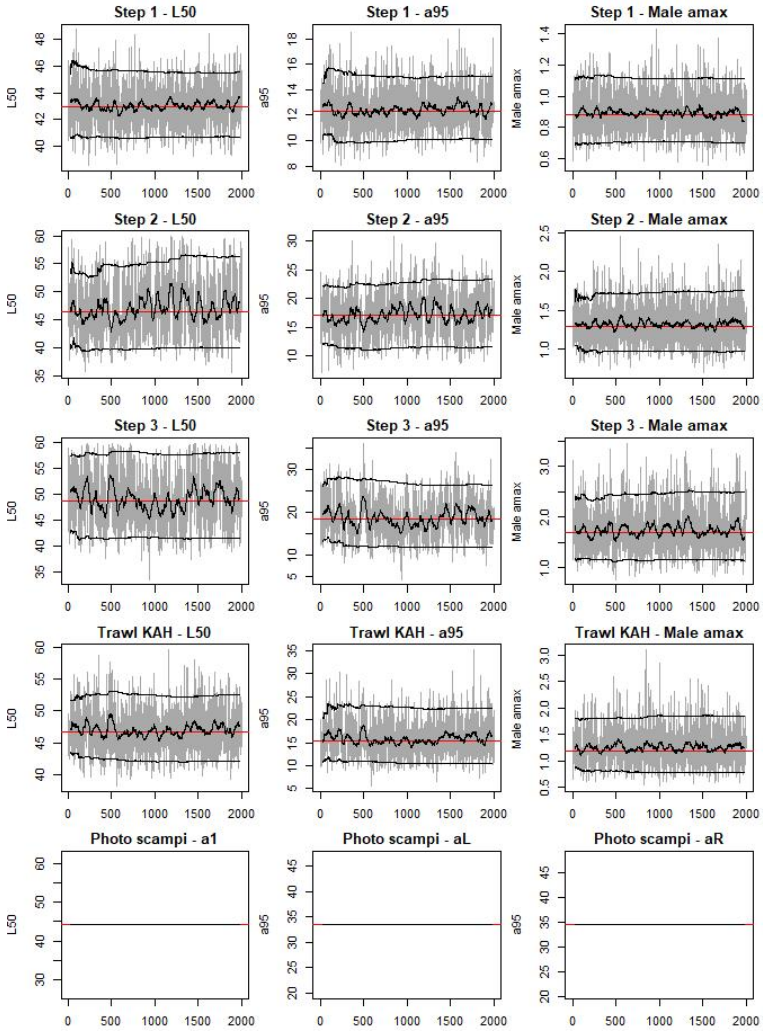

A5. 25: MCMC traces for selectivity terms for the SCI 6A low *M* model. Photo scampi selectivity fixed at MPD estimate within the MCMC.

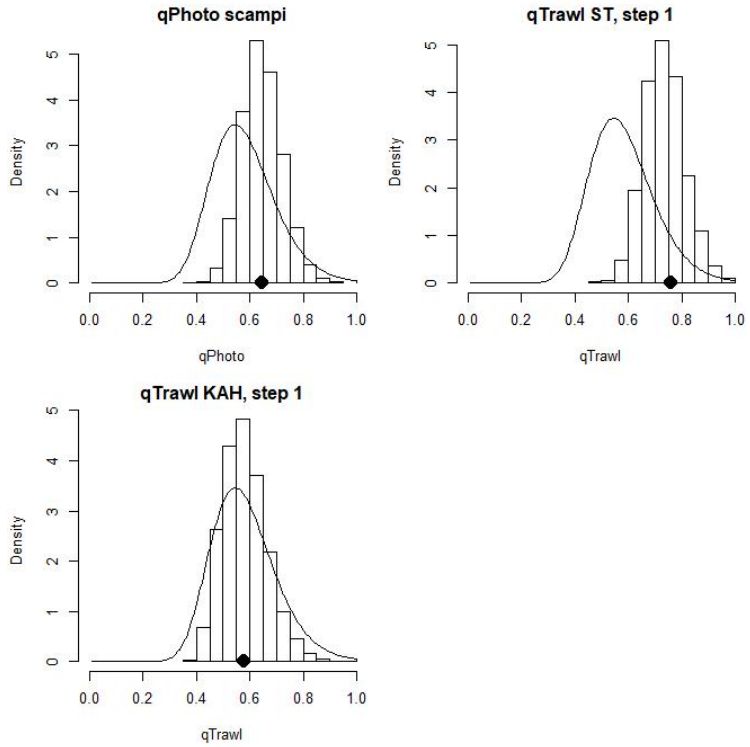

A5. 26: Marginal posterior distributions (histograms), MPD estimates (solid symbols), and distributions of priors (lines) for catchability terms for the SCI 6A low *M* model.

APPENDIX 6. SCI 6A CPUE excluded model plots

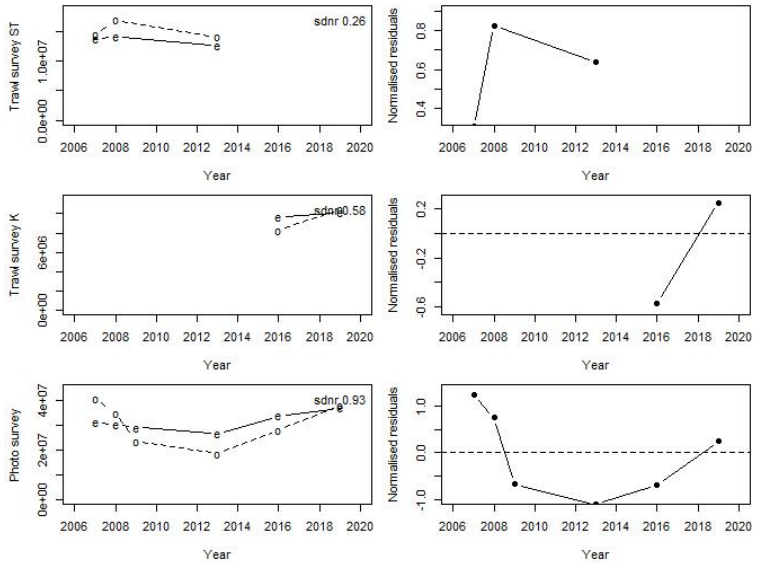

A6. 1: Fits to abundance indices (left column) and normalised residuals (right column) for standardised CPUE index (top row) *San Tongariro* (ST) trawl survey abundance index (second row), *Kaharoa* (K) trawl survey abundance index (third row), and photo survey emerged scampi abundance index for the SCI 6A CPUE excluded model.

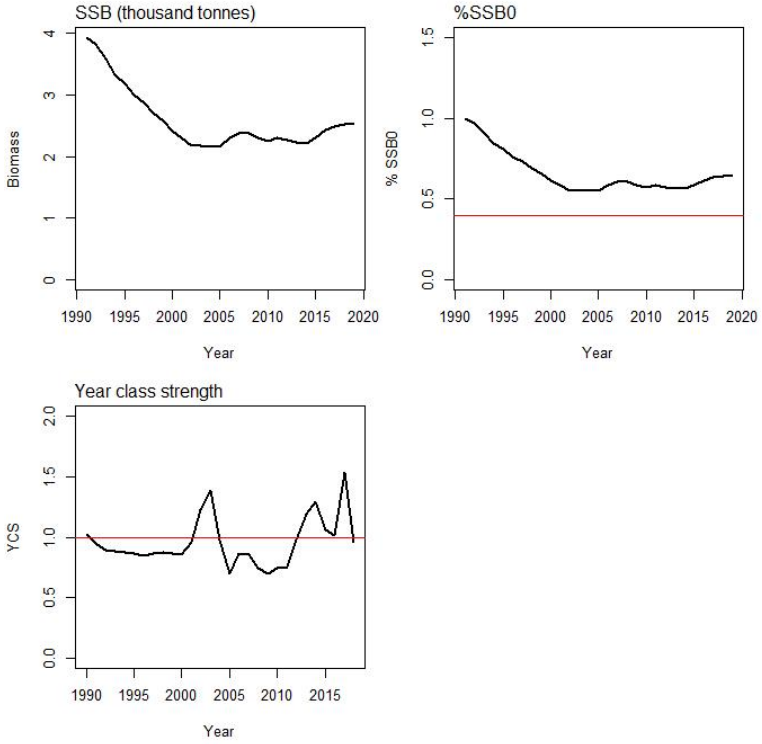

A6. 2: Spawning stock biomass trajectory (upper left), stock status (upper right), and year class strength (lower left) for the SCI 6A CPUE excluded model.

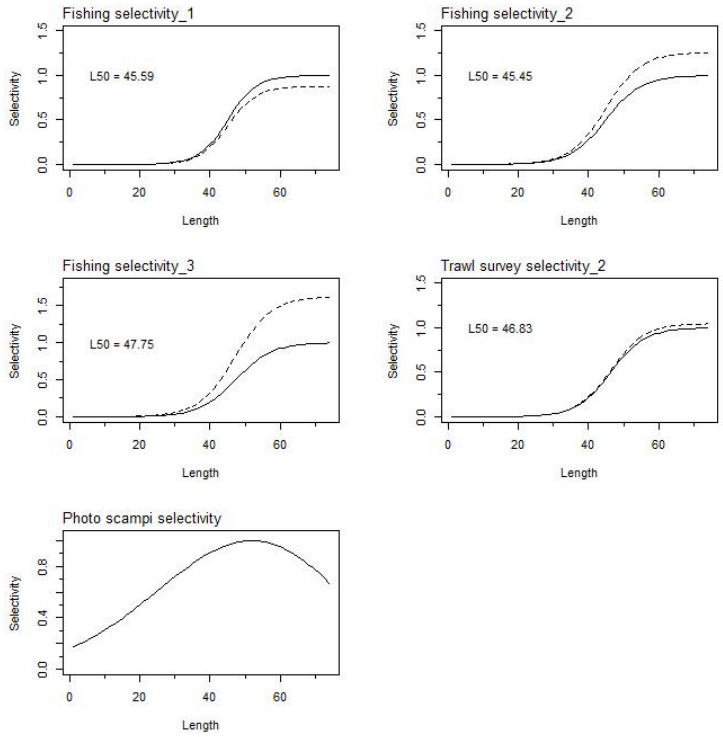

A6. 3: Fishery and survey selectivity curves for SCI 6A CPUE excluded model. Solid line – females, dotted line – males. The scampi photo index is not sexed, and a single selectivity applies.

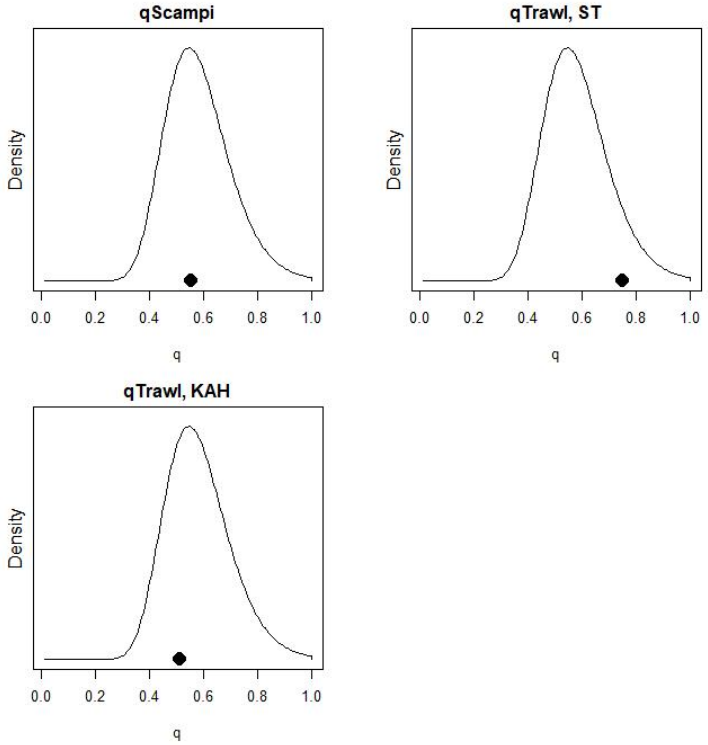

A6. 4: Catchability estimates from MPD model run, plotted in relation to prior distribution for SCI 6A CPUE excluded model.

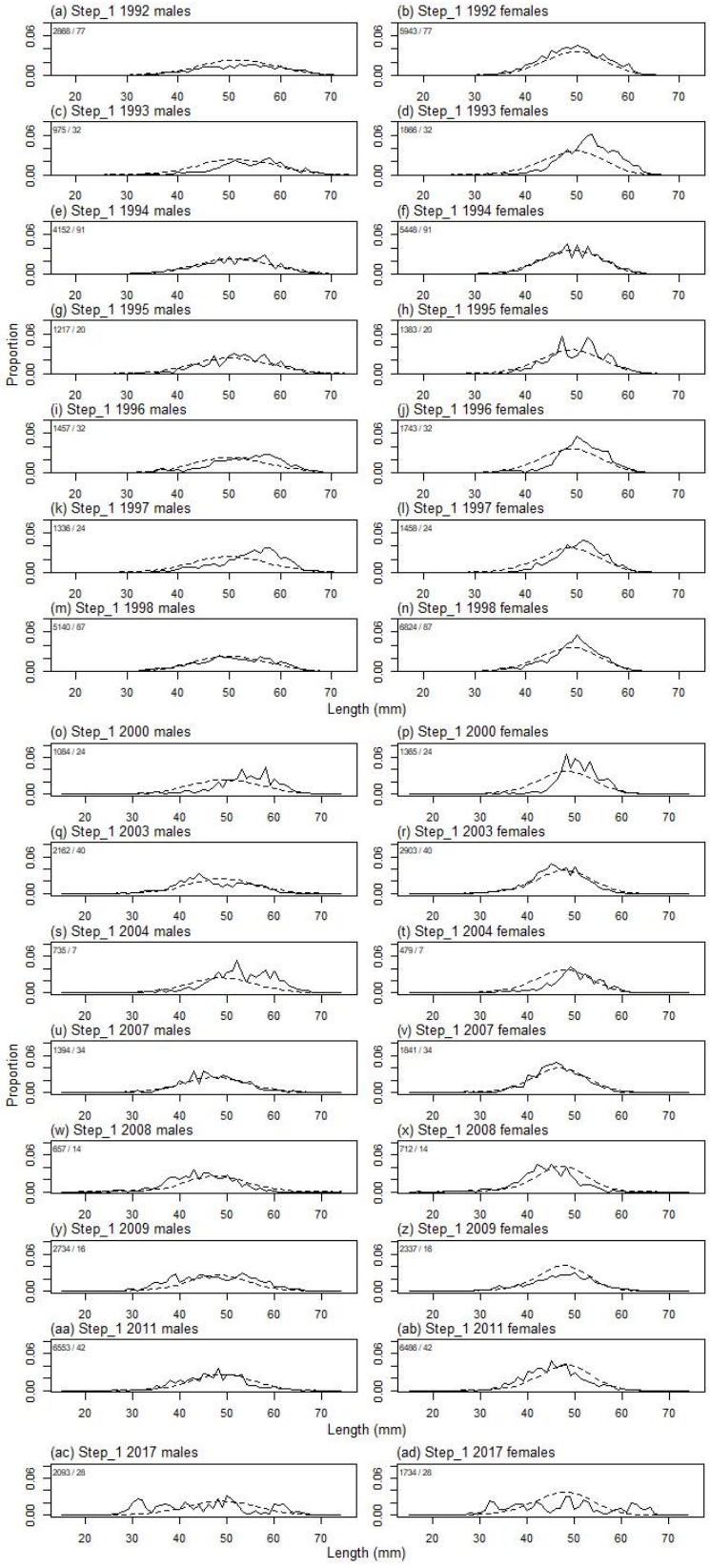

A6. 5: Observed (solid line) and fitted (dashed line) length frequency distributions from observer samples, time step 1 for the SCI 6A CPUE excluded model. Numbers in top left corner of each plot represent number of scampi measured / number of events sampled.

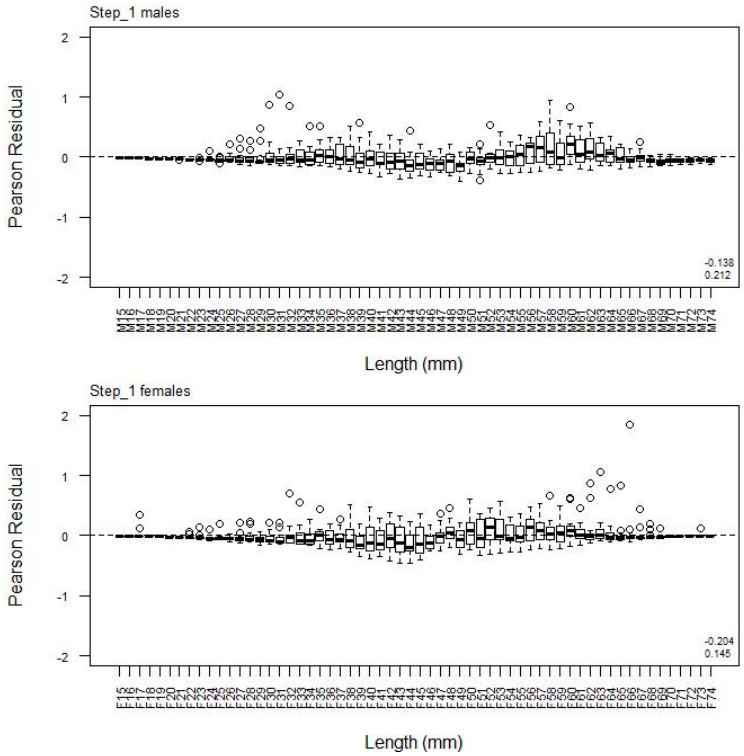

A6. 6: Box plots of Pearson residuals from the fit to length frequency distributions by length from observer sampling by sex for time step 1 for the SCI 6A CPUE excluded model.

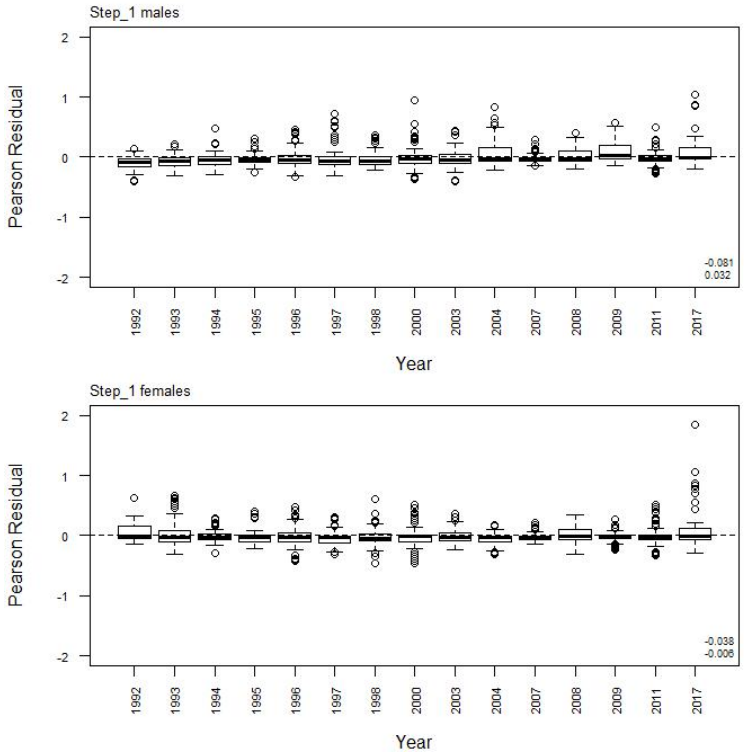

A6. 7: Box plots of Pearson residuals from the fit to length frequency distributions by year from observer sampling by sex for time step 1 for the SCI 6A CPUE excluded model.

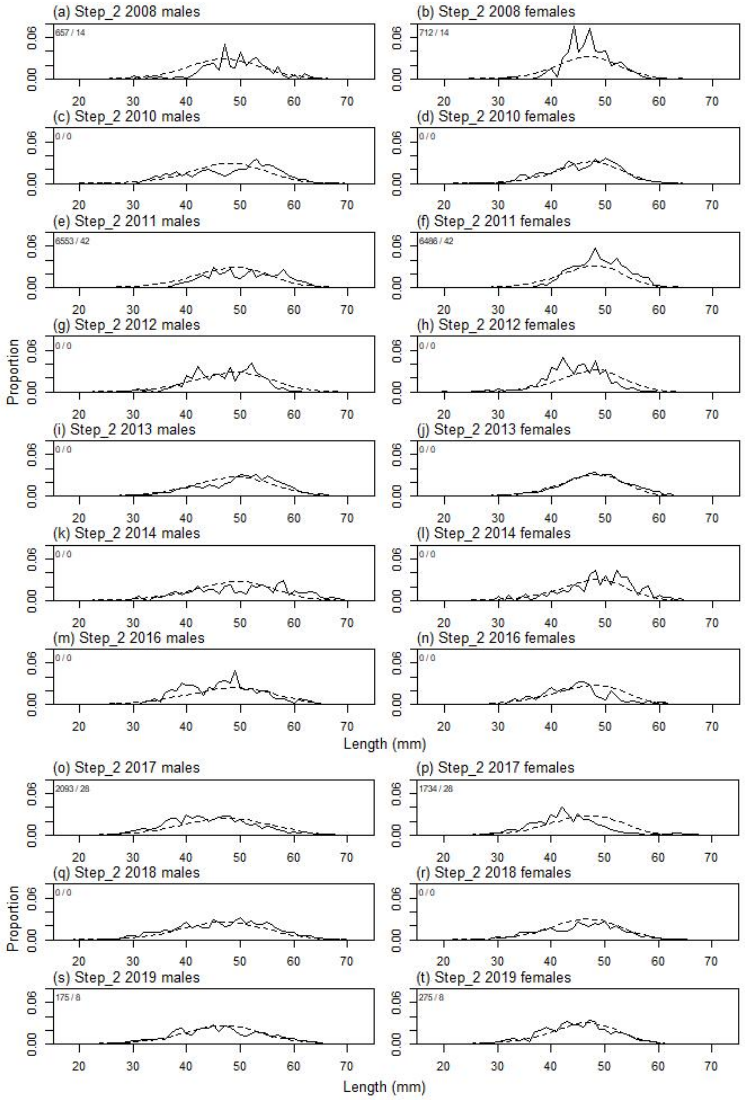

A6. 8: Observed (solid line) and fitted (dashed line) length frequency distributions from observer samples, time step 2 for the SCI 6A CPUE excluded model. Numbers in top left corner of each plot represent number of scampi measured / number of events sampled.

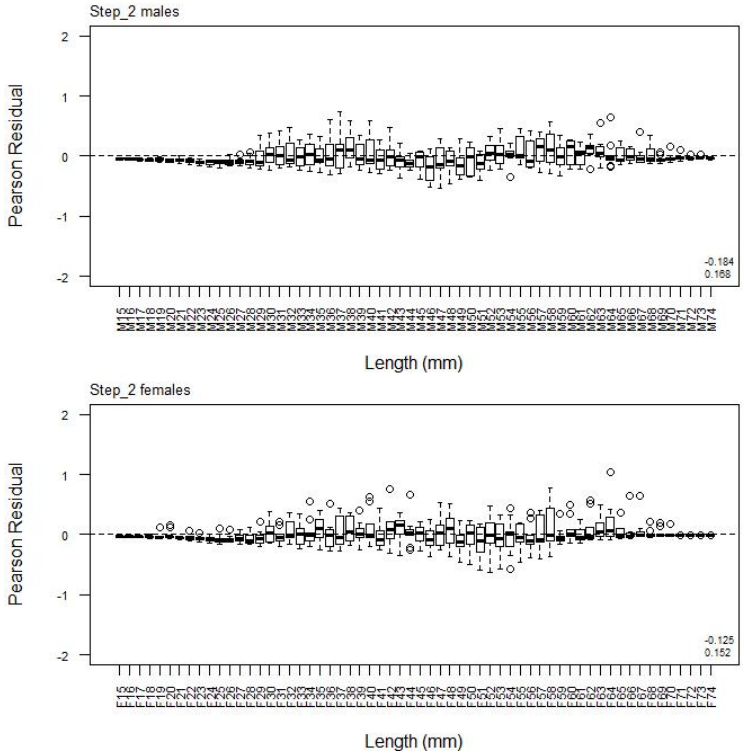

A6. 9: Box plots of Pearson residuals from the fit to length frequency distributions by length from observer sampling by sex for time step 2 for the SCI 6A CPUE excluded model.

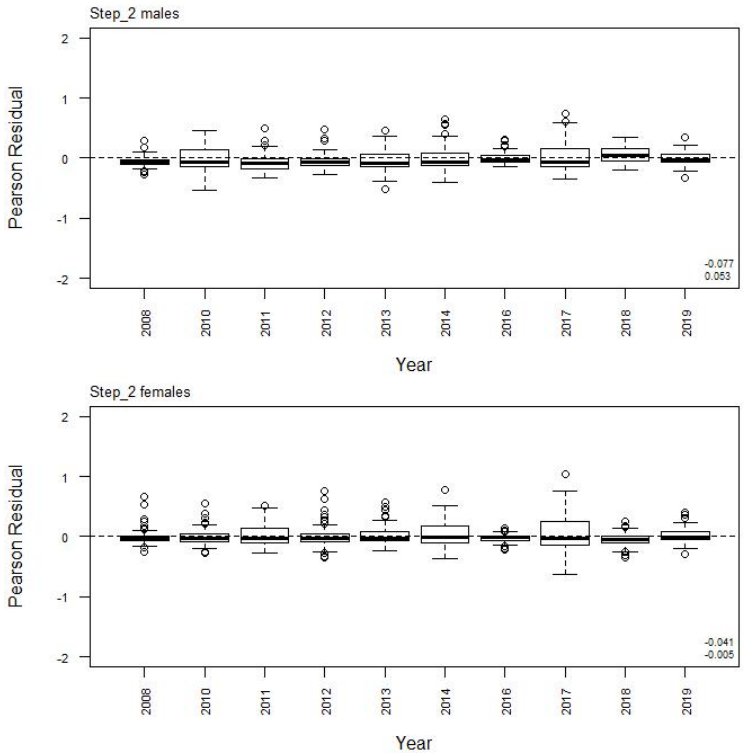

A6. 10: Box plots of Pearson residuals from the fit to length frequency distributions by year from observer sampling by sex for time step 2 for the SCI 6A CPUE excluded model.

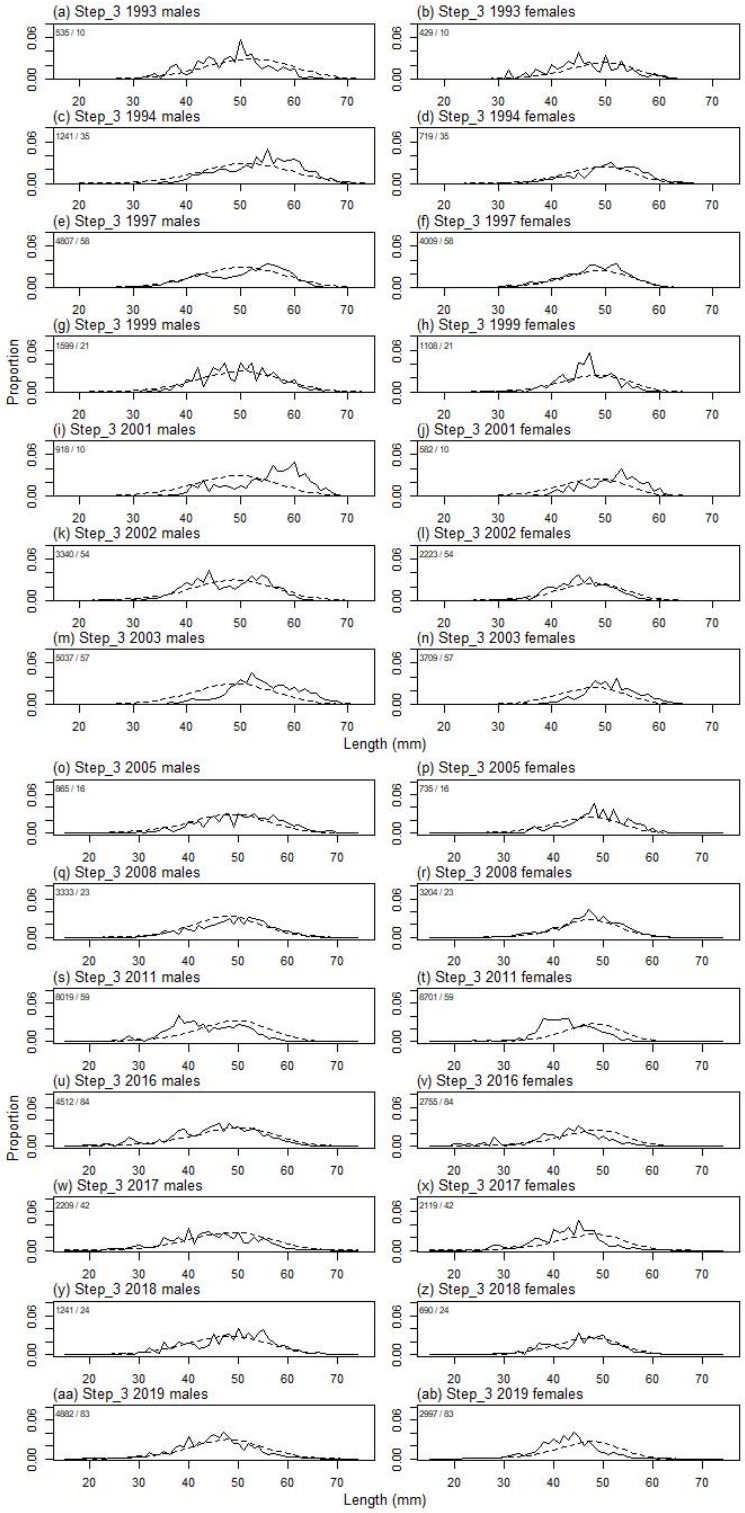

A6. 11: Observed (solid line) and fitted (dashed line) length frequency distributions from observer samples, time step 3 for the SCI 6A CPUE excluded model. Numbers in top left corner of each plot represent number of scampi measured / number of events sampled.

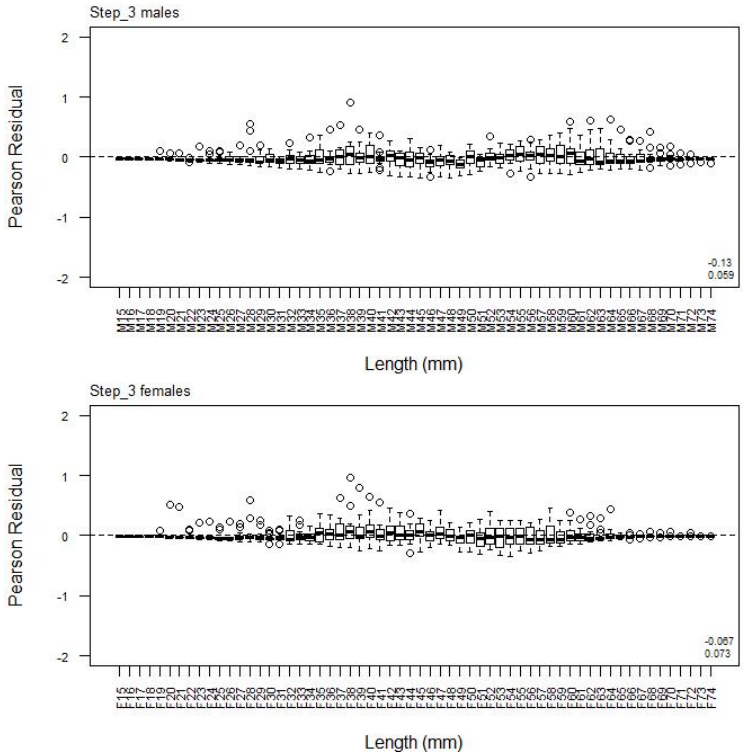

A6. 12: Box plots of Pearson residuals from the fit to length frequency distributions by length from observer sampling by sex for time step 3 for the SCI 6A CPUE excluded model.

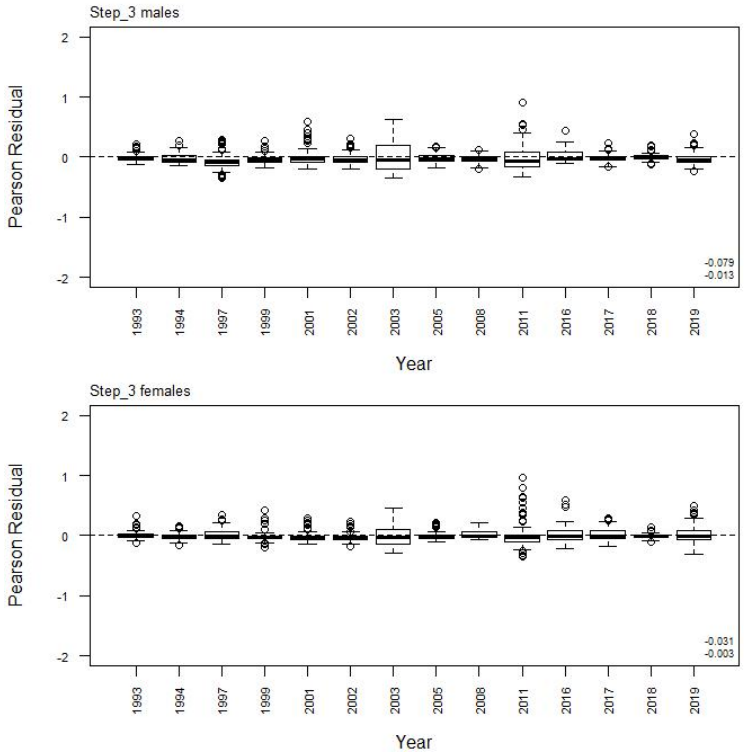

A6. 13: Box plots of Pearson residuals from the fit to length frequency distributions by year from observer sampling by sex for time step 3 for the SCI 6A CPUE excluded model.

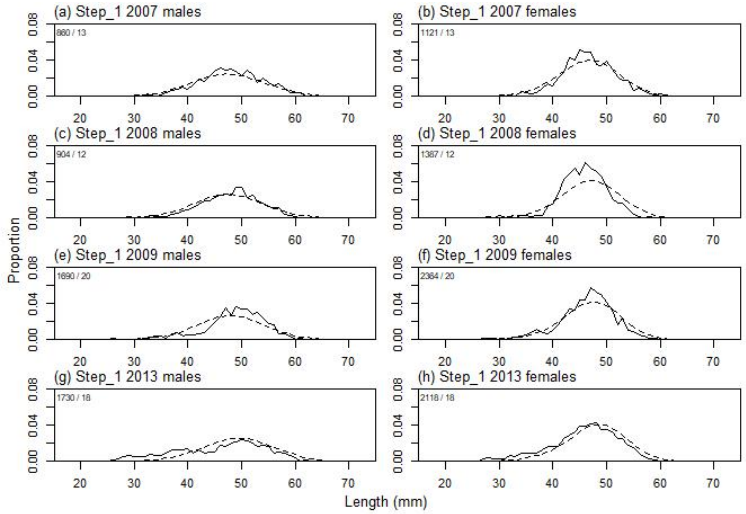

A6. 14: Observed (solid line) and fitted (dashed line) length frequency distributions from *San Tongariro* trawl survey samples for SCI 6A CPUE excluded model. Numbers in top left corner of each plot represent number of scampi measured / number of events sampled.

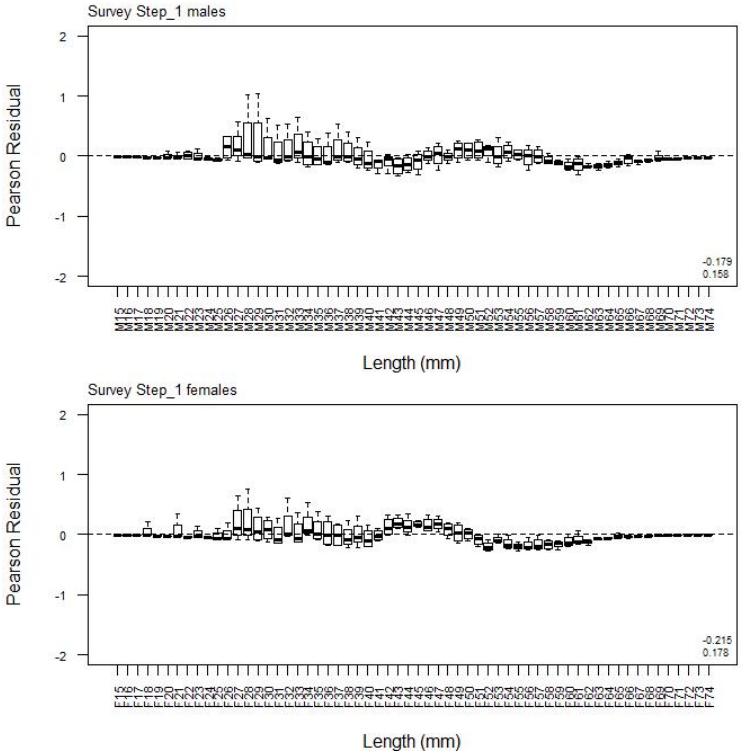

A6. 15: Box plots of Pearson residuals from the fit to length frequency distributions by length from *San Tongariro* trawl survey by sex for the SCI 6A CPUE excluded model.

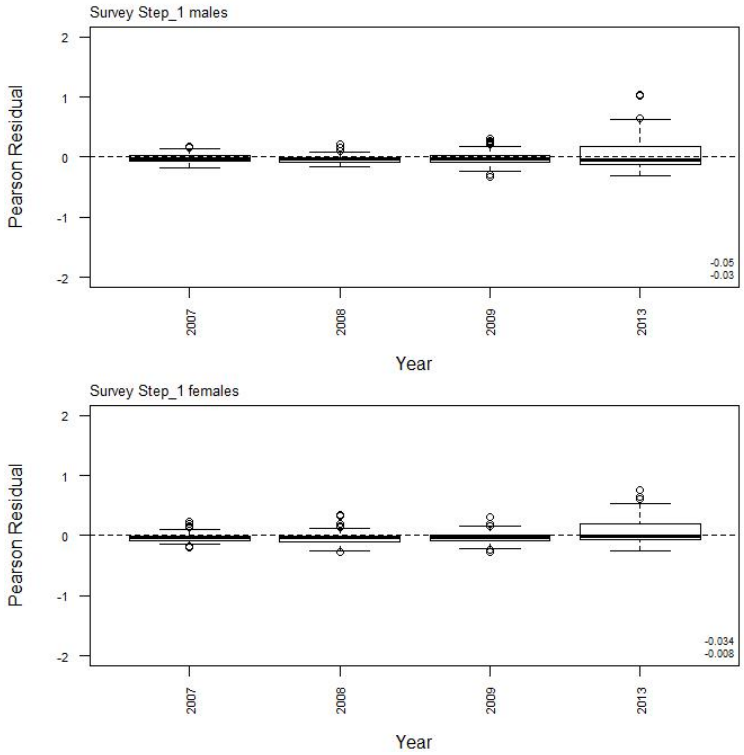

A6. 16: Box plots of Pearson residuals from the fit to length frequency distributions by year from *San Tongariro* trawl survey by sex for the SCI 6A CPUE excluded model.

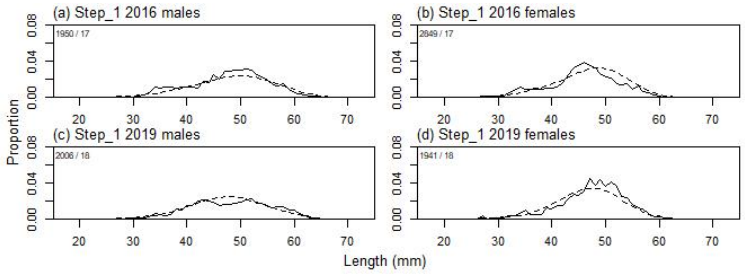

A6. 17: Observed (solid line) and fitted (dashed line) length frequency distributions from *Kaharoa* trawl survey samples for SCI 6A CPUE excluded model. Numbers in top left corner of each plot represent number of scampi measured / number of events sampled.

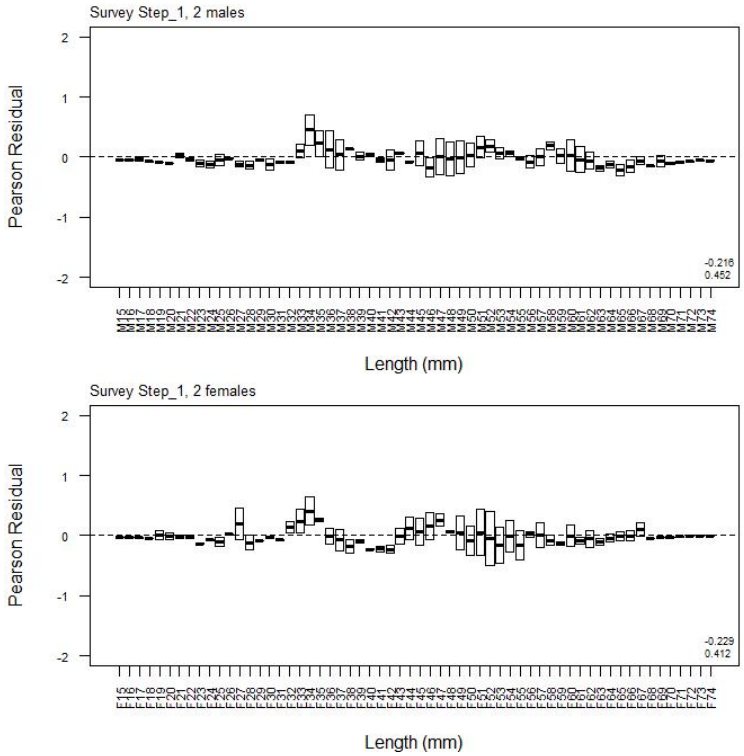

A6. 18: Box plots of Pearson residuals from the fit to length frequency distributions by length from *Kaharoa* trawl survey by sex for the SCI 6A CPUE excluded model.

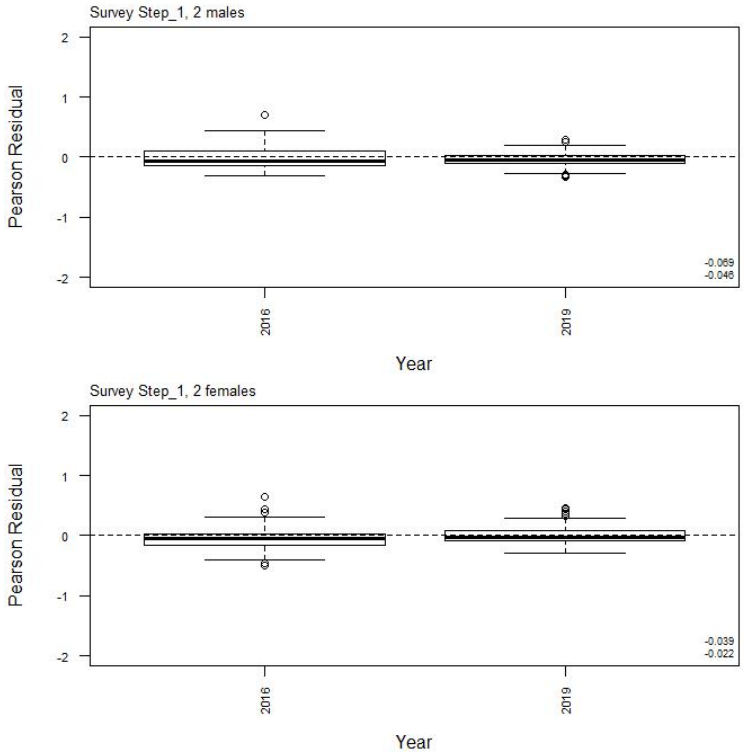

A6. 19: Box plots of Pearson residuals from the fit to length frequency distributions by year from *Kaharoa* trawl survey by sex for the SCI 6A CPUE excluded model.

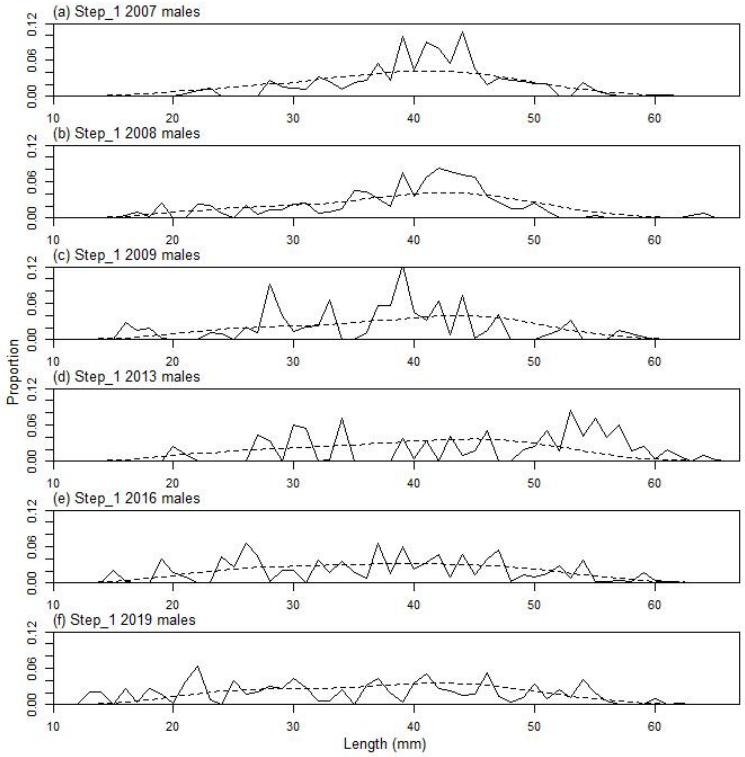

A6. 20: Observed (solid line) and fitted (dashed line) length frequency distributions from photo survey samples for the SCI 6A CPUE excluded model.

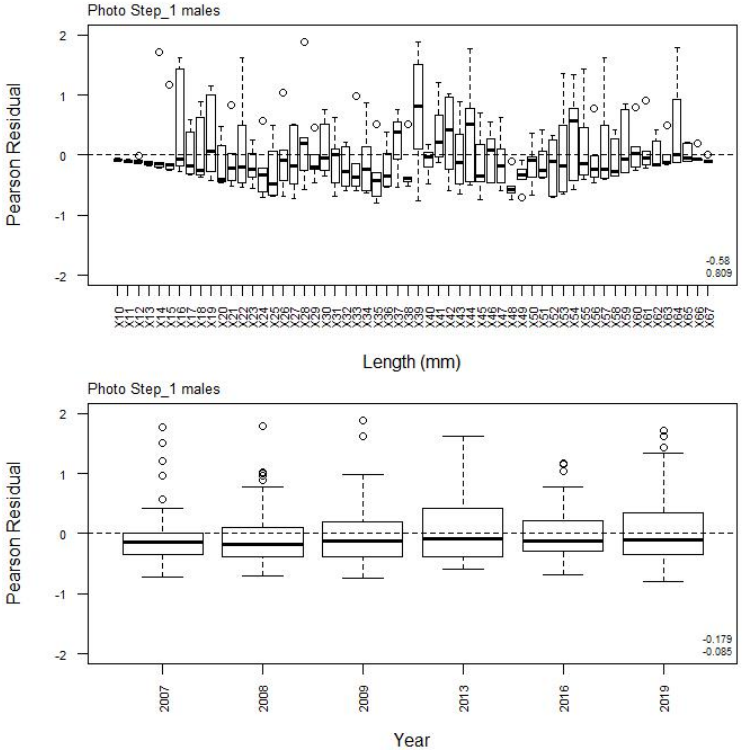

A6. 21: Box plots of Pearson residuals from the fit to length frequency distributions by length (top plot) and year (bottom plot) from photo survey sampling by sex for the SCI 6A CPUE excluded model.

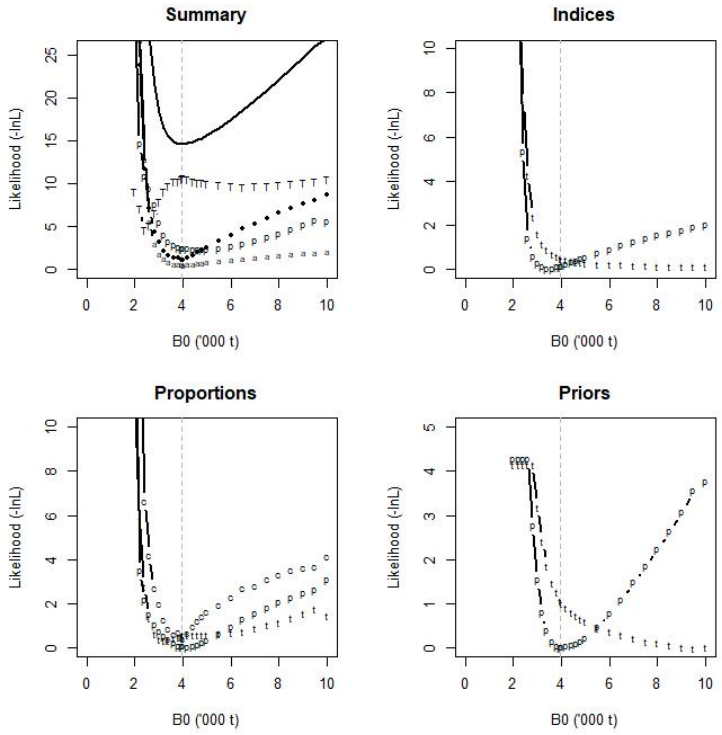

A6. 22: Likelihood profiles for the SCI 6A CPUE excluded model when B_0 is fixed in the model. Figures show profiles for main priors (top left, p – priors, a – abundance indices, • – proportions at length, T – tag recaptures), abundance indices (top right, t – trawl survey step, c – CPUE, p – photo survey), proportion at length data (bottom left, p-photo, t – trawl, c – observer), and priors (bottom right, p – *q-Scampi*, t – *q-Trawl*).

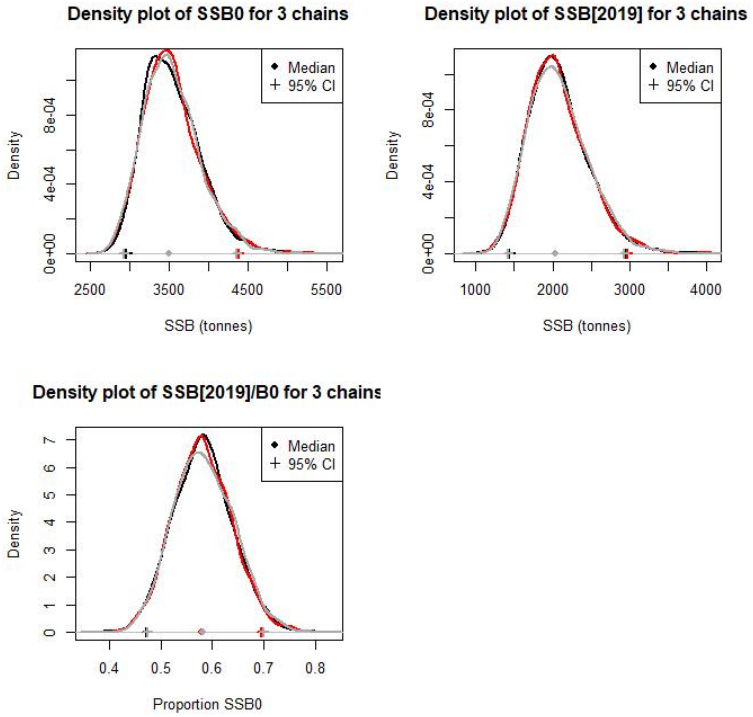

A6. 23: Density plots for SSB_0, SSB_{2019}, and SSB_{2019}/SSB_0 for the SCI 6A CPUE excluded model for three independent MCMC chains, with median and 95% confidence intervals.

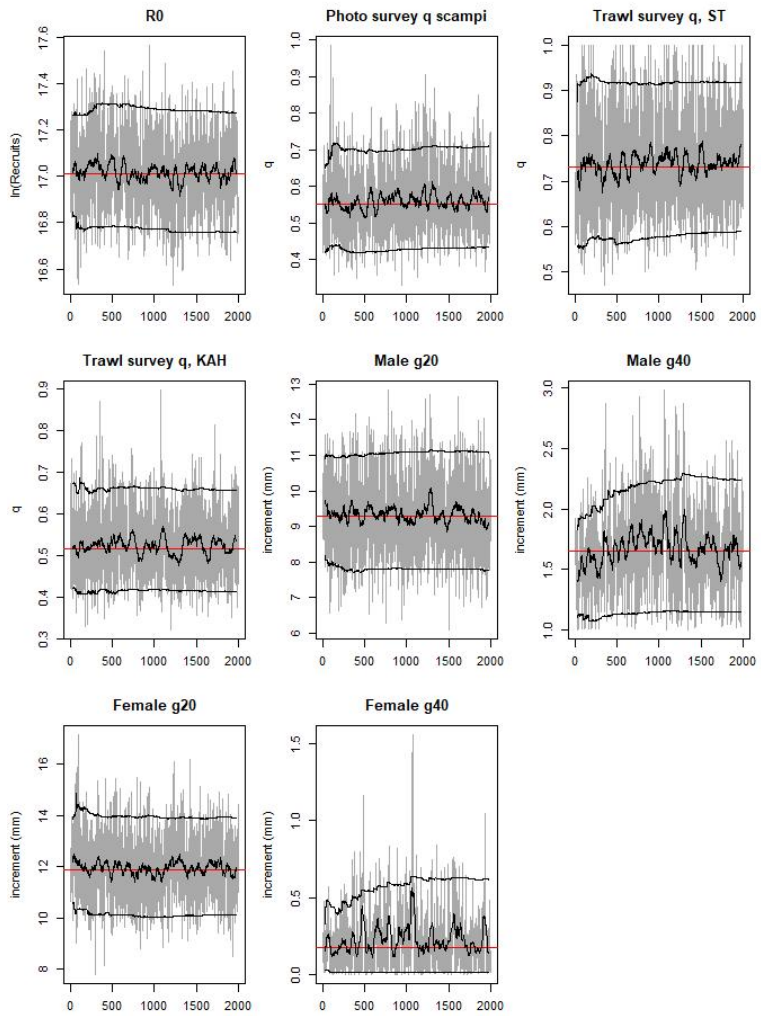

A6. 24: MCMC traces for R_0, catchability, and growth terms for the SCI 6A CPUE excluded model.

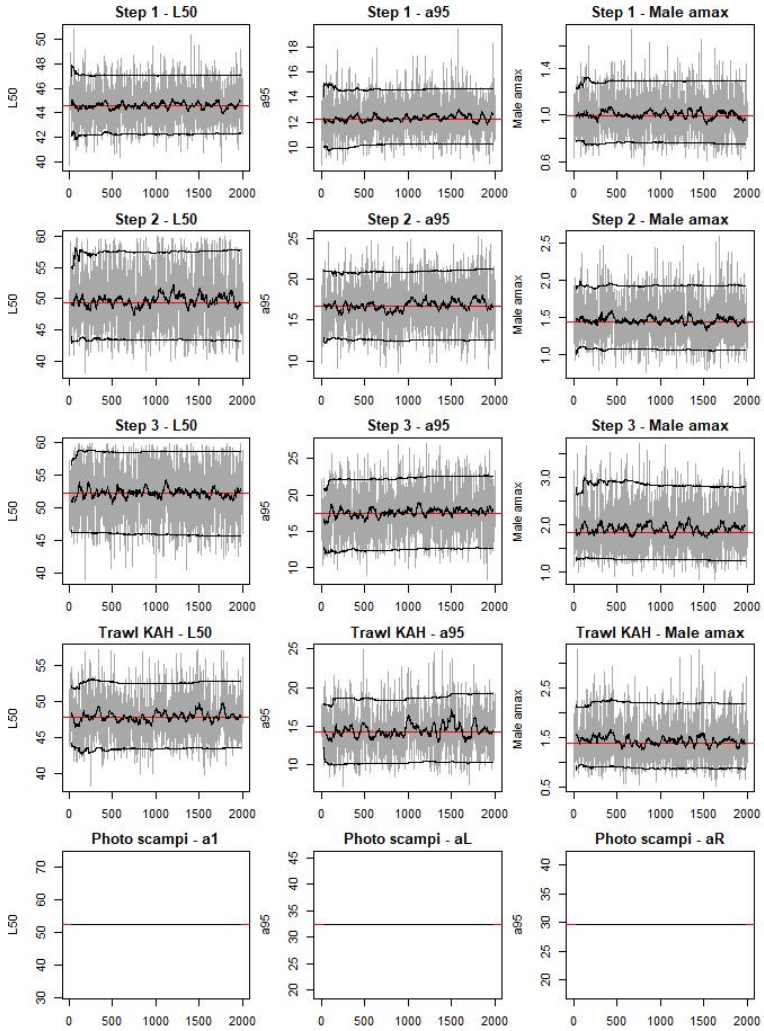

A6. 25: MCMC traces for selectivity terms for the SCI 6A CPUE excluded model. Photo scampi selectivity fixed at MPD estimate within the MCMC.

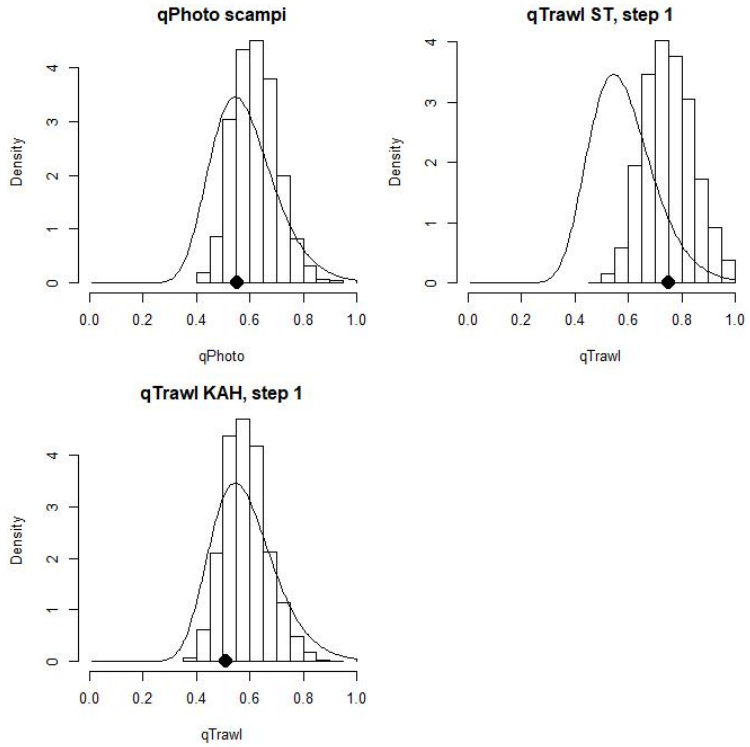

A6. 26: Marginal posterior distributions (histograms), MPD estimates (solid symbols), and distributions of priors (lines) for catchability terms for the SCI 6A CPUE excluded model.